Modelling Kallmann Syndrome in the Zebrafish

by

Steven Mark Cadman

A thesis submitted to University College London
for the degree of Doctor of Philosophy

December 2010

Centre for Neuroendocrinology
University College London Medical School
Royal Free Campus, London NW3 2PF

Declaration

I, Steven Mark Cadman, confirm that the work presented in this thesis is my own. Where information has been derived from other sources, I confirm that this has been indicated in the thesis.

....

Steven Mark Cadman **Date**

Abstract

Kallmann syndrome (KS) is a human genetic disorder characterised by delayed/absent pubertal development, associated with lack of olfaction. KS is proposed to result from disrupted migration and targeting of olfactory sensory axons and hypothalamic gonadotrophin releasing hormone (GnRH1) neurons during early embryogenesis. Mutations in anosmin-1 (*KAL1*), fibroblast growth factor receptor 1 (*FGFR1*) and fibroblast growth factor 8 (*FGF8*) are responsible for some cases of KS. Previously, in *ex vivo* human GnRH neuroblast culture, anosmin-1 was shown to enhance FGFR1 signalling in an FGF-dependent manner. Here, using a zebrafish *in vivo* system, the biological functions of anosmin-1- and FGF-mediated signalling during olfactory and GnRH system development have been investigated.

Characterisation of the zebrafish GnRH system, and the role of olfactory axonogenesis in its development, was aided by the generation of a transgenic reporter line: pGnRH3:mCherry. Two notable mCherry populations were visualised by 36 hours post-fertilisation (hpf): the well-characterised terminal nerve cells, and an early, hitherto unreported, hypothalamic cluster of cells.

Antisense morpholino approaches were used to demonstrate that knocking down both *Kal1a* and *Kal1b* genes, the two zebrafish *KAL1* orthologues, caused noticeable deficiency in the number of olfactory sensory neurons accurately projecting to the olfactory bulbs, concomitant with disruption in the terminal nerve GnRH cells and presence of fewer presumptive hypothalamic GnRH cells by 36hpf. Moreover, there was a notable failure in formation of one or both of the two forebrain commissures in these morphants. In parallel experiments, knocking down one of the two *FGF8* orthologues, Fgf8a, or specific temporal pharmacological inhibition of FGFR signalling at 14-22hpf, resulted in similar phenotypes by 36hpf. Interestingly, co-injection of Kal1a/Kal1b and Fgf8a morpholinos at concentrations which would give no phenotype individually was able to replicate the commissural mutant phenotype. Combined, these data strongly suggest that Kal1a/Kal1b may act via the Fgf8a pathway *in vivo*.

Acknowledgements

I would firstly like to thank my two supervisors, Prof. Pierre Bouloux and Prof. Ivor Mason, for their continued help, support, and guidance throughout my PhD. I am so grateful to them both for giving me the opportunity to carry out my PhD studies in their labs.

I'm also greatly indebted to Soo-Hyun Kim, Laxmi Iyengar, Youli Hu, and Suba Poopalasundaram, for all their helpful discussions and advice; as well as their endless encouragement and moral support.

I'd also like to thank Panna, Rajit, Naila, James M, Annabelle, Sheona, and Suresh, as well as many others from the MRC Centre for Developmental Neurobiology (King's College London) and Royal Free Medical School who have helped to ensure that my experiences over the past few years have been so enjoyable and memorable.

I am also very grateful to Gregory Philp for helping to initiate this project at King's College, and for teaching me some of the techniques, including zebrafish embryo micro-injection.

I'd also like to acknowledge Sharon, David, and Swapna for helping to ensure that my zebrafish were healthy and always happy to spare me some of their eggs!

Finally, I'd like to thank my parents for their patience and endless love and support; this PhD thesis is dedicated to them both.

"Nothing is more memorable than a smell. One scent can be unexpected, momentary and fleeting, yet conjure up a childhood summer beside a lake in the mountains."

Diane Ackerman

Table of Contents

Figure list

Page:

Table list

Abbreviations

AC: anterior commissure

CNS: central nervous system

coMO: Control MO

DAB: (3,3′-Diaminobenzidine)

dnFGFR: dominant negative FGFR

ECM: extracellular matrix

FGFR1: fibroblast growth factor receptor 1

FGF8: fibroblast growth factor 8

FSH: follicle-stimulating hormone

G3MC: pGnRH3:mCherry

GFP: green fluorescent protein

GnRH: gonadotrophin releasing hormone

HH: hypogonadotrophic hypogonadism

Hpf: hours post fertilisation

HPG: hypothalamic-pituitary-gonadal axis

HS: heparan sulphate

HSPG: HS proteoglycan

KS: Kallmann syndrome

KWT: King's wild-type

LH: luteinising hormone

MAPK: classic mitogen-activated protein kinase (Erk1/2)

MHB: mid-hindbrain

MO: morpholino

MYA: million years ago

OB: olfactory bulb

OE: olfactory epithelium

OECs: olfactory ensheathing cells

OMPG: pOMP:TauEGFP transgene

OP: olfactory placode

OR: odorant receptor

ORNs: olfactory receptor neurons

PCR: polymerase chain reaction

pERK: phosporylated Erk1/Erk2

PI3K: phosphoinositide 3-kinase

PLLP: posterior lateral line primordium

POC: post-optic commissure

PK: Proteinase K

PTU: phenylthiourea

RT: room temperature

sbMO: splice-blocking MO

SPR: surface plasmon resonance

tbMO: translation-blocking MO

VNN: vomeronasal nerve

VNO: vomeronasal organ

VRNs: vomeronasal receptor neurons

X-KS: X-linked KS

Chapter 1
Introduction

1.1 Kallmann Syndrome

Kallmann syndrome (KS) is a developmental genetic disorder that affects about 1 in 8,000 males and 1 in 40,000 females (Hu et al., 2003). The defining clinical features of KS are hypogonadotrophic hypogonadism (HH; failure of pubertal development) combined with an absent or deficient sense of smell (anosmia/ hyposmia).

KS is named after Franz Josef Kallmann (Kallmann et al., 1944), who, in 1944, demonstrated the genetic transmission of HH with anosmia in three different families; but it is Aureliano Maestre de San Juan (Maestre de San Juan, 1856) who was first to publish a report on KS back in 1856: an autopsy finding of a hypogonadal man with small testes and absent olfactory bulbs.

In KS, anosmia and HH result from olfactory bulb dysgenesis and hypothalamic gonadotrophin releasing hormone (GnRH) deficiency, respectively. These combined defects are proposed to result from disrupted migration and targeting of olfactory sensory axons and hypothalamic GnRH neurons during early embryogenesis (MacColl et al., 2002).

KS patients can be brought through puberty, with gonadotrophin or GnRH therapy, and may subsequently gain normal fertility; but, there is no treatment for the reversal of anosmia (Cadman et al., 2007). Moreover, the HH may occasionally be reversible (Pitteloud et al., 2005; *see below*).

1.2 Human reproductive axis

In humans, pulsatile release of hypothalamic GnRH is essential for the correct functioning of the hypothalamic-pituitary-gonadal (HPG) axis. At the hypothalamus, GnRH is secreted into the hypophyseal portal circulation of the median eminence, where it activates the GnRH receptor (GnRHR1), expressed by the anterior pituitary gonadotrophs, thereby stimulating expression, synthesis and secretion of the two pituitary gonadotrophins: luteinising hormone (LH) and follicle-stimulating hormone (FSH) into the systemic bloodstream. LH and FSH then stimulate steroid production and gametogenesis in both sexes. *Refer to Figure 1.01 for an illustration of the HPG axis and further discussion on its role in the acquisition of secondary sexual characteristics at the time of puberty and the maintenance of reproductive competence thereafter.*

Production of gonadotrophins and resulting reproductive competence are therefore dependent on correct development and coordinate functioning of hypothalamic GnRH-secreting cells and pituitary gonadotrophs. HH is a disorder of the reproductive axis presenting as complete or partial failure of secondary sexual development at the time of puberty. In the clinic, HH is most typically characterised by abnormally low levels of the gonadotrophins in the systemic bloodstream, in the presence of low or undetetctable circulating sex steroid concentrations (Achermann et al., 2001; Silveira et al., 2002).

The onset of puberty

Postnatally, in the male, GnRH secretion is temporarily activated (for 3-6 months), but then remains quiescent until the onset of puberty, when the HPG axis is reawakened and secondary sexual maturation begins (Cadman et al., 2007). In recent years it has been demonstrated that it is the kisspeptin-GPR54 signalling pathway that plays a significant role in determining the actual time that GnRH secretion is re-activated at the time of pubertal onset.

Figure 1.01 The hypothalamic-pituitary-gonadal (HPG) axis

INSET: *Summary of the HPG axis: GnRH, secreted by the hypothalamus acts on the anterior pituitary, causing it to release LH and FSH into the systemic bloodstream, which act on the gonads. Direction of hormone release is indicated by green arrows.*

The structure of the hypothalamic-pituitary region is depicted towards the top right of the figure and the downstream effects on the gonads are depicted towards the bottom left. The GnRH neurons (in green) secrete GnRH at the median eminence into the hypophyseal network of capillaries which leads into the anterior pituitary. Here the GnRH binds to its receptor on the gonadotrophs, which stimulates these cells to secrete FSH and LH which pass into the efferent veins and enter the systemic bloodstream. LH and FSH act on the gonads (orange ovals) to bring about secondary sexual maturation at the time of puberty and maintain subsequent reproductive competency. Specifically, LH acts on the testes in men to induce testosterone production, which helps to bring about the male secondary sexual characteristics at puberty (e.g. deepening of voice, body/facial hair growth etc) and acts with FSH to bring about spermatogenesis. In women, LH and FSH act on the ovaries to induce oestrogen production which helps to bring about the female secondary sexual characteristics (e.g. widening of hips and breast development) and ovulation.
GnRH= gonadotrophin-releasing hormone; LH= luteinising hormone; FSH= follicle-stimulating hormone.

Figure 1.01 (overleaf) was assembled using two figures from the PhD thesis of Alexis Robertson (Robertson, 2000)

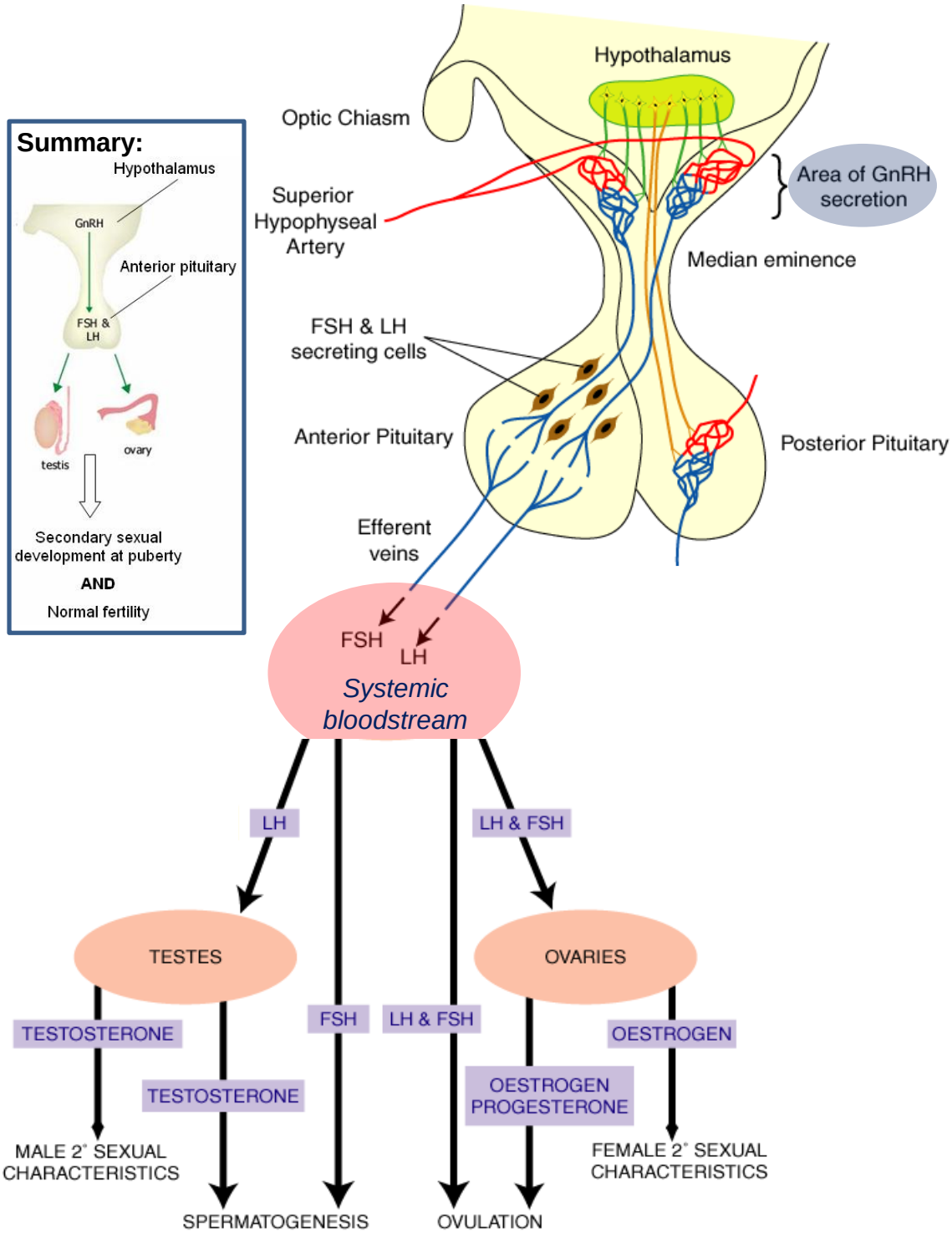

Figure 1.01 The hypothalamic-pituitary-gonadal (HPG) axis

Kisspeptin, a 54-amino acid peptide derived from the *KiSS1* gene product, is the natural ligand for GPR54, a previously 'orphan' G-protein-coupled receptor. Shorter C-terminal derivatives of human kisspeptin, designated kisspeptin-14, -13, and -10, have similar high-affinity binding to GPR54 (Kotani et al., 2001).

Intracerebroventricular kisspeptin-10 administration induces dramatic release of GnRH in sheep (Messager et al., 2005), and intracerebroventricular kisspeptin-10 administered to primates results in an immediate gonadotrophin surge (Plant et al., 2006). *Gpr54* knockout mice (Seminara et al., 2003) fail to secrete FSH and LH in response to exogenous murine kisspeptin-15, despite having anatomically normal hypothalamic GnRH neurons, indicating that their hypogonadism results from abnormalities of GnRH neuronal secretion, and not defective GnRH neuronal migration (Messager et al., 2005).

Intravenous kisspeptin injection has also been shown to stimulate LH, FSH, and testosterone secretion in human male volunteers (Dhillo et al., 2005). However, when infused continuously into male juvenile rhesus monkeys, human kisspeptin-10 appeared to desensitise/downregulate Gpr54-induced GnRH release, as monitored indirectly by gonadotrophin release (Seminara et al., 2006). Kisspeptin-induced GPR54 signalling, in concert with other signalling pathways (e.g. leptin), is thus thought to be a major regulatory control point for GnRH release, and is likely to have a determining role in pubertal onset (Dhillo et al., 2005).

These findings have significant potential therapeutic implications for a range of human reproductive conditions: for example, modulating GnRH secretion by pharmacological manipulation of the GPR54 system may provide a new avenue for altering reproductive competency in adults, in terms of fertility and contraception. *See Chapter 3 for further discussion.*

1.3 Human olfactory & vomeronasal systems

Odorant detection

The odours in the air which we perceive when we smell are detected by olfactory receptor neurons (ORNs), which occupy a small area in the upper part of the nasal epithelium, at the back of the nose (*see Figure 1.02*). Specifically, when odorant molecules (such as the scent of a flower) pass through our nose, they bind to their specific odorant receptor located on the cilia which project from the ORN into the nasal cavity. Once activated, these ORNs relay their signal (via their axons which traverse the cribriform plate of the ethmoid bone) to specific glomeruli in the olfactory bulbs. Within the glomerulus, the ORN nerve endings excite mitral cells within the olfactory bulb which forward the signal to higher regions of the brain, such as the olfactory cortex, where the olfactory information is then processed (Rinaldi, 2007).

Every ORN expresses only one odorant receptor (OR). ORNs of the same type (expressing the same OR) are randomly distributed in the nasal epithelium, but converge on the same set of glomeruli within the olfactory bulb. The mouse has approximately 1200 ORs, whilst humans make do with less than 400. Each odorant is detected by a specific combination of ORs, and our brain then translates the 'receptor code' for that odorant into a distinct smell, thus accounting for the ability of humans to detect a wide variety of exogenous olfactory ligands. Olfactory receptors, in fact, account for the greatest number of G-protein-coupled receptor genes within the human genome (Rinaldi, 2007).

Olfactory system development and regeneration

During the formation of the olfactory system, in early embryogenesis, olfactory axons traverse tiny pores in the cribriform plate and extend towards the olfactory bulb anlage, where they form synapses with dendrites of mitral cells within the glomerular layer. Mitral cell axons then extend to form the lateral olfactory tract which relays olfactory information to the piriform cortex (Rinaldi, 2007).

Figure 1.02 Organisation of the human olfactory system

Odorant receptors are localised along the membrane of olfactory receptor neurons (ORNs), which are located in a small area of the upper part of the olfactory epithelium at the back of the nose. Each ORN expresses just one specific type of odorant receptor, as represented by three different colours (red, blue and green). Odorant molecules in the air bind to their specific receptor, and, once activated, these ORNs then relay this signal to their specific glomeruli within the olfactory bulb. ORNs of the same type are randomly distributed in the olfactory epithelium, but their processes converge at the same glomerulus within the olfactory bulbs. At each glomerulus, the ORN axons excite mitral cells within the olfactory bulb which forward the odorant signal to higher regions of the brain, including the olfactory cortex, where the olfactory signals are interpreted.

Figure 1.02 (overleaf) reprinted by permission from Macmillan Publishers Ltd: EMBO Rep. 8, 629-633, Copyright 2007. Credit for original figure: Karolinska Institutet and Nobel Foundation, Stockholm, Sweden.

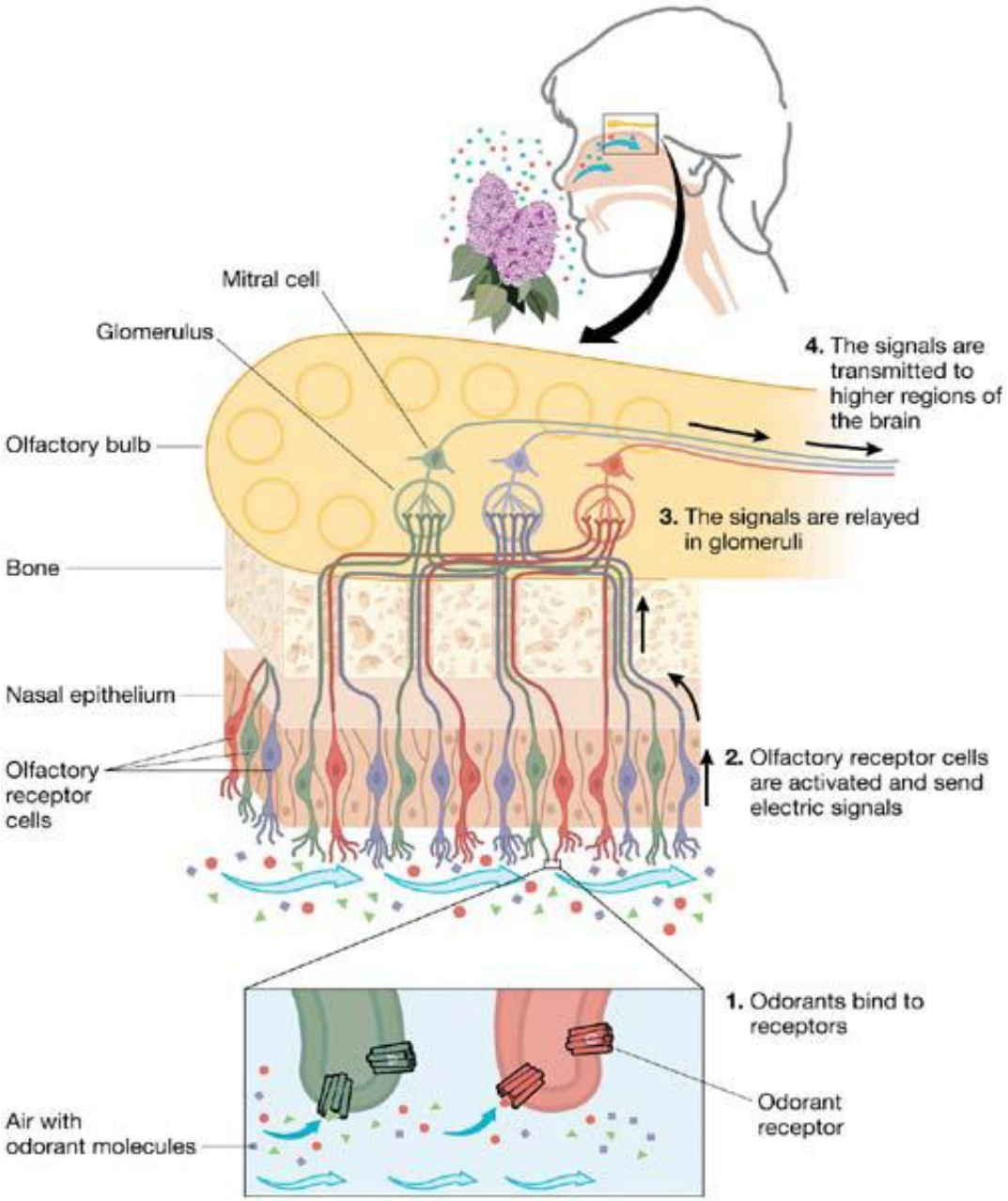

Figure 1.02 Organisation of the human olfactory system

An interesting, and important, facet of the ORNs is their ability to regenerate throughout adult life due to a neurogenetic process which continually provides new primary sensory neurons at the olfactory epithelium (Graziadei and Graziadei, 1979a; Graziadei and Graziadei, 1979b). Since the ORNs have an average lifespan of 6-8 weeks, in part due to inhalation of smoke and other air toxicants, it is essential that they are replaced regularly. New ORNs, which arise from the base of the olfactory epithelium, must project to one of the olfactory bulbs and re-establish functional synapses. Olfactory ensheathing cells (OECs) are a type of glial cell which helps to support and maintain extension of the ORN axons from within the olfactory epithelium to their targets in the olfactory bulbs. Due to their rare ability of being able to traverse both the peripheral and central nervous systems, OECs are being investigated for their potential usage during spinal cord repair (Ruitenberg et al., 2006; Raisman et al., 2010). Moreover, proteins, such as anosmin-1, which are thought to have a role in olfactory axonogenesis during development, may provide new avenues of research in the field of neural repair.

Pheromone detection

The vomeronasal organ (VNO) is located at the base of the nasal cavity in most mammals, where it has a role in pheromone detection. The vomeronasal receptor neurons (VRNs), analogous to the ORNs, project to the accessory olfactory bulb. VRNs express their own array of distinct receptors, including, for example, the ion channel TRPC2, a member of the superfamily of transient receptor potential channels. TRPC2 is expressed on the microvilli of VRNs, where it plays an important role in the signal transduction of most, but not all, VRNs. Interestingly, TRPC2 has been completely lost from the human genome. However, TRPC2-knockout mice have severe behavioural abnormalities, including a strong reduction in electrophysiological responses of the VRNs to urine and uncharacteristic indiscriminate courtship behaviour of male mice with females (Tirindelli et al., 2009).

Destruction of the main olfactory epithelium does not impair male hamster mating behaviour; however, specifically severing the VRN projections produced

severe sexual behavioural deficits in one-third of treated animals, whereas combined deafferentation of both vomeronasal and olfactory systems completely abolishes copulation in treated animals. The apparent importance of the vomeronasal system in these rodents makes it all the more surprising that humans seem to completely lack a clearly distinguishable VNO. However, it has been proposed that humans can instead detect pheromones via their main olfactory epithelium (Tirindelli et al., 2009). Moreover, there is evidence that the VNO does form during human embryogenesis, but then later regresses, as is the case with some other mammals including apes and bats (Smith et al., 2001).

Pheromone receptors in the mammalian VNO are encoded by V1R and V2R gene superfamilies. All human V2R sequences so far identified have been shown to be pseudogenes; whilst only four of the approximately 200 V1R genes have demonstrably intact open reading frames in most human individual. This massive V1R pseudogenization observed in the human genome is believed to have begun shortly before the separation of the hominoids (i.e. humans and apes) from the Old World monkeys, most likely due to the reduced importance of vomeronasal pheromone communications. Therefore, it is unlikely that the putative remnant of the human vomeronasal system has any major role in modulating human reproductive activity, as it is believed to in the rodent species discussed above (Grus et al., 2005).

1.4 An olfactory origin for GnRH neurons

The migratory route of GnRH neurons from the nasal compartment to the hypothalamus was originally characterised using immunohistochemical comparisons at certain developmental stages from various model organisms (including the rat, mouse, chick, and, rarely, human embryos), assisted by DiI labelling and olfactory ablations. However, these characterisations have sometimes been complicated because several species have more than one GnRH gene (humans have two: GnRH1 and GnRH2), as well as two or more different GnRH-expressing

cell populations in the brain, some of which will probably not contribute directly to the regulation of pituitary gonadotrophin secretion (Tobet and Schwarting, 2006).

Furthermore, immortalised GnRH cell lines, explants, and mouse head slices, and more recently, transgenic approaches, have also helped in our understanding of GnRH neuronal migration (Tobet and Schwarting, 2006). Mice and rats in which living GnRH neurons can be traced by GnRH1 promoter-driven green fluorescent protein (GFP) expression have allowed us to observe GnRH cell migration in *real* time (Kim et al., 2002). This transgenic technology has also been used more recently in two fish models: zebrafish and medaka (Palevitch et al., 2007; Okubo et al., 2006), which have the added advantage of producing transparent embryos that develop *ex utero*, permitting all developmental stages to be visualised more easily in living embryos.

In most vertebrates, olfactory and GnRH neurons both originate from the nasal compartment, although the exact area of origin within the nasal compartment may vary in different species, including, most notably, the zebrafish (*see chapter 3*). The olfactory axons extend and establish contact with the olfactory bulb anlage on the telencephalon, a prerequisite for olfactory bulb morphogenesis (Graziadei and Monti Graziadei, 1986; Wray et al., 1989) and the GnRH neurons migrate into the hypothalamus (Schwanzel-Fukuda and Pfaff, 1989). These migratory steps are strictly regulated by specific spatiotemporal expression of certain axonal guidance cues, cell adhesion molecules and extracellular matrix (ECM) proteins, as well as specific transcription and growth factors and neurotransmitters that determine GnRH neuronal fate (Gonzalez-Martinez et al., 2004a). Specifically, the GnRH neurons are believed to migrate along a nasal mesenchymal scaffold of olfactory, vomeronasal and terminal nerves, expressing neural cell adhesion molecule (NCAM) along their central processes, prior to dispersing in the mediobasal part of the anterior hypothalamus, where they undergo terminal differentiation and GnRH secretion (Schwanzel-Fukuda et al., 1992).

GnRH neuronal migration in the mouse forebrain

In the mouse, the hypothalamic GnRH cells originate anteriorly at the nasal compartment area, in and/or around the vomeronasal organ. During embryogenesis, these GnRH neurons appear to associate with the vomeronasal nerve (VNN) whilst it traverses the nasal septum- through the cribriform plate of the ethmoid bone towards the telencephalon. When it reaches its telencephalic target, the VNN then defasciculates, leaving the GnRH neurons to follow only a subset of VNN axons that take a more caudal and ventral route into the forebrain. Towards the terminal part of this migration, the GnRH cells separate from their guiding VNN axons and disperse at their final positions within the hypothalamus (Cariboni et al., 2007; Tobet and Schwarting, 2006). See Figure 1.03 for a schematic representation of this migratory process.

This migratory route can be separated into at least three regions: (1) within the nasal compartment; (2) traversing the cribriform plate; and (3) within the forebrain (Cariboni et al., 2007). Each domain is equally important for the correct migration of the GnRH cells, and different guidance cues and signalling molecules may be present within each of these three individual domains. Deciphering molecular constituents of each domain, and the molecular changes which occur in the GnRH cells along their route, in response to these external cues, will be fundamental for understanding the complexities of GnRH neuron migration (*see chapter 6 for further discussion*).

Evidence from an aborted X-KS embryo

In 1989, Schwanzel-Fukuda et al. (Schwanzel-Fukuda et al., 1989) described a human foetus with X-linked KS (X-KS) whose GnRH neurons terminated in a tangle beneath the forebrain on the dorsal surface of the cribriform plate; suggesting that the HH in KS might result from a GnRH neuronal migratory defect. Since the initial differentiation and migration of olfactory and GnRH neurons appeared normal, it was proposed that the developmental defects seen in XKS patients result from abnormalities in subsequent axonal elongation, pathfinding, and/or terminal

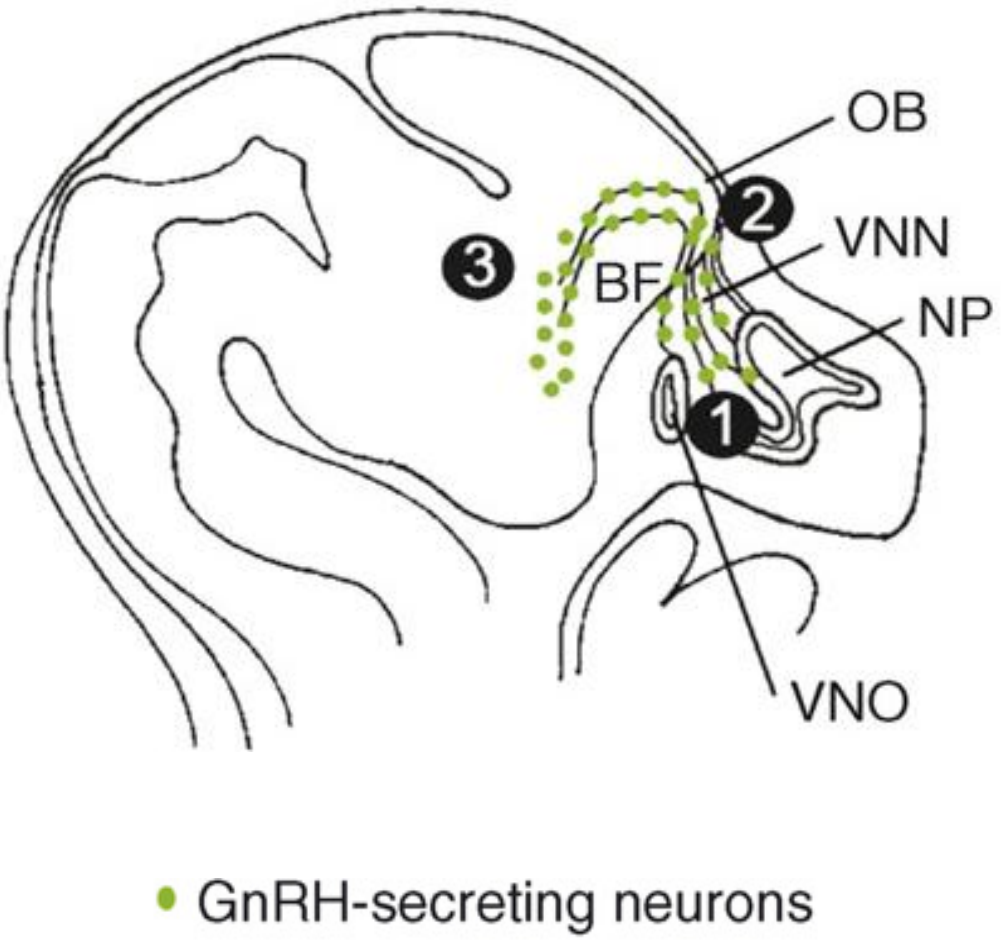

Figure 1.03 GnRH neuronal migration in the mouse forebrain

Schematic diagram of the migratory route of GnRH neurons (green dots) from their nasal placodal (NP) origin, close to the vomeronasal organ (VNO). From here, the GnRH neurons can be visualised traversing along olfactory/vomeronasal nerves (VNN) into the forebrain, in the proximity of the olfactory bulbs (OB). Their migration then continues on into the basal forebrain (BF), towards the hypothalamus, where they will finally reside. During this migratory journey, the GnRH neurons traverse 3 distinct regions: (1) the nasal compartment; (2) the nasal-forebrain junction; and (3) the basal forebrain. The precise levels of specific guidance and signal molecules within these 3 regions determines the correct targeting of the GnRH neurons along this migratory route.

Figure 1.03 reprinted from Trends Neurosci. 30, Cariboni et al., 'From nose to fertility: the long migratory journey of gonadotropin-releasing hormone neurons', pp.638-644, Copyright 2007, with permission from Elsevier.

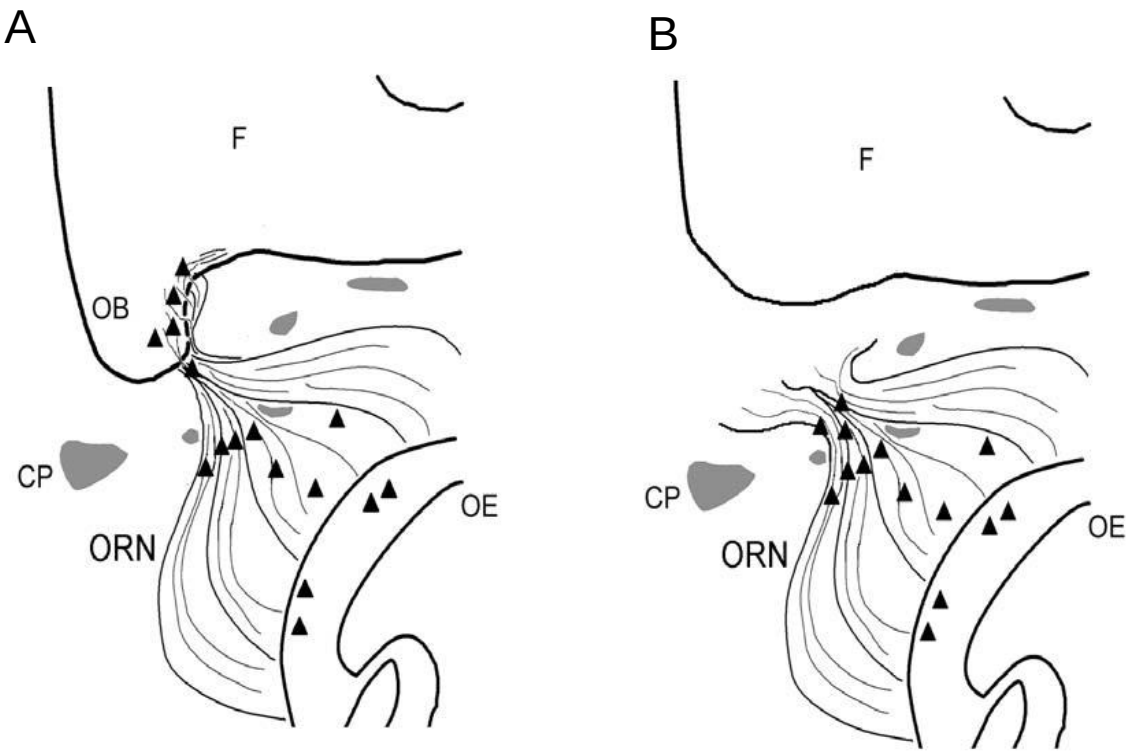

Figure 1.04 Evidence from an aborted embryo with X-linked KS

These diagrams illustrate the disruption to the olfactory and GnRH neuronal pathways in an aborted 19-week human foetus with X-linked KS, based on immunohistochemical analysis carried out by Schwanzel-Fukuda et al., in 1989. **A**: depicts normal co-development of the olfactory receptor neuronal (ORN) pathway and GnRH neuronal (▲) migration from the olfactory epithelium (OE), through the cribriform plate (CP), and on into the developing forebrain. **B:** depicts a disrupted olfactory pathway in a 19-week aborted foetus with a *KAL1* mutation. The initial trajectory of the ORNs appears normal. However, the ORN axons are abruptly arrested, along with the GnRH neurons beneath the dura at the level of the cribriform plate; and the olfactory bulbs fail to form.

Figure 1.04 is used with permission from the PhD thesis of Youli Hu (Hu, 2005)

differentiation. Briefly: in the absence of olfactory nerve synaptogenesis with the olfactory bulb anlage, GnRH neurons are denied a navigational pathway towards the forebrain, explaining the deficiency of hypothalamic GnRH-secreting neurons in KS, as well as olfactory bulb dysgenesis (*see Figure 1.04*). However, this hypothesis remains to be fully tested and proven *in vivo*.

1.5 The known KS genetic loci

Application of conventional linkage studies in the investigation of the genetic basis of KS (as well as HH disorders in general) has proven difficult because of the rarity and infrequency of familial transmission, and because the pedigrees tend to be small as the majority of patients, without treatment, remain infertile (Cadman et al., 2007). Nonetheless, six KS-associated genes have been identified, accounting for approximately 30-40% of all KS cases (Dode and Hardelin, 2010). These include: ***KAL1*** (OMIM[1]: 308700), *KAL2* (***FGFR1***, OMIM: 147950), *KAL3* (***PKR2***, OMIM: 607123), *KAL4* (***PK2***, OMIM: 607002), *KAL5* (***CHD7***, OMIM: 612370), and *KAL6* (***FGF8***, OMIM: 612702).

KAL1 (anosmin-1)

KAL1, the gene responsible for X-linked KS, and the first KS-causative gene to be identified, in 1991, accounts for ~10% of total KS cases. The phenotype associated with *KAL1* mutations varies significantly, even amongst monozygotic twins sharing the same mutation (Matsuo et al., 2000), emphasising the likely role of modifier genes, epigenetic factors and environmental factors in the penetrance of *KAL1* mutations. Whilst the majority of patients with *KAL1* mutations have HH and some degree of anosmia, other neurological and non-neurological symptoms may co-exist. Specifically, up to 30% of X-linked KS patients have a missing or

[1] OMIM: Online Mendelian Inheritance in Man (http://www.ncbi.nlm.nih.gov/omim)

malformed kidney (renal aplasia), and up to 75% have upper body mirror movements (bimanual synkinesis), suggesting that *KAL1* has a significant role in these other important developmental processes (Kim et al., 2008).

KAL1 is located on Xp22.3 and encodes a ~100kDa extracellular-matrix glycoprotein, anosmin-1. Anosmin-1 is a multi-domain protein consisting of an N-terminal cysteine-rich region (Cys box), followed by a whey acidic protein-like (WAP) four disulphide core motif, four tandem fibronectin type III (FnIII) domains and a C-terminal histidine-rich region (*see Figure 1.05A*). The Cys box contains ten cysteine residues, resembling the cysteine-rich region of the insulin-like growth factor receptor (Hu et al., 2005). The eight cysteines of the WAP domain form four disulphide bonds, highly conserved throughout the serine protease inhibitors of the WAP protein family, which includes elafin, SLPI and PS20 (Hu et al., 2004). Large positively charged basic regions on the FnIII domains, particularly the first, were shown by surface plasmon resonance to be essential for high-affinity dose-dependent binding of anosmin-1 to negatively charged heparan sulphate (HS) (Hu et al., 2004).

Using X-ray scattering and analytical ultracentrifugation, along with constrained homology modelling, it has been shown that the six domains of anosmin-1 are extended with flexible inter-domain linkers (*see Figure 1.05B*), suggesting anosmin-1 may act as a platform for coordinate interaction with HS and its other biomacromolecular ligands (Hu et al., 2005). *Further analysis of the expression and function of anosmin-1, including its interaction with the FGF signalling pathway, is discussed below.*

KAL2 (FGFR1)

In 2003, *loss-of-function* mutations in fibroblast growth factor receptor 1 (*FGFR1*; referred to as *KAL2*) were subsequently shown to account for another ~10% of total KS cases (Dode et al., 2003). By contrast, *gain-of-function* mutations in *FGFR1* had previously been shown to result in another disorder, craniosynostosis (*see Table 1.1 for a summary of the human disorders that are known to be caused by mutations in the FGF receptors*). Amongst patients with *FGFR1* (loss-of-function)

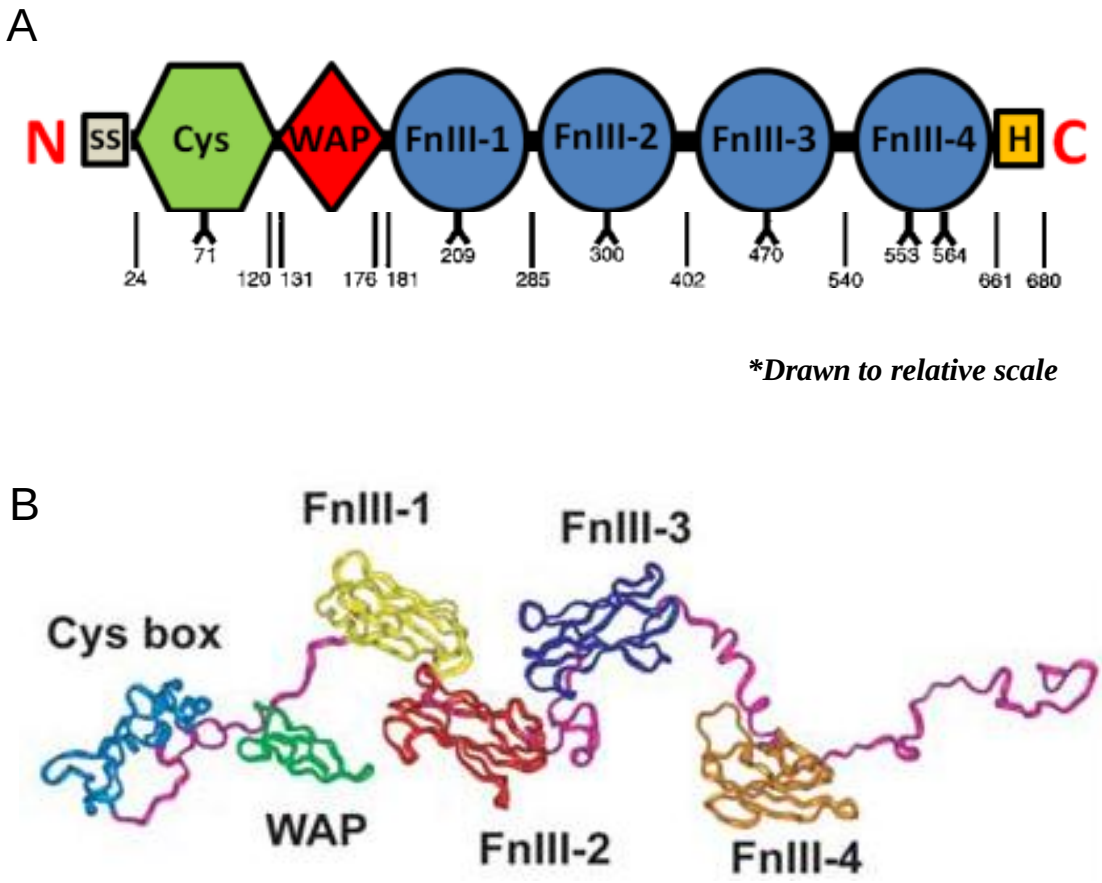

Figure 1.05 The structure of anosmin-1

A: the domain-structure diagram of anosmin-1 comprising an N-terminal secretory sequence (SS), Cysteine box (Cys), whey acidic protein-like motif (WAP), and four fibronectin type III domains (FnIII-1 to -4), and a C-terminal histidine-rich region (H). Lines underneath indicate amino acid positions; 'Y's indicate six putative N-glycosylation sites.

B:Illustrates the X-ray scattering solution structure best-fit model for recombinant anosmin-1 using an unglycosylated α-carbon ribbon trace (RCSB Protein Data Bank accession number 1zlg.). The domains are coloured as follows: Cys-box, blue; WAP, green; FnIII-1, yellow; FnIII-2, red; FnIII-3, dark blue; FnIII-4, orange. The linker peptides in this model are shown in purple.

Figure 1.05(B) reprinted from J. Mol. Biol. 350, Hu et al., 'Extended and flexible domain solution structure of the extracellular matrix protein anosmin-1 by X-ray scattering, analytical ultracentrifugation and constrained modelling', pp553-570, Copyright 2005, with permission from Elsevier.

Table 1.1 Human syndromes with FGFR/FGF mutations

Gene	Disease	Common or characteristic mutations
FGFR1	Kallmann syndrome*	Widespread (haploinsufficiency)
	Pfeiffer syndrome	P252R
	Osteoglophonic dysplasia	N330I, Y374C, C381R
FGFR2	Apert syndrome	S252W, P253R
	Crouzon/Pfeffer/Jackson-Weiss/Antley-Bixler syndromes	D3, TKD**, D1
	Beare Stevenson syndrome	Y375C, S372C
FGFR3	Muenke syndrome	P250R
	Hypochondroplasis Achondroplasia SADDAN*** thanatophoric dysplasia I thanatophoric dysplasia II	N540K G380R K650M R248C, Y373C K650E
	Crouzon syndrome with acanthosis nigricans	A391E
	New syndrome	R621H

* Loss-of-function mutations (all other known disorders are believed to result from gain-of-function FGFR mutations). **TKD= tyrosine kinase domain, *** Severe chondroplasia with developmental delay and acanthosis nigricans.

Adapted from (Wilkie, 2005)

mutations, there is a high level of variability in the degree of HH with or without anosmia (i.e. they may have KS or isolated (normosmic) HH) (Pitteloud et al., 2006). Moreover, as with *KAL1* mutations, penetrance of *KAL2* mutations varies considerably, even within the same kindred. Thus, Pitteloud et al. (Pitteloud et al., 2005) have described 3 subjects from the same family who share an identical tyrosine kinase domain *FGFR1* mutation, but each with a different phenotype. The pedigree comprised a male proband with KS (who later recovered from his HH), whose mother had delayed puberty and whose maternal grandfather had isolated anosmia. Patients with *FGFR1* mutations may also present with cleft palate and dental agenesis, but do not normally present with renal agenesis or bimanual synkinesis, as these symptoms tend to be specific to those with *KAL1* mutations (Kim et al., 2008).

FGFR1 signalling has been known to play a wide-ranging role during embryogenesis, including promoting proliferation, differentiation and survival of neuronal stem cells and progenitor cells. In humans, there are four known members of the FGFR family of receptor tyrosine kinases (FGFR1, FGFR2, FGFR3, and FGFR4), which specifically bind to particular members of the 22 FGF ligands (*see Figure 1.06*), in different cellular contexts. As well as requiring two FGF ligands, heparan sulphate (HS) is also essential for FGF receptor dimerisation and activation (Mohammadi et al., 2005; Eswarakumar et al., 2005).

FGFRs consist of an extracellular region of three immunoglobulin (Ig)-like domains (D1, D2, and D3), a single transmembrane helix, and a cytoplasmic tyrosine kinase domain (*see Figure 1.07*). The D1-D2 linker region contains a stretch of negatively charged amino acids (‘the acid box’), and there is a HS-binding site (HBS) within the first half of D2 (Mohammadi et al., 2005).

Alternative splice variants exist for FGFR1-3. The common 'IIIa exon' (exon 7) that encodes the first half of D3 can be spliced to either exon 8A or 8B, resulting in 'FGFR1 IIIb' and 'FGFR1 IIIc' isoforms. When neither 8A nor 8B is used, the result is a soluble 'FGFR1 IIIa' variant, reviewed in (Mohammadi et al., 2005).

A specific mutation (L342S) which affects the IIIc isoform of FGFR1, was shown by surface plasmon resonance (SPR) analysis to reduce the binding affinity

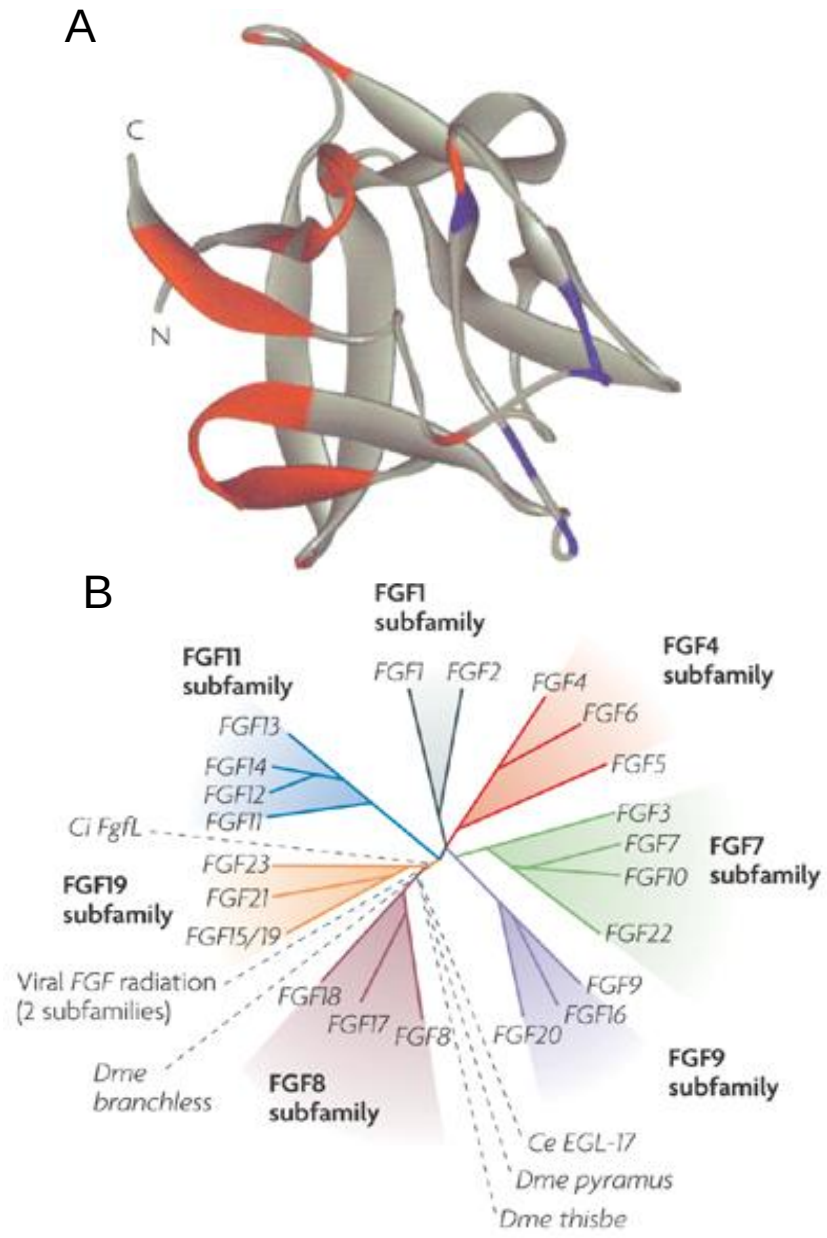

Figure 1.06 FGF ligand structure and phylogeny

A: ribbon model of the FGF protein structure and folding, with contact sites for the FGF receptor marked in red and those for heparan sulphate proteoglycan marked in blue.

B: schematic diagram illustrating the seven mammalian FGF sub-families (FGF1, FGF4, FGF7, FGF9, FGF8, FGF19, and FGF11) . FGF8 belongs to the FGF8 subfamily, along with FGF17 and FGF18. Evolutionary affinities of *Ciona intestinalis* (Ci) FgfL, the viral FGF radiation, *Drosophila melanogaster* (Dme) branchless, pyramus and thisbe, and *Caenorhabditis elegans* (Ce) EGL-17 are superimposed onto this diagram by dashed lines.

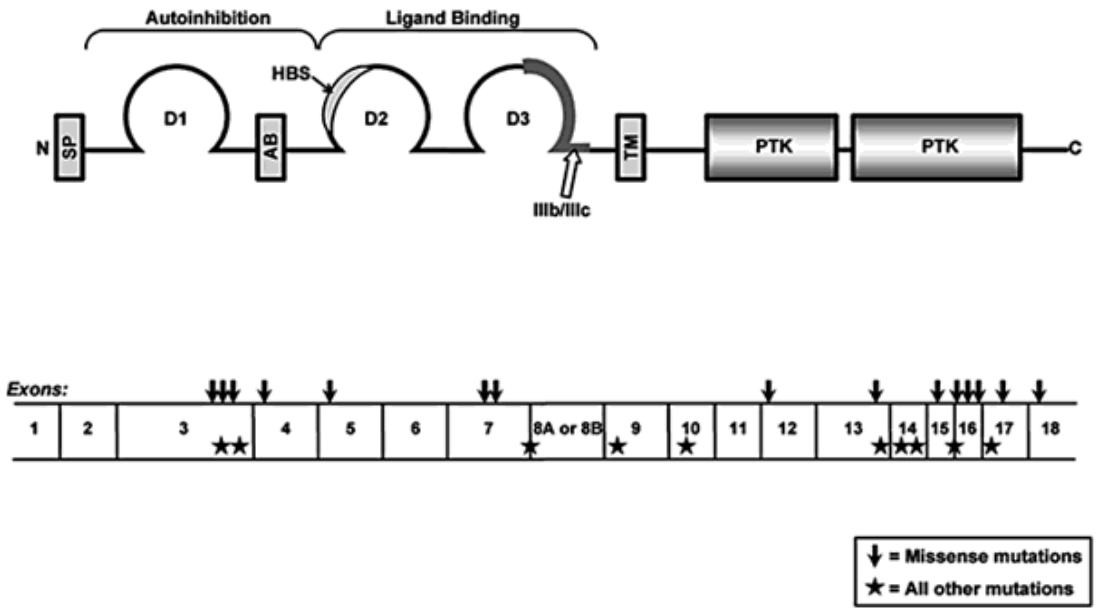

Figure 1.07 Structure of FGFR1 and its KS-associated mutations

Schematic domain-structure diagram of FGFR1. The protein (top) and the corresponding exons (bottom) are shown. The extracellular regions of FGFR1 that have a role in autoinhibition or ligand binding are indicated (see main text for further discussion). SP = Signal peptide; D1, D2, and D3 = the three immunoglobulin-like domains; AB = acid box; HBS = HS binding site; IIIb/IIIc refers to two major splice isoforms; TM = transmembrane helix, and PTK refers to the intracellular protein tyrosine kinase domain. Some characteristic KS-associated (loss-of-function) mutations are shown: missense mutations are indicated by arrows; all other mutations are represented by stars.

Figure 1.07 reprinted by permission from S. Karger AG, Basel: Cadman, S.M. et al: Horm Res 2007;67:231-242.

to FGF8 by 20 fold, compared with only a minor reduction in binding affinity for FGF1 and FGF2 (Pitteloud et al., 2007). Furthermore, mice homozygous for a hypomorphic *Fgf8* allele lacked hypothalamic GnRH neurons, while heterozygous mice had far fewer hypothalamic GnRH neurons. Together, these data suggested that FGF8 could be an important ligand for FGFR1 during GnRH neuronal development, and has since been shown to be a KS-causative gene (Falardeau et al., 2008) (*see below*).

As with other receptor tyrosine kinases, FGFR1 plays a significant role in cell proliferation and differentiation, so its activity is therefore under tight regulation. According to the 'autoinhibition model', in quiescent cells, the acidic box may bind to the positively charged HBS, consequently bringing the D1 domain into a position that will interfere with HS and FGF ligand binding to the D2-D3 regions, resulting in a closed, autoinhibited state. The presence of FGF, which has a higher affinity for the D2-D3 ligand binding sites, is hypothesised to open up the closed configuration, making the HBS accessible to HS (the obligatory cofactor for functional activation of the whole signalling complex). In quiescent cells, 'closed' (autoinhibited) FGFR1 is in equilibrium with the 'open' (*active*) FGFR1 configuration. Therefore, upon binding of HS and FGF, the equilibrium shifts towards the 'open' state and FGFR1 dimerises and becomes fully active. KS patients, whose loss-of-function mutations map to D1 or the acid box, may have a more autoinhibited FGFR1, thus disturbing the equilibrium and resulting in FGFR1 signalling insufficiency (Eswarakumar et al., 2005; Schlessinger, 2003).

Specific FGF ligands, along with precisely modified HS, bind to their target FGFR to form an ‘active’ FGF/FGFR/HS signalling complex. This results in receptor dimerisation, followed by autophosphorylation of the receptor tyrosine residues on the intracellular kinase domain and activation of downstream signalling pathways (*see Figure 1.08*). Then, by recruitment of specific signalling and docking proteins, activated FGF receptors transmit their signal intracellularly, normally via one of three major downstream signalling cascades: classic mitogen-activated protein kinase (MAPK) (Erk1/2), phosphoinositide 3-kinase (PI3K) or via phospholipase C (PLC)γ activation; the last two are capable of activating protein kinase C (PKC) which in turn stimulates Erk1/2 signalling. As an example, in the

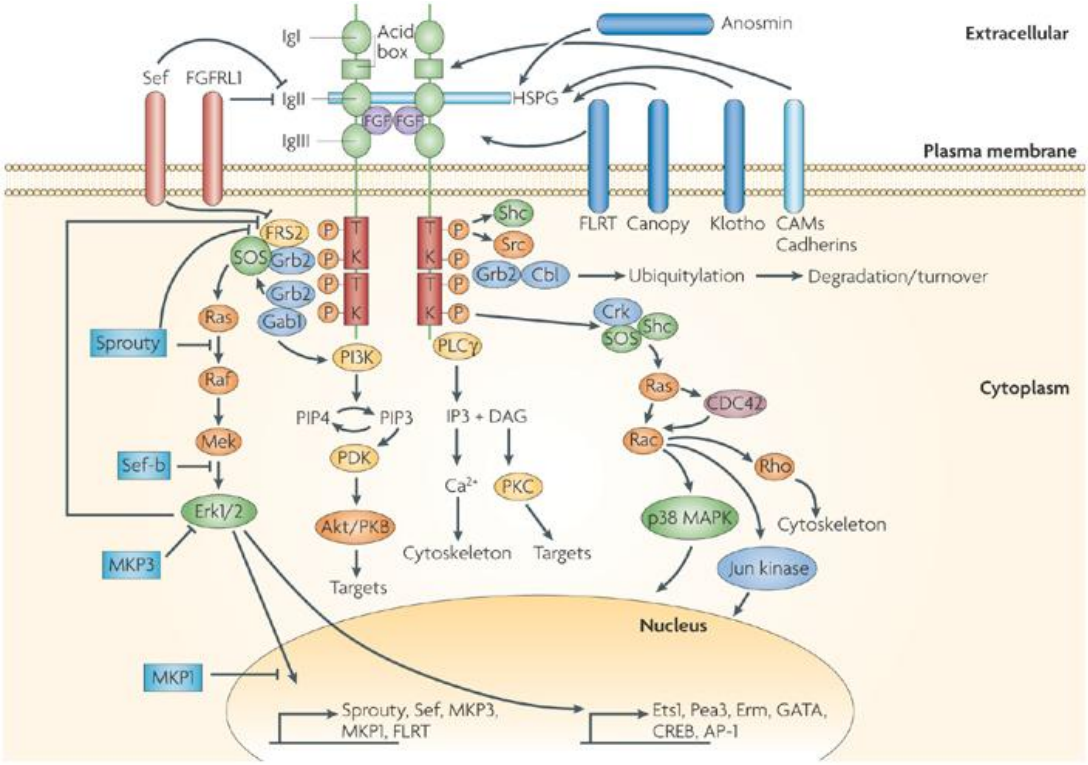

Figure 1.08 FGF receptor downstream signal transduction

Schematic diagram illustrating the downstream signalling events that occur intracellularly after FGF ligand binding and receptor dimerisation. Adaptor proteins such as the FRS2a/SOS/Grb2 complex are recruited to the tyrosine kinase domains of the FGF receptor, initiating Ras activation, leading to Raf, MEK and then ERK1/2 phosphorylation . Activation of Ras by other adapter complexes leads to PI3K and p38/Jun kinase activation. Other downstream cascades that are activated may include PLCγ, calcium signalling and ubiquitinylation via Cbl proteins. Regulatory proteins such as MKP3 (intracellular) and Sef (membrane-localised) are indicated by blue and pink boxes, respectively.

Figure 1.08 reprinted by permission from Macmillan Publishers Ltd: Nat. Rev. Neurosci. 8, 583-596, Copyright 2007.

MAPK cascade, the FGF signal is transduced via RAS downstream of an FRS2-SOS-Grb2 complex, culminating in the phosphorylation of Erk1/2 (also known as p42/44) which enters the nucleus and modulates transcription of specific target genes (*see Chapter 4*). This FGFR signalling is tightly-regulated by a multitude of endogenous agonists and antagonists, including anosmin-1 (*see below*) that may act both up- and downstream of the FGF receptor in order to regulate and maintain the fine-tuning of FGFR activity (Mason, 2007; Kim et al., 2008).

Significantly, it was recently reported that mutations in SEF (Similar Expression as FGF; *see Figure 1.08*), a conserved transmembrane protein which potently inhibits FGF8 signalling, accounts for some cases of KS. Specifically, out of total of 225 KS patients studied, six missense SEF mutations were found, which were absent from 200 healthy controls. Two of the mutations were homozygous (p.P306S and p.P577Q), whilst the remaing four were heterozygous (p.K162R, p.Y379C, pS468L, pA735V). Using an AP1-luciferase reporter assay as readout of FGF signalling, it was found that the K162R, S468L, and A735V mutations decreased FGF signalling; P306S *increased* signalling; and, P577Q and Y379C had no effect. This data, together with its expression in olfactory and hypothalamic regions, suggests that SEF may have an important role in regulating FGF signalling during GnRH and olfactory system development (Feng et al., 2010).

FGF8 (KAL6)

In 2008, six *FGF8* missense mutations were identified in HH patients with varying levels of olfaction. Such *FGF8* mutations account for approximately 5% of total KS cases (Falardeau et al., 2008). Figure 1.09 illustrates the alternative splicing at the N-terminus that gives rise to the four splice isoforms of FGF8 in humans.

Four of the mutations that were identified affected all four FGF8 splice isoforms (Fgf8a, Fgf8b, FGF8e, and FGF8f), whilst the other two affected only the FGF8e and FGF8f isoforms. Two of the *FGF8* mutations identified, P26L and R127G (both heterozygous), occurred in patients with hyposmia or anosmia (i.e.

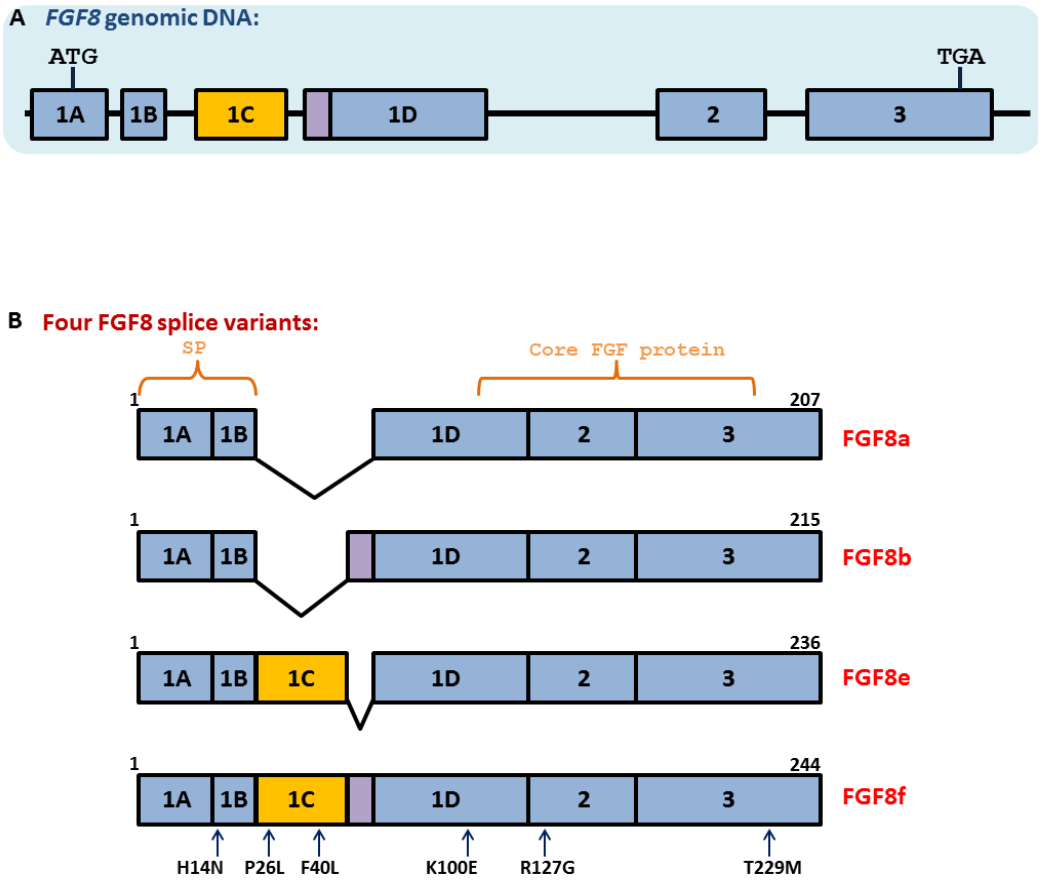

Figure 1.09 Differential splicing of the human *FGF8* gene

A: Genomic structure of *FGF8*. Boxes denote exons; lines denote introns.
B: Schematic diagram of the four FGF8 splice variants identified in humans, which differ by whether or not they include exon 1C and part of exon 1D. Most of the conserved FGF core is encoded by exons 2 and 3. The numbers above the exons indicate amino acid numberings for each splice variant. KS mutations identified by Falardeau *et al* (2008) are indicated by arrows and have been numbered according to the FGF8f isoform.
SP = Signal peptide (for secretion).

typical KS). The R127G mutation is located on exon 2, encoding a common region of the 'core' FGF8 protein. The P26L mutation is located in exon 1C, thus affecting both FGF8e and FGF8f isoforms, suggesting an essential requirement for one or both of these isoforms in GnRH and olfactory neuronal ontogeny. Consistent with the loss-of-function prediction for these *FGF8* mutations, P26L-mutated FGF8f showed reduced signalling activity in an FGFR1c luciferase assay, compared with wild-type FGF8f: the same was true for the four other *FGF8* mutations that were tested in this assay (Falardeau et al., 2008).

More recently, two unique heterozygous ***nonsense*** mutations in *FGF8* (p.R127X and p.R129X) have been reported, resulting in variable degrees of GnRH deficiency and olfactory phenotypes, confirming that it is *loss-of-function* mutations in *FGF8* that cause human GnRH deficiency (normosmic HH or KS) (Trarbach et al., 2010).

NELF

Nelf, the Nasal Embryonic LHRH[2] Factor gene, encodes a guidance molecule required for olfactory axonal outgrowth and hypothalamic GnRH neuronal migration in mice (Kramer and Wray, 2000) and zebrafish (Palevitch et al., 2009). The human orthologue, *NELF*, therefore, for several years, seemed to be a likely candidate as another potential KS-associated locus (Miura et al., 2004). In fact, N.Pitteloud and colleagues have now subsequently proposed a 'digenic model' whereby the synergistic action of a *NELF* mutation in the presence of certain *FGFR1* mutations results in a more severe KS phenotype, whilst patients with either one of these two mutations alone do not present with full KS (Pitteloud et al., 2007).

[2] now called GnRH

PKR2 (KAL3) and *PK2 (KAL4)*

Prokineticin receptors 1 and 2 (PKR1 and PKR2) are G-protein-coupled receptors which are activated by the prokineticins, PK1 and PK2. Mice with Pk2 deficiency have smaller olfactory bulbs with abnormal architecture (Ng et al., 2005). Similarly, *Pkr2* knockout mice exhibit olfactory bulb hypoplasia, which is associated with a disrupted reproductive system including severe atrophy of the testis, ovary, uterus, vagina, and mammary glands, along with decreased plasma levels of testosterone and FSH, and an absence of hypothalamic GnRH neurons (Matsumoto et al., 2006). This suggested that *PK2* and *PKR2* represented two more KS-associated genes.

In a cohort of 192 KS patients, ten mutations were found in *PKR2* and four mutations were found in *PK2*; together these two genes therefore account for around 5-10% of total KS cases. The *PK2* mutations were found in the heterozygous state, whereas, the *PKR2* mutations were found in the heterozygous, homozygous, or compound heterozygous state. Moreover, one of the patients with a heterozygous mutation in *PKR2* also had a mutation in *KAL1*, suggesting a possible digenic inheritance pattern for that patient; however, whether or not there is any cross-talk between these molecules and their signalling pathways requires further investigation (Dode et al., 2006; Monnier et al., 2009).

Both anosmin-1 and PK2 bind to HSPG, the obligatory cofactor for FGF signalling. It can therefore be speculated that anosmin-1 *may* have a role in modulating prokineticin-signalling via PKR2, as well as its previously defined role in the FGF signalling through FGFR1 (Gonzalez-Martinez et al., 2004b; Kim et al., 2008). It is interesting to note that only homozygous mouse mutants for *Pk2*, *Pkr2*, and *Fgfr1* have abnormal olfactory bulbs, whereas heterozygous mutations in their human orthologues are sufficient to cause KS in humans. This may be because anosmin-1 is required at a critical minimum dosage to exert its modulatory role on both the FGFR1 and PKR2 signalling complexes in humans. The hitherto unidentified murine *Kal1*, which thus far hasn't been isolated from the X-chromosome, may have translocated to an autosomal region, as has happened in other amniotes, such as the chicken, where it is found on chromosome 1 (Ensembl

gene: ENSGALG00000016616). This would mean that ansomin-1 is expressed at much higher levels compared with its X-linked human orthologues, resulting in a comparatively higher dosage of anosmin-1 in the mouse, thus protecting it from developmental abnormalities that result from Fgfr1 and Pkr2 signalling insufficiency (Kim et al., 2008).

CHD7 (KAL5)

CHD7 mutations are responsible for some cases of CHARGE syndrome (Vissers et al., 2004), a developmental disorder defined by coloboma, congenital heart disease, choanal atresia, mental and growth retardation, genital hypoplasia, and ear malformations and/or deafness (Hall, 1979; Pagon et al., 1981). Significantly, the defining clinical features of KS, HH with olfactory deficiency, are also present in patients with CHARGE syndrome (Chalouhi et al., 2005). In fact, some cases of KS had previously been reported with additional phenotypes including choanal atresia, mental retardation, and hearing loss (Klein et al., 1987; Coatesworth and Woodhead, 2002), thus demonstrating a degree of overlap between KS and CHARGE syndrome.

The protein encoded by *CHD7*, chromodomain helicase DNA-binding protein-7, is a member of a superfamily of proteins that uniquely comprise two N-terminal chromodomains, an SNF2-like ATPase/helicase domain and a DNA-binding domain (Woodage et al., 1997). It is expressed in many foetal (and adult) tissues, including the developing brain, and is predicted to affect both chromatin structure and gene expression during early embryonic development (Vissers et al., 2004). Kim et al., (2008) carried out mutation-screening of the 37-protein coding exons of *CHD7* and found seven heterozygous mutations, two splice and five missense, in three sporadic KS and four sporadic normosmic HH patients. They estimated that CHD7 mutations occur in approximately 6% of sporadic KS cases. Given the overlap of KS with CHARGE syndrome, it seems plausible that both normosmic HH and KS are mild allelic variants of CHARGE syndrome resulting from certain, less severe, *CHD7* mutations (Kim et al., 2008).

Non-KS loci

The division between normosmic (nHH) and anosmic HH (KS) is becoming more and more arbitrary as we learn more about the complicated genetics of HH, as illustrated by *FGFR1* mutations which can cause both nHH and KS. It is therefore prudent to be aware of the genes underlying cases of nHH, which have thus far not been implicated in KS, but may nevertheless be important modifiers that may affect the penetrance of other KS-causing genes. These include the two most obvious candidates: the GnRH receptor (*GnRHR1*) and, more rarely, the gene encoding its ligand, G*nRH1* (Chan et al., 2009). Other examples include the gonadotrophin β-subunits, and transcription factors that are involved in pituitary gland development (e.g. *LHX3*, *PROP1*, and *HESX1*). *DAX1* mutations cause HH that is associated with adrenal insufficiency (adrenal hypoplasia congenita), and mutations of leptin and its receptor, as well as mutations in prohormone convertase 1, cause HH that is linked with obesity. Moreover, recently, mutations in *TAC3* and *TACR3* have also been shown to cause some cases of nHH (Topaloglu et al., 2009). HH also results from mutations in *GPR54* and in the gene encoding its ligand, *KiSS1;* a signalling pathway that is implicated in the initiation and regulation of pubertal onset (*see above*). With the exception of *GnRH1*, *TAC3* and *TACR3*, which are more recent findings, all of these genes have been reviewed in (Cadman et al., 2007).

Some other gene products which have been shown to have a significant role in the migration of GnRH neurons in various model organisms or *ex vivo* systems, but have yet to be identified as KS or nHH-causing loci include: hepatocyte growth factor (HGF) and its receptor, c-met; the pleiotropic cytokine, Leukemia inhibitory factor (LIF); the transcription factor, EBF2; reelin, an extracellular matrix protein, Reelin; chemokine stromal cell-derived factor-1 (SDF-1) and its receptor CXCR4; the neurotransmitter γ-aminobutyric acid (GABA) and the neuropeptide cholecystokinin (CCK) and CCK-1R receptor; Ephrin A3/A5 and EphA5; Neuropilin-2 (Npn-2), acts as a co-receptor for class 3 semaphorins and some isoforms of vascular endothelial growth factor (VEGF); and the cell surface glycoconjugate lactosamine. These are just some examples of the many factors that affect the migration of the GnRH neurons from the nasal compartment to the hypothalamus.

1.6 The role of anosmin-1 in KS

In vitro and *ex vivo* analyses

During human embryogenesis, anosmin-1 expression is restricted to basement membranes and interstitial matrices of discrete embryonic areas, including the developing olfactory bulb, retina, and kidney (Lutz et al., 1994; Duke et al., 1995); regions which correlate well with the distribution of phenotypic abnormalities seen in X-KS patients.

In vitro, it has been demonstrated that human anosmin-1 stimulates migratory activity in immortalised rodent GnRH-producing neurons (Cariboni et al., 2004). Anosmin-1 also modulates neurite outgrowth in a cell-type specific manner (Soussi-Yanicostas et al., 1998) and stimulates collateral branch formation from rat olfactory bulb output neurons (the mitral and tufted cells) (Soussi-Yanicostas et al., 2002). However, observations from an aborted KS embryo suggested that olfactory defects seen in KS patients are the result of earlier abnormalities in olfactory system development; specifically, elongation and pathfinding of sensory axons towards, and connection with, the olfactory bulb anlage in the developing forebrain (Schwanzel-Fukuda et al., 1989). However, observations made from this isolated study may not be representative of all KS cases. Nontheless, according to this model, anosmin-1 expressed in the presumptive olfactory bulb area is hypothesised to attract olfactory sensory axons towards the forebrain during the latter stages of their trajectory. In the absence of olfactory nerve synaptogenesis with the olfactory bulb anlage, GnRH neurons are denied a navigational pathway towards the forebrain, explaining the deficiency of hypothalamic GnRH-secreting neurons in KS (Soussi-Yanicostas et al., 2002).

Anosmin-1 has also been shown to significantly enhance the amidolytic activity of urokinase-type plasminogen activator (uPA) *in vitro*. This is hypothesized to enhance the uPA-induced activation of the plasmin cascade at the cell surface and consequently result in proteolytic degradation of ECM components that subsequently release cell-cell and cell-ECM interactions that facilitate cell migration. Also, the anosmin-1-HS-uPA interaction was shown to induce cell

proliferation in the PC-3 prostate carcinoma cell line, in an FGFR1-independent manner (as these cells lack this receptor) (Hu et al., 2004). Furthermore, FGF2 induces uPA expression in mouse brain capillary endothelial cells, which suggests that there could also be a functional relationship between uPA and FGF signalling *in vivo* (Mochizuki et al., 2002). Alternatively, anosmin-1 may be a multifunction protein with FGFR1-independent activities (Hu et al., 2004).

In vivo studies

KAL1 orthologues are present throughout animals as diverse as chicken, zebrafish, fruitfly, and nematode worm, providing a wide choice of invertebrate and vertebrate model organisms for studying X-KS (i.e. anosmin-1 *in vivo* function). A phylogenetic analysis of the various *KAL1* orthologues present across 50 different species is illustrated in Figure 1.10.

Invertebrate X-KS model (fruitfly & nematode worm)

During development, the ability of anosmin-1 to confer GnRH neurons with cell-specific chemotactic responsivity, as well as branch-promoting and guidance functions in olfactory neurons, is dependent on heparan sulphate proteoglycan (HSPG) interactions. In fact, HSPGs are a critical component of the ECM, playing a vital role in neuronal navigation during CNS development (Van et al., 2006).

HSPGs are cell-surface or secreted proteins containing the glycosaminoglycan HS. During HS chain biosynthesis, alternating glucuronic acid (GlcA) and N-acetylglucosamine (GlcNAc) subunits are extended from the core tetrasaccharide attached to a serine residue on the protein. Some of the GlcNAc residues are then modified by N-deacetylation/N-sulphation to form N-sulphated glucosamine (GlcNS) regions (NS domains) which are interspersed within the unmodified GlcNAc regions (NA domains). The polymer is then further modified by epimerisation of GlcA to iduronic acid (IdoA) and by three types of sulphation; the 2-O-sulphation of IdoA (or more rarely GlcA) to form IdoA(2S) or GlcA(2S); the 6-O-sulphation of GlcNS residues to form GlcNS(6S); and the 3-O-sulphation of

Figure 1.10 Phylogenetic tree of the *KAL1* gene

An Ensembl gene tree was generated using the Gene Orthology/Paralogy prediction method pipeline at http://www.ensembl.org. This phylogenetic tree represents the evolutionary history of the *KAL1* gene family from a common ancestor around 580 million years ago (MYA). The position of the common primate/rodent ancestor at approximately 107 MYA is indicated on the tree by a purple arrow. The *KAL1* orthologues for several important organisms are indicated by red arrows along with their common names. These include:

Human *KAL1*: ENSG00000011201;

Zebrafish *Kal1a*: ENSDARG00000012896;

Zebrafish *Kal1b*: ENSDARG00000004932;

Squirrel *Kal1*: ENSSTOG00000000380;

Guinea Pig *Kal1*: ENSCPOG00000013143

Chick *Kal1*: ENSGALG00000016616

Fruitfly *Kal1*: FBgn0039155

Nematode worm *Kal1*: WBGene00002181

**Ensembl gene numbers are stated for each organism, except for fruitfly where the FlyBase gene name is given and the nematode worm where the WormBase gene name is given.*

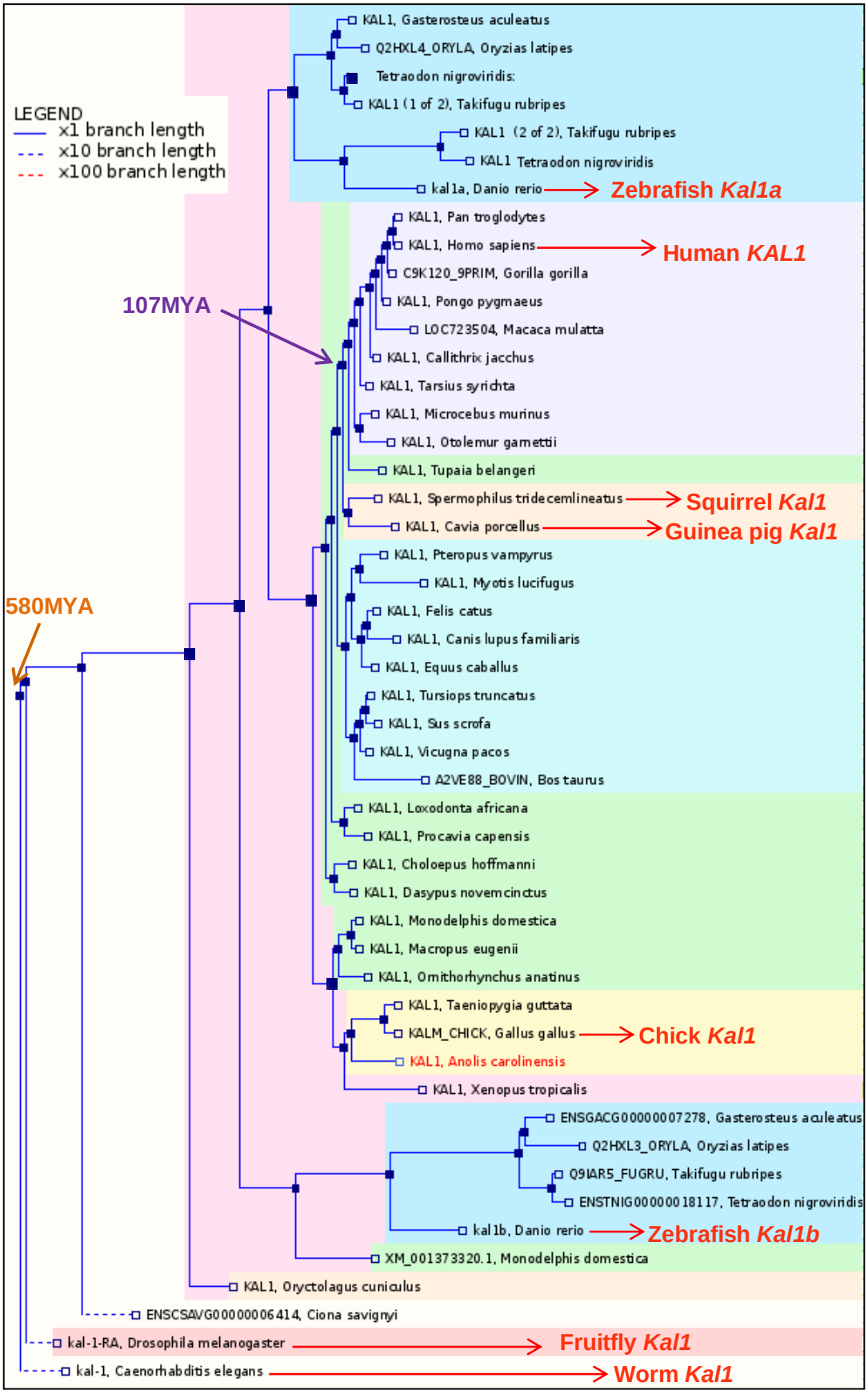

Figure 1.10 Phylogenetic tree of the *KAL1* gene

GlcNS(6S) to form GlcNS(3S,6S). All modification reactions are incomplete *in vivo*, generating many HS chain variants with distinct, highly variable, domains of charge density, thereby altering their molecular binding specificities (Van et al., 2006).

In *C. elegans*, particular HS modifications are required for anosmin-1 activity in certain cell types. 'AIY interneurons' are a subclass of *C. elegans* neurons which receive synaptic input from olfactory neurons. The *C. elegans* orthologue of anosmin-1 (ceKal1) induces a specific axonal branching phenotype in these cells, which was abolished in worms lacking 6-O-sulphotransferase (hst-6) or C5-epimerase (hse-5), but not in those lacking 2-O-sulphotransferase (hst-2). However, hypodermal defects induced by *ceKal1* over-expression were suppressed only in those worms lacking hse-5, but not by those lacking hst-6 or hst-2. It was therefore proposed that anosmin-1 function requires distinct HS modifications in different developmental contexts (Bulow et al., 2002; Bulow and Hobert, 2004). Significantly, specific HS saccharide alterations were also shown to affect binding specificity of ligand-receptor interactions of the fibroblast growth factor receptor 1 (FGFR1) (Guimond and Turnbull, 1999).

In the fruitfly, *Kal1* is expressed during important morphogenetic processes such as germ band retraction, dorsal closure and head involution and has a complex and dynamic pattern of expression in the second half of embryogenesis. Also, *Kal1* is notably expressed in cells of the antennal organ, which has olfactory function in the fruitfly (Andrenacci et al., 2004), demonstrating that the role of anosmin-1 in olfactory system development is highly conserved across the vertebrates and invertebrates

However, neither of these invertebrate models can satisfactorily recapitulate human olfactory/GnRH neuronal development (and KS-associated defects therein) in the same way as a vertebrate model organisms, which have homologous olfactory/GnRH systems. Moreover, when the evolutionary gap is so wide between two organisms, the signalling pathways have sometimes diverged significantly. For example, the *C. elegans* has only one FGFR orthologue, EGL-15. However, unlike vertebrates, *C. elegans* FGF receptor signalling can occur independently of the

multi-substrate adapter FRS2 during processes such as sex myoblast migration guidance and fluid homeostasis (Lo et al., 2010). This notable divergence in FGFR signalling mechanism suggests that *C. elegans* may not be an appropriate model for studying FGF signalling mechanisms which occur in vertebrates.

Vertebrate X-KS model (rodents, chicken, fish)

Whilst anosmin-1 is highly conserved (especially the WAP and first FNIII domain) across many species, a mouse/rat homologue has remained elusive, frustrating attempts to develop a rodent X-KS model, although one group has shown that anti-human anosmin-1 antibodies cross-react with a 100-kDa protein in cerebellum and olfactory bulb extracts from both the rat and mouse, indicating that a mouse/rat anosmin-1 orthologue may exist (Soussi-Yanicostas et al., 2002). However, growing evidence casts doubt on this, and the consensus at the moment is that a rodent *KAL1* orthologue probably does not exist. Firstly, the availability of the virtually complete mouse and rat genome sequences in recent years has proven that they do not have a homologous sequence for *KAL1*, despite conservation of homology between human and nematode worm *KAL1* sequences across a much greater evolutionary distance. Furthermore, the putative *KAL1* locus is pseudoautosomal in rodents and synteny abruptly terminates just before the expected location of the *KAL1* gene. In fact, steroid sulphatase (STS), the gene most adjacent to *KAL1* on the human X chromosome is present in the syntenic region in the rodent, but there is no *KAL1* orthologue beside it (Kim et al., 2008).

In fact, *KAL1* orthologues do exist in two other rodents (*see Figure 1.10*): the guinea pig (*Cavia porcellus*; Ensembl gene ID: ENSCPOG00000013143) and the squirrel (*Spermophilus tridecemlineatus*; Ensembl gene ID: ENSSTOG00000000380) (Bribian et al., 2008), but these two rodent animals are less amenable to developmental studies. This has meant that several groups have turned to fish models (zebrafish and medaka, *see below*) or the nematode worm (*C. elegans*) to model X-KS *in vivo*.

Chicken anosmin-1

An extensive spatio-temporal expression analysis of anosmin-1 in the chicken (*Gallus gallus*) has been reported in the literature (*see below*); however, a full functional characterisation of anosmin-1 in this species has hitherto been unreported. It should however be noted that the chicken *KAL1* orthologue is located on an autosomal chromosome (chr. 1) (Legouis et al., 1993b), and may therefore be expressed at higher levels compared with the human X-chromosome orthologue. This may give the chicken an anosmin-1 dosage advantage in certain developmental processes, thus potentially causing complications in the comparative analysis of anosmin-1 function in this organism.

During the second half of chicken embryonic life, *Kal1* transcript is mainly found in the neurons of the central nervous system (CNS), including particularly high levels of transcript in the mitral neurons of the olfactory bulbs, in the Purkinje cells of the cerebellum, in retinal neurons, and in discrete neuronal populations of the brainstem and spinal cord. A low level expression is observed in some mesenchymal derivatives, including that of the developing kidney (i.e. the small blood vessel walls and glomeruli of the mesonephros). Notably, unlike human embryos, *Kal1* expression is not detected at any stage in the chick embryonic epithelium or the surrounding nasal mesenchyme. From embryonic day 8, the expression is therefore almost entirely restricted to definite neuronal populations of the CNS, some of which (including the optic tectum and striatum) continue to express *Kal1* after hatching. However, during early chick development (days 2-8), Kal1 is transiently expressed in endodermal and mesodermal derivatives (preceding cell differentiation); and is also expressed in post-mitotic neuroectodermal derivatives which continue to express the gene after differentiation. Therefore, *Kal1* appears to have a role in morphogenetic events and in late neuronal differentiation and/or neuronal trophicity (Legouis et al., 1993a; Legouis et al., 1993b; Legouis et al., 1994).

Zebrafish/medaka anosmin-1

Two fish models (zebrafish and medaka) have been used to demonstrate the phenotypic consequences of knocking down *KAL1* gene function. Zebrafish and medaka both have two *KAL1* orthologues (*Kal1a* and *Kal1b*) (Whitlock et al., 2005b; Okubo et al., 2006). Knocking down one of these orthologues, *Kal1a*, in the medaka resulted in both the GnRH1 and GnRH3 cells losing their ability to migrate into the forebrain, and instead accumulating in the olfactory compartment (Okubo and Nagahama, 2008b). Similarly, knockdown of *Kal1a* gene function in the zebrafish was shown to result in specific complete loss of 'endocrine' GnRH cells migrating to the hypothalamus, whilst not affecting the 'neuromodulatory' GnRH cells of the terminal nerve and midbrain. However, knockdown of the other orthologue, *Kal1b*, resulted in only a very slight decrease in hypothalamic GnRH cell number (Whitlock et al., 2005b). More recently, it has also been demonstrated in zebrafish that *Kal1a* (but not *Kal1b*) is also required for fasciculation and terminal targeting of olfactory sensory neuronal axons in the olfactory system (Yanicostas et al., 2009) (*see chapter 5 for further discussion*), as well as in the correct migration of the posterior lateral line primordium (Yanicostas et al., 2008).

The advantages of a zebrafish model

The unavailability of a rodent model for X-KS lead us to choose the zebrafish as our vertebrate KS model, for investigating the role of anosmin-1 and its putative role in the FGF signalling pathway during olfactory and GnRH system development. The zebrafish is a very useful vertebrate model organism for studying these early developmental processes, for the following reasons:

i) Zebrafish are small (4-5cm long) and relatively cheap and easy to maintain.

ii) They are prolific layers: each female can lay around 200 eggs, 2 to 3 times per week.

iii) Zebrafish embryos are transparent and develop externally (*ex utero*), thus allowing all developmental stages to be visualised under the microscope in real-time.

iv) Zebrafish development is very fast: by 24 hours post fertilisation (hpf), the body plan has been established and the major organs are visible.

Sequencing of the zebrafish genome, which began in 2001, has demonstrated that many of the genes that have so far been annotated have very good homology to their human orthologues (http://www.ensembl.org). However, during evolution (around 350 million years ago), a whole genome duplication event occurred in the ray-fin fish lineage, prior to the teleost radiation, meaning that zebrafish often have two orthologues for the corresponding tetraplod (human) gene. Since this divergence, the zebrafish genome has been resolving back to a diploid state again; however, this process is incomplete, and many orthologue pairs have been retained (Kleinjan et al., 2008). For example, zebrafish have two orthologues each of *KAL1*, *FGF8*, and *FGFR1* (Ardouin et al., 2000; Jovelin et al., 2007; Rohner et al., 2009). Among the remaining co-orthologues, there has sometimes been a partitioning of different ancestral gene subfunctions within different teleost lineages: a process known as sub-functionalisation (Kleinjan et al., 2008). This process may have occurred for the two *KAL1* orthologues, where *Kal1a*, according to recent reports, has retained a role in olfactory and GnRH system development, whereas a role for *Kal1b* is yet to be established (Ardouin et al., 2000) (*see chapter 5*).

Analysis and characterisation of the zebrafish GnRH and olfactory systems is further discussed in chapter 3.

1.7 The role of FGF signalling in forebrain development

A summary of the phenotypes of FGFR knockout mouse models is shown in Table 1.2. Due to defects in cell migration through the primitive streak, *Fgfr1* gene inactivation causes embryonic lethality at E9.5-E12.5. Whilst, specific loss of the *Fgfr1c* isoform shows an identical phenotype, the *Fgfr1b* knockout caused no obvious phenotype. This data suggests that only Fgfr1c (not Fgfr1b) is required during embryonic development (Eswarakumar et al., 2005; Kim et al., 2008). The targeted abolition of *Fgfr1* in the developing mouse telencephalon resulted in olfactory bulb aplasia, confirming that Fgfr1 signalling is essential for olfactory bulb morphogenesis (Hebert et al., 2003).

However, in some cases of KS, *FGFR1* mutations may result in an isolated GnRH deficiency without affecting formation of the olfactory bulbs (Pitteloud et al., 2006). This suggests that reduced FGFR1 signalling may affect GnRH neuronal migration, differentiation or survival within the hypothalamus, without causing olfactory bulb defects.

In fact, specific expression of a dominant-negative Fgfr1 (dnFgfr) in GnRH neurons in mice has been shown to result in a 30% decrease in the number of GnRH neurons to reach the forebrain, as well as a significant reduction in GnRH axonal projections to the median eminence. These mice exhibited delayed puberty and premature ovarian senescence. dnFgfr lacks the intracellular tyrosine kinase domain, and upon binding ligand, forms a non-functional heterodimer with wild-type Fgfr1, Fgfr2, and Fgfr3, which then blocks downstream Fgfr signalling (Tsai et al., 2005). This demonstrates that FGF signalling is important for normal GnRH neuronal migration, differentiation and/or survival in the hypothalamus, as well as playing an essential role during telencephalon morphogenesis, particularly in the olfactory bulb.

There have been some reports of patients with FGFR1 mutations whose KS was reversible, whereby normal pulsatile GnRH secretion was activated after they

Table 1.2 FGFR knockout mouse phenotype

Gene	Survival	Phenotype
Fgfr1	Lethal (E9.5-E12.5)	Defective cell migration through primitive streak, posterior axis defects
Fgfr1b	Viable	No obvious phenotype
Fgfr1c	Lethal (E9.5)	Defective cell migration through primitive streak, posterior axis defects
Fgfr2	Lethal (E10.5)	Defective placenta and limb bud formation
Fgfr2b	Lethal (P0)	Agenesis or lungs, anterior pituitary, thyroid, teeth and limbs
Fgfr2c	Viable	Delayed ossification, proportionate dwarfism, chondrocranium
Fgfr3	Viable	Bone overgrowth, inner ear defect
Fgfr4	Viable	No obvious phenotype, growth retardation and lung defects in FGFR3 null background

Adapted from (Eswarakumar et al., 2005) and (Kim et al., 2008)

were given initial gonadotrophin treatments (Pitteloud et al., 2005). And, as mentioned above, female mice expressing a dominant negative FGFR1 specifically within their GnRH neurons had delayed puberty, yet had normal fertility when they reached adulthood (Tsai et al., 2005). These observations suggest that FGFR1 plays an important role during foetal development of the forebrain GnRH system, as indicated by a decreased number of hypothalamic GnRH neurons in these mice, but, postnatally, other factors may lead to the recovery of the hypothalamic GnRH neuronal population, in an FGFR1-independent manner (Kim et al., 2008).

FGF8 expression is detected in the mouse invaginating-nasal pit and has been shown to be a particularly important ligand for olfactory development in mice. In fact, mice with a targeted loss of *Fgf8* failed to develop a definitive olfactory epithelium, vomeronasal organ, and nasal cavity due to apoptosis of cells within the morphogenetic centre and in the developing neuroepithelium, despite initial invagination of the nasal pit and normal olfactory epithelium neurogenesis. Furthermore, *Fgf8* knockout mice have absent olfactory bulb development as well as midline defects (Kawauchi et al., 2005). Consistently, *Fgf8a* mutant 'acerebellar' zebrafish have fewer olfactory sensory neuronal condensations at the olfactory bulbs (Shanmugalingam et al., 2000) (*see chapter 4*). As mentioned earlier, Fgf8 also has an essential role in forebrain GnRH neuronal development; hence mice hypomorphic for *Fgf8* lack GnRH neurons of the hypothalamus (Falardeau et al., 2008). *FGF2* is co-expressed with *FGFR1* in the nasal epithelium, and may therefore represent a further FGFR1 ligand for signalling during olfactory and GnRH system development (Britto et al., 2002), although its presence here clearly cannot compensate for absence of FGF8 in this region.

Both *Fgfr1* and *Fgfr3* are expressed in developing GnRH neurons and are capable of binding to Fgf8 equally well. However, the total number of GnRH neurons decreased only in homozygous *Fgfr1* hypomorphs, but not homozygous *Fgfr3* knockout mice. Therefore, it is believed that the effects of FGF8 are mediated through FGFR1 alone during forebrain GnRH development, and that its action is directed on the target migrating GnRH cells, as they themselves express FGFR1 (Chung et al., 2008).

Zebrafish *Fgf3* ('Lia') mutants lack an adenohypophysis (anterior pituitary) due to specific apoptosis of adenohypophyseal cells (Herzog et al., 2004), as well as defects in forebrain development, including failure of forebrain commissure formation (Walshe and Mason, 2003). It been proposed that, in zebrafish, hypothalamic GnRH cells may originate from the anterior pituitary placodal region (Whitlock, 2005a; Whitlock et al., 2005b). Therefore, it may be interesting to find out whether these *Fgf3* mutants also lack hypothalamic GnRH neurons. Moreover, *Fgf8a* morphant embryos also had forebrain commissure defects which were worsened by concomitant knock down of *Fgf3*, suggesting that both ligands are required for developmental processes within the forebrain (Walshe and Mason, 2003) (*see chapter 3*).

1.8 Anosmin-1 modulates FGF signalling

A functional interaction between anosmin-1 and the FGF signalling pathway was identified using two *in vitro*-based cell systems. The first system to be used were FNCB4, which is a primary neuroblast cell culture derived from human foetal olfactory neuroepithelium, which expresses olfactory and GnRH markers, and responds to autocrine GnRH stimulation. Addition of recombinant anosmin-1 to these cells induces neurite outgrowth and cytoskeletal rearrangements through an FGFR1-dependent mechanism. Specifically, sustained MAPK (p42/44 and p38) phosphorylation and Cdc42/Rac1 activation was achieved in these cells, at levels equivalent to or higher than those induced by addition of high concentrations of exogenous FGF2 alone (*see Figure 1.11*). The second *in vitro* cell system utilised BaF3 cells, which express specific isoforms of FGFRs and respond to FGF in a heparan sulphate dependent manner. Using this system, it was demonstrated that the effects of anosmin-1 action on the FGF signalling pathway may be specific to the FGFR1 IIIc isoform. The proliferative response to suboptimal concentrations of FGF2 in these cells was significantly increased upon addition of anosmin-1, suggesting that anosmin-1 may be an isoform-specific co-ligand enhancer for FGFR1 (Gonzalez-Martinez et al., 2004b; Kim et al., 2008).

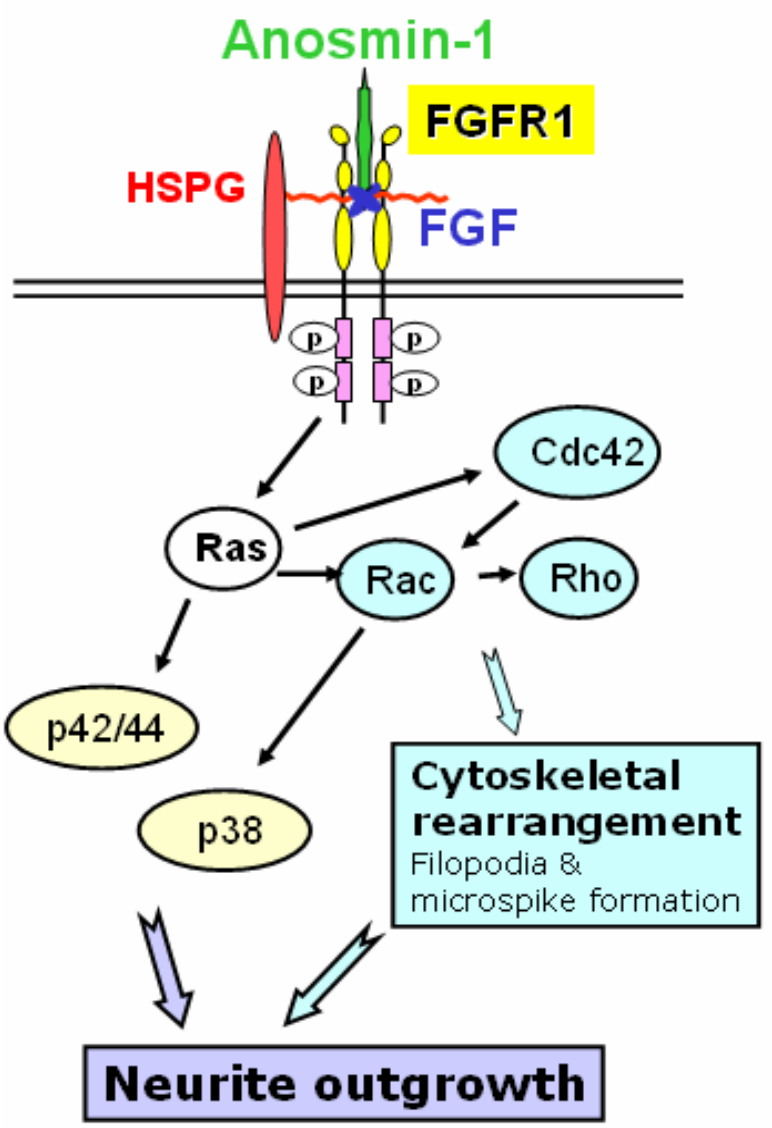

Figure 1.11 A role for anosmin-1 in neurite outgrowth via FGFR1 signalling

A schematic diagram illustrating the downstream pathways that were stimulated by anosmin-1 in *ex vivo* cell culture. In human embryonic GnRH olfactory neuroblasts, anosmin-1 induces neurite outgrowth and cytoskeletal rearrangements through FGFR1-dependent mechanisms involving p42/44 (ERK1/2) and p38 mitogen-activated protein kinases and Cdc42/Rac1 activation. These effects were not seen when anosmin-1 with KS-specific point mutations were used.

During human embryogenesis, anosmin-1 and FGFR1 are expressed in the olfactory placode from as early as 4.5 weeks, and later, at 8 weeks, are both present at the terminal nerve region, part of the migratory route for GnRH-expressing neurons as they navigate towards the hypothalamus. This close proximity of anosmin-1 with FGFR1 at these stages, as well as the data which shows their *in vitro* interaction, supports the possibility of their interaction during human olfactory and GnRH system development (Gonzalez-Martinez et al., 2004b; Cadman et al., 2007) (*see Figure 1.12; a more detailed summary of the spatio-temporal expression of anosmin-1 and FGFR1 during early human embryogenesis is presented in Figure 1.14 at the end of this section*).

Activation of FGF signalling is initiated by multi-protein complex formation between FGF ligand, FGF receptor, and HS proteoglycan (HSPG) on the cell surface. However, other factors, such as anosmin-1, have recently been shown to affect the ***assembly*** of this complex and in this way modulate the response of the cell to the FGF ligand, depending on the specific concentration of anosmin-1 (Hu et al., 2009). This has significantly enhanced our understanding of the molecular mechanism of anosmin-1 action on FGFR1 signalling. However, until now, there has been an absence of an *in vivo* model to demonstrate that this phenomenon is physiologically relevant, during vertebrate embryogenesis (*see chapter 5*).

It has been demonstrated recently that anosmin-1 binds directly with FGFR1 at high affinity, and that this interaction involves the N-terminus of anosmin-1 (cysteine-rich region, whey acidic protein-like domain and the first fibronectin type III domain) and the D2–D3 extracellular domains of FGFR1. Whilst an FGFR1-bound anosmin-1 can bind to FGF2 alone, it cannot bind to an FGF2-heparin complex, thus preventing formation of an ‘active’ FGF signalling complex. In contrast, heparin-bound anosmin-1 *does* bind to a preformed FGF2-FGFR1 complex, resulting in an ‘active’ anosmin-1-FGFR1-FGF2-heparin signalling complex (*see Figure 1.13*). However, anosmin-1 binds to FGFR2IIIc with much lower affinity and has negligible binding affinity for FGFR3IIIc (Hu et al., 2009).

Furthermore, it was also shown, using transwell migration assays, that anosmin-1 induces opposing effects in the chemotaxis of human neuronal cells i.e. it

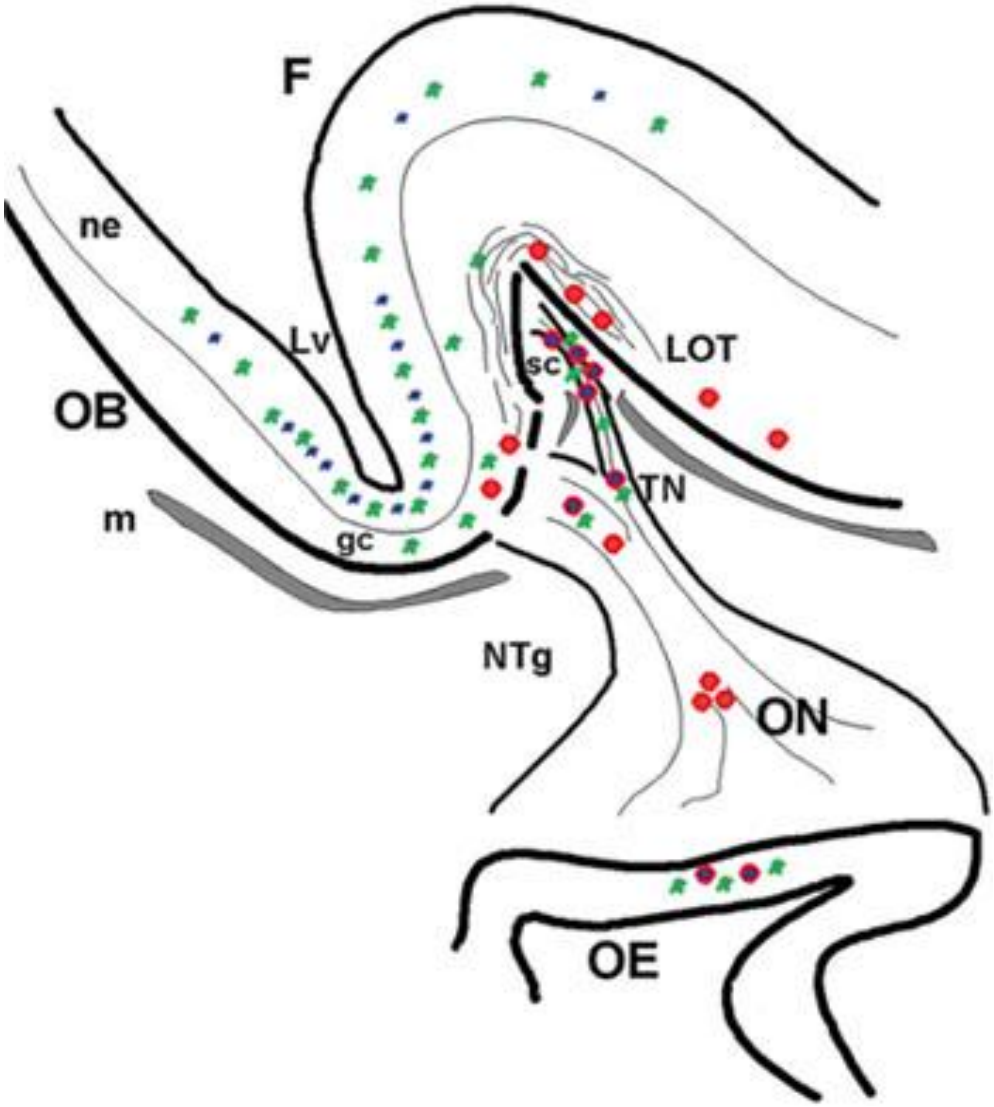

Figure 1.12 Anosmin-1 & FGFR1 expression during human olfactory and GnRH neuronal development

Schematic drawing depicting anosmin-1 (green star), FGFR1 (blue star), and GnRH (red circle) immunoreactivity in the olfactory system and rostral forebrain during human embryogenesis after 53–54 days (CS21). Red circles with blue stars at their centre represent GnRH cells that co-express FGFR1. F= Forebrain; OB= olfactory bulb; OE= olfactory epithelium; ON= olfactory nerve; TN= terminal nerve; NTg= terminal nerve ganglion cells, sc= sulcus circularis, LOT= lateral olfactory tract, gc= granule cells, m= meninges, Lv= lateral ventricle, ne= neuroepithelium.

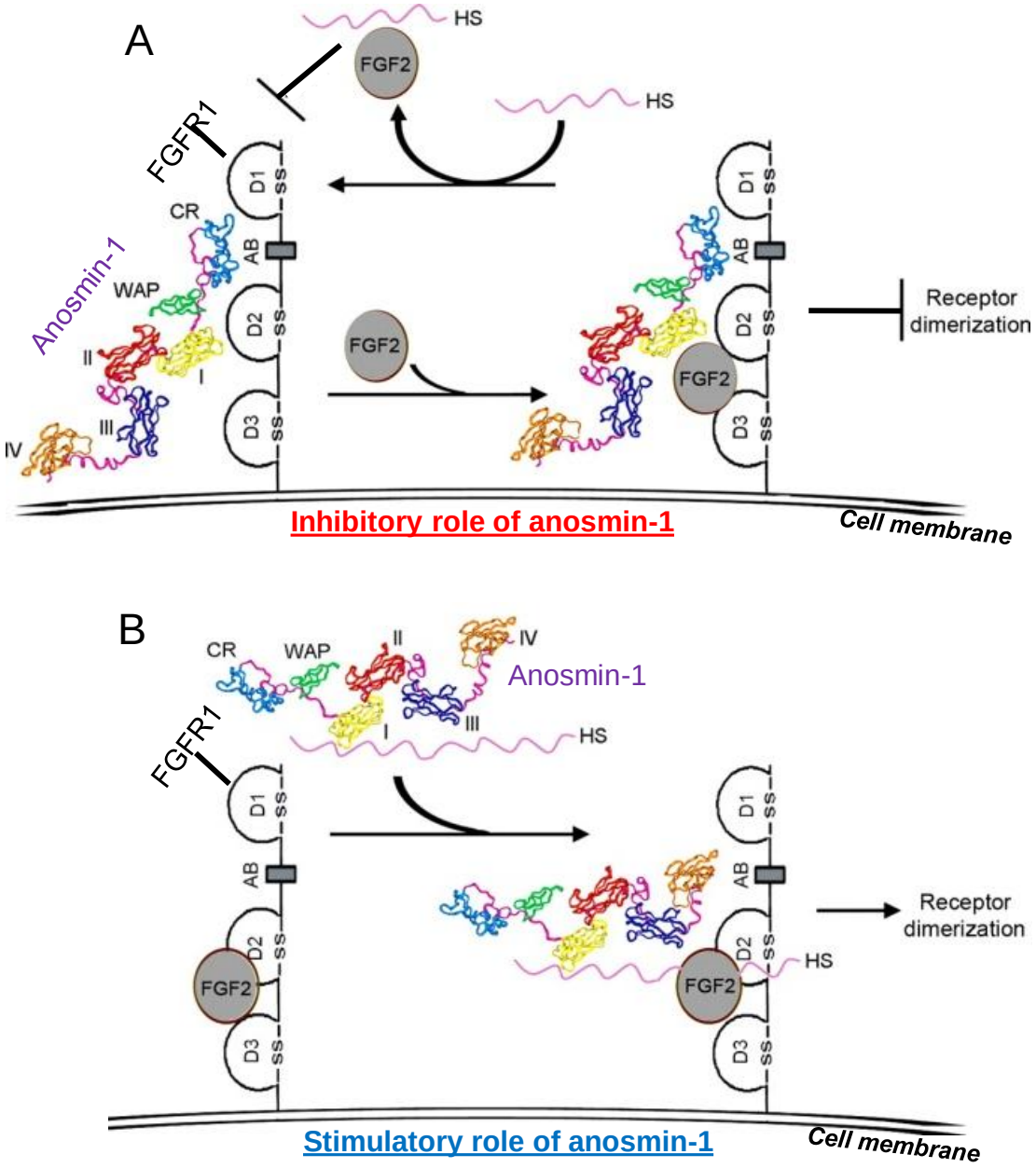

Figure 1.13 Putative model for the dual role of anosmin-1 in inhibiting and stimulating FGFR1 signalling

Model A: Anosmin-1 binding to FGFR1 ***inhibits*** FGF2/FGFR1/HS complex formation. FGF2 is able to bind to pre-formed anosmin-1/FGFR1 complex to form anosmin-1/FGF2/FGFR1 complex, but HS is able to 'strip' the FGF2 from this complex. FGF2/HS complex cannot bind to anosmin-1/FGFR1, so active FGF2/FGFR1 signalling complex cannot form.

Model B: anosmin-1 binding to HS ***facilitates*** FGF2/FGFR1/HS complex formation. HS-bound anosmin-1 preferentially binds to pre-formed FGF2/FGFR1 complex, resulting in active anosmin-1/FGF2/FGFR1/HS complex formation. *Figure modified from Hu et al., 2009.*

was shown to promote GnRH neuroblast migration at lower concentrations, but inhibit this migration at higher concentrations. These dual properties of chemoattractance and chemorepellance may be used to direct cell migration and axon targeting in different cellular contexts, at differing anosmin-1 concentrations. The binding capacity of HSPG and the expression levels of anosmin-1 may determine these opposing actions of anosmin-1, depending on whether the anosmin-1 is in an FGFR1-bound or a heparan sulphate-bound state. These observations may help to explain why *FGFR1* mutations cause KS with a wide spectrum of reproductive phenotypes. Furthermore, FGF8, another of the six currently identified KS genes may form an FGF8-FGFR1-HS signalling complex, whose formation and activation is regulated by anosmin-1 in a similar manner, during GnRH and olfactory neurogenesis (Hu et al., 2009).

Finally, these studies may also help to explain the five-fold higher prevalence of KS in males compared to females. As anosmin-1 dose-dependently enhances GnRH cell migration and neurite outgrowth via the FGFR1 signalling pathway, higher *KAL1* gene expression in females, due to partial escape from X inactivation, might compensate for haploinsufficiency of *FGFR1* in heterozygous females (Cadman et al., 2007; Hu et al., 2009).

Figure 1.14 Anosmin-1 and FGFR1 expression in the olfactory system and rostral forebrain during human embryogenesis.

This schematic diagram illustrates anosmin-1 (red dots; •) and FGFR1 (green dots; •) immuno-reactivity at 4 weeks (**A**), 5.5 weeks (**B**), and 6 weeks (**C**) gestation; corresponding to Carniege Stage (CS) 13, 17, and 18, respectively. GnRH cells are depicted as triangles (▲). **A'** shows an immunofluorescently labelled sagittal section from a 4.5-week-old human embryo illustrating FGFR1 (green labelling) and anosmin-1 (red labelling) distribution at the olfactory placode (OP), corresponding to the region demarcated by a dotted box in part **A**.
A: During human embryogenesis, GnRH-positive neurons are first visualised at around 4.5weeks gestation in the medial OP. Anosmin-1 and FGFR1 are also first detected around this stage in the OP (*see **A'***). FGFR1 and GnRH are co-expressed in some cells at the medial positions of the OP (indicated by green triangles, ▲).
B: Between 5 and 5.5 weeks (CS15-16), FGFR1 and anosmin-1 expression is more widespread, and in addition to the OP, now becomes detectable in the neuroepithelium of the ventral telencephalic and diencephalic part of the forebrain.

C: By 6 weeks gestation, FGFR1 and anosmin-1 are no longer readily detectable in the olfactory epithelium, and, instead become more restricted to the olfactory bulb region and ventral telencephalic and diencephalic regions; a region where GnRH neurons are actively migrating towards the preoptic hypothalamus (as demonstrated by a blue dotted arrow). In fact, by this stage, several GnRH-positive cells are already present in the ventral forebrain surface, suggesting that the initial migration of GnRH cells through the forebrain may be independent of olfactory bulb morphogenesis.

See Figure 1.12 for the GnRH, FGFR1, and anosmin-1 immuno-expression at a later human embryonic stage, CS21; which is approximately 7.5 weeks gestation).
OP=olfactory placode; PON=primary olfactory neurons; bv= blood vessel; NM=nasal mesenchyma; CP=cribriform plate; F=forebrain; ORN=olfactory receptor neurons; OE= olfactory epithelium; OB=olfactory bulb; ONT=olfactory nerve tract; TN=terminal nerve; NTg=terminal nerve ganglion cells; r=rostral.

Figure 1.14 (A), (B), and (C) modified from Front Neuroendocrinol. 25, Gonzalez-Martinez et al., 'Ontogeny of GnRH and olfactory neuronal systems in man: novel insights from the investigation of inherited forms of Kallmann's syndrome.', pp. 108-130, Copyright 2004, with permission from Elsevier. Figure 1.14 (A') is from Gonzalez-Martinez et al., 2004b. Copyright 2004 by the Society for Neuroscience.

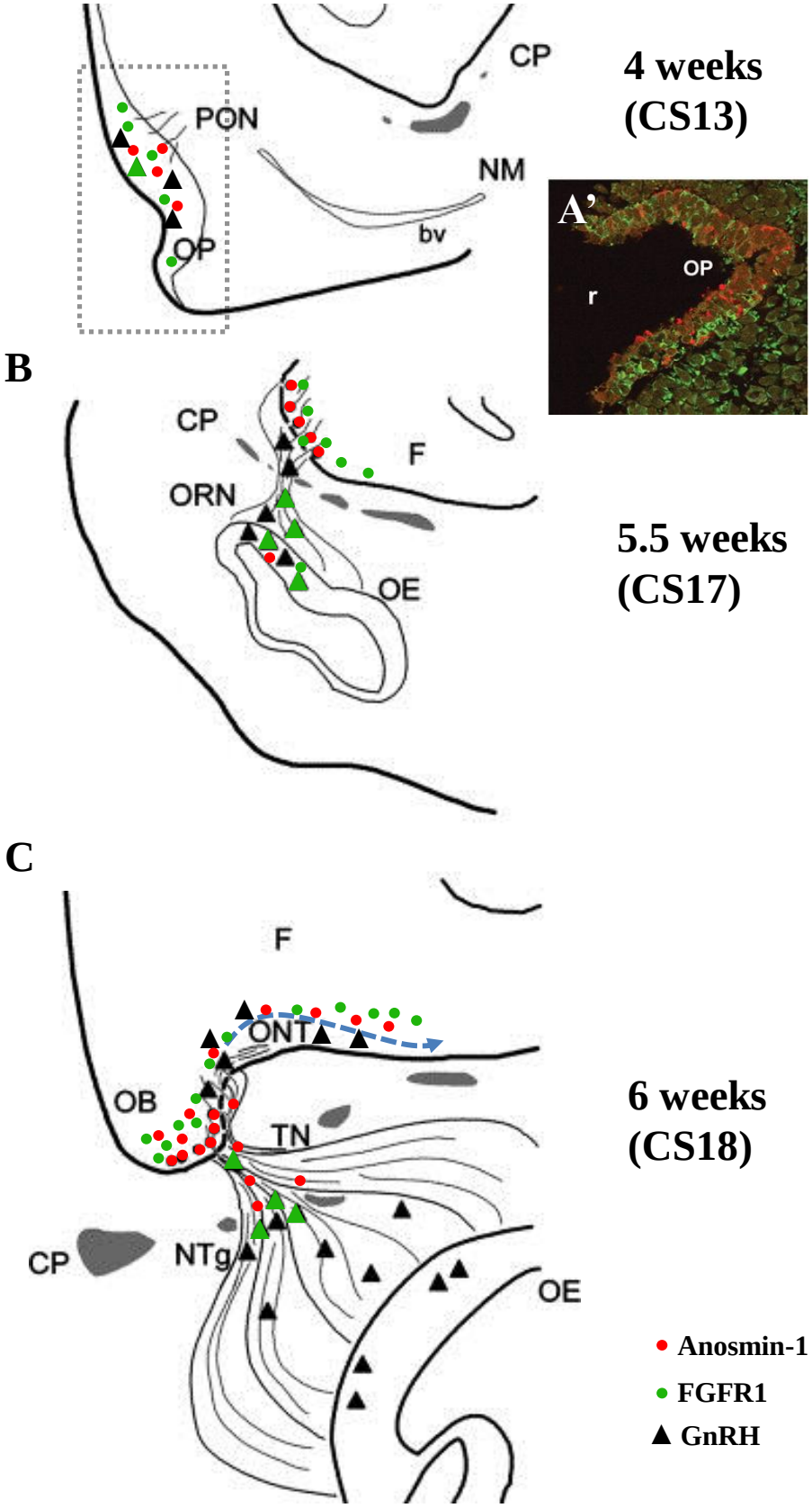

Figure 1.14 Anosmin-1 and FGFR1 expression in the olfactory system and rostral forebrain during human embryogenesis.

1.9 Aims of thesis

- To characterise and re-assess our understanding of GnRH and olfactory neuronal development in zebrafish, and, in the process, establish an *in vivo* model for Kallmann syndrome and other (normosmic) disorders that include hypogonadotrophic hypogonadism in their aetiologies. **[Chapter 3]**.

-To ascertain the developmental origins of the forebrain GnRH neurons and investigate whether early up-regulation of the kisspeptin signalling pathway can affect their migration and/or accumulation at the hypothalamus **[Chapter 3]**.

-To investigate the involvement of FGFR signalling, and, in particular, the role of the two zebrafish FGF8 orthologues therein, during the development of the olfactory and GnRH neuronal systems **[Chapter 4]**.

-To investigate the role of the two zebrafish anosmin-1 orthologues during development of the olfactory and GnRH neuronal systems, by means of gene knockdown **and** over-expression **[Chapter 5]**.

-To identify whether or not the two anosmin-1 orthologues are involved in formation of the forebrain commissures in zebrafish; and, if so, to use this developmental process to explore a putative role for anosmin-1 action on the Fgf8 signalling pathway *in vivo* **[Chapter 5]**.

Chapter 2
Materials & Methods

2.1 Buffers and solutions

Note: *All reagents were supplied by BDH or Sigma and dissolved in water unless otherwise stated. % means weight/volume, unless specified as v/v (volume/volume).*

1% Agarose gel: 1g agarose in 100ml 1X TAE

BBR: 10% Boehringer Blocking Reagent (Roche) in MAB

Block buffer for TCA protocol: 10% (v/v) DMSO, 2% (v/v) goat serum, 1% BSA in PBSTx

CHAPS: 10% (v/v) [(3-cholamidopropyl)-dimethylammonio]-1-propanesulfonate in DEPC-treated PBS.

DEPC treatment: diethylpyrocyanate, 1ml added to 1L solution, left overnight and autoclaved.

DExB: 10mM Tris pH8.2, 10mM EDTA, 200mM NaCl, 0.5% SDS, 200μg/ml Proteinase K

Goat serum: (Invitrogen) heat-inactivated by heating to 60^{o}C for 30 minutes, aliquoted and stored at -20^{o}C

GS/BBR blocking buffer: 20% (v/v) goat serum, 20% BBR in MABT

Hybridisation (hyb) solution: 50% (v/v) Formamide (Fluka), 5X SSC, 5 mM EDTA, 50 μg/ml yeast tRNA (Invitrogen), 0.2% (v/v) Tween-20, 0.5% CHAPS, 100 μg/ml Heparin in DEPC-treated water

Incubation buffer (IB): 10% goat serum (v/v), 1% (v/v) DMSO in PBSTx

LB: Luria Bertani medium, 10g Bacto-Tryptone (BD), 5g Bacto-yeast extract (BD), 10g NaCl in 1L water (then autoclaved)

MAB: 100mM Maleic acid, 150mM NaCl, adjusted to pH7.5 (autoclaved)

MABT: 0.1% Tween-20 (v/v) in MAB

Memfa fix: 10% (v/v) MEMFA-10X salts, 10% (v/v) formaldehyde (37%)

Milk block: 5% powdered milk in 1X TBST (for Western blots)

MEMFA-10X Salts: 1M MOPS, 20mM EGTA, 10mM $MgSO_4$ adjusted to pH 7.8 with NaOH, filter sterilised and stored at 4^{o}C.

5X MO buffer: 600mM KCl, 100mM Hepes (pH7.5), 1.25% phenol red

NBT/BCIP: 4-nitroblue-tetrazolium chloride and 5-bromo-4-chloro-3indolyl-phosphate (Roche)

NTMT (pH9.5): 5 M NaCl, 2 M Tris pH 9.5, 2 M $MgCl_2$, 10% (v/v) Tween-20

PBS: 0.16 M NaCl, 3 mM KCl, 8 mM Na_2HPO_4, 1 mM KH_2PO_4 (Oxoid), autoclaved

PBSTx: 0.1% (v/v) triton X-100 in PBS.

PBSTw: 0.1% (v/v) Tween-20 in PBS.

4% PFA: 4% paraformaldehyde and 7% sucrose in PBS, heated to 70^{o}C until dissolved, whilst adding NaOH drop-wise to approximately pH10, then adjusted to pH 7.5 with HCl, aliquoted and stored -20^{o}C

1000X PK: 10mg/ml Proteinase K, aliquoted and stored at -20^{o}C.

PTU (100X)**:** 0.3% phenylthiourea, pH7.0

SDS-PAGE running buffer: 10g SDS, 30.3g Tris, 144g Glycine in 1L water

20X SSC: 3 M NaCl, 0.3 M Sodium citrate, adjusted with citric acid to pH 4.5, DEPC treated and autoclaved.

TLB-WB: 1X TLB-10X, 10mM sodium orthovanadate, one Complete Mini-Protease inhibitor cocktail tablet (Roche)

TLB-10X: 1% (v/v) triton X-100, 50mM Tris HCl, 150mM NaCl

2% TCA: 2% (v/v) trichloracetic acid

Tricaine: 0.01% tricaine methanesulfonate (MS222), pH7.0

2YT: 16g Tryptone (BD), 10g Yeast (BD) 5g NaCl in 1 L water

10X transfer buffer: 30.3g Tris, 144g Glycine in 1L water

1X transfer buffer: 20% (v/v) methanol in 1X transfer buffer (for Western blots)

10X TBS: 10X stock, 20mM Tris, 150mM NaCl in water, pH 7.5

TBST: 1X TBS with 0.1% (v/v) Tween-20

TAE: 40 mM Tris-Acetate, 1mM EDTA

2.2 Animals

2.2.1 Adult zebrafish

Adult zebrafish were maintained at a constant light/dark cycle (14 hours with lights on, followed by 10 hours of lights off) to ensure a reliable breeding pattern.

Zebrafish strains used in this study:

- Wild-type zebrafish: King's College Wild-type ('**KWT**')
- Transgenic zebrafish: **Nkx2.1a:YFP** (Danesin et al., 2009), **pOMP:tauEGFP** (Yoshida et al., 2002), **pTRPC2:Venus** (Sato et al., 2005), **pSox10:GFP** (Wada et al., 2005), **Dusp6:d2GFP** (Molina et al., 2007), **hsp70l:dnfgfr1-EGFP** (Lee et al., 2005).
- Mutant zebrafish: **Ace** (*Fgf8a* mutant) (Shanmugalingam et al., 2000)

2.2.2 Harvesting zebrafish & medaka embryos

Zebrafish and medaka both lay their eggs *ex utero* at the beginning of a new light cycle each day (i.e. when lights are first switched on in the morning). Their embryos were harvested and maintained in 90mm Petri dishes containing aquarium water supplemented with methylene blue (to deter microbial contamination), and then incubated at 28.5^{o}C. To ensure that the embryos remained pigment-free and transparent after 24hpf, phenylthiourea (PTU) was also added to the Petri dishes, at a final concentration of 0.003%.

2.2.3 Chicken embryos

Fertilised brown chicken eggs (from Henry Stuart Farms) were incubated at 38^{o}C in a humidified room. Chick embryos were then dissected from these eggs and staged according to Hamburger and Hamilton (Hamburger and Hamilton, 1992).
Note: All chicken embryo dissections were performed by Dr Panna Tandon.

2.3 Immunohistochemistry of whole embryos

Note: the following protocol is suitable for immuno-labelling embryos with anti-GFP, anti-mCherry, or anti-calretinin. However, certain adjustments to this protocol were required when using other antibodies listed in Table 2.1, or when sections were being used. These modifications are described in sections 2.3.2 through to 2.3.6.

2.3.1 The standard protocol

Embryos were fixed in 4% PFA for 3 hours at room temperature (RT, or overnight at 4^{o}C), and then washed five times in PBSTx for 5mins each. Embryos older than 24hpf were then permeabilised using 1000X Proteinase K (PK), diluted in PBSTx at the following stage-dependent concentrations:

For **24hpf**: 15min of 1X PK;

For **48hpf**: 45min of 1X PK;

For **72hpf**: 45min of 2X PK;

For **96hpf**: 45min of 3X PK;

For **120hpf**: 45min of 4X PK.

PK treatments were carried out on a platform rocker at RT, and embryos were then re-fixed in 4% PFA for 20mins. Embryos were then washed in PBSTx another five times for 10mins each, and 'blocked' in IB for at least one hour at RT. Embryos were then incubated in IB with primary antibody at 4^{o}C overnight *(see Table 2.1 for appropriate dilutions).*

Table 2.1 Primary antibodies

Antibody	Species	Company	Application	Dilution
anti-mCherry	Rabbit	MBL International (*PM005)*	IHC	1:500
anti-GFP	Rabbit	Invitrogen *(A6455)*	IHC	1:500
anti-calretinin	Rabbit	Swant *(7699/3H)*	IHC	1:500
anti GnRH (LRH13)	Mouse	Gift from K. Wakabayashi *(Gunma University, Japan)*	IHC	1:200
anti-acetylated tubulin	Mouse	Sigma-Aldrich *(T6793)*	IHC	1:1000
anti-phospho-p44/42 MAPK (Erk1/2) (Thr202/Tyr204)	Rabbit	Cell Signalling Technology (#9101)	IHC	1:500
anti-anosmin1a	Rabbit	Gift of N. Soussi-Yanicostas *(INSERM, France)*	IHC WB	1:500 1:2000
anti-anosmin-1b	Rabbit	Gift of N. Soussi-Yanicostas *(INSERM, France)*	IHC WB	1:500 1:2000
anti-GAPDH	Rabbit	Abcam *(ab8245)*	WB	1:5000

If Alexa-488 (green fluorescent) or Alexa-594 (red fluorescent) secondary antibodies (Invitrogen) were used, embryos were then mounted and visualised using confocal microscopy.

Alternatively, if HRP-conjugated secondary antibody was used, a DAB (3,3′-Diaminobenzidine) colour reaction was then carried out using SigmaFast DAB reagent (Sigma-Aldrich), as per the manufacturer's instructions. Embryos were incubated in SigmaFast DAB for approximately 10 minutes at RT, so that a 'brown precipitate' could form wherever immuno-complexes were present. When sufficient labelling was achieved, the DAB reaction was stopped ('quenched') by removal of the DAB reagent and application of several PBSTx washes. Embryos were then brought into 80% (v/v) glycerol/PBS (mountant), via 30% (v/v), then 50% (v/v) glycerol/PBS washes, and visualised by standard compound light microscopy.

2.3.2 Anti-GnRH (LRH13)

LRH13 is a monoclonal antibody which detects GnRH1 or GnRH3 decapeptide (but not GnRH2) from birds, mammals, and fish (Park and Wakabayashi, 1986).

Because the GnRH decapeptide is very small, two modifications to the above protocol were applied. Embryos were fixed for 2 hours at RT in 4% PFA *supplemented with 7%* (v/v) *saturated picric acid*. Also, instead of PK treatment, embryos were permeabilised using ice-cold *acetone* at -20^{o}C for 10mins.

2.3.3 Anti-anosmin-1a/-1b and anti-pERK

Embryos were fixed in 5ml of **memfa fix** at 4^{o}C overnight. The next day, 2.5ml of fix was replaced with 2.5ml of ice-cold ethanol, and agitated on a rocker (in an ice bucket) for 10 minutes. The 50% (v/v) fix/ 50% (v/v) ethanol was then replaced with 100% ice-cold ethanol, and repeated for another 10mins; and then repeated again for another 30mins with new ethanol. 2.5ml of ethanol was then replaced with 2.5ml ice-cold PBS for another 10mins (still on ice). The ethanol/PBS

was then replaced with PBS for another 10mins. The embryos were then removed from the ice and allowed to return to RT in new ice-cold PBS, followed by five washes in PBSTx. The standard immunohistochemistry protocol (2.3.1) was then followed, but **without** the PK permeabilisation/ post-fix steps.

2.3.4 Anti-acetylated tubulin

Embryos were fixed in **2% (v/v) TCA** fixative for 2hrs at RT, and then washed five times in PBSTx for 10 minutes each. They were then blocked for 1-2 hrs at RT in **'TCA block buffer'**, and then subsequently incubated in anti-acetylated tubulin antibody (diluted in 'TCA block buffer') overnight at 4^{o}C. The standard protocol (2.3.1) was then followed for post-primary antibody incubation.

2.3.5 Cryostat sections

Cryostat sections of embryos that were adhered to glass slides were washed in PBSTx several times, before being blocked in IB. A hydrophobic layer was then marked around the cryostat section, and a 'droplet' of antibody (diluted in IB) was placed on top of the section. This was then kept in a moist box in the fridge overnight. The standard protocol (2.3.1) was then followed, but with secondary antibody applied in this same manner.

2.3.6 Vibratome sections

Dissected chick embryo heads or adult zebrafish brains were fixed and then embedded in 3% agarose, before being sectioned using a vibratory microtome ('Vibratome'). Immuno-labelling was then carried out as described in 2.3.1 on these *'free-floating'* sections *in vitro* (without the PK treatment step).

Note: All cryostat and Vibrotome sectioning was carried out by Dr Laxmi Iyengar.

2.4 *In situ* hybridisation for whole embryos

2.4.1 DIG-labelled probe synthesis

The following reaction mix was assembled for synthesising antisense probe (*all reagents from Roche*): 11.5µl of Nuclease-free H_2O; 4.0µl of '5X' transcription buffer; 2.0µl of DIG-labelled nucleotide mix; ~1.0µl linearised plasmid* (from ~1mg/ml stock); 0.5µl of RNase inhibitor; 1.0µl of polymerase. The reaction was then incubated at 37^{o}C for 2 hours. The DIG-labelled RNA probes were then purified using a microspin G-50 column (GE Healthcare).

** Unless otherwise specified, all plasmids used to synthesise DIG-labelled probes were kindly provided by the following research groups (see references for experimental details):* ***GnRH2*** *&* ***GnRH3*** *(Palevitch et al., 2007);* ***Fgfr1a*** *(Scholpp et al., 2004);* ***Fgfr1b*** *(Rohner et al., 2009);* ***Fgfr2*** *(Tonou-Fujimori et al., 2002);* ***Fgfr3*** *(Sleptsova-Friedrich et al., 2001);* ***Fgfr4*** *(Thisse et al., 1995);* ***Fgf3*** *(Walshe et al., 2002);* ***Fgf8a*** *(Shanmugalingam et al., 2000);* ***Fgf8b*** *(Reifers et al., 2000);* ***Sprouty4*** *(Furthauer et al., 2001);* ***Dusp6*** *(Tsang et al., 2004);* ***Kal1a*** *&* ***Kal1b*** *(Ardouin et al., 2000).*

Kiss1*,* ***Kiss2****,* ***Gpr54a****, and* ***Gpr54b*** *were all previously cloned into a TOPO vector (Invitrogen) using full length coding sequences for each gene (Cadman et al, unpublished). Kiss1, Gpr54a, and Gpr54b plasmids were linearised with SacI and a T7 polymerase was then used for probe synthesis; whereas for Kiss2, NcoI was used for linearisation, and an SP6 polymerase was used for probe synthesis.*

2.4.2 Embryo fixation and dehydration

Embryos were fixed in 4% PFA for 3 hours at RT, or overnight at 4^{o}C. Embryos were then washed three times in PBSTw for 10mins each; followed by one wash in 1:1 PBSTw/methanol, and then two washes in 100% methanol, and then stored at -20^{o}C overnight (or up to 2 months).

2.4.3 Hybridisation with RNA probe

The zebrafish embryos were rehydrated through 1:1 methanol/PBSTw, and then PBSTw. They were then washed three more times in PBSTw at RT, before undergoing PK treatment as described in **section 2.2.1** *(except the PK was diluted in PBSTw)**. Embryos were then washed briefly 3 times in PBSTw, re-fixed in 4% PFA for 20mins at RT, and then washed another four times in PBSTw (5mins each wash). Embryos were then rinsed twice (5mins each) in 1:1 PBSTw/hybridisation (hyb) solution, and then transferred to 100% hyb solution and incubated at 65^{o}C for at least 30mins. Embryos were then incubated overnight at 65^{o}C in hyb solution containing 1μg/ml RNA probe.

2.4.4 Incubation with anti-DIG antibody

Probes were removed the next day and embryos were rinsed once with pre-warmed hyb solution (used probes were kept at -20^{o}C, and used 1-2 more times). Embryos were then washed twice in 1:1 hyb solution/MABT for at least 30mins and then rinsed three more times in MABT for 5mins each at RT. Embryos were then pre-incubated in GS/BBR blocking buffer for 2-3 hours at RT, before incubation overnight at 4^{o}C in anti-DIG-AP antibody (Roche) at a dilution of 1:2000 in the same blocking buffer.

The next day, embryos were rinsed briefly at least 3 times with MABT, and then washed three times for 1 hour each in MABT at RT. Embryos were then rinsed with NTMT (pH9.5) and then transferred to a multi-well plate. Embryos were then incubated at RT with NTMT containing 20μl/ml NBT/BCIP stock solution (Roche), until the appropriate 'purple' staining was achieved. Embryos were then transferred to 80% (v/v) glycerol/PBS, ready for analysis by standard optical microscopy.

2.5 Molecular biology techniques

2.5.1 DNA electrophoresis

A 1.5% agarose in TAE gel containing 0.5µg/ml ethidium bromide was used to analyse DNA and RNA products diluted in 10X 'Orange G' loading dye to a final 1X concentration and run at 150V with 1µg of 1Kb plus DNA Ladder (Invitrogen). A UV illuminator with camera was then used to visualise and photograph the gel.

2.5.2 Genomic DNA extraction from zebrafish embryos

Approximately fifty 96hpf embryos were killed by tricaine-overdose and added to a 1.5ml tube. All liquid was removed from the tube and replaced with 200µl of DNA extraction buffer (DExB) and then incubated at 50^{o}C for 3 hours, with vortexing every 10-20mins. 500µl of ethanol was then added, and the tube placed on ice for 30mins. This was then centrifuged on full speed for 10mins, and the supernatant was removed. The pellet was then washed with 500µl 70% (v/v) ethanol and centrifuged again for 2mins. The resulting pellet was then dried and resuspended in 20µl of nuclease-free water and stored at -20^{o}C.

2.5.3 RNA extraction from zebrafish embryos

The following protocol describes the extraction of RNA from a single embryo, but can the same protocol was used to extract RNA from a 'pool' of embryos, by multiplying all reagent volumes, as appropriate.

One embryo was added to 100µl Trizol (Invitrogen) in a 1.5ml tube and lysed by pipetting until the embryo fully dissolved, and was then incubated at RT for 5mins. 20µl of chloroform was then added and the tube was flicked vigorously for 15secs, and then incubated at RT for 2-3mins. The tube was then centrifuged at 4^{o}C at 10,000rpm for 10mins in an Eppendorf desktop centrifuge. The 'upper layer' was then transferred into a fresh tube and precipitated with 50µl of isopropanol.

This was incubated at RT for 10mins and then centrifuged again, as above. The resulting pellet was then washed with 100µl of 75% (v/v) ethanol and centrifuged again, but this time at 6,000rpm for 5mins (at 4^{o}C). The pellet was then air dried for several minutes, and then resuspended in 20µl of nuclease-free water.

2.5.4 cDNA synthesis

1µl of N_6 random primer (from Transcriptor reverse transcriptase kit, Roche) was added to 14µl of RNA sample, which had been extracted as described in section 2.5.3. The tube was then placed on a 95^{o}C heat-block for 5mins, and then put straight back on ice again. The cDNA synthesis reaction was then assembled on ice by adding the following components (all from Roche): 2µl 10X RT buffer, 2µl (5mM) dNTPs, 0.5µl (5U) RNase inhibitor (Roche), and 0.5µl (2.5U) Reverse transcriptase. The reaction was then allowed to proceed for 2 hours at 37^{o}C, and the resulting cDNA was then used in a standard PCR reaction (section 2.5.5). Therefore the entire 'RT-PCR protocol' consists of sections 2.5.3 through to 2.5.5.

2.5.5 Polymerase chain reaction (PCR)

The following standard PCR reaction was assembled (*see Table 2.2 for primer sequences*): ≤1µg of DNA* diluted with 10X HotStarTaq buffer (Qiagen) to a final concentration of 1X with nuclease-free water and 5µM of forward and reverse primer, 5mM dNTPs (Roche), and 2.5 units of HotStarTaq Polymerase (Qiagen), to a final volume of 25µl. * *cDNA (from 2.5.4) or genomic DNA (from 2.5.3).*

Table 2.2 Primer sequences

Name	Nucleotide sequence (5'→ 3')	Annealing temp (^{o}C) for PCR	Expected product size (bp)
GnRH3 promoter (For) *GnRH3* promoter (Rev)	CCACTAGTCTCACATGAATGTGATTG CCGGATCCGCTAAAACTAAAACACAG	55	2432*
Whole *Kal1a* (For) Whole *Kal1a* (Rev)	GCTCTAGAATGCGCGACGGGCTCACC GCGTCGACTCAGTGACGTTCAATCAC	55	1966
Whole *Kal1b* (For) Whole *Kal1b* (Rev)	GGTCTAGAATGCTGCTTTTGAGGAATCTCT GGGTCGACTCAGTGGATGGTGCTGTTTAAA	62	1910
Fgf8b Exon1(For) *Fgf8b* Exon5(Rev)	AATACCGCGAGGAAACAATG AACTTATGTGTGGCTTGGGC	58	1486
Kal1a Exon1 (For) *Kal1a* Exon7 (Rev)	GGGAGTTGAAAGACGGACCTTG TGAGTTTGGGTGGCAGATTGTG	55	750
Kal1b Exon1 (For) *Kal1b* Exon6 (Rev1) ***or*** *Kal1b* Exon7 (Rev2)**	TGTGTGTTTGAGGTGAGCGTTG AGAAATGCTTGCTGGGAGTGG CTCCCACAGGACCAGAACAC	62 62	754 858
GAPDH (For) *GAPDH* (Rev)	TCAATGGATTTGGCCGTATT GAGCTGAGGCCTTCTCAATG	55	306

**Encompassing nucleotides 365–2797 (Genbank no.: AF490354) of the zebrafish GnRH3 promoter (Palevitch et al, 2007).*

***This reverse primer is used for the RT-PCR confirmation of the Exon 6 Kal1b splice ('KB6').*

****Genbank codes:* ***Kal1a****: AF163310;* ***Kal1b****: AF163311;* ***Fgf8b****: NM_182856;* **GAPDH**: AY818346

Standard PCR cycle parameters

Using a Thermocycler (Eppendorf), the following standard PCR cycle was used:

[1] 95^{o}C for 15mins

[2] *45 cycles of:*

(i) 95^{o}C for 40sec;

(ii) 52^{o}C** for 50secs;

(iii) 72^{o}C for 1min***

[3] 72^{o}C for 10mins

***See Table 2.2 for specific annealing temperatures*

****1 minute of extension time for every 500bp of DNA template*

2.5.6 DNA digestion by restriction endonucleases

1µg of plasmid DNA was diluted in 10X enzyme buffer (Roche) to a final 1X concentration with nuclease-free water (Sigma) and 5 units of desired restriction endonuclease(s) (Roche). This reaction was then incubated at 37^{o}C for 1-2 hours. Digestion products were either loaded on to a 1.5% agarose gel and extracted using a 'Gel Extraction kit' (Qiagen), or purified directly using a 'PCR purification kit' (Qiagen).

2.5.7 Plasmid ligation, transformation, and purification

Linearised vector DNA (100ng) was added to desired 'insert DNA' at a molar ratio of 1:3 or 1:6 to give a final volume of 10µl. 10µl of 2X quick ligation buffer (NEB) was added to this reaction mix, followed by 1µl of T4 DNA 'quick' ligase. This was then incubated for 5 minutes at 25^{o}C, and then chilled on ice.

When transforming sub-cloned fragments, XL10-Gold 'ultracompetent' cells (Stratagene) were used, due to their greater efficiency at taking up ligated DNA. At all other times, XL1-Blue 'competent' cells (Stratagene) were used for general

cloning of supercoiled plasmids. In both cases, the standard manufacturer's protocols were used.

Miniprep kits (Qiagen) were used according to manufacturer's instructions in order to extract and purify plasmid DNA from single bacterial clones that were grown in either LB or 2YT media, supplemented with appropriate antibiotics.

2.6 Cloning strategies

2.6.1 Constructing pGnRH3:mCherry

- PCR amplification of the GnRH3 promoter

The previously described ~2.4kb zebrafish GnRH3 promoter region was PCR amplified from zebrafish genomic DNA as described in section 2.2.3.2 and 2.2.3.5, but with the following modifications. Standard PCR was used (*see above*), with an annealing temperature of 55^{o}C and an extension time of 6mins. Moreover, when the first round of PCR had finished, 1µl of the PCR reaction was removed and used in place of the genomic DNA in a second round of PCR, thus greatly amplifying the otherwise low amount of PCR product. Also, the PCR primers that were used introduce SpeI and BamHI sites at the 5' and 3' ends, respectively (*see Table 2.2*).

- Cloning mCherry into I-SceI plasmid

The mCherry coding sequence was cut from the pBA2-memb-mCherry plasmid (Shaner et al., 2005) by AgeI/ApaI digestion, and then cloned into the XmaI/ApaI site of the *I-SceI pBS SK+ (Stratagene)* plasmid.

- Cloning GnRH3 promoter into the I-SceI-mCherry plasmid

The GnRH3 promoter PCR product was gel purified (as described above). This was then digested with SpeI/BamHI and gel purified again. This was then cloned into the XbaI/BamHI site of the I-SceI-mCherry plasmid (*see Figure 2.01A*).

2.6.2 Sub-cloning pOMP:TauEGFP transgene into I-SceI vector

The I-SceI plasmid was digested with SpeI, gel-purified, and then treated with Antarctic phosphatase (NEB), following manufacturer's instructions, to prevent re-ligation of the digested vector. The whole pOMP:tauEGFP transgene (Yoshida et al., 2002) was then removed from its original vector by SpeI digestion, and cloned into the SpeI-digested I-SceI vector (*see Figure 2.01B*).

2.6.3 Cloning Kiss1, Kiss2, Gpr54a, Gpr54b into pBUT3 and hsp70l:MCS-IRES-EGFP plasmid

Full length Kiss1, Kiss2, Gpr54a, and Gpr54b were previously PCR-amplified and cloned into TOPO vectors *(unpublished, S. Cadman et al)*. For this current project, these full length coding sequences were sub-cloned into the pBUT3 vector, which, by addition of extra 5' and 3' sequences, improves the stability of the *in vitro* transcribed mRNA. Using standard PCR conditions (*see above*), with an annealing temperature of 58^{o}C and an extension time of 4mins, the full length Kiss1, Kiss2, Gpr54a, and Gpr54b were amplified from their TOPO plasmids using primers designed to introduce XbaI/SalI sites at the end of the coding sequences (*see Table 2.2*). These PCR products were then XbaI/SalI digested, gel-purified, and

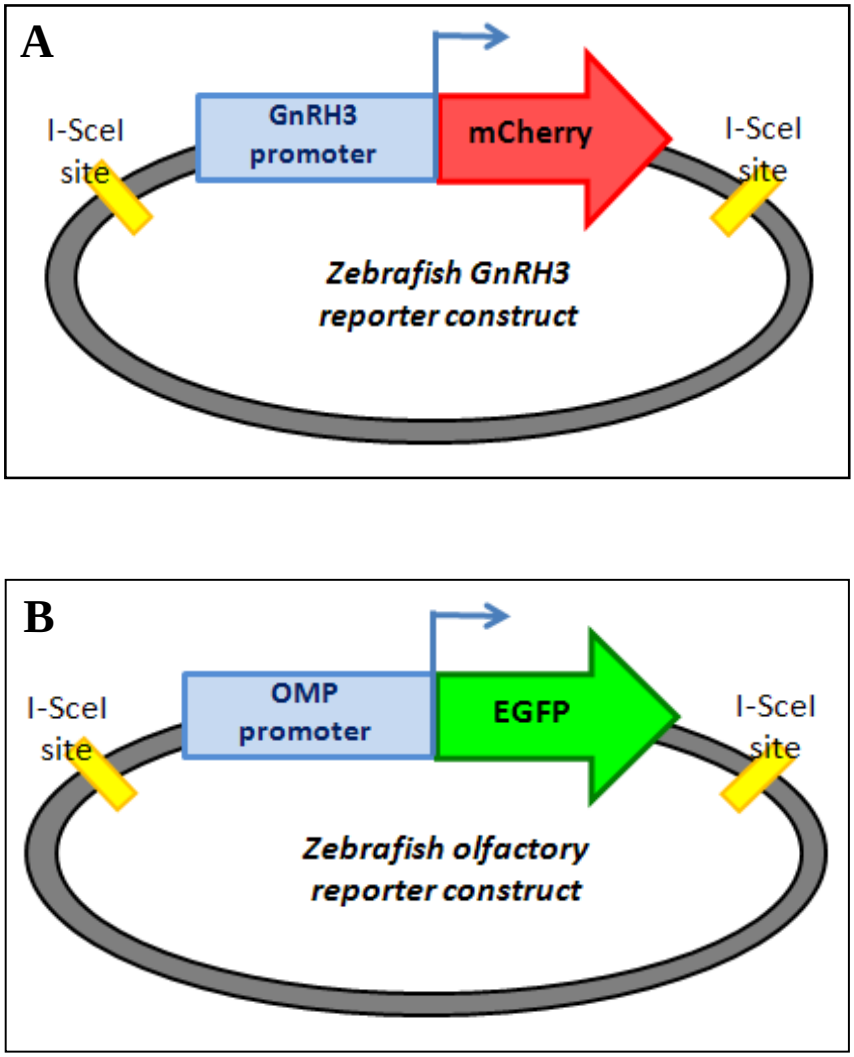

Figure 2.01 I-SceI plasmid constructs for transgenesis

A illustrates the pGnRH3:mCherry construct and **B** shows the pOMP:tauEGFP construct. Both transgenes are flanked by I-SceI recognition sites (in yellow), which had previously been incorporated into a pBluescript vector (pBS SK+) scaffold.

cloned into the XbaI/SalI site of the pBUT3 or Heat-shock (hsp70l:MCS-IRES-EGFP) vectors.

2.6.4 Cloning *Kal1a* and *Kal1b* into pBUT3 plasmid

Full length *Kal1a* and *Kal1b* sequences were PCR-amplified from zebrafish whole embryo cDNA, using primers that introduced XbaI/SalI and cloned into pBUT3, as described in section 2.2.4.3. Subsequently, the plasmids were fully sequenced to ensure that there were no errors introduced to the *Kal1a*/*Kal1b* sequences during this process.

2.7 *In vitro* transcription of Kiss1, Kiss2, Gpr54a, Gpr54b, *Kal1a*, and *Kal1b*

2.7.1 'Capped' mRNA synthesis

The pBut3 plasmids were linearised by digestion with SfiI, gel-purified, and then eluted into nuclease-free water. An mMESSAGE mMACHINE T3 kit (Ambion) was then used to *in vitro* transcribe 'capped' RNA from these linearised plasmids by assembling the following reaction: 10µl of 2X NTP/CAP, 6µl of linearised plasmid (~1µg), 2µl of 10X reaction buffer, and 2µl of T3 RNA polymerase. This reaction was then allowed to proceed for 2 hours at 37^{o}C.

2.7.2 mRNA purification & quantification

1µl RNAse-free DNAse was then added to the reaction mix and incubated at 37°C for a further 15mins. 15µl of ammonium acetate 'stop' solution was then added, followed by 115µl of nuclease-free water and mixed thoroughly by pipetting. The RNA was then precipitated by adding 115µl of isopropanol, mixed again, and

then placed at -20°C for 15 min. This was then centrifuged at 14,000rpm for 15 min using a desktop centrifuge, and the resulting pellet was washed three times with 70% (v/v) ethanol, and centrifuged at 14,000rpm for 5mins between each of these washes. All traces of ethanol were removed and the pellet was then dried for 20mins at RT. Finally, the mRNA pellet was re-suspended in 20µl of nuclease-free water and quantified using standard UV spectrophotometry. The RNA was also run on a 1% agarose gel to confirm the stability of the mRNA, and then stored as single-use aliquots at -80°C.

2.8 Zebrafish embryo micro-injections

Using a microinjection needle and Pico-Spritzer apparatus, zebrafish embryos were injected at the 1-cell or 2-cell stage with a droplet of morpholino, RNA, and/or DNA at a size of 1/8 of the diameter of the embryo yolk. Prior to microinjection, morpholinos and DNA (but ***not*** RNA) were diluted to a final concentration of 1X using 5X MO buffer, to aid in the visualisation of the droplet size and embryonic localisation.

2.8.1 Plasmid DNA micro-injection

There are two commonly used approaches for generating stably transgenic zebrafish. The first approach involves linearising the plasmid DNA construct (containing desired transgene) with a specific restriction endonuclease, then simply injecting the linearised DNA into the cell of one-cell-stage embryos. The other common approach (*see section 2.6.1*) is to use a vector which has the transgene flanked by two I-SceI recognition sites. I-SceI is a meganuclease, which is similar to a restriction endonuclease, but has a large 18bp recognition sequence. With this approach, the plasmid construct is pre-incubated with the I-SceI meganuclease before micro-injection into the one-cell-stage embryos. The I-SceI recognition sequence is predicted to be absent from the zebrafish genome, so the exact method of genome integration is unknown. However, it is believed that the I-SceI pre-

incubation makes the flanking ends of the transgene highly recombinogenic, causing the transgene to integrate very early (at the one cell stage), thus increasing the likelihood of germ-line transmission (Rembold et al., 2006).

Generating stable transgenic zebrafish (the I-SceI meganuclease approach)

i.e. pGnRH3:mCherry; pOMP:tauEGFP

The following reaction was assembled on ice one hour prior to micro-injection: 300ng of plasmid DNA was diluted with 10X I-SceI buffer (NEB) to a final concentration of 1X with nuclease-free water and 2.5U of I-SceI enzyme (NEB) to a final volume of 10µl. This was incubated at RT for 1 hour. Then, 2µl of MO buffer was added and the tube was placed on ice. This was then micro-injected into the cell cytoplasm of one-cell stage embryos, using a droplet size of approximately 1/10 diameter of the cell. Injected embryos were then incubated at 28.5 ^{o}C overnight, and then visualised at ~24-36hpf using a fluorescent microscope. All fluorescent embryos were separated and allowed to mature into adult zebrafish in the fish facility. When they reached sexual maturity (~3 months), these F0 fish were crossed with wild-type fish in order to identify any stable transgenic carriers.

Transient transgenesis

i.e. pGnRH1(Medaka):EGF; pGnRH3(Medaka):EGF

When only transient transgenesis was required, the whole circular plasmid DNA containing the transgene was microinjected at a concentration of 30ng/µl.

2.8.2 RNA micro-injection

In vitro transcribed *Kal1a*/ *Kal1b* mRNA (section 2.2.5) was micro-injected at concentrations of 0.5-2.0µM (0.05-0.2µg/µl) to determine the optimal

concentration. For the over-expression experiments, *Kal1a* and/or *Kal1b* mRNA was injected as described above, but without any 5X MO buffer. Similarly, for the 'rescue experiments', *Kal1a*/*Kal1b* mRNA was diluted to the same pre-determined optimal concentration with the *Kal1a*/*Kal1b* morpholinos.

2.8.3 Morpholino micro-injection

An antisense oligonucleotide (morpholino) approach was used to knockdown *Fgf8a*, *Fgf8b*, *Kal1a*, and *Kal1b* gene function in the zebrafish (*see Table 2.3 for specific morpholino sequences*). There are two types of morpholinos that Gene Tools (Oregon, USA) provide: one which blocks translation of the target gene ('translation-blockers'), and the other which blocks its correct splicing ('splice-blockers'). The mechanism for how both types of morpholino work is demonstrated in Figure 2.02. Upon arrival, the lyophilised morpholinos were reconstituted in nuclease-free water to a final concentration of 5mM, and then stored at -80^{o}C in 5µl aliquots.

To determine the optimal concentration, each morpholino was initially diluted to a final concentration of 0.5mM, 1.0 mM, 1.5 mM, and 2.0 mM. For the gene knockdown experiments, the morpholinos were then micro-injected at these pre-determined optimal concentrations (as described above).

2.9 Lypophilic dye lineage tracing (DiI, DiD, and DiO)

Whole embryo DiI labelling of external membranes was carried out using a previously described procedure (Dynes and Ngai, 1998). Specifically, 20hpf wild-type embryos were dechorionated using watchmaker's forceps and then placed in a multi-well dish, with 1% agarose at the bottom of each well to protect the integrity of the embryos. A 250µM stock solution of DiI dissolved in DMSO was then added

Table 2.3 Morpholino sequences

Name	**Sequence**	**Optimal conc. (mM)**
Fgf8a (Sp.bl*)	GAGTCTCATGTTTATAGCCTCAGTA	1.0
Fgf8b (Sp.bl)	CTTATAAAACTGTGACTTGCCATGA	1.5
Kal1a (Tr.bl)	GAGCCCGTCGCGCATCTTGAAGAAC	1.0-1.5
Kal1b (Tr.bl)	GCAGAGATTCCTCAAAAGCAGCATC	1.0-1.5
KA4	TTCAGGTCTTACCTCTGTAGAGGTT	1.0
KA6	GTTGTTATCTGAAGCCCACCTTTAG	2.0
KB4	GTGTGTTTTACCTTTGAACAGGTTG	1.0
KB6	GAAAGAGTTTTGCTGTACCTCGCAC	1.0
coMO**	CCTCTTACCTCAGTTACAATTTATA	1.5

**Sp.bl= splice blocking; Tr.bl=translation blocking*

*** Standard control morpholino from Gene Tools (Oregon, USA)*

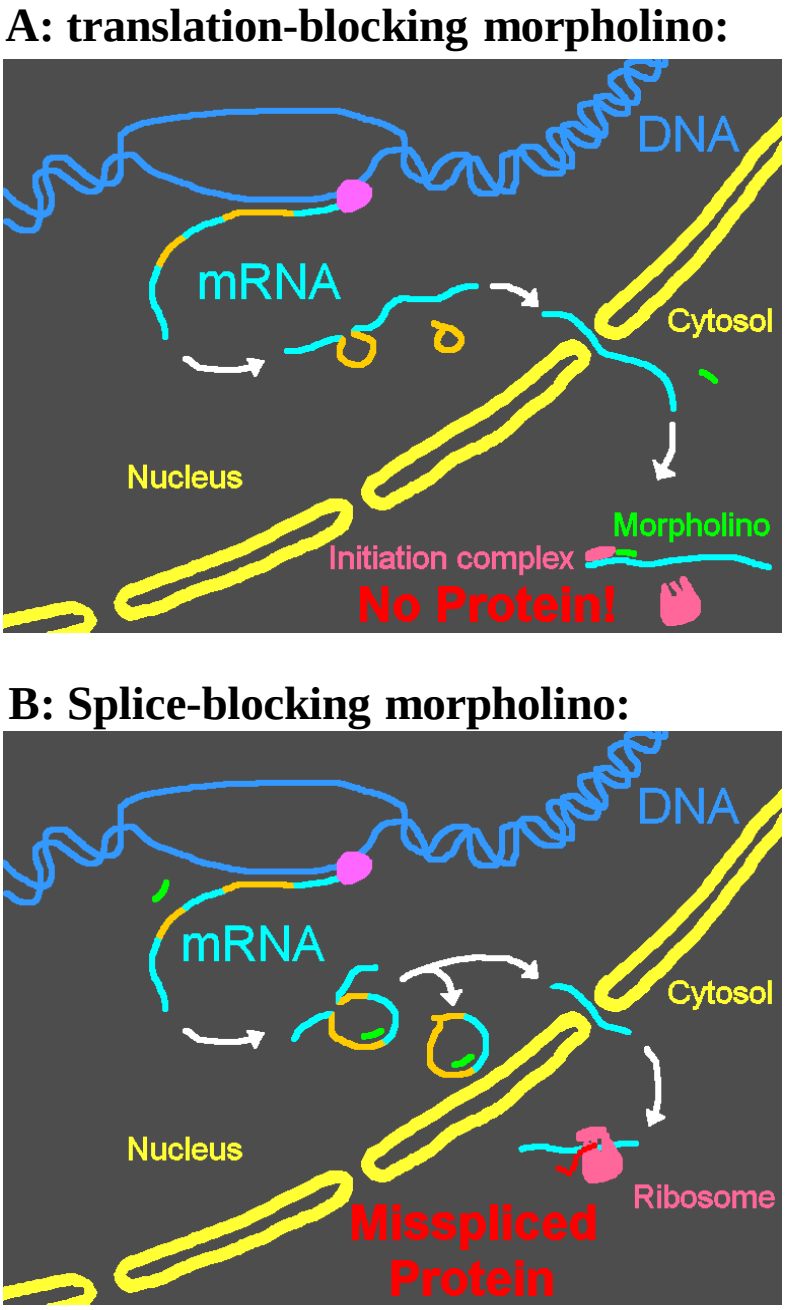

Figure 2.02 The two types of morpholino

A illustrates the gene knockdown mechanism of the 'translation-blockers' and **B** illustrates the 'splice-blockers'. In **A**, the morpholino binds to a the 'start site' region of the target mRNA in the cytoplasm and prevents the initiation complex from translating the RNA into protein. In **B**, the morpholino enters the nucleus and binds to a specific exon-intron region of the pre-spliced target mRNA. This results in the loss of an entire exon; resulting in an aberrant 'mis-spliced protein, which may be truncated or lack a certain amino acid sequence. (Morpholinos are depicted in green).

Dr Jon D. Moulton of 'Gene Tools' (http://www.gene-tools.com), who holds the copyright for these images, kindly allowed me to reproduce them here.

to each well containing embryos, to a final concentration of 2.5μM (dissolved in the aquarium water). Embryos were then incubated at 32°C for 45mins, rinsed several times in aquarium water, and then permitted to develop as usual at 28.5°C. Embryos were then visualised using confocal microscopy (using the 'Cy3' filter) from around 24hpf onwards to visualise the olfactory epithelium and other placodally-derived cells.

The same procedure worked well using DiD, another lypophilic dye (using the 'Cy5' filter); however, this procedure failed to work with DiO, as this lypophilic dye quickly precipitated out in aquarium water and therefore was not available to be absorbed by the cell membranes.

2.10 FGFR inhibition strategies

2.10.1 Using SU5402 inhibitors

A 10mM stock of SU5402 (Mohammadi et al., 1997; Maroon et al., 2002; Walshe and Mason, 2003) dissolved in DMSO was added to dechorionated embryos (at 14hpf or 22hpf) in 1%-coated wells to final concentration of 100μM. Embryos were then allowed to develop for 8-14 hours at 28.5°C before the SU5402 was removed and embryos could then develop as usual. *See Figure 4*.08 *for a detailed summary of the SU5402 treatments that were carried out*.

2.10.2 Heat–shock using dnFGFR

HSP70:dnFGFR-EGFP (Lee et al., 2005) heterozygous carriers were bred together to obtain a clutch of embryos that were 50% dnFGFR (EGFP-positive) and 50% wild-type (EGFP-negative). These embryos were 'heat-shocked' at 18hpf or 22hpf by placing their dish into a 37°C incubator for 45minutes. From around 2 hours later, all dnFGFR embryos could be identified by their green-fluorescence, and were separated from the non-fluorescent embryos (the 'non-dnFGFR' controls).

2.11 Western blotting (immunoblotting)

Immunoblotting was performed using standard procedures (Laemmli, 1970). Briefly, 10-20 embryos were dechorionated and added to 0.5ml of 'ice-cold' triton lysis buffer (TLB-WB, see section 2.1.1). A needle with a very narrow aperture was then used to lyse the embryos completely, and then left on ice for 15 minutes to allow the completion of cell lysis. The resulting cell lysate was then centrifuged at high speed (13,000rpm) at 4^{o}C, using a desktop centrifuge. The resulting supernatants were then transferred to new tubes, and the 'total protein' yield was quantified on a spectrophotometer. Proteins were then separated electrophoretically using 10% acrylamide gels; transferred to nitrocellulose membranes; and probed with anti-anosmin-1a/-1b or anti-GAPDH antibodies (*see Table 2.1*).

2.12 Microscopy

Live embryos anaesthetised using tricaine and visualised in their Petri dish and visualised using a Leica MZFLIII dissecting microscope with or without fluorescence.

All embryos stained by *in situ* hybridisation and some of the immuno-labelled embryos, and adult/ embryo sections, were mounted in 80% (v/v) glycerol in PBS and visualised using a Zeiss Axioskop compound microscope.

Most of the fluorescently labelled embryos, whether live or fixed, were mounted in 1% low melting point agarose in PBS and visualised using an Olympus FV500 confocal microscope, with Fluoview (Olympus) software analysis. 3D rendering analysis was carried out using bioView3D software (Center for BioImage Informatics, UCSB).

Chapter 3
Results (I)

Establishing an *in vivo* system for modelling Kallmann syndrome: a characterisation of zebrafish GnRH and olfactory neuronal ontogeny

3.1 Introduction

Comparative endocrinology of GnRH neuronal development has contributed greatly to our understanding of the human reproductive axis. Using morphological, physiological, molecular, and behavioural approaches, GnRH neurons have been studied extensively in many vertebrate model organisms, including mammals, birds, and fish.

The ontogeny of the three GnRH neuronal systems of the adult teleost fish is, in fact, very similar to that of the amniotes. In particular, the two forebrain GnRH systems in the adult teleost are distributed in a similar way to other vertebrates, rostro-caudally along the ventral telencephalon and diencephalon, thus making the teleost, particularly the zebrafish, an attractive model for studying vertebrate GnRH system development in live, transparent embryos, in 'real-time'.

3.1.1 The zebrafish GnRH neuronal system

At least 24 distinct forms of GnRH decapeptide have been described across different species. In most vertebrates, GnRH decapeptides are processed from the

gene products of 2 to 3 GnRH genes present in their genomes. One of these decapeptides is found at each of three brain regions across mammals and fish: an 'endocrine' type found at the hypothalamus/ preoptic area, and two 'neuromodulatory' types present at the midbrain and terminal nerve/ nasal compartment (*see Figure 3.01*). The function of GnRH at the hypothalamus is known to be in the hormonal control of reproduction via its regulation of gonadotrophin secretion from the pituitary gland. However, less is known about the role of GnRH neurons at the midbrain and terminal nerve, other than their proposed 'neuromodulatory' action on reproductive behaviour (Parhar, 2002).

The GnRH2 decapeptide is highly conserved across most vertebrate species; however, the sequence of GnRH1 and GnRH3 differs throughout these species. The prevailing hypothesis for why there is an extra form of GnRH (GnRH3) in teleost fish, is that the GnRH1 gene duplicated in a teleost fish ancestor some time after its evolutionary split from the lineage that would eventually give rise to mammals. Whereas some fish, such as the medaka, have retained GnRH1 and GnRH3 (as well as GnRH2); other fish, such as the zebrafish, have lost GnRH1 from their genome and only retained GnRH3 and GnRH2 (Kuo et al., 2005).

Hypophysiotropic GnRH system

Although the GnRH1 gene is absent from the zebrafish genome, it has been shown that GnRH3 is expressed at the hypothalamus (as well as the terminal nerve) in zebrafish and has therefore likely assumed the hypophysiotropic role (regulation of pituitary gonadotrophin secretion) that is carried out by GnRH1 in humans, and in some other fish, such as the medaka (Palevitch et al., 2007; Abraham et al., 2009). In proof of this, injection of mammalian kisspeptin-10 (a molecule implicated in the 'molecular switch', which re-awakens GnRH pulsatile secretion at the time of puberty) into the flathead minnow (a fish belonging to the cyprinid family, which includes the zebrafish) increased GnRH3, but not GnRH2 secretion. This provided evidence that GnRH3 is the main hypophysiotropic form of GnRH in cyprinid fish that have only two forms of GnRH (i.e. GnRH2 and GnRH3) (Filby et al., 2008).

A

Role:	Endocrine	Neuromodulatory	
	Hypothalamus/ preoptic area	Midbrain	Terminal Nerve/ nasal region
Amniotes (e.g. human, chick)	GnRH1	GnRH2*	GnRH1
Fish (e.g. Medaka)	GnRH1	GnRH2	GnRH3
Fish (e.g. zebrafish)	GnRH3	GnRH2	GnRH3

except rodents which lack GnRH2

B

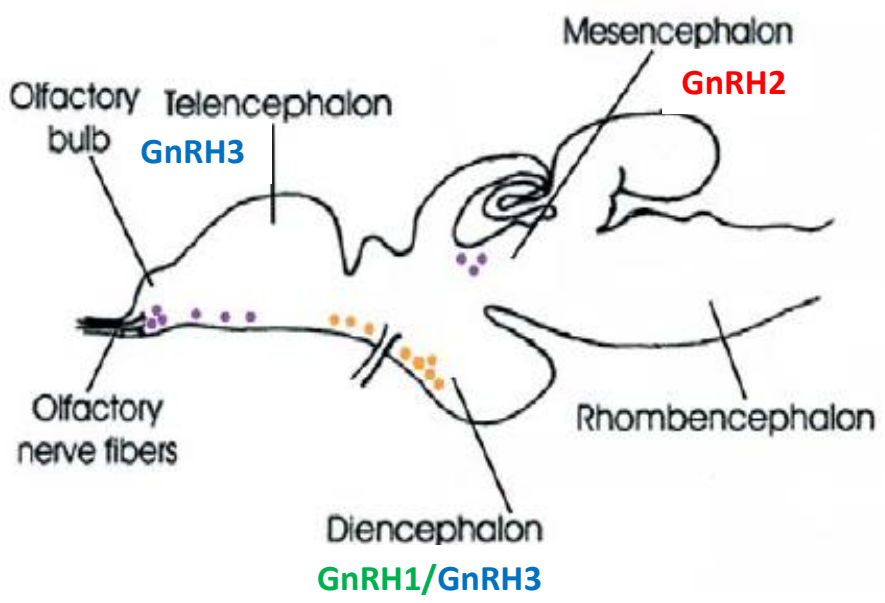

Figure 3.01 Vertebrate GnRH neuronal system

A: Table illustrating the different forms of GnRH expressed at the three well-characterised GnRH-expressing brain regions.

B: schematic of a typical adult fish brain. 'Purple dots' represent the neuromodulatory GnRH populations of the terminal nerve and midbrain; 'orange dots' represent the hypothalamic GnRH population.

Figure 3.01 (B) modified from Trends Endocrinol. Metab 16, Whitlock,K.E, 'Origin and development of GnRH neurons.', pp. 145-151, Copyright 2005, with permission from Elsevier.

Terminal nerve GnRH system

GnRH is present within only some of the neurons of the terminal nerve (*nervus terminalus*), the rostral-most cranial nerve ("nerve 0"). In most vertebrates, the terminal nerve consists of a bundle of neurons embedded within olfactory or vomeronasal axons at the nasal cavity, except in sharks, where it is a separate nerve (Demski and Schwanzel-Fukuda, 1987; Whitlock, 2004). Although the terminal nerve GnRH system has been studied mainly in teleosts, the terminal nerve is also likely to be the main source of the GnRH-immuno-reactive fibres that are distributed throughout the mammalian olfactory system (Kawai et al., 2009). In fact, lesions of the terminal nerve cause deficits in male hamster mating behaviour, as well as abnormalities in male fish nest building behaviour (Wirsig and Leonard, 1987). This highlights the significant role played by the terminal nerve GnRH system in modifying how olfactory information is perceived, perhaps by altering the sensitivity to certain pheromones at reproductively auspicious times. In humans too, GnRH cells remain present in the olfactory epithelium throughout adulthood; however, their putative neuromodulatory role in this region remains speculative (Gonzalez-Martinez et al., 2004a).

3.1.2 Zebrafish GnRH system development: controversial origins

It has been extensively shown in amniotes that hypothalamic GnRH neurons originate in the olfactory placode, wherefrom they migrate across the nasal-forebrain junction, through the basal forebrain and into the hypothalamus during early development. This well-characterised 'migratory stream' is understood so well because the GnRH cells begin expressing GnRH soon after they are born in the medial olfactory placode (at E10.5 in the mouse, or stage 19 in the chick) and continue to express GnRH throughout their migratory route to the hypothalamus (Gonzalez-Martinez et al., 2004a).

In most amniotes studied, including the chick and mouse, the GnRH cells appear to begin their migration soon after the first olfactory axons have extended towards the forebrain, and they are then believed to migrate along this olfactory (or

vomeronasal) axonal scaffold towards the forebrain. An analogous stage during zebrafish development is between 24-48hpf, when the olfactory placodes have formed and olfactory axonogenesis has begun. However, the exact involvement of olfactory axonogenesis during GnRH system development is not well understood in the zebrafish. In fact, it is has even been proposed that the hypothalamic GnRH neurons do not originate from the olfactory placode in zebrafish, but have an anterior pituitary placode origin instead. Moreover, the terminal nerve and midbrain GnRH cells have been proposed to originate from cranial neural crest cells (Whitlock, 2005a), but this requires confirmation.

3.1.3 Two 'waves' of GnRH neuronal migration

During human embryogenesis, GnRH cells are first detected in the terminal nerve region from 6 weeks gestation (Carniege Stage 17, CS17); although studies have shown that they are actually 'born' at around 5.5 weeks (CS16) at the olfactory placode. By this stage, the olfactory axons have already established contact with the presumptive olfactory bulb anlage; however, actual olfactory bulb morphogenesis does not become truly distinct until around week 7 (CS19) (Gonzalez-Martinez et al., 2004a).

Comparable results were also found in the rhesus monkey, where it was shown that there are in fact two 'waves' of GnRH neuronal migration from the olfactory placode to the basal forebrain. At a stage equivalent to CS14, prior to olfactory bulb morphogenesis, the *'early wave'* of pioneer GnRH neurons establishes the migratory pathway; and this is followed by a *'later wave'* of GnRH migration around the time of olfactory bulb morphogenesis (as described above, in human embryos) (Cadman et al., 2007). This *later wave* of migrating GnRH neurons may form direct or indirect connections with the *early wave* GnRH neurons in order to reach the septo-preoptic hypothalamus, but this is yet to be fully established (Gonzalez-Martinez et al., 2004a). This work highlights the complexities of forebrain GnRH neuronal migration across different vertebrates, and emphasises that a 'migratory stream' of GnRH neurons occurring in association with olfactory

axonogenesis, may not always be the entire explanation for how the forebrain GnRH neuronal system is formed during embryogenesis.

3.1.4 The zebrafish olfactory system

In zebrafish, the olfactory placodes (OP) appear as thickenings of the ectoderm at approximately 17-18 hours post-fertilisation (hpf) (Whitlock and Westerfield, 2000). These thickenings then invaginate by 32hpf to form the naris (the external part of the nasal cavity/ nose). At 22-24hpf the first axons extend from the OP into the CNS at the presumptive olfactory bulb region; these are the pioneer neurons and they establish the preliminary olfactory pathway (labelled green in Figure 3.02A). The olfactory receptor neurons (ORNs, labelled red) extend their axons into the CNS, following the axons of the pioneer neurons (and thus replacing them) by approximately 48hpf, so that by 60hpf the outline of the zebrafish olfactory system has already been completed. In recent years, olfactory transgenic reporter fish have been developed, which has permitted 'real-time' fluorescent visualisation of these pioneer and secondary (ORN) olfactory neurons in living embryos (Whitlock and Westerfield, 1998).

Olfactory interneurons within the olfactory bulbs project their axons across the anterior commissure (Figure 3.02B-C), which allows communication between both sides of the olfactory system. In humans too, the anterior commissure serves to connect the two temporal lobes of the brain, but also contains decussating fibers from the olfactory tracts. As with other vertebrates, odorant perception is ultimately interpreted by higher regions of the brain, including the olfactory cortex, where the olfactory information has been relayed via the olfactory tract, which projects from the olfactory bulbs (Whitlock and Westerfield, 1998).

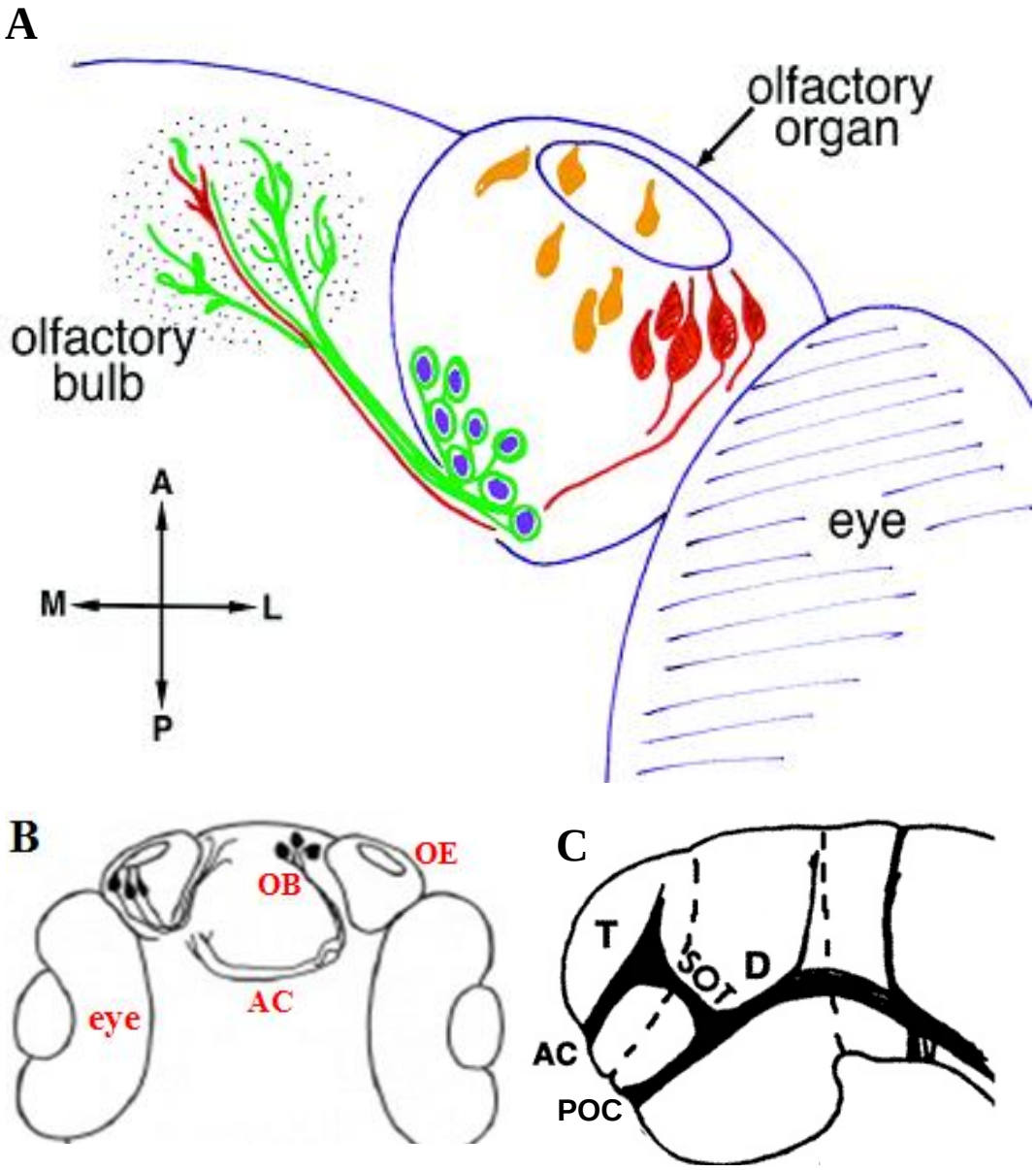

Figure 3.02 Zebrafish olfactory system development

A: Schematic diagram of the olfactory projections from one olfactory organ. Pioneer axons are labelled in green, and olfactory receptor neurons are labelled in red. **B**: Schematic diagram of the projections from the olfactory bulb interneurons which cross the anterior commissure.

C: Schematic diagram of the brain commissures at approx 24hpf; with the anterior commissure (AC) and post-optic commissure (POC) indicated in the telencephalon. *A and B are Ventral views; C is a lateral view.*

OB= olfactory bulb; OE= olfactory epithelium; T= telencephalon; D= diencephalon; SOT= supraoptic tract.

Figure 3.02 (A) is from Whitlock and Westerfield, 1998. Copyright 1998 by the Society for Neuroscience. Figure 3.02 (B) adapted with permission from Development (Whitlock and Westerfield, 2000).

3.1.5 Aims of this chapter

The proposal that terminal nerve and hypothalamic GnRH neurons have completely different origins and developmental pathways in the zebrafish, even though they appear to occupy positions along the same migratory route into the forebrain, remains controversial. To improve our understanding of zebrafish forebrain GnRH system development, and in turn establish a *'zebrafish model'* for studying the molecular pathogenesis of Kallmann syndrome, the following aims are set out for this chapter:

-To confirm spatial and temporal GnRH protein/ transcript expression during zebrafish early embryogenesis; and compare this expression with that from another teleost (the medaka) and an amniote (the chick).

- To generate, and spatio-temporally characterise a stable transgenic GnRH3 reporter zebrafish line, and use it to further understand GnRH neuronal migration to the hypothalamus, in '**real-time**'.

- To use olfactory transgenic reporter lines to characterise the involvement of olfactory and vomeronasal axonogenesis during forebrain GnRH neuronal migration.

-To obtain a greater understanding of the **origins** of the hypothalamic GnRH neurons, and ascertain whether or not they have an olfactory placodal origin in zebrafish.

-To investigate whether or not early embryonic upregulation of the kisspeptin/Gpr54 signalling pathway influences the development of the zebrafish GnRH neuronal system.

3.2 Results

3.2.1 GnRH expression in the zebrafish: from embryogenesis to adulthood

Adult GnRH immuno-expression

GnRH immuno-labelling on a para-sagittal section of a 3 month post-fertilisation (adult) zebrafish brain (Figure 3.03-A) demonstrated the expected three GnRH neuronal populations in the adult brain: at the telencephalon (terminal nerve/ olfactory region), diencephalon (preoptic area/hypothalamus), and the mesencephalon. There was also some unexpected immuno-labelling in other parts of the brain, including a very large cluster of cells at the centre of the rhombencephalon.

Beginning at the anterior of the adult forebrain ('TN', Figure 3.03-A), a few GnRH cells are detected along the olfactory nerve region (presumably in association with olfactory/ terminal nerve axonal fibres), projecting their axons throughout the whole of the olfactory bulb. These GnRH axons are then visualised coursing through the basal perimeter of the anterior telencephalon. Posteriorly, there is then a cluster of GnRH immuno-labelled cells in the preoptic area, as well as a large number of axonal processes throughout the posterior forebrain, including at the hypothalamic region. The GnRH immuno-labelled cells of the mesencephalon appear to mainly occupy the ventricular boundary regions of the tectum.

Embryonic GnRH immuno-expression

GnRH immuno-expression is first detected in zebrafish embryos from around 30-36hpf as a group of 3-6 cells medial to the olfactory pits; defined previously as the 'terminal nerve GnRH cells'. By 36hpf, these cells have extended axons towards the presumptive olfactory bulbs, and across both forebrain commissures: the anterior commissure (*towards top*, Figure 3.04A) and post-optic

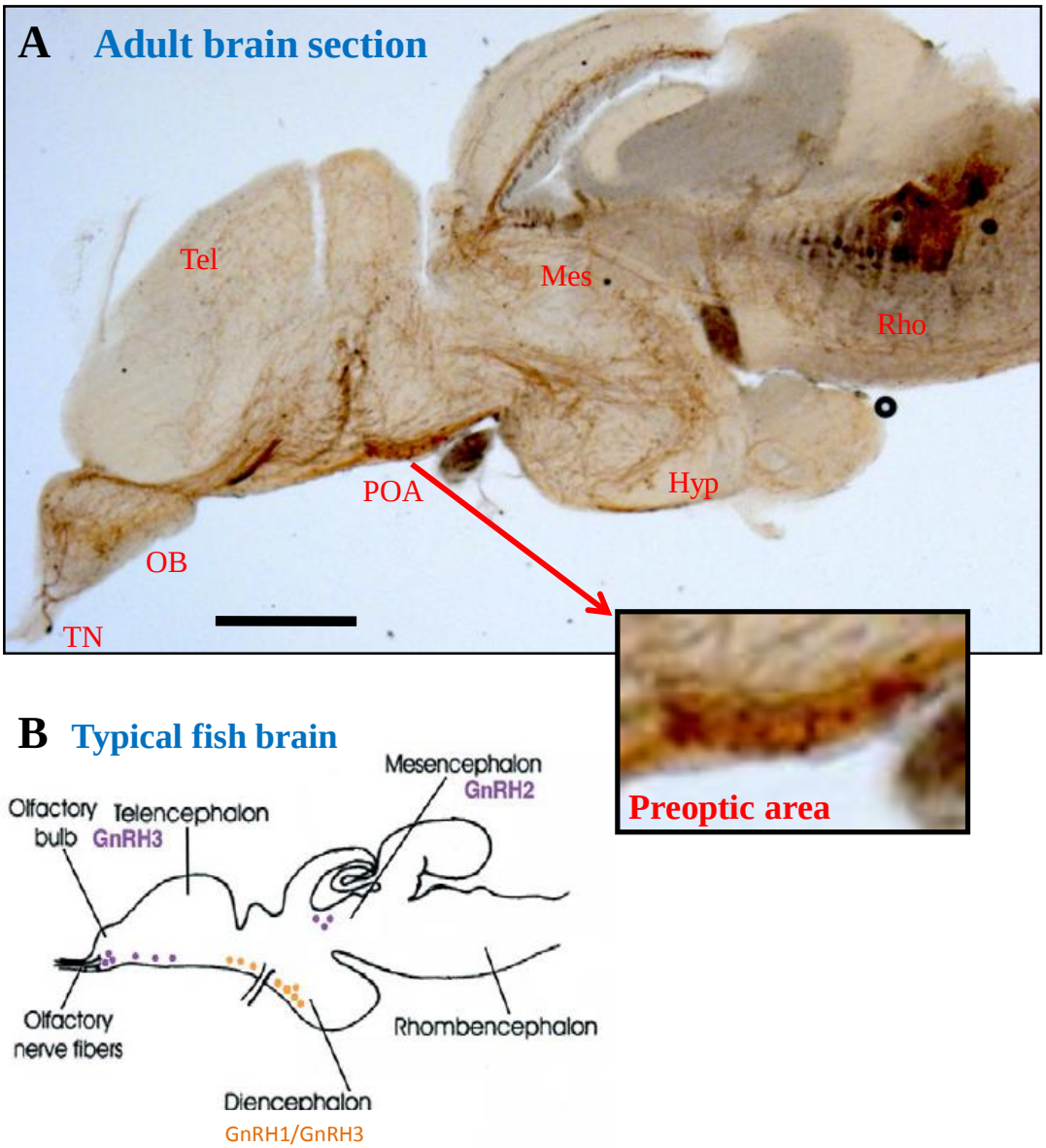

Figure 3.03 GnRH immuno-expression in the adult zebrafish brain

A: Anti-GnRH immuno-labelling in a parasagittal section of an adult (3 months post-fertilisation) female zebrafish brain. Anterior is to the left.

B: schematic of a typical adult fish brain. 'Purple dots' represent the neuromodulatory GnRH populations of the terminal nerve and midbrain; 'orange dots' represent the hypothalamic GnRH population.

Scale bar is 500µm.

TN= terminal nerve; OB= olfactory bulb; tel= telencephalon; POA= preoptic area; hyp= hypothalamus; mesencephalon; rhombencephalon. ***Figure 3.03 (B) modified from Trends Endocrinol. Metab 16, Whitlock,K.E, 'Origin and development of GnRH neurons.', pp. 145-151, Copyright 2005, with permission from Elsevier.***

commissure (*towards bottom*). These two forebrain commissures are illustrated in Figure 3.02C, from a lateral view; and, in Figure 3.02B, the olfactory bulb interneuronal projections which project across the anterior commissure are also demonstrated schematically.

By 60hpf, the same GnRH expression was visualised, except now there was also some GnRH immuno-labelling within retinal cells in the eyes (Figure 3.04B). Conspicuously, there were no GnRH-positive cells detected in the hypothalamus (*marked by an asterisk*) by 60hpf. Moreover, it was not possible to visualise the 'migrating' stream of hypothalamic GnRH cells which had previously been described at around 56hpf (Whitlock et al., 2005), using the same anti-GnRH antibody. To ensure that these 'migrating' GnRH cells were not over-looked, embryos were fixed between 36-60hpf at 4hr intervals and immuno-labelled exactly how Whitlock and colleagues had described; this included using a HRP-conjugated secondary antibody with peroxidase anti-peroxidase ('PAP') amplification and subsequent DAB colour reaction. However, it was still not possible to detect these 'migrating' hypothalamic GnRH cells or indeed any hypothalamic GnRH cells at all, as seen in the representative image at 60hpf (Figure 3.04B'). In fact, PAP amplification with DAB gave even less GnRH immuno-labelling than using a fluorescently-labelled secondary antibody, which, as mentioned above, also labelled the forebrain commissure projections.

By 6dpf, there is still GnRH immuno-labelling at the terminal nerve, as well as GnRH-positive neuronal tracts extending across both forebrain commissures and the optic nerve (Figure 3.04C). Furthermore, there are also some GnRH-positive cells behind the eyes (indicated by an asterisk in Figure 3.04C), which may be trigeminal ganglion cell bodies. However, even by 6dpf it was still not possible to detect any GnRH-positive cell bodies in the hypothalamic region. To investigate whether *'incomplete antibody penetration'* could be the reason for this, GnRH immuno-labelling was carried out on 10μm-thick sagittal cryostat sections of 60hpf (data not shown) and 6dpf (Figure 3.04D) embryos, in order to increase the exposure of the hypothalamic GnRH antigen to the anti-GnRH antibody. However, after checking all sagittal sections, only GnRH-positive terminal nerve cells could be detected at these stages.

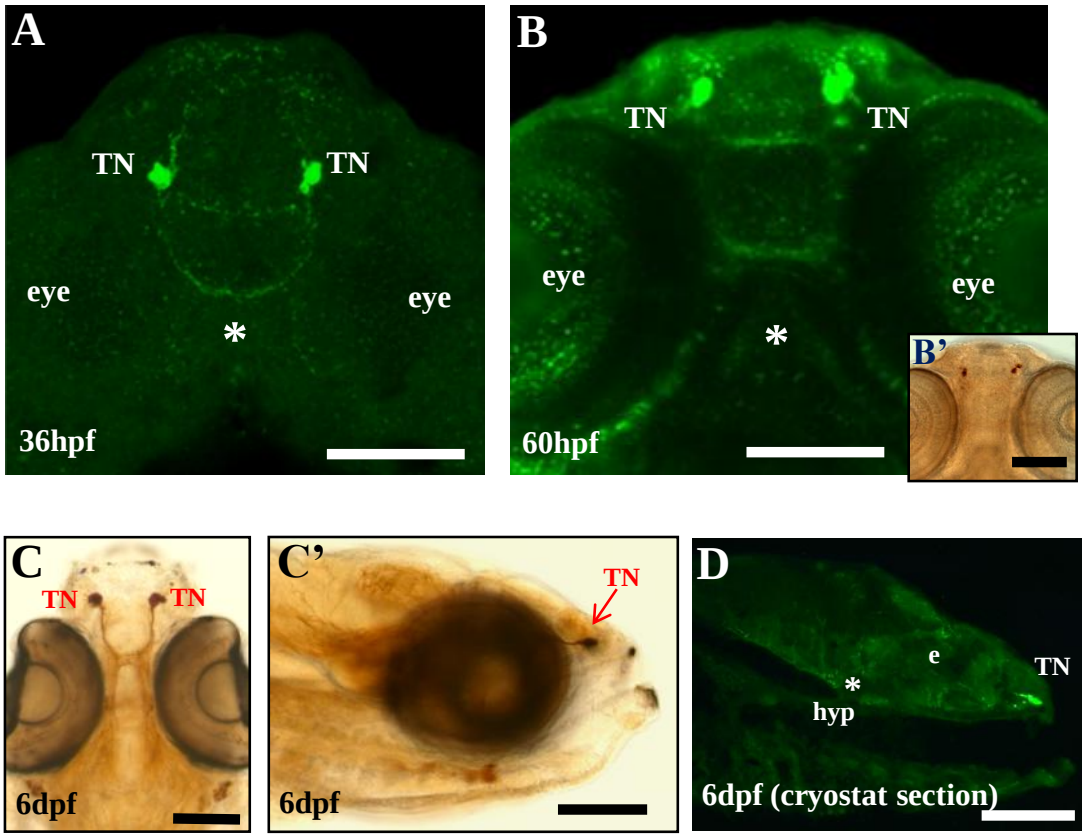

Figure 3.04 GnRH immuno-expression during zebrafish embryonic development

Anti-GnRH immuno-labelling in zebrafish embryos at 36hpf (A), 60hpf (B) and 6dpf (C, C', D). A, B, and D are confocal images; B', C, and C' were treated with DAB and visualised using light microscopy. A-C are ventral views; C' is a lateral view, and D is a parasagittal cryostat section. The asterisk in A, B and D indicates the centre of the hypothalamic region.
Scale bars are 100µm.
TN= terminal nerve; hyp= hypothalamus; e=eye

Throughout this project phenylthiourea (PTU) was added to the zebrafish embryos to keep them pigment-free beyond 24hpf, thereby keeping the embryos transparent and making microscopy/ photography easier. There have been some reports that PTU disrupts thyroid hormone production at the thyroid in developing zebrafish (Elsalini and Rohr, 2003). To ensure that PTU was not interfering with GnRH production at the hypothalamus as well, some embryos were allowed to develop in PTU-free water, and immuno-labelled for GnRH at 36hpf, 60hpf, and 6dpf. However, the resulting GnRH immuno-labelling was the same as that shown for the PTU-treated embryos shown in Figure 3.04.

GnRH3 & GnRH2 mRNA expression

Zebrafish have just two GnRH genes: GnRH3 and GnRH2. *In situ* hybridisation analysis using GnRH2 and GnRH3 antisense probes was carried out on zebrafish embryos from 1-15dpf. GnRH3 transcript was first detected at around 30hpf in the terminal nerve region (Figure 3.05A) and this expression persisted through to 60hpf (Figure 3.05B) and 6dpf (Figure 3.05C). Post-*in situ* GnRH immuno-labelling demonstrated that GnRH3 transcript is localised to the same cells in the terminal nerve that were GnRH immuno-labelled (Figure 3.05B'). Most GnRH3 transcript remains localised to the terminal nerve region by 6dpf (Figure 3.05C), except in one anomalous case (n=1/24) where there was some GnRH3 *in situ* labelling in the diencephalic region by this stage (Figure 3.05D). By 15dpf, GnRH3 transcript remains localised to the terminal nerve/olfactory region, but labelling is faint and is obscured by pigment cells in Figure 3.05E. There is also some faint GnRH3 *in situ* labelling in the diencephalic-midbrain region at 15dpf (Figure 3.05E').

GnRH2 transcript was first detected in the midbrain region at 30hpf (Figure 3.05F), and remained localised to this region at 60hpf, 6dpf, and 15dpf (Figure 3.05G-J). However, post-*in situ* GnRH immuno-labelling at 60hpf failed to co-label any midbrain cells expressing GnRH2 transcript. Notably, there was some GnRH2 *in situ* labelling at the anterior commissure region in the forebrain at 60hpf and 15dpf, which closely abuts the GnRH immuno-labelled terminal nerve GnRH3 cells.

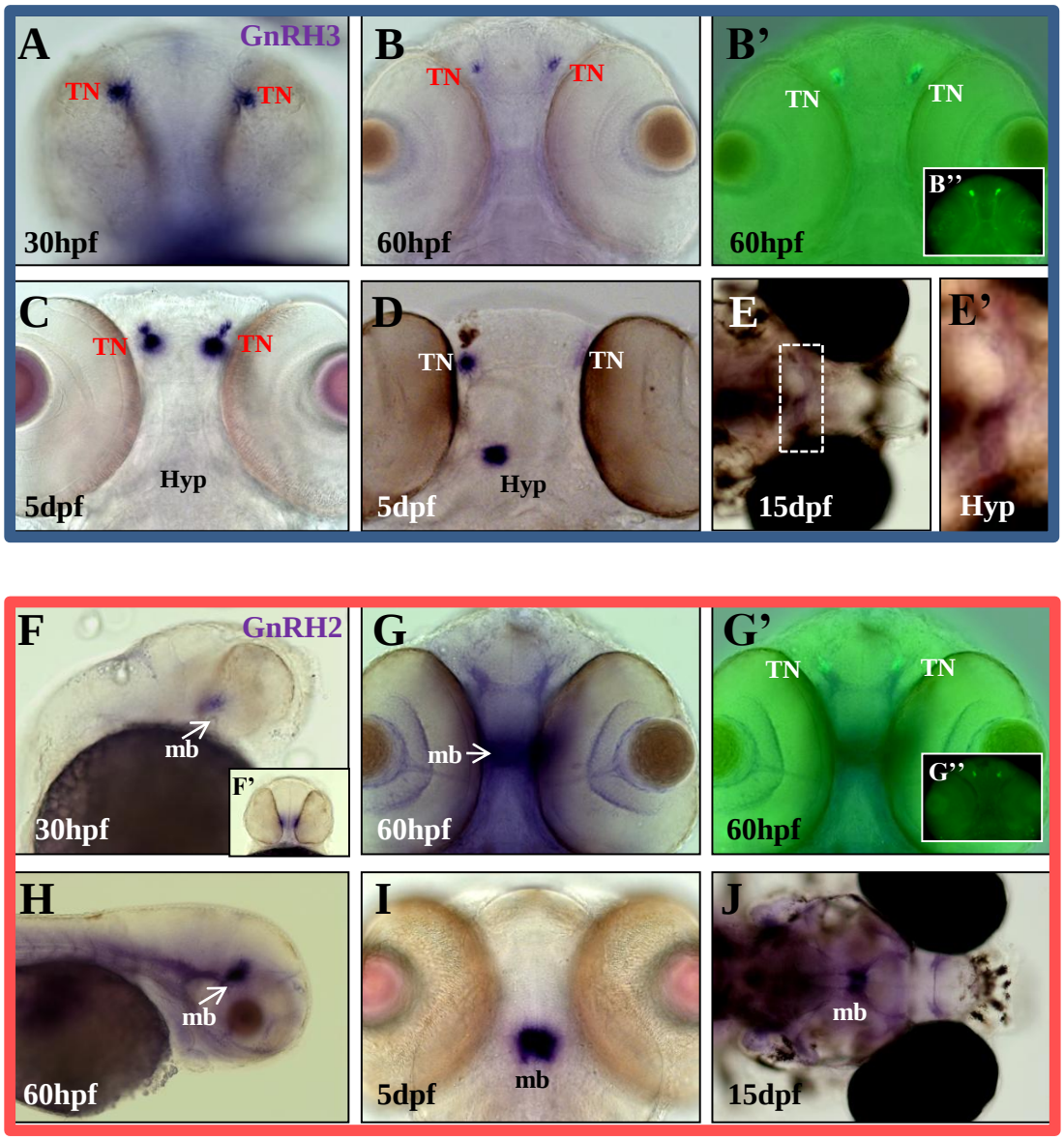

Figure 3.05 Zebrafish GnRH3 & GnRH2 *in situ* hybridisation expression analysis

Expression of GnRH3 (A-E) and GnRH2 (F-J) at 30hpf (A, F), 60hpf (B, H), 5dpf (C, D, I) and 15dpf (E, J). A-E are ventral views; F and H are lateral views; G, I, and J are dorsal views. B' and G' show the overlay of anti-GnRH expression (shown inset: B'' and G'') with GnRH3 (B) and GnRH2 (G) transcript, respectively. The dotted box in E indicates the hypothalamic region which is shown in more detail in E', demonstrating very weak labelling.
TN= terminal nerve; hyp= hypothalamus; mb= midbrain

3.2.2 GnRH expression in another teleost (medaka fish) and an amniote (the chick)

Embryogenesis proceeds more slowly in the medaka, and by 2dpf there is no GnRH immuno-labelling in the forebrain; however, there was some immuno-reactivity in the midbrain (Figure 3.06A), but this is no longer apparent from 3dpf onwards. At 3dpf terminal nerve GnRH immuno-labelling is first detected (Figure 3.06B), and remains present at 5dpf (Figure 3.06C) and through to 7dpf (Figure 3.06D). By 7dpf there is also GnRH immuno-reactivity in 2-4 cells in the hypothalamic region, as indicated by arrows in Figure 3.06D''.

Zebrafish and medaka both have GnRH2 and GnRH3 genes; however, medaka also have a third GnRH gene (GnRH1), which is homologous to the human GnRH1 gene; the form expressed by human hypothalamic GnRH neurons. Medaka GnRH1 and GnRH3 GFP-reporter plasmids provided to us (Okubo et al., 2006) were injected in to one-cell stage *zebrafish* embryos. These injected zebrafish embryos were then allowed to develop to 48hpf, and then subsequently fixed and subjected to GnRH immuno-labelling (Figure 3.07). Some embryos were also allowed to grow until 4dpf, but were found to lack any GFP expression by this stage, so were not analysed further. Zebrafish injected with either the GnRH1 or GnRH3 medaka reporter constructs showed GFP fluorescence in the terminal nerve cells, as confirmed by GnRH co-immuno-labelling of these cells. The pGnRH1(medaka):GFP-injected zebrafish embryos also had some telencephalic GFP fluorescent cells (Figure 3.07A), whilst those injected with pGnRH3(medaka):GFP showed some optic nerve GFP-fluorescence (Figure 3.07B). Furthermore, both constructs showed some GFP fluorescence in external epithelial cells, and, occasionally, in muscle-like cells along the trunk *(*data not shown*)*. However, these latter occurrences of GFP fluorescence, whilst reproduceable, were not corroborated by anti-GnRH immuno-labelling, and could therefore just be experimental artefacts.

GnRH immuno-labelling was also carried out on chick embryos at embryonic days 4 and 5 (E4 and E5), to permit a comparison of amniote and fish

GnRH system ontogenies, whilst also testing the reliability of the anti-GnRH antibody (LRH13). Weak GnRH immuno-labelling was first visualised in the olfactory epithelium of E4 chick embryos, Hamburger-Hamilton (HH) stage 20 (data not shown). However, the GnRH immuno-labelling becomes much more prominent in the olfactory epithelium of E5 (HH St.26) embryos, as shown in a parasagittal section in Figure 3.06E. A 'stream' of GnRH immuno-reactive cells can be seen along the entire process of the olfactory nerve as it extends towards the telencephalon (Figure 3.06E'); although the telencephalon is not present in this section, it is located at the same level as the eye in subsequent sections *(not shown)*.

3.2.3 Generation and characterisation of a zebrafish pGnRH3:mCherry reporter line

A 2.4kb genomic fragment of zebrafish GnRH3 promoter sequence (as determined previously (Palevitch et al., 2007)) was amplified and cloned upstream of mCherry coding sequence, flanked by two I-SceI recognition sites in a modified pBUT3 plasmid (Figure 3.08A). Approximately 100 wild-type embryos were injected with this pGnRH3:mCherry ('G3MC') construct at the one-cell stage, using the I-SceI meganuclease approach (Rembold et al., 2006). These injected 'F0' embryos were screened by fluorescence microscopy at 48hpf (Figure 3.08B), and 52 were transferred to the fish nursery and grown to adulthood (i.e. beyond 3 months post-fertilisation). Of the 33 embryos that survived to adulthood, 4 stable transgenic G3MC carriers were isolated and named G3MC1 (strongest red fluorescence) through to G3MC4 (weakest fluorescence). All four carriers were outcrossed to wild-type fish, and their 'F1' progeny were grown to adulthood and used to generate the 'F2'G3MC embryos that were used for the experiments in this thesis.

The mCherry fluorescence pattern for all four carriers were carefully compared with each other, and were found to be identical (both spatially and temporally), despite the difference in fluorescence intensity between the four groups. Therefore, only G3MC-1 (now just called 'G3MC') was used for all subsequent analysis and experiments because it showed the strongest G3MC

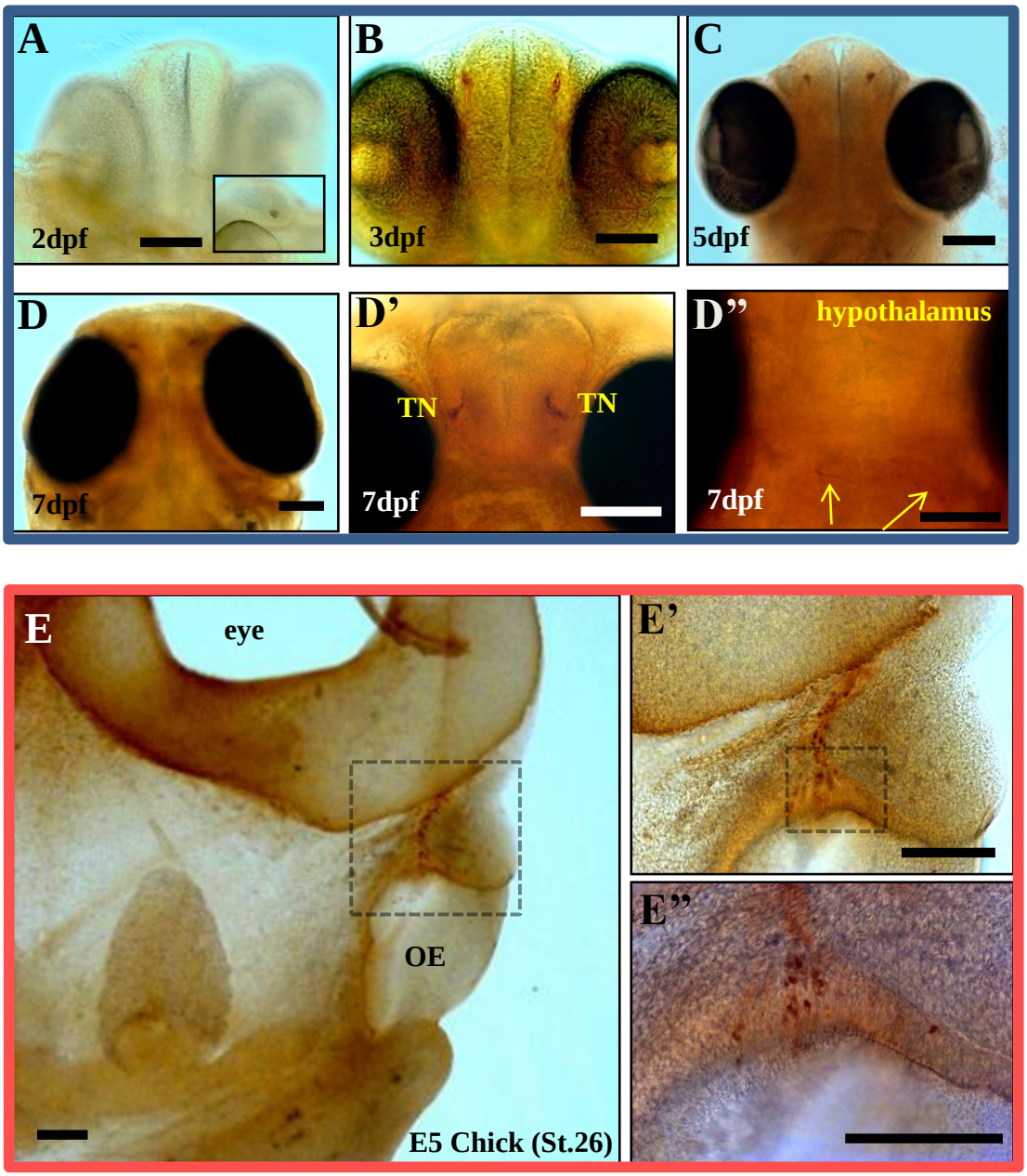

Figure 3.06 GnRH immuno-expression in another teleost (medaka fish) and an amniote (the chick)

Anti-GnRH immuno-labelling in medaka embryos at 2dpf (A), 3dpf (B), 5dpf (C) and 7dpf (D); and an E5 (Hamburger-Hamilton stage 26) chick embryo sagittal section (E). A-D and D'' are ventral views; in D' the anterior axis is projecting from the page. The inset in A shows midbrain labeling. D'': Yellow arrows indicate two hypothalamic immuno-stained cells. E-E'': the dotted boxes indicate the area which is amplified in the subsequent picture. Scale bars are 100μm (A-D) and 250μm (E)

TN= terminal nerve; OE= olfactory epithelium, E5= embryonic day 5

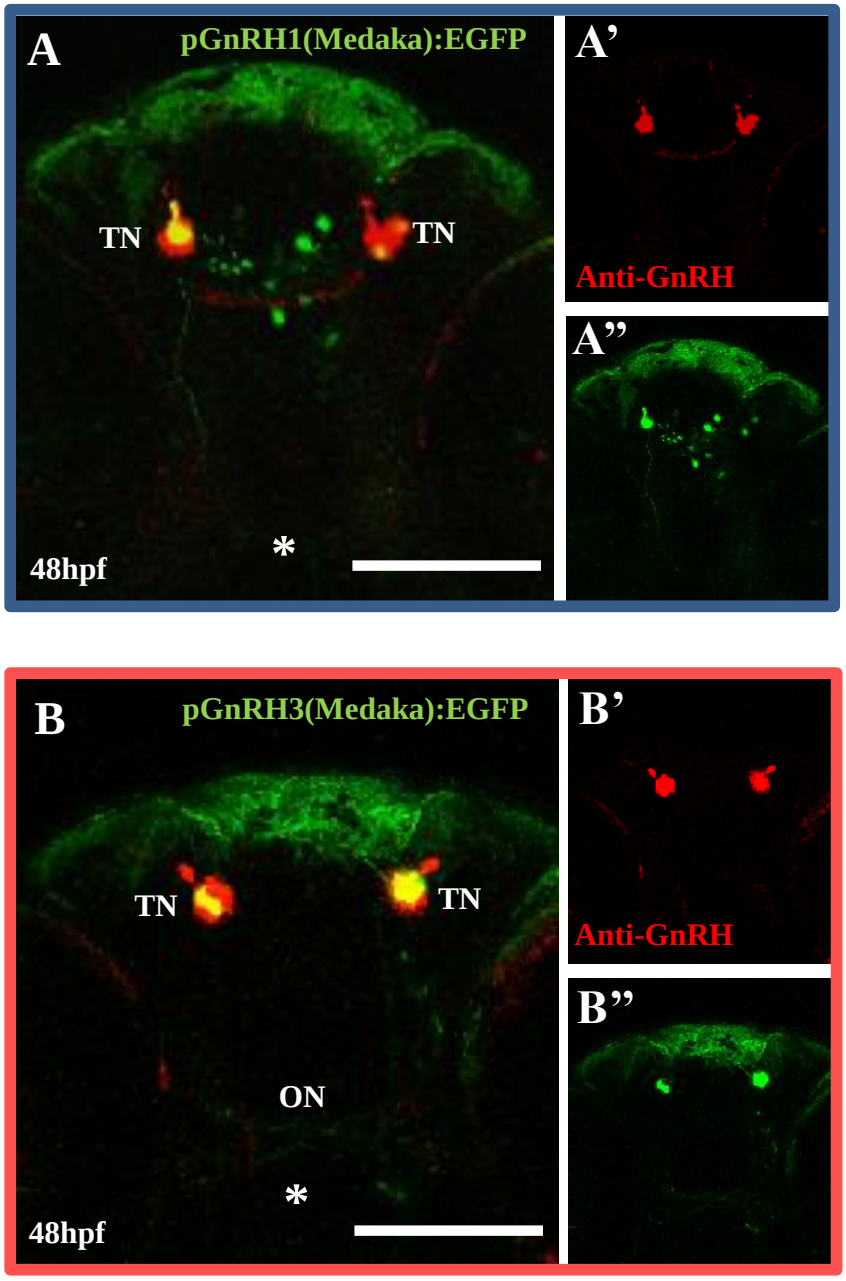

Figure 3.07 Transient expression of medaka pGnRH1:GFP and pGnRH3:GFP reporter constructs in the zebrafish

A'' and B'': zebrafish transiently expressing pGnRH1:GFP and pGnRH3:GFP constructs, respectively (shown in green). A' and B' shows the corresponding anti-GnRH expression (in red) in these embryos; and the overlay of this is shown in A and B, respectively. All views are ventral and are at 48hpf. An asterisk indicates the hypothalamic region.
Scale bars are 100μm.
TN= terminal nerve; ON= optic nerve

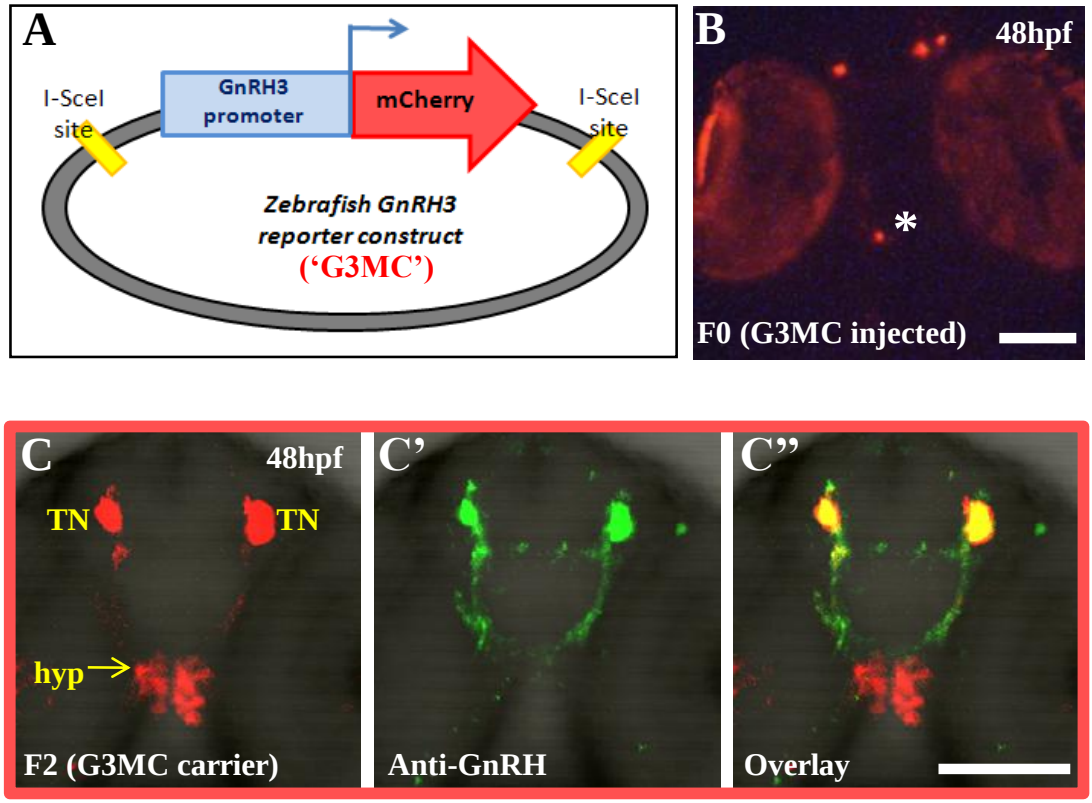

Figure 3.08 Generation of a zebrafish pGnRH3:mCherry reporter line

A: Schematic of the zebrafish 'pGnRH3:mcherry' plasmid (abbreviated as 'G3MC'). B: An example of a G3MC-injected embryo at 48hpf: an asterisk indicates the hypothalamic region. C is a ventral view at 48hpf of a G3MC stable transgenic (in red). C' shows anti-GnRH immuno-staining of the same embryo (in green): and C'' shows the overlay. Scale bar 100µm.
TN= terminal nerve; hyp= hypothalamus

fluorescence. This also helped to ensure that all G3MC phenotypes were consistent, and therefore comparable (that is assuming that there were no male/ female differences in GnRH3 expression during embryogenesis).

To begin with, a time-course of mCherry fluorescence between 0hpf and 120hpf was carried out in order to characterise the G3MC stable transgenic line (Figure 3.09). At least six embryos were visualised for each time-point, and the representative image for each is shown. mCherry fluorescence was first detected at 20hpf in 2-4 cells at the dorsal part of the anterior neural tube (Figure 3.09A). By 24hpf, there is now mCherry expression in 1-2 cells at the terminal nerve on one or both sides, directly medial to the olfactory pits (Figure 3.09B). By 26hpf, there are 2-4 mCherry-positive terminal nerve cells on each side and they begin to project ventrally and/or dorsally to targets within the forebrain (Figure 3.09C). From around 28hpf, some of these ventral projections extend across the forming anterior commissure in the telencephalon, whilst others project more caudally towards the diencephalon, across the developing post-optic commissure (Figure 3.09D). By 32hpf, some mCherry-positive axons have now extended across the midline, traversing both forebrain commissures and the supra-optic tract (Figure 3.09F).

From a lateral view at 30hpf, another group of mCherry cells behind the eyes become apparent: the trigeminal ganglion cells. These cells project to several targets in the midbrain, hindbrain and spinal cord/trunk (Figure 3.09E).

From 32hpf (Figure 3.09E), mCherry cells begin to accumulate in the diencephalon, and by 36hpf (Figure 3.09G, G') they number between 20-50 cells, with an average of approximately 40 cells per embryo (cell counts were estimated to within an accuracy of 5 cells, across 20 different 36hpf embryos).

By 60hpf, the presumptive hypothalamic mCherry cell number and position is similar to that specified for the 36hpf time-point; however, the fluorescence intensity is somewhat reduced, so some of the previously weak-fluorescent cells may no longer be detectable by 60hpf (Figure 3.09H). In contrast, the terminal nerve mCherry cells and associated forebrain tracts remain intensely fluorescent at 60hpf, as do the retinal mCherry cells and their associated optic nerve projections which had first became apparent at around 36hpf (Figure 3.09G, H). By 120hpf, the

Figure 3.09 Temporal characterisation of the pGnRH3:mCherry stable transgenic line

The F2 generation from the G3MC carrier (out of a total of four carriers) with the brightest fluorescence is shown here, and was used for all experiments henceforward.

Except I, J and J' (which are light microscopy images), A-I' all show confocal images of representative live-mounted G3MC embryos at 20hpf (A), 24hpf (B), 26hpf (C; *showing terminal nerve detail*), 28hpf (D), 30hpf (E), 32hpf (F), 36hpf (G; *with hypothalamic cells shown in more detail in G'*), 60hpf (H), 120hpf (I'). J and J' show a fixed 60hpf embryo that was immuno-stained with anti-mCherry, as shown by brown DAB precipitate.
A-D, F-H, and J are ventral views; E and J' are lateral views; I and I' are dorsal views. The dotted box in J and J' indicates the hypothalamic mCherry-positive cells at 60hpf from ventral and lateral views, respectively.
Scale bars are 100μm.
OE= olfactory epithelium; TN= terminal nerve; AC= anterior commissure; POC= post-optic commissure; Tg= trigeminal ganglion; hyp= hypothalamus; OC= optic chiasm

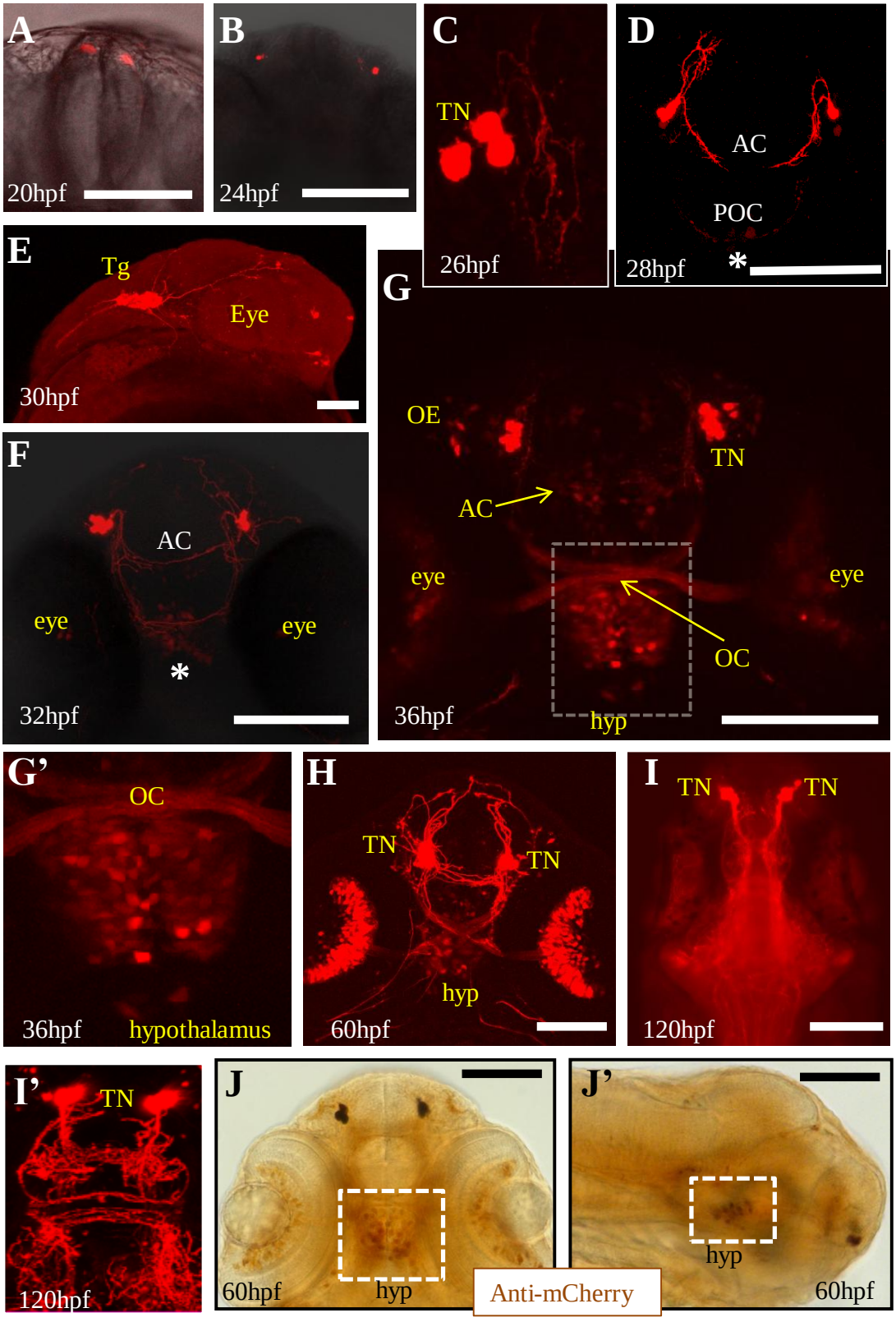

Figure 3.09 Temporal characterisation of the pGnRH3:mCherry stable transgenic line

terminal nerve and trigeminal ganglion mCherry cells have remained intensely fluorescent (Figure 3.09I), and there are extensive mCherry-positive axonal tracts across several commissures throughout the whole brain, but it is less easy to decipher which of these has emanated from the two aforementioned mCherry cell clusters, or perhaps new mCherry neuronal populations (Figure 3.09I'). By 120hpf, it was no longer possible to distinguish a hypothalamic cluster of mCherry cells, presumably because they had, by then, stopped expressing mCherry.

mCherry immuno-labelling (with DAB colour reaction) was carried out to confirm the localisation of the diencephalic mCherry cluster by 60hpf (Figure 3.09J, J'). From these ventral and lateral views of the same embryo, it is immediately apparent that this cluster is indeed located within the hypothalamic region of the brain. To take this one step further, a hypothalamic-region reporter line, pNkx2.1a:YFP, was crossed with G3MC and the resulting embryos were visualised at 32hpf and 60hpf (Figure 3.09J, J'). At 32hpf, the initial diencephalic mCherry cells are located within a cluster of Nkx2.1a (YFP-expressing) hypothalamic cells (Figure 3.10A) and remain so by 60hpf (Figure 3.10B), despite the increment in G3MC cell number in this region. Conspicuously, none of the hypothalamic G3MC cells actually co-express Nkx2.1a (YFP), as demonstrated in the inset, although they are clearly located within the exact same brain region (the hypothalamus).

Finally, parasagittal sections of an adult zebrafish G3MC (3 months post-fertilisation) whole brain were analysed for mCherry (GnRH3) expression (Figure 3.11). To permit straightforward comparisons with the GnRH-immuno-labelled brain in Figure 3.03A, a female brain was again used. Consistently, mCherry expressing cells located along the olfactory nerve and anterior limit of the olfactory bulb, presumably the terminal nerve GnRH cells, were found to project to regions throughout the olfactory bulb (*not present in section shown*), as well as along the basal part of the anterior telencephalon, towards the preoptic area (Figure 3.11A''). Within the preoptic area, and to a lesser extent within the anterior hypothalamus, scattered GnRH cells were also detected, mainly along the basal parts (Figure 3.11'). There were some other regions, especially in the mesencephalon, which had some mCherry expression, but for the most part it was not cellular.

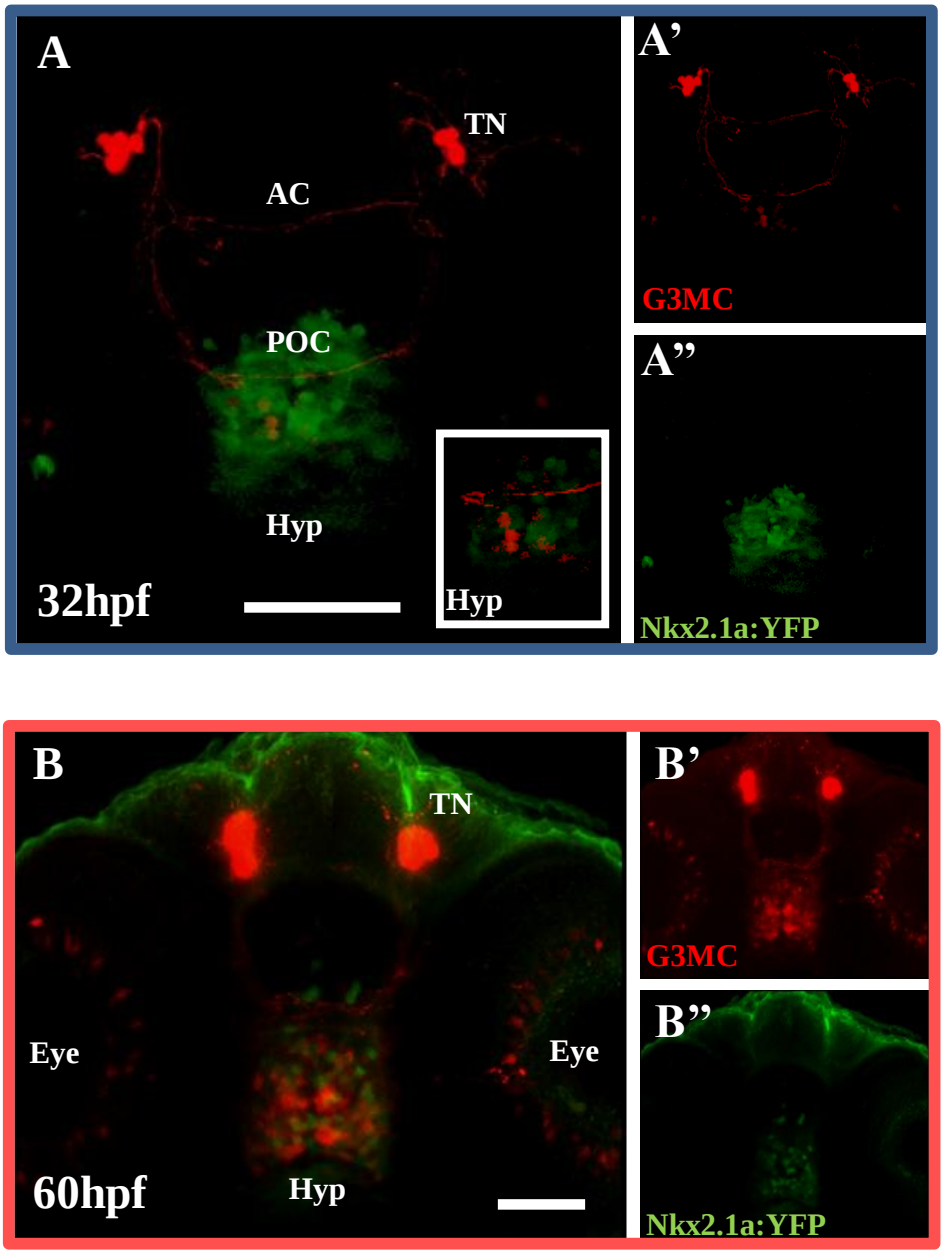

Figure 3.10 Confirming regional identity for the presumptive hypothalamic population in G3MC

G3MC was crossed with a hypothalamic reporter line: Nkx2.1a:YFP (shown in green). Ventral views of this cross are shown in A and B; at 32hpf and 60hpf, respectively. The corresponding images of G3MC alone (A' and B') and Nkx2.1a:YFP alone (A'' and B'') are also shown. The inset in A shows a single Z-layer from the corresponding total confocal stack in A; demonstrating a lack of overlay between individual mCherry-positive cells and Nkx2.1a:YFP cells within the hypothalamus. Scale bars are 100µm.
TN= terminal nerve; AC= anterior commissure; POC= post-optic commissure; hyp= hypothalamus

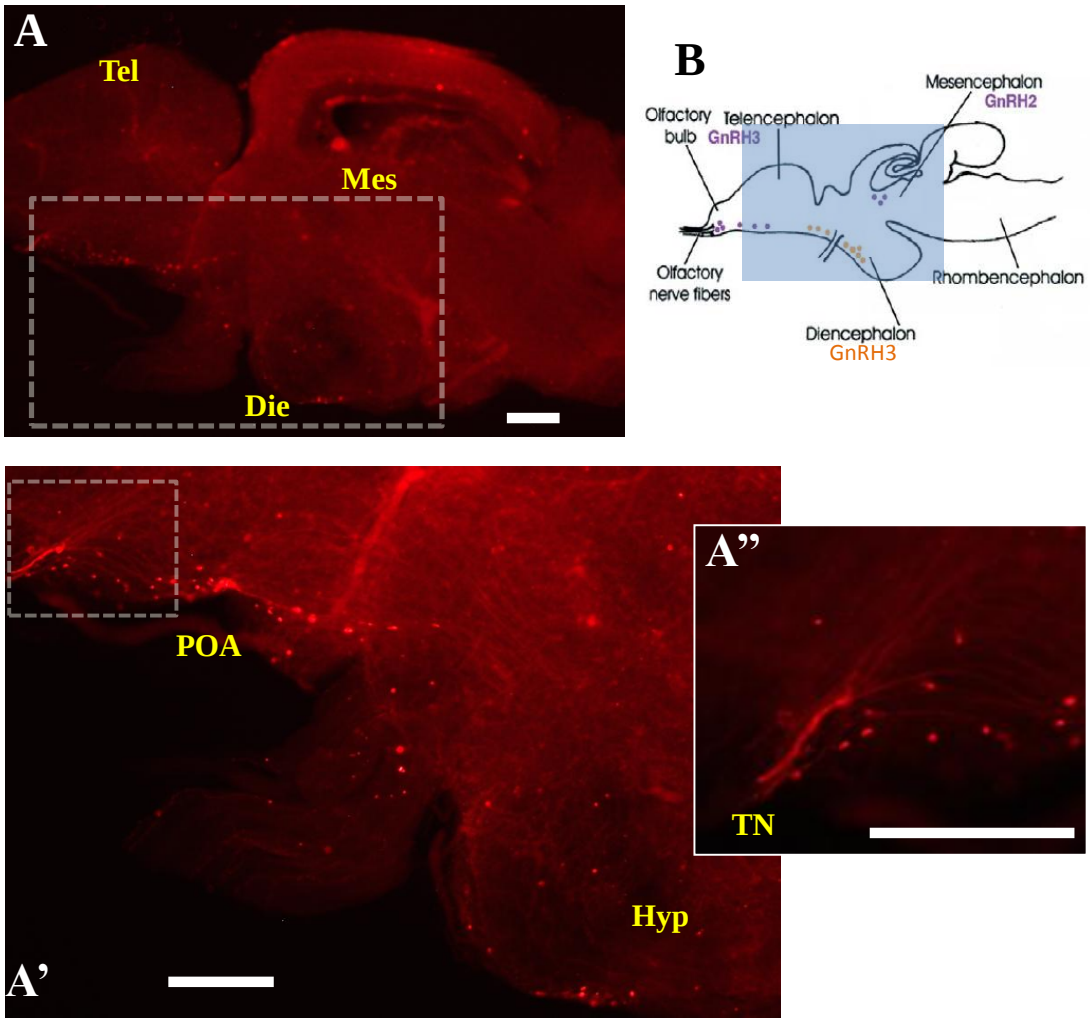

Figure 3.11 mCherry expression in an adult G3MC brain

A: Parasagittal section of an adult (3 months post-fertilisation) female G3MC brain. Anterior is to the left. **B**: Schematic of an adult fish brain (see 3.02(b) for more details). The blue shaded area in B indicates the region of the brain which is shown in A. The dotted box in A demarks the telencephalic-diencephalic area which is shown in more detail in A'; in turn, the terminal nerve region demarked in A' is then shown in more detail in A''. Scale bar is 250µm.

Tel= telencephalon; Mes= mesencephalon; Die= Diencephalon; POA= preoptic area; hyp= hypothalamus; TN=terminal nerve.

Figure 3.11 (B) modified from Trends Endocrinol. Metab 16, Whitlock,K.E, 'Origin and development of GnRH neurons.', pp. 145-151, Copyright 2005, with permission from Elsevier.

GnRH immuno-labelling was carried out on G3MC embryos at 48hpf to confirm the specificity of the mCherry fluorescence, i.e. whether it was reliably reporting GnRH3 expression (Figure 3.08C). Unfortunately it was not possible to use anti-mCherry to boost the mCherry fluorescence (post-fixation) because this antibody was not compatible with the anti-GnRH immuno-labelling protocol (and *vice versa*). However, the remaining mCherry fluorescence in the terminal nerve cells was sufficient to allow complete overlay with GnRH-immunoreactivity in these cells, and thus verifying their GnRH3 neuronal identity. However, as expected (*see Figure 3.04B*), there was no GnRH immuno-labelling of the mCherry-positive hypothalamic cells, meaning that these cells could not be definitively authenticated as '*real'* hypothalamic (i.e. hypophysiotropic) GnRH cells, using this strategy.

3.2.4 The relationship between olfactory axonogenesis and early GnRH system development

OMP (olfactory marker protein) is an early marker for a major subset of olfactory receptor neurons (ORNs), and the OMP promoter (pOMP) was previously shown to be a very reliable reporter for early olfactory axonogenesis (Yoshida et al., 2002). Here, the pOMP:TauEGFP transgene ('OMPG'), provided by M. Mishina (Yoshida et al., 2002), was sub-cloned into a pBUT3 plasmid, so that it became flanked by two I-SceI recognition sites (Figure 3.12A), and then micro-injected into 100 wild-type embryos (Figure 3.12B); once again using the I-SceI meganuclease strategy. However, on this occasion, of the 37 F0 adults that were screened, only one stable transgenic OMPG fish was identified. Unfortunately, in the subsequent OMPG F1/F2 offspring, initiation of GFP expression within the ORNs was a day later than previously reported by M. Mishina, i.e. from 48hpf onwards, instead of the expected 24hpf onwards. This was sufficient to label the secondary 'mature' ORNs at 60hpf (Figure 3.12C) and 96hpf (Figure 3.12D), but was inadequate for labelling the pioneer ORNs which are present between 24hpf and 36hpf.

Fortunately, M. Mishina later agreed to provide us with their strain of stable transgenic OMPG fish which showed GFP expression in the ORNs from around 24hpf onwards (when pioneer ORN axonogenesis is initiated), and this OMPG

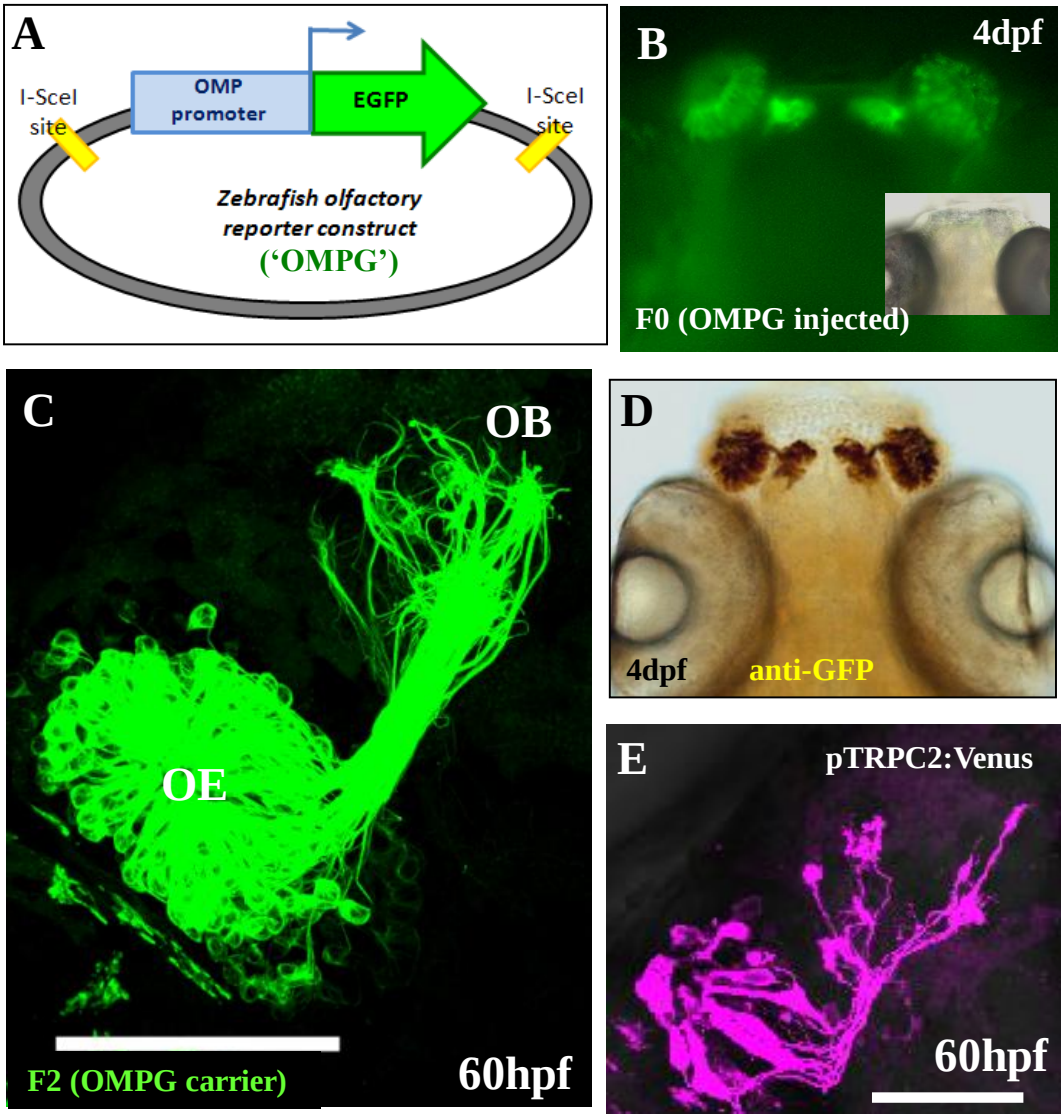

Figure 3.12 Generation of a zebrafish olfactory reporter line

A: Schematic of the zebrafish 'pOMP:EGFP' plasmid (abbreviated as 'OMPG'). B: An example of an OMPG-injected embryo at 4dpf, with an inset indicating the morphology of the embryo. C shows a single olfactory pit from a 60hpf OMPG stable transgenic (in green). D: Anti-GFP immuno-stained OMPG embryo at 4dpf (brown DAB precipitate). Whilst OMPG labels a 'ciliated-type' of olfactory sensory neuron (OSN), the pTRPC2:Venus transgenic line labels a mutually exclusive 'microvillous-type' ('vomeronasal-type') of OSN. To emphasize that these two types of OSN are entirely separate, the TRPC2:venus olfactory pit in E (at 60hpf) is shown in 'magenta'.
Scale bars are 50μm. *OE= olfactory epithelium; OB= olfactory bulb.*

strain was used for all subsequent experiments in this thesis. Furthermore, Y.Yoshihara (Sato et al., 2005) kindly agreed to provide another stable transgenic line: pTRPC2:Venus, which labels a *mutually exclusive* 'micro-villous type' ('vomeronasal-type') of ORN, in contrast to the 'ciliated-type' of ORN labelled by OMPG. In Figure 3.12E, the TRPC2-positive ORNs are re-coloured in 'magenta' to emphasise that these ORNs are an entirely separate subset, which show *no overlap* with those labelled by OMPG (Figure 3.12C).

To investigate possible co-development of the G3MC terminal nerve cells with olfactory axonogenesis, the OMPG line was crossed with G3MC (Figure 3.13). Expression of both GFP (OMP) and mCherry (GnRH3) was first detected from around 24hpf, in embryos that had inherited both transgenes (Figure 3.13). By 24hpf, olfactory axonogenesis has already begun, and a tightly fasciculated bundle of olfactory axons can be seen projecting towards the olfactory bulbs (Figure 3.13A). At this stage, one or two terminal nerve G3MC cells are located medial to the olfactory epithelium, below where the olfactory axons are seen to emanate from the olfactory pit. However, despite this close proximately, there was no co-expression of GFP (OMP) and mCherry (GnRH3) detected at this stage.

In Figure 3.13B (at 28hpf) a small cluster of four terminal nerve G3MC cells (and up to four other low-expressing cells, on this occasion) are seen projecting **towards** (dorso-caudally) the ORN fasciculated bundle and also directly **away** from it. Figure 3.13C (at 32hpf) demonstrates this asymmetry that is often found during *early* terminal nerve axonogenesis, but is no longer noticeable by 60hpf onwards. There is no bias for this asymmetry; however, in the case of Figure 3.13C, on the *left* side, the terminal nerve projections are seen extending further dorso-caudally across the entire length of the olfactory axonal bundle, all the way to the presumptive olfactory bulb region of the telencephalon. This is in contrast to the *right* side where the axons do not extend as far dorso-caudally and 'loop back' towards more caudal-ventral parts of the forebrain, as happens on the left side as well, to a lesser degree. Moreover, some axons were seen 'looping back around' the olfactory pit itself, thus highlighting the seemingly close interactivity between the olfactory and terminal nerve GnRH systems.

Figure 3.13 Co-development of the G3MC terminal nerve and OMPG olfactory projections

G3MC (in red) was crossed with OMPG (in green) and a representative image of one olfactory pit (A, B, D) or both pits (C) is shown at 24hpf (A), 28hpf (B), 32hpf (C), and 36hpf (D). All olfactory pits were visualised by confocal microscopy from a ventral view. A 3D-rendered image (using BioView3D software) is shown in A. D' shows OMPG alone and D' shows G3MC alone at 36hpf; whilst the overlay of the two is shown in D''. The dotted box in D highlights a single cell which co-expresses OMPG (GFP; in the membrane) and G3MC (mCherry) throughout the cell: in the inset this is shown in more detail as a single Z-layer from the total confocal Z-stack. Scale bars are 25μm.

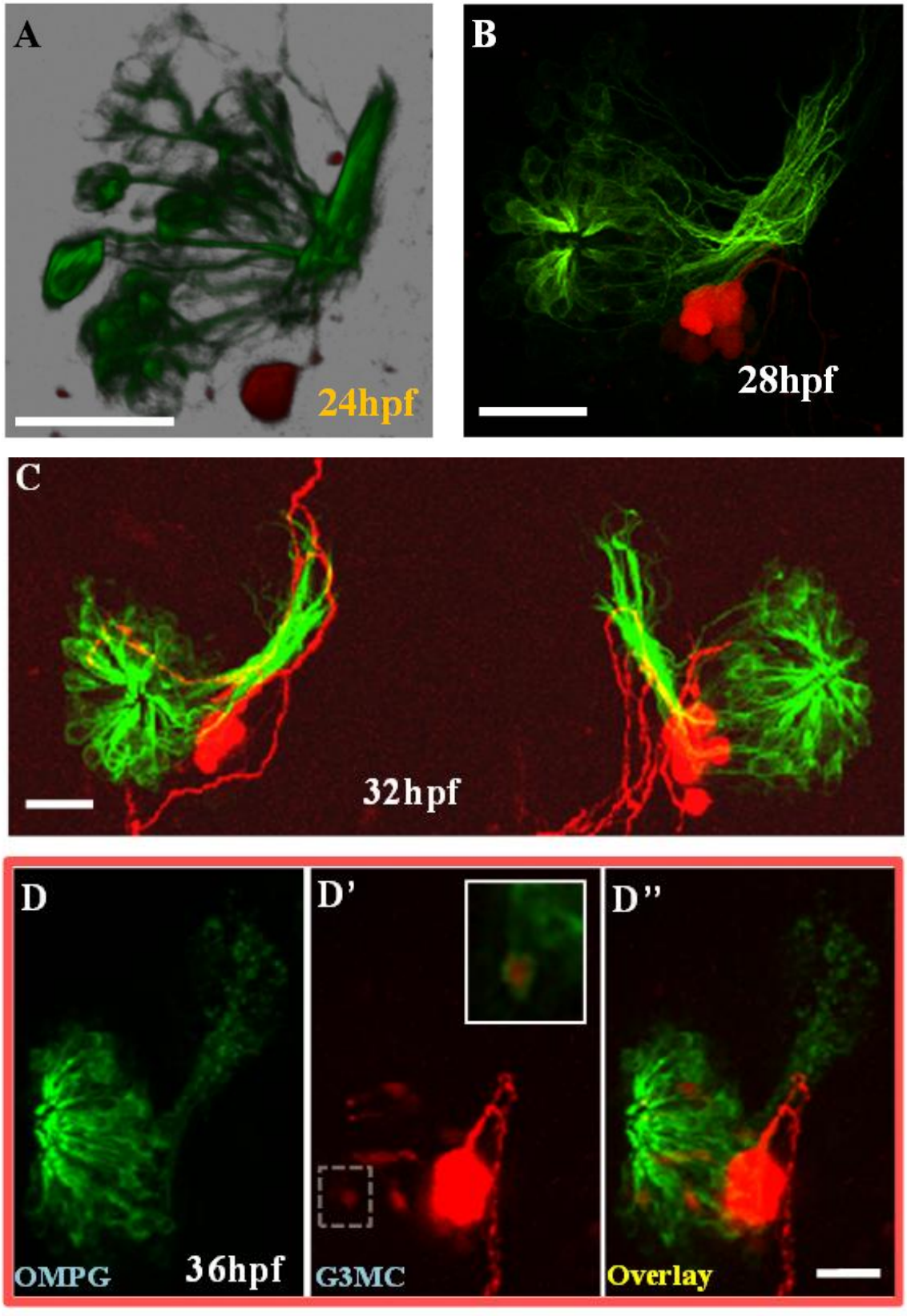

Figure 3.13 Co-development of the G3MC terminal nerve and OMPG olfactory projections

Interestingly, by 36hpf, there was co-expression of mCherry (GnRH3) and GFP (OMP) in several (4-8) ORN cell bodies in the olfactory epithelium (Figure 3.13D''). A closer view of one such co-expressing cell is shown in the inset in Figure 3.13D'; illustrating membrane-localised GFP (due to the 'Tau' tag) with whole-cell localised mCherry. This finding may have implications for understanding the origin of the hypothalamic G3MC cells which also begin to appear during this stage of development, i.e. between 32-36hpf (*see discussion*).

Figure 3.14A illustrates a typical anti-acetylated tubulin immuno-stained 60hpf embryo with all newly formed neuronal tracts labelled with DAB brown precipitate, emphasising the outline of the olfactory system and its associated tracts at this time-point. Figure 3.14B reveals that there is still some mCherry/GFP co-expression in the olfactory pits at 60hpf, and that the terminal nerve G3MC cells have maintained/increased their projections to the olfactory bulb regions and the forebrain commissures; particularly the anterior commissure. Whilst it is known (and seen in Fig.12A) that olfactory interneurons within the olfactory bulbs project their axons along the anterior commissure; it becomes apparent that significant number of these commissural tracts belong to the terminal nerve cells (Figure 3.14B), thus providing further opportunities for the olfactory and GnRH systems to interact.

The pTRPC2:Venus line, which labels the other major subset of ORNs, was also crossed with G3MC, and the resulting double transgenic embryo (at 36hpf) is shown in Figure 3.15. Whilst several mCherry-positive cells are again seen in the olfactory epithelium, none appear to co-express Venus (TRPC2), suggesting that only ciliated (OMP-positive) ORNs are capable of giving rise to these GnRH3 (mCherry) cells at 36hpf. In fact, there were some cells which did appear to co-express mCherry and Venus (inset in Figure 3.15A'). However, on closer inspection, it became apparent that these cells *strongly* expressed Venus (YFP), so it seems likely that this membrane-only red fluorescence was just 'bleed-through' from the YFP fluorescence, and not mCherry (GnRH3).

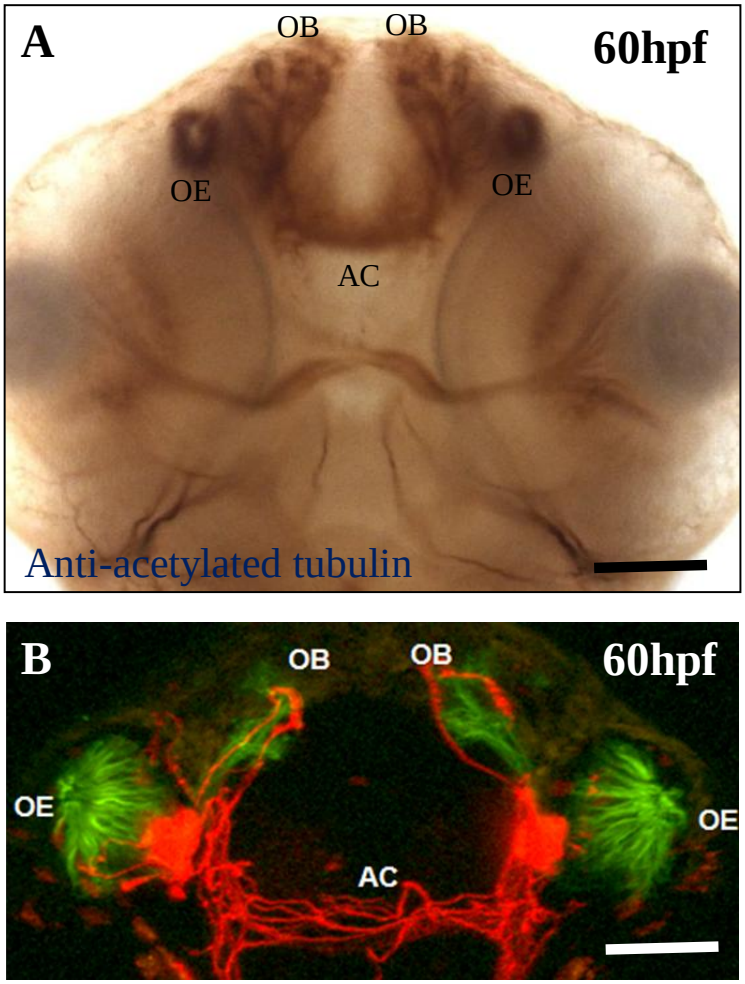

Figure 3.14 Terminal nerve GnRH axons project across the anterior commissure

A: anti-acetylated tubulin immuno-stained embryo (with DAB), labelling all neuronal tracts. B: Detailed view of G3MC-positive axons projecting across the anterior commissure (-which is also labelled in A). For B: OMPG (in green) and G3MC (in red).
Scale bars are 50µm (B) and 100µm (A)
OE= olfactory epithelium; OB= olfactory bulb; AC= anterior commissure.

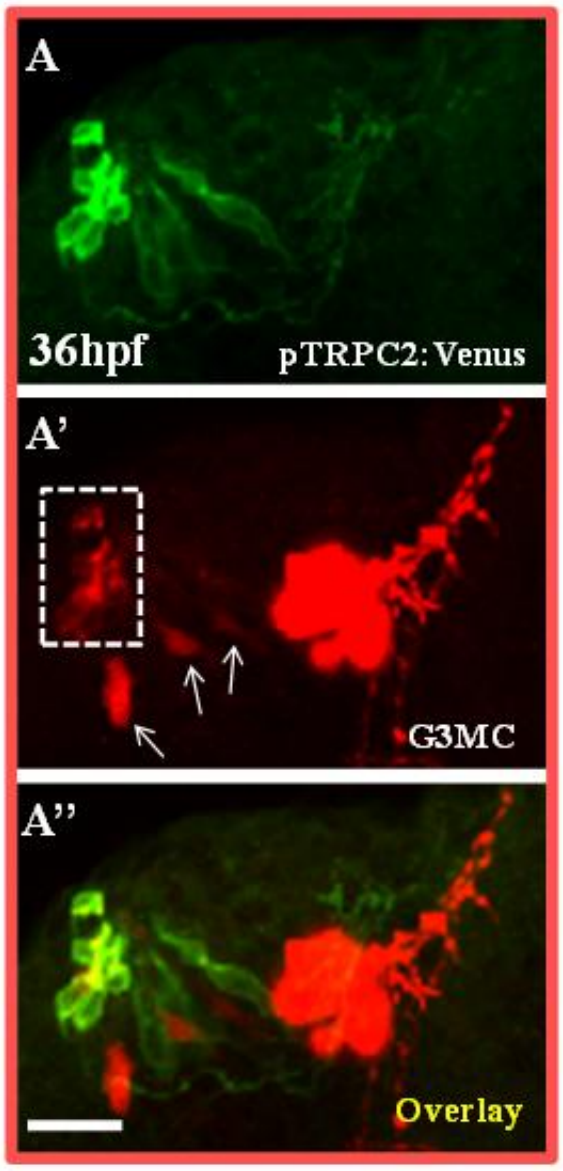

Figure 3.15 Co-development of the G3MC terminal nerve and pTRPC2:Venus vomeronasal* projections

G3MC (in red) was crossed with pTRPC2:Venus (in green) and a representative image of one olfactory pit (A, A', A") is shown at 36hpf (confocal ventral view). TRPC2:Venus alone is shown in A, G3MC in A', and the overlay of the two is shown in A". The dotted box in A' indicates likely bleed-through from Venus (YFP) fluorescence in A. The arrows indicate three mCherry-positive cells in the olfactory epithelium which do not co-express TRPC2:Venus in A". Scale bar is 25μm.

**For clarity, TRPC2:Venus olfactory projections will henceforth be called 'vomeronasal' projections*

3.2.5 An olfactory placodal origin for the hypothalamic GnRH cells?

In 2005, evidence was reported showing that the terminal nerve (and midbrain) GnRH cells had a cranial neural crest origin, but that the hypothalamic GnRH cells had a different (anterior pituitary placodal) origin (Whitlock, 2005b). SOX10 has been shown to be a good marker for migrating neural crest cells, and the pSox10:EGFP transgenic line faithfully recapitulates this SOX10 expression (Wada et al., 2005). However, when the G3MC line was crossed with pSOX10:EGFP, none of the terminal nerve *or hypothalamic* G3MC cells co-expressed GFP (SOX10), casting some doubt on whether they do actually have a neural crest origin (Figure 3.16).

So, can an olfactory origin for the hypothalamic GnRH (G3MC) cells still be excluded? In an attempt to find this out, lypophilic tracer dyes (DiI, DiO, and DiD) were used to label the olfactory placode, using a method that had been reported previously (Dynes and Ngai, 1998). DiI fluoresces at a 'red' wavelength, whilst DiO is 'yellow/green', and DiD is in the 'far red' part of the spectrum. These lypophilic dyes were applied externally to embryo water, so that they could be absorbed by *all external membranes*, including, of course, the olfactory placodes/ epithelia. However, it became apparent that DiO was unusable because it readily precipitated out of the water (so could not be absorbed at membrane surfaces). Fortunately, both DiD (data not shown) and DiI successfully labelled the olfactory pits (and all other external membranes) from around 24hpf onwards (Figure 3.17A), and this labelling was retained until at least 60hpf (Figure 3.17B). However, none of these externally labelled ORNs migrated to the hypothalamus; as there was no observable DiI/DiD labelling in the hypothalamic region (*see asterisk*), suggesting that the G3MC hypothalamic cells which appear between 32-60hpf may not have an external, placodal origin.

Neither DiI nor DiD could be applied to the G3MC line because they both emit fluorescence in the 'red' region of the emission spectrum, and therefore could not be differentiated from mCherry fluorescence at the hypothalamus. In any case,

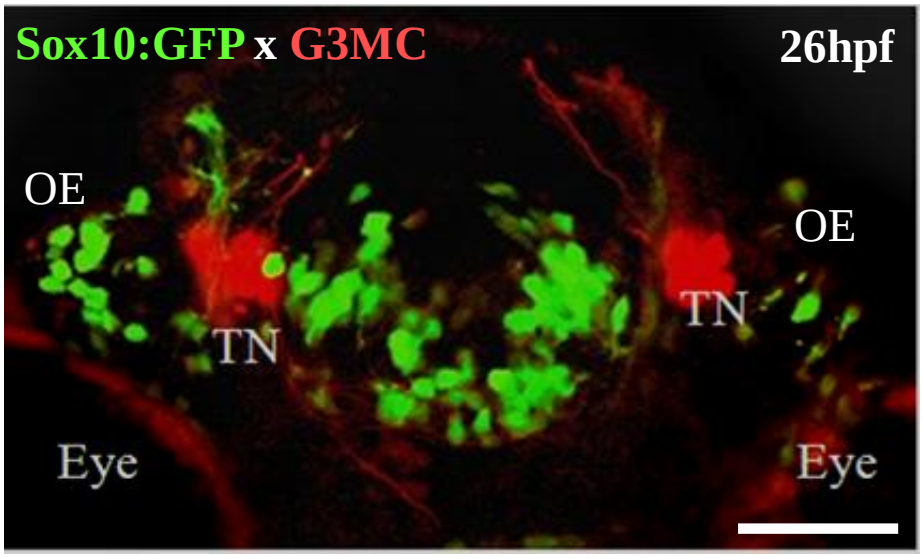

Figure 3.16 The terminal nerve G3MC cells do not co-express a migrating neural crest marker

The Sox10:GFP line (a migrating neural crest reporter line) was crossed with G3MC and a representative image at 26hpf is shown above (ventral view). None of the terminal nerve G3MC cells (in red) co-express GFP (i.e. Sox10; in green). The hypothalamic G3MC cells at 32-36hpf do not express sox10 (GFP) either *(data not shown)*. Scale bar is 50µm.
OE= olfactory epithelium; TN= terminal nerve

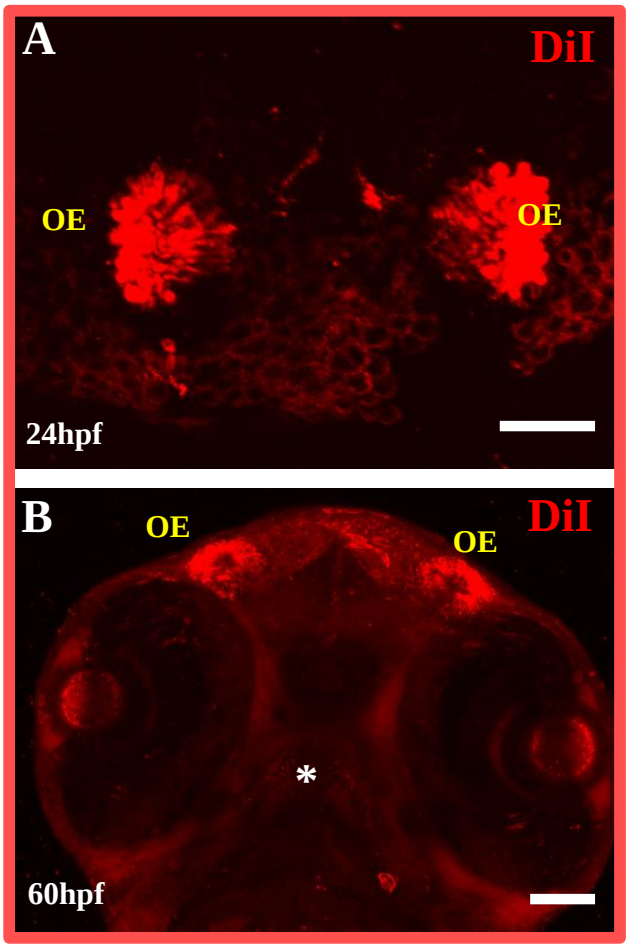

Figure 3.17 An olfactory epithelium origin for hypothalamic G3MC cells could not be confirmed by external application of lypophilic tracer dye, DiI

DiI was added externally to dechorionated wild-type embryos at 20hpf, and uptake of DiI at the olfactory epithelium can be seen by 24hpf in A , as well as all other external membranes *(data not shown)*. By 60hpf (B) the olfactory epithelial cells still contain DiI, but the hypothalamic region has not acquired any DiI-containing cells (as shown by an asterisk). Scale bars are 50µm.
OE= olfactory epithelium.

the result was negative: an olfactory origin for hypothalamic (GnRH/G3MC) cells could not be confirmed (*or ruled out*).

3.2.6 Over-expression of Kiss1/-2 and Gpr54a/-b had no affect on embryonic GnRH immuno-expression at the hypothalamus

In recent years, there have been many reports, across many different vertebrates, regarding the role of Kisspeptin-GPR54 signalling in the initiation of GnRH pulsatile secretion at the time of puberty. Zebrafish have two kisspeptin orthologues (*Kiss1* and *Kiss2*) and two GPR54 orthologues (*Gpr54a* and *Gpr54b*) (Oakley et al., 2009). In adult brains, Gpr54a and Gpr54b are both highly expressed in the hindbrain. Also, Gpr54a has moderate telencephalon expression, whereas Gpr54b has moderate diencephalon and midbrain expression. Kiss1 is predominantly found in the ventromedial region of the habenula, and Kiss2 in the posterior tuberal nucleus and periventricular hypothalamus (Oakley et al., 2009). Both Kiss1 and Kiss2, along with GnRH3, show a gradual increase in expression at the start of the pubertal phase, indicating that kisspeptin-signalling may have a role in the control of puberty in the zebrafish. Significantly, it was also shown that intra-peritoneal injections of the Kiss2 (but not Kiss1) decapeptide into sexually mature female zebrafish up-regulated pituitary gonadotrophin gene expression (Lhβ and Fshβ) (Kitahashi et al., 2009). This data, together with its periventricular hypothalamus expression, suggests that, in teleosts, Kisspeptin-2 may have adopted the role of neuroendocrine control of reproduction carried out by Kisspeptin-1 in mammals.

To characterise spatio-temporal expression of Kiss1, Kiss2, Gpr54a, and Gpr54b during zebrafish embryogenesis, *in situ* hybridisation was carried out on embryos at three different stages (24hpf, 36hpf and 60hpf). However, *in situ* expression was found only at 60hpf (Figure 3.18); although the actual initiation of expression begins between 36-60hpf, and possibly even earlier, as shown by RT-PCR (data not shown). The expression pattern obtained for all four members of the kisspeptin/Gpr54 signalling pathway were the same; which, interestingly, is the

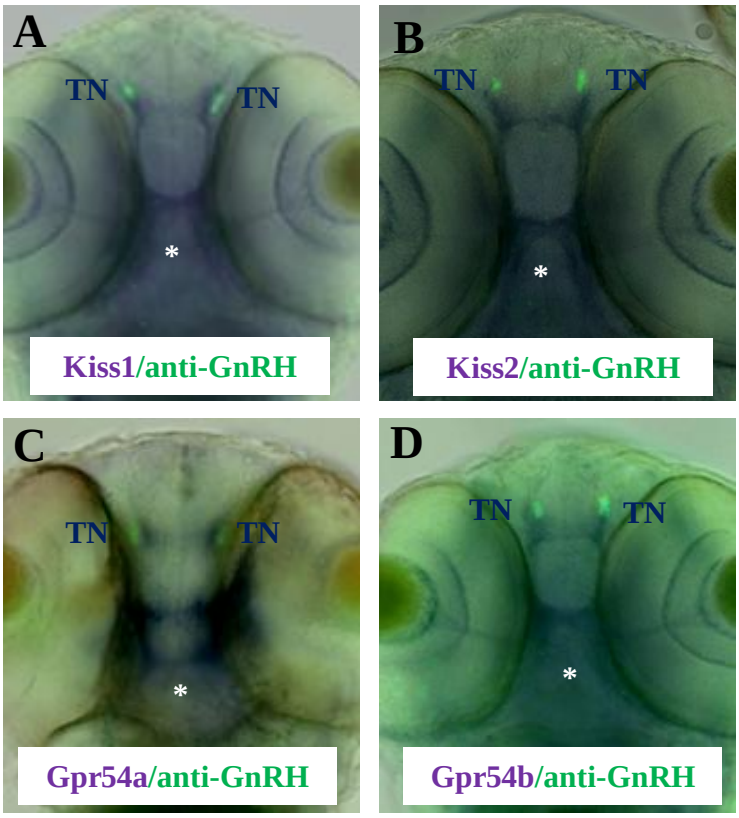

Figure 3.18 Expression analysis of Kiss1, Kiss2, Gpr54a and Gpr54b

A-D: *In situ* hybridisation analysis of Kiss1, Kiss2 , Gpr54a,, and Gpr54b (in purple) with anti-GnRH immuno-labelling (in green) at 48hpf (all ventral views). An asterisk marks the hypothalamic region in A-D.
TN=terminal nerve

same as the GnRH2 *in situ* staining pattern at the same stage (Figure 3.03G) i.e. in both forebrain commissures and their associated tracts, including those that extend towards the terminal nerve GnRH cells (as shown by GnRH immuno-labelling; '*green' labelling* in Figure 3.18A-D).

To ascertain whether or not embryonic up-regulation of kisspeptin-Gpr54 signalling altered forebrain GnRH neuronal ontogeny, full length (5' and 3' capped) RNA for Kiss1, Kiss2, Gpr54a, and Gpr54b were injected individually (data not shown), or as the four alternate Kiss/Gpr54 pairs (data not shown) or all together (Figure 3.19) into 1-cell stage embryos. However, upregulating the kisspeptin/Gpr54 signalling pathway in this manner had no effect on GnRH immuno-labelling at 36hpf (data not shown) or 60hpf (Figure 3.19B, C). The untreated control embryo (Figure 3.19B) showed the same terminal nerve/ commissural GnRH immuno-labelling as the Kiss1/Gpr54 RNA-injected embryo (Figure 3.19C), and no quiescent hypothalamic (*see asterisk*) GnRH-immuno-labelled cells were revealed ('unmasked') using this approach. Moreover, the G3MC expression pattern was equally unaffected by the kisspeptin/Gpr54 over-expression *(*data not shown*)*.

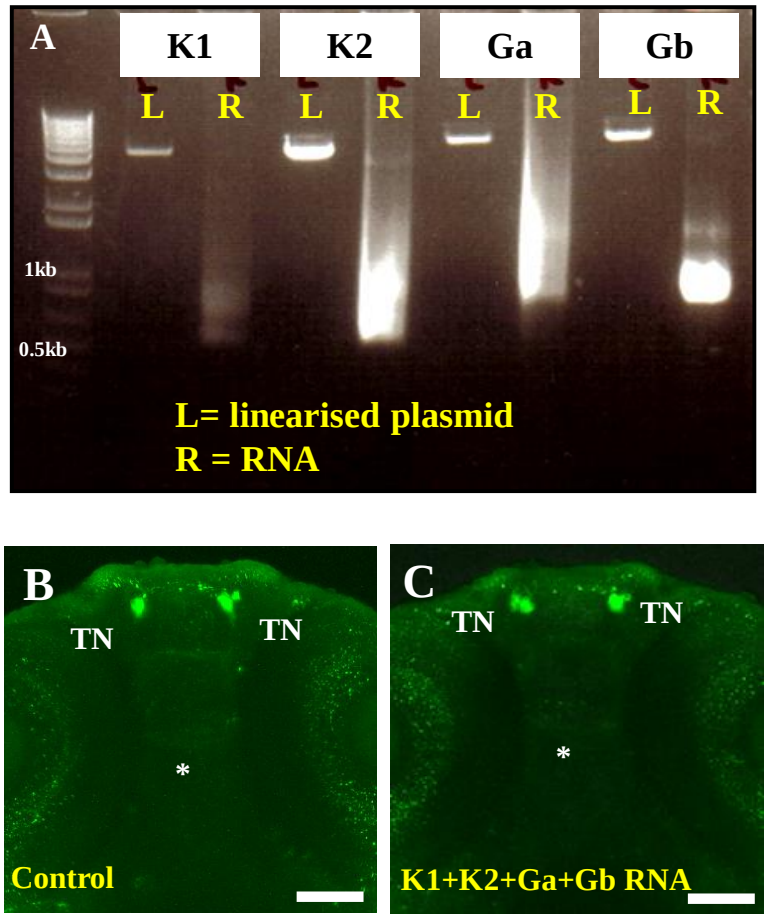

Figure 3.19 Over-expression of Kiss1, Kiss2, Gpr54a, and Gpr54b does not lead to any noticeable changes in GnRH immuno-labelling

A: An agarose gel showing that RNA for Kiss1/-2 and Gpr54a/-b are all successfully transcribed *in vitro*. B and C show confocal images of anti-GnRH immuno-stained embryos (in green) at 60hpf: B was untreated, whilst C was injected with Kiss1, Kiss2, Gpr54a and Gpr54b RNA at the one-cell stage. An asterisk marks the hypothalamic region in B and C.
Scale bars are 100μm.
TN=terminal nerve

3.3 Discussion

Using standard immuno-histochemical techniques, amniotic forebrain GnRH system development has previously been well characterised, in several different model organisms. These studies showed that the entire migratory route of the GnRH neurons can be reliably traced from their medial olfactory placodal origin, across the terminal nerve, and then finally at their septo-preoptic hypothalamic destination. However, an analogous migratory stream was not detected during *early* zebrafish embryogenesis; and may not occur in this manner until at much later developmental stages- in what may be a *'second wave'* of GnRH neuronal migration.

3.3.1 GnRH protein/ transcript is absent in the hypothalamus during early embryogenesis.

LRH13 is a monoclonal anti-GnRH antibody that recognises forms of GnRH that contain serine at position 4 and tyrosine at position 5 (of the decapeptide) (Park and Wakabayashi, 1986). In agreement with previously described adult zebrafish brain expression patterns (Figure 3.03B)**,** LRH13 reliably detected both of the neuromodulatory (terminal nerve and midbrain) populations; and also, importantly, the hypophysiotropic (preoptic area/ hypothalamus) population. As LRH13 is predicted to bind to GnRH3 more avidly than to GnRH2, the midbrain GnRH immuno-labelling was unexpected. The reason may be that GnRH3 is also present in the midbrain (and some other regions) or it could be that the levels of GnRH2 present in the midbrain are very high, thus amplifying the possibly weaker anti-GnRH labelling in this region. It should also be noted that although the brain sections were treated with hydrogen peroxide, residual endogenous peroxidase activity may account for some of the unexpected 'background' brain immuno-labelling, although this was not seen in the negative controls, so is unlikely.

As well as showing that GnRH is actively being synthesised in these adult brain regions (as would be expected for a sexually competent zebrafish of 3 months old), it also demonstrated the reliability of the anti-GnRH antibody (LRH13), as well as the actual immuno-labelling protocol itself. However, unexpectedly, the LRH13 immuno-expression patterns for zebrafish embryos and larvae were less consistent with previously reported expressions patterns (Whitlock et al., 2005b).

Another lab has reported the presence of LRH13-labelled GnRH cells migrating towards the preoptic area and hypothalamus in embryos at around 56hpf (Whitlock et al., 2005b). However, it was not possible for us to replicate this expression pattern using the same protocol. Indeed, despite the fact that LRH13 consistently labelled the terminal nerve GnRH cells between 30hpf and 6dpf, there were no GnRH-immuno-reactive cells detected in (or migrating to) the hypothalamic region during these developmental stages. Moreover, using a fluorescently labelled secondary antibody, hitherto unreported labelling of both forebrain commissures could also be demonstrated by us; axonal tracts which presumably emanate from the terminal nerve GnRH cells. Whilst this would suggest our protocol is both accurate and sensitive, the possibility still remains that the reported hypothalamic LRH13-labelled GnRH cells are present and do indeed express GnRH at these stages, but at very low levels and/or for a very short period of time. This type of expression pattern could have been missed by our analysis. So, in an attempt to try and rule out this possibility, embryos at 4-hour intervals between 36-60hpf were immuno-labelled for GnRH- but, again, no hypothalamic cells were detected.

To make sure that this was not simply a case of poor antibody penetration, sections of 60hpf and 6dpf embryos were immuno-labelled for GnRH. Again, whilst the terminal nerve GnRH cells were readily detected at both stages, no hypothalamic GnRH cells were found. However, here it is possible that the high ‘background’ fluorescence in these sections may have masked very low levels of hypothalamic GnRH expression. Finally, the removal of PTU from embryo medium had no affect on hypothalamic GnRH cell immuno-labelling. However, this does not mean that PTU has no influence on hypophysiotropic GnRH synthesis, as it does with thyroid

hormone synthesis; further analysis at later stages (when hypothalamic GnRH cells are present) would be required.

In situ hybridisation data subsequently demonstrated that most of the GnRH immuno-labelling could be accounted for by GnRH3 transcript alone. From 30hpf through to 15dpf, GnRH2 transcript localised mainly to the midbrain region, in accordance with previously reported data (Palevitch et al., 2007), none of which overlaid with the GnRH immuno-labelling. Interestingly though, there was some GnRH2 transcript localised to the forebrain commissural regions (where no GnRH3 transcript was found), which, as mentioned above, also showed immuno-labelling by LRH13.

Up until 5dpf, GnRH3 transcript remains largely restricted to the terminal nerve cells, matching almost exactly the GnRH immuno-labelling at these stages (apart from the forebrain commissure expression). In an isolated case at 5dpf, there was some GnRH3 transcript detected in the diencephalic region, but the infrequency of such labelling makes it questionable that this represents *bona fide* hypothalamic (hypophysiotropic) GnRH cell staining. Later, at 15dpf, there was some GnRH3 transcript found in the diencephalic-midbrain region; however, its veracity is again questionable because of the weakness and diffuseness of the staining.

Palevitch *et al* (Palevitch et al., 2007) similarly showed that GnRH3 transcript is restricted to the terminal nerve region until 5dpf, and then between 20-25dpf a 'continuum' of GnRH3 neurons is visualised extending from the olfactory area, through the terminal nerve ganglion, along the lateral aspects of the telencephalon, and then on into the preoptic area and hypothalamus by 30dpf. Considering the fast early development of the zebrafish (major organs and brain regions are formed by 1dpf, and embryos are free-swimming by 2dpf), this represents a very long delay in hypothalamic GnRH cell migration, compared with other vertebrates (amniotes) which have a spatially similar migratory route into the hypothalamus. Therefore, it could be speculated that instead of revealing the migrating cells in 'real time', in fact the migratory pathway is 'unmasked' approximately 28 days after the cells actually migrated to the hypothalamus by this *in situ* hybridisation analysis. So, the 'migratory pathway' becomes 'revealed' as the

cells that have remained along its route begin to transcribe GnRH3 closer to the time of zebrafish 'puberty' at 35-45dpf, and *not* at the time that they were migrating.

Assuming that the terminal nerve cells represent an entirely separate population from the cells which give rise to the hypothalamic GnRH cells, how can the hypothalamic (hypophysiotropic) cells be distinguished (visually) from the 'neuromodulatory' terminal nerve cells? And, if they are actually distinguishable (i.e. different types of cell), and therefore separate, why do the hypothalamic cells only appear after 20-30dpf; and, when and where were they specified? Conversely, if the hypothalamic and terminal nerve GnRH cells are not distinguishable (i.e. they are the same type of cell); do they have a common origin e.g. at the olfactory placode? The remainder of this chapter aims to tackle these questions and tries to unravel some of the other complexities of the zebrafish GnRH system compared with that of the amniotes.

3.3.2 The differences in GnRH neuronal ontogeny of amniotes compared with teleost fish

The medaka is another teleost fish, which is estimated to have diverged from zebrafish around 110–160 million years ago (Wittbrodt et al., 2002), showed very similar GnRH immuno-labelling. That is, terminal nerve GnRH cells were immuno-labelled from 3dpf onwards, at an analogous developmental stage to the faster-developing zebrafish embryo. Notably, there were a few GnRH immuno-labelled cells in the hypothalamus by 7dpf in some medaka; however, these were very low in number i.e. often only 2-4 cells. Further work would need to be carried out to fully characterise these cells, to ensure they are indeed the hypophysiotropic GnRH cells, and to find out if their number increases past 7dpf. Work by Okubo *et al* showed that both GnRH1 and GnRH3 genes were expressed by cells in the preoptic area/ hypothalamus by this stage (Okubo et al., 2006); however, it would be interesting to ascertain which of these two genes was being expressed by the LRH13-labelled cells in this study, as further proof of their identity.

Using GFP transgenic reporter lines for GnRH1 and GnRH3, Okubo and colleagues (Okubo et al., 2006) showed that by 4dpf GnRH1-GFP cells had reached the ventral preoptic area, and by 20dpf that these neurons had extended projections to the anterior pituitary. Similarly, GnRH3-GFP cells had also reached the preoptic area/anterior mesencephalon by this stage, but did not project to the anterior pituitary. Teleost fish, unlike mammals, do not have a hypophyseal portal circulation that transports the secreted GnRH to the pituitary. Instead, the GnRH neurons need to directly innervate their target pituitary cells (the gonadotrophs). This would suggest that, in medaka, only GnRH1 hypothalamic neurons have the hypophysiotropic role. However, because zebrafish don't have a GnRH1 gene, they must surely have to rely on GnRH3-expressing hypothalamic neurons to fulfil this role?

The medaka GnRH1 and GnRH3 GFP-reporter plasmids, provided by Okubo *et al (Okubo et al., 2006),* were injected into zebrafish embryos to find out whether the medaka promoter function was conserved, despite the large evolutionary distance between the two teleost fish. The presence of GFP in the terminal nerve cells, as proven by anti-GnRH immuno-labelling in these cells, showed that the regulatory elements in the medaka GnRH promoters could still be used by the zebrafish, either because the zebrafish still uses the same regulatory elements, or because its terminal nerve cells still harbour the required regulatory transcription factors. Both of the medaka reporter constructs gave some GFP expression in cells which were not co-labelled by GnRH immuno-labelling, including in the telencephalon; but neither constructs gave any hypothalamic or preoptic area expression by 48hpf. Moreover, although some embryos were allowed to develop until 4dpf, by 3dpf the expression in the terminal nerve region had diminished, and by 4dpf, the GFP expression in the terminal nerve was very weak or absent, with just some residual GFP expression in the external epithelial cells. This was most likely because the plasmid construct had been lost/ degraded by this stage in these *transient* transgenics, but could also be because the required regulatory factors were no longer available for continued transcription of GnRH1 and GnRH3 in those cells.

Whilst the medaka constructs did recapitulate terminal nerve GnRH expression, and could be expected to continue doing so in a *stable* transgenic, to ensure that all native zebrafish GnRH3 expression is correctly reported, especially hypophysiotropic GnRH, it was decided that using the native zebrafish GnRH3 promoter to generate the stable transgenic line would be preferable.

3.3.3 pGnRH3:mCherry embryos recapitulate normal terminal nerve GnRH expression and also label a novel *early* hypothalamic population

In 2002, Torgersen *et al* characterised the 1.6 kb upstream promoter region of the zebrafish GnRH3 gene and found that it contained an enhancer at -976, with adjacent binding sites for Oct-1, CREB and Sp1, which were required for GnRH3 expression at the terminal nerve. However, using reporter constructs containing this upstream regulatory region, they were unable to demonstrate any hypothalamic GnRH3 expression (Torgersen et al., 2002).

In 2006, Palevitch *et al* (Palevitch et al., 2007) used a similar strategy, except that their GnRH3 reporter construct also contained downstream regions comprising exon 1, intron 1, and part of exon 2 of GnRH3. Using this construct, they were able to confirm the terminal nerve labelling previously reported by Torgersen *et al*; and much later, at 10dpf, GFP fluorescence was first seen in the presumptive hypothalamus. However, this was a transient transgenic analysis and a stable GnRH3 transgenic reporter line had not yet been reported.

To study the role of olfactory axonogenesis during GnRH neuronal development, a pOMP:tauEGFP reporter line had already been acquired from another group (Yoshida et al., 2002), that allowed a subset of olfactory sensory neurons to express GFP from around 24hpf. It was therefore deemed advantageous to use mCherry (a form of red fluorescent protein) to co-label the GnRH3 neurons, so that both GnRH neurons and olfactory neurons could be identified independently of each other (in red and green, respectively). Therefore, to make a stable transgenic GnRH3 reporter line, the promoter region reported by Palevitch *et al* (Palevitch et al., 2007) was PCR-amplified from whole genomic DNA and then cloned upstream

of mCherry coding sequence, thus generating a 'pGnRH3:mCherry' reporter construct ('G3MC'). mCherry was the best choice of red fluorescent protein due to its high level of fluorescence intensity, its high photostability, and also its very fast maturation time (Shaner et al., 2005).

The temporal characterisation of G3MC from 0-120hpf (Figure 3.09) revealed that mCherry expression could be detected in the terminal nerve cells from around 24hpf onwards, but that the first mCherry cells were visualised in the anterior neural tube region around 4 hours earlier. This analysis didn't reveal whether these earlier mCherry cells gave rise to the terminal nerve cells, or some other later population. However, previously it has been suggested that the terminal nerve cells do arise from cranial neural crest cells, so these cells located in the anterior neural tube may indeed be migrating towards the terminal nerve region; though time-lapse video imaging would be required to determine whether or not this is true.

By 32hpf, axons from the terminal nerve cells have extended up towards the olfactory bulbs and also across both forebrain commissures. This closely resembles the GnRH immuno-labelling that is also seen around this time-point (Figure 3.04A); which proves that the transgenic expression is faithfully reporting 'real' GnRH3 expression. Unexpectedly, from around 32-36hpf onwards, mCherry-positive cells began to appear in the presumptive hypothalamic region. This was subsequently confirmed by crossing G3MC with pNkx2.1:YFP (a marker of the hypothalamic region). However, when GnRH immuno-labelling was carried out on G3MC, these hypothalamic cells, of course, were not co-labelled (as there is no LRH13-labelling in the hypothalamus at these stages). Therefore, further proof was required to show that these hypothalamic mCherry cells were really the hypophysiotropic GnRH cells.

Interestingly, when brain sections from a 3 month old female G3MC zebrafish were analysed, the mCherry expression was found to be very similar to the LRH13 immuno-labelled brain sections (Fig 3.03A). Specifically, there were many mCherry-expressing cells found in the preoptic area and hypothalamus in a similar region to where GnRH immuno-labelled cells were found. This would certainly

suggest that these mCherry cells are 'real' hypothalamic (hypophysiotropic) GnRH cells. However, this is not proof that these adult brain hypothalamic GnRH cells are related to the early hypothalamic mCherry cells detected between 32-60hpf in G3MC embryos.

Only adult female brains were used in this study, to minimise the confusion caused by possible gender differences in GnRH3 spatial expression. Further work will be required to find out if there are actually any differences in male/female GnRH expression levels; and, in particular, how this relates to the sexual dimorphic expression of the kisspeptin receptors (Gpr54a and Gpr54b) in sexually competent zebrafish (Oakley et al., 2009).

Whilst the hypothalamic GnRH cells are most clearly visible between 32-60hpf, they become less apparent by around 120hpf. This is most likely because these cells are no longer expressing mCherry i.e. the cells have become quiescent-similar to the hypophysiotropic GnRH cells in amniotes, prior to puberty. Instead, at 120hpf, there are extensive mCherry-positive tracts present throughout the brain, only some of which emanate from the terminal nerve cells. It is not yet clear whether some of these projections belong to the hypothalamic cells, and, if so, whether they project to the anterior pituitary cells. Prior to 120hpf, when the hypothalamic GnRH cells are most visible (due to high mCherry expression levels), it is not apparent whether these cells are innervating the anterior pituitary at these early stages. However, anosmin-1b immuno-labelling in the presumptive pituitary (Figure 5.04, *see later*), certainly suggest that these hypothalamic G3MC cells are in very close proximity to the hypothalamic cells.

Abraham *et al* (Abraham et al., 2009; Abraham et al., 2008) recently reported the characterisation of a *stable* transgenic pGnRH3:EGFP line, which gave considerably-improved clarity on their previous transient expression analysis. Because, in generating G3MC, we used the same promoter region that they had previously reported, our expression data closely resembles their recent stable transgenic line analysis (with a few exceptions). Their description of the GnRH3 axonal projections between 26-48hpf matches very closely what we see with the G3MC line. They first visualise the GnRH3 perikarya around the olfactory placodal

region at 24hpf, which, to avoid confusion, has been referred to by us as the 'terminal nerve GnRH cells' at this time-point. From around 3dpf, some of these perikarya re-position themselves between the olfactory epithelium and olfactory bulbs, and can perhaps now be more properly called 'terminal nerve cells', forming a continuum from the olfactory epithelium to the terminal nerve ganglion, which, by 6dpf extends into the ventral telencephalon; and this can also be seen in our characterisation of G3MC at 5dpf (Figure 3.09I).

However, in their characterisation of pGnRH3:EGFP, Abraham *et al* make no mention of the early hypothalamic cluster of cells that we see between 32hpf and 60hpf.

The 'tangential migration' route that forebrain GnRH neurons traverse, from the olfactory region, is thought to be axophilic: migrating along olfactory and terminal nerve tracts, along the terminal nerve ganglion, into the ventral telencephalon, and then on into the preoptic area and hypothalamus (Abraham et al., 2009; Palevitch et al., 2007). In zebrafish, it has even been suggested that GnRH3 perikarya may associate with their own axonal tracts during this migration.

Whilst we didn't study the 'terminal nerve GnRH cells' beyond 5dpf (except at adulthood), we can assume that they would continue to follow the same migratory route that is described by Abraham *et al* (*see Figure 3.20*) (Abraham et al., 2008). That is, between 7-12dpf, a few GnRH3 perikarya extend caudally into the ventral telencephalon, along existing GnRH3 axonal tracts that project to the hypothalamic region. By day 12, one or two will have migrated along the terminal nerve ganglion, and will have reached the presumptive preoptic area (Figure 3.20D, (Palevitch et al., 2009)). This process of perikarya 'migrating' along their own neurites into the hypothalamic region could be visualised all the way up to 30dpf (Abraham et al., 2008). So, whilst this 'continuum' of forebrain GnRH neurons is very similar to that which occurs in amniotes, the process has apparently taken *vastly* longer in the zebrafish.

So, what about the much earlier, hitherto unreported, cluster of hypothalamic GnRH cells seen in the G3MC embryos between 32-60hpf? Whilst these '*early'* hypothalamic cells accumulate once GnRH neuronal projections have already been

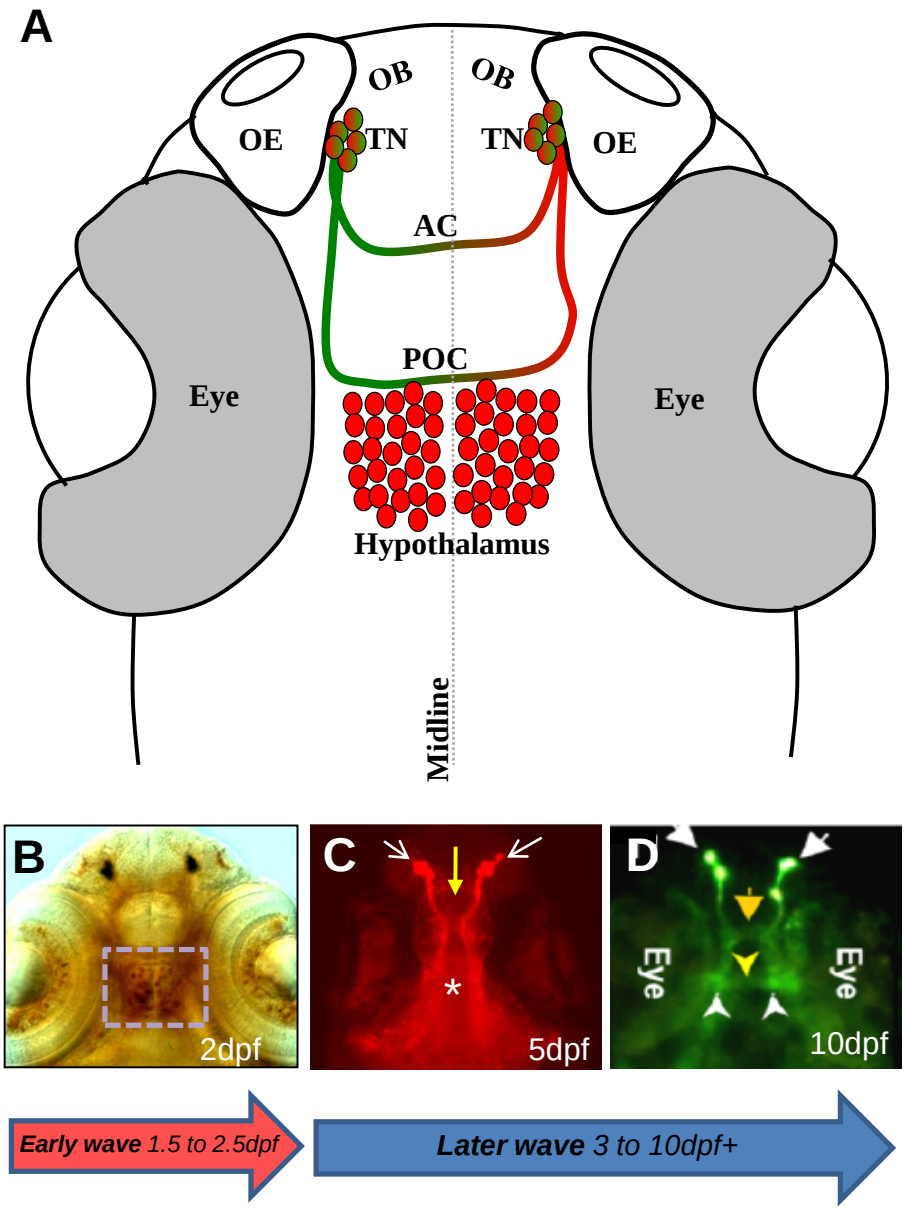

Figure 3.20 'Two wave' model for hypothalamic GnRH neuronal migration/ accumulation during zebrafish embryogenesis

A: Schematic diagram illustrating pGnRH3:EGFP (*Palevitch et al, 2009, in green*) and G3MC fluorescence (*this study, in red*) at 2dpf. A green-red gradient is used to indicate terminal nerve cells ( ) and projections ( ) which are detected in both transgenic lines, whereas solid red is used to demonstrate G3MC-specific expression at the hypothalamus ( ).
B-D show representative images of the 'early wave' (**B**), and progress of the 'later wave' (**C-D**). The hypothalamus is indicated by a 'dotted box' in **B**; an asterisk in **C**; and white arrow heads in **D**. Yellow arrows show the proposed direction of GnRH3 neuronal migration to the hypothalamus, from the terminal nerve region (white arrows).

Figure 3.20 (D) reprinted from Developmental Dynamics (Palevitch et al, 2009), with permission from John Wiley and Sons.

established across the forebrain commissures, it is not clear whether the migrating GnRH neurons (or their perikarya) use these axons to reach the hypothalamus; in an analogous way to how the 'later' wave of GnRH cells are believed to reach the hypothalamus at around 12dpf (i.e. axophilically).

So, are there two 'waves' of GnRH neuronal migration to the hypothalamus during zebrafish embryogenesis: an '*early'* wave (at around 1.5dpf to 2.5dpf), followed by a much '*later'* wave (at around 3dpf to 12dpf+)? Two waves of GnRH cell migration have already been identified during primate embryogenesis: the first wave of GnRH cell migration precedes olfactory bulb formation, whereas the other wave occurs in association with olfactory bulb formation. During this 'second wave' of migration, GnRH cells migrate along a nasal mesenchymal scaffold of olfactory, vomeronasal and terminal nerves. So, we may speculate that the two apparent waves of GnRH cell migration that occur in zebrafish, may be comparable to these two waves of migration that have been described in human embryos (although, perhaps at different equivalent stages of embryogenesis).

It has been shown recently that bilateral removal of EGFP-positive GnRH3 cells, from the terminal nerve region, in pGnRH3:EGFP embryos, subsequently resulted in complete lack of hypothalamic GnRH3 neurons in the adult (at 12-weeks old). However, surprisingly, regeneration rates of these hypothalamic GnRH3 cells were much higher in embryos that were ablated early (at 2dpf), compared to those that were ablated much later (at 4dpf or 6dpf) (Abraham et al., 2010). This would suggest that the *'later wave'* of GnRH cell migration has a much more significant contribution to the number of hypophysiotropic GnRH cells in sexually competent adults. However, if they do not make a direct contribution in terms of cell number, the *'early wave'* of GnRH cell migration may still nonetheless make a significant, perhaps necessary, contribution to the correct-functioning of the adult hypophysiotropic GnRH cells, but this will need to be confirmed. Terminal nerve ablations at 4dpf and 6dpf abolish the extensive GnRH3-positve axonal tracts in the forebrain; some of which may form essential synaptic contacts with the *'early wave'* hypothalamic GnRH3 neurons, which may be important for the prolonged survival of these cells i.e. by the secretion of specific cell survival factors. So, an alternative interpretation of the ablation experiments could be that the terminal nerve GnRH

system may have a very important role in the survival and/or correct physiological activity of the hypophysiotropic GnRH neurons (especially after 4-6dpf).

Assuming that the mCherry-positive cells (from G3MC embryos) which accumulate at the hypothalamus between 32hf and 60hpf represent 'real' hypophysiotropic GnRH3 cells (the so-called *'early wave'*), why are there no GnRH immuno-labelled or GnRH3 *in-situ*-stained cells in this region, during these stages? One possible explanation could be that the pre-migratory GnRH cells down-regulate GnRH expression before or during their migration to the hypothalamus (and do not start expressing GnRH there until much later, probably after 6dpf). If this is case, the G3MC promoter may lack a regulatory element that would normally allow GnRH expression to be down-regulated at these early stages. Fortuitously for us, this has meant that we have been able to visualise these early-appearing hypothalamic GnRH cells, where normally they would have been untraceable by standard immuno-labelling or *in situ* hybridisation techniques.

The intriguing question is why Abraham & colleagues (Abraham et al., 2008) did not report the appearance of these early hypothalamic GnRH3 cells when they characterised their pGnRH3:EGFP line, which uses the same promoter region? During this project, four separate G3MC founder stable transgenics were identified, and they all had the same spatial expression pattern. Therefore, it can be assumed that the early appearance of hypothalamic GnRH3 cells were not the result of transgene insertion positional differences. However, whilst the reason for this discrepancy remains elusive, further characterisation of this early hypothalamic population was sought, to gain a better understanding of its identity. Moreover, in subsequent experiments herein, the early development of the 'terminal nerve GnRH3 cells' is also further investigated; as these are proposed to, at a much slower rate, give rise to the *'later wave'* of GnRH cells that reach the hypothalamus from around 12dpf onwards.

3.3.4 Olfactory and terminal nerve GnRH3 axons are apparently closely associated, and there is some evidence for olfactory epithelium-derived GnRH3 cells

To understand the role of the olfactory region in the specification and early migration of GnRH3 neurons during early development, two olfactory reporter lines, labelling both major subsets of olfactory receptor neurons (ORNs), were crossed with G3MC. pOMP:tauEGFP, which labels the ciliated-type of ORN, broadly demarcates the outline of the olfactory epithelia. Between 24-32hpf, the terminal nerve G3MC cells accumulate medially to the olfactory pit, and project their axons along a similar navigational route as the ORN axonal bundle- dorso-caudally towards the presumptive olfactory bulb region at the telencephalon. The 'intertwining' and close proximity of the terminal nerve and olfactory axons is similar to the morphology of the neurites in amniotes. However, rather than axophilically follow the olfactory/terminal nerve axons (as is seen in the amniotes), the *'later wave'* ('terminal nerve GnRH neurons') are found to follow axophilically a more caudal-ventral route into the ventral telencephalon. It is not, however, possible yet to say whether the *'early wave'* of GnRH3 neurons follow this same route into the hypothalamus, and if, by doing so, they establish the migratory pathway for the later wave, as is believed to happen in primates.

Interestingly, at around 36hpf, within the olfactory epithelium there are some mCherry-expressing (G3MC) ciliated ORNs (pOMP:EGFP positive cells). However, there does not seem to be any mCherry co-expression within the micro-villous ('vomeronasal') ORNs (pTRPC2:Venus positive cells). Therefore, some GnRH3 cells, which originate from the olfactory placode, arise from OMP-positive ORN progenitor cells, but not vomeronasal-type ORN progenitors. Whilst these mCherry (G3MC) cells can be detected within the olfactory epithelium as late as 5dpf (and possibly even later); the lack of GnRH3 protein (or transcript) in these olfactory cells is most likely due to the absence of a repressor element in the G3MC promoter, which would ordinarily repress GnRH3 expression in these cells.

Previous reports have shown that pre-migratory GnRH cells, which originate within the olfactory placode, do co-express both olfactory and GnRH markers

(Gonzalez-Martinez et al., 2004a), so this result is consistent with other vertebrate model organisms. However, whilst, this data supports a possible olfactory origin for the hypothalamic GnRH cells in fish, time-lapse imaging of the olfactory-GnRH3 cells will be required to ascertain whether or not this is true.

Assuming that the olfactory-derived GnRH3 cells do contribute to the hypothalamic GnRH population, it is not clear whether they migrate during the *'early wave'* or the *'later wave'*. The *'early wave'* GnRH3 cells begin to accumulate in the hypothalamus around the same time-point (36hpf) that the OMP/GnRH3 co-expressing cells first appear at the olfactory epithelium. However, if these olfactory-GnRH cells do contribute to the *'early wave'*, the migration would have to happen very fast, as there has been little evidence of these cells actively migrating from the olfactory epithelium to the hypothalamus between 24pf and 36hpf. Alternatively, if they contribute to the *'later wave'*, the olfactory-GnRH cells must down-regulate EGFP expression by the time they reach the terminal nerve, as none of the GnRH3 cells in the terminal nerve region were found to co-express EGFP (OMP); although low levels of residual GFP in these cells may in future be revealed by anti-GFP immuno-labelling, or similar technique.

To further investigate a putative olfactory origin for the *'early wave'* hypothalamic GnRH3 cells, lypophilic tracer dyes were used; and DiI was found to be most useful. When DiI was applied externally to live zebrafish embryos at 20hpf, by 24hpf the olfactory pits were very strongly labelled (as were all other external epithelial cells). However, by 60hpf, whilst the olfactory epithelia remained strongly labelled, there was no DiI labelling in the hypothalamic region. This suggested that the *'early wave'* of GnRH migration to the hypothalamus did not have an olfactory epithelium origin; unless, of course, the *'early wave'* GnRH cells were specified at the olfactory placode *before* 20hpf, and migrated away from the 'external epithelial thickening' before 20hpf as well. In fact, the olfactory placode actually forms at around 17hpf, but when DiI was applied to embryos at this time-point the toxicity was high, the subsequent olfactory epithelial labelling was poor, and the embryos looked morphologically defective by 24hpf (and showed no hypothalamic DiI labelling by 60hpf, data not shown). Of course, the *'later wave'* hypothalamic

GnRH cells may have an olfactory placode origin; but to determine this will require looking at much later embryos (12dpf+), after a DiI-incubation.

An alternative, more precise, approach to using lypophilic dyes, would be to use a 'caged fluorophore', such as *Kaede* (Hatta et al., 2006). In this case, a laser is used to photo-activate the *Kaede* specifically at the olfactory placode of zebrafish embryos, so that those cells fluoresce 'red' amongst a background of green-fluorescing cells. Therefore, if any of these olfactory-derived 'red' cells migrate to the hypothalamus, this can be easily traced. Unfortunately, this approach cannot be used on G3MC embryos because the mCherry-positive cells will also fluoresce 'red', meaning that they could not be distinguished from the photo-activated cells. Moreover, whilst more precise, using Kaede may not be any more informative than the DiI experiment above; which also, incidentally, cannot be used on G3MC embryos anyway because it too fluoresces red. Regardless, DiI proved, at least, that the *'early wave'* GnRH3 cells are unlikely to originate from the olfactory placode.

As mentioned earlier, it has been suggested that the terminal nerve GnRH cells originate from cranial neural crest cells. However, mCherry-positive terminal nerve GnRH3 cells did not co-express a migrating neural crest cell marker (pSOX10:EGFP, (Wada et al., 2005)), and nor did the hypothalamic GnRH3 cells at 36hpf. This data casts some doubt on whether the terminal nerve GnRH cells do in fact originate from neural crest cells; and also whether the terminal nerve cells actually do have a different origin from the hypothalamic GnRH cells; however, this is yet to be confirmed. Moreover, it has also been suggested previously that the hypothalamic GnRH cells which appear around 56hpf may arise from the anterior pituitary placode (Whitlock, 2005b). Whilst this was not specifically investigated here, the DiI experiment which labelled all external placodes, also labelled the anterior pituitary placode. But, as already mentioned, no hypothalamic cells were DiI-positive by 60hpf, so an anterior pituitary placode origin for the hypothalamic cells is also less likely. However, as before, the time of DiI application may have been too late, or the time-point for examination (60hpf) may have been too early to definitively rule this out; and this would therefore need to be investigated further.

3.3.5 Embryonic upregulation of kisspeptin signalling does not induce early hypothalamic GnRH protein expression

The 4 genes that comprise the Kisspeptin/Gpr54 signalling pathway (Kiss1, Kiss2, Gpr54a, and Gpr54b) are all expressed predominately in the forebrain commissure regions by 48hpf. The *in situ* staining prior to this time-point was either very weak, or non-existent; however, previous RT-PCR data (*unpublished*) revealed that all 4 genes are expressed much earlier, from around 24hpf onwards. Therefore, it would seem that whilst the genes are expressed much earlier, the lower sensitivity of the *in situ* hybridisation protocol means that the expression pattern is seen only much later, at around 48hpf.

The kisspeptin/GPR54 signalling pathway was previously shown to increase GnRH expression/secretion both *in vitro* and *in vivo*, in pre-pubescent and sexually mature animals (Oakley et al., 2009). So, if this signalling pathway was activated/ upregulated prematurely, during early zebrafish embryogenesis, could it 'unmask' *migrating* GnRH cells and/or the *'early wave'* hypothalamic G3MC cells?

In fact, injecting the RNA for Kiss1, Kiss2, Gpr54a, and Gpr54b individually, in pairs, or all 4 together, had no measurable effect on embryonic GnRH protein expression i.e. the protein expression remained localised to the terminal nerve region and forebrain commissures, and no early embryonic hypothalamic expression was 'revealed'. However, whilst the stability of the 4 different RNA molecules was confirmed electrophoretically (Figure 3.19A), the unavailability of specific antibodies meant that the longevity of these RNA transcripts *in vivo* could not be proven. Therefore, the possibility remains that the RNA is degraded too quickly *in vivo*, and that this is the reason for the kisspeptin-Gpr54 pathway upregulation having no effect.

As the G3MC spatio-temporal expression pattern was also unaffected, it would seem that kisspeptin/Gpr54 over-expression does not affect the migration of the *'early wave'* GnRH3 cells; however, this study does not reveal whether the *'later wave'* of GnRH neuron migration is affected by the kisspeptin/Gpr54 over-expression; although it is unlikely that the RNA would persist long enough to affect this later GnRH neuronal migration.

To solve the possible problem of RNA instability *in vivo*, plasmids have been constructed whereby Kiss1, Kiss2, Gpr54a, and Gpr54b expression is controlled by a heat-shock promoter, thus permitting temporal control over the upregulation of kisspeptin-Gpr54 signalling during early zebrafish development *(*data not shown*)*. In future experiments, this would allow precise control of kisspeptin/Gpr54 signalling at certain critical time-points during GnRH neuronal migration. Moreover, because these constructs are also designed to simultaneously translate GFP, as a separate protein, from the same transcript, the longevity of the Kiss1, Kiss2, Gpr54a, and Gpr54b transcripts can be better understood. Similarly, the physiological and behavioural consequences of upregulating these genes (by heat-shock) in *adult* zebrafish could also be investigated.

3.4 Conclusions

The rostro-caudal distribution of GnRH neurons along the ventral telencephalon and diencephalon in the adult zebrafish brain is very similar to the spatial expression pattern that can be seen in the brain of an amniote, such as the chick or mouse. However, there are some notable differences in forebrain GnRH neuronal system development in the zebrafish, compared with these amniotes, which have been characterised in the course of this chapter.

To begin with, GnRH immuno-labelling of chick embryos illustrated the characteristic GnRH neuronal 'migratory stream' as it extended towards the hypothalamus, along the olfactory/ terminal nerve fibres. In contrast, using the same GnRH antibody, at a similar developmental stage in zebrafish or medaka, immuno-labelling was detected only in the terminal nerve GnRH cells and their associated projections across the two forebrain commissures. This suggested that, in zebrafish, the hypophysiotropic GnRH neurons migrated at a much later stage (i.e. later than 6dpf); or, that unlike amniotes, they do not express GnRH decapeptide throughout their whole migratory route to the hypothalamus (or, that the GnRH decapeptide antigen was 'masked' in some way, preventing immuno-labelling of these migratory cells).

There have been several conflicting reports regarding the arrival of the hypophysiotropic GnRH neurons to the preoptic area/ hypothalamus in zebrafish and medaka. There have been reports showing GnRH immuno-labelled cells migrating to the hypothalamus at around 56hpf, and other reports using *in situ* hybridisation to conversely show that GnRH3 transcript is restricted to the terminal nerve cells at this time-point, and that there is no transcript found in the hypothalamus until much later, at around 20-30dpf. Moreover, GnRH transgenic reporter analyses showed that GnRH cells do not reach the preoptic hypothalamus until around 12dpf in zebrafish, or around 4dpf in medaka. Together with results from this current study, a **'two wave'** model for GnRH neuronal migration to the hypothalamus has now been proposed by us, in a manner similar to what has previously been described in primate forebrain GnRH neuronal development.

Using a zebrafish GnRH3 reporter line, similar to the one used in this study, it was recently demonstrated that GnRH3 cells in the terminal nerve region extend into the ventral telencephalon between 7-12dpf, and reach the preoptic area from around 12dpf onwards. The extension of terminal nerve GnRH cells into the telencephalon in this way was also found in this current study, using our G3MC line (Figure 3.20C); so, it can be envisaged that there is indeed such a late migration of GnRH cells to the hypothalamus. However, in the case of G3MC, this *considerably later* wave of migration is superseded by a much *earlier* wave of migration into the hypothalamus at around 36-60hpf. But, unlike the *later wave* of migration, there was no migratory '*trail'* of GnRH cells along the ventral forebrain, which would have alluded to the origin and migratory route of these cells. Therefore, until more information is known about this *'early wave'*, it is perhaps better referred to as an '*early accumulation'* at the hypothalamic region.

During this study, a placodal (olfactory) origin for this *'early accumulation'* of hypothalamic GnRH3 cells could not be proven, nor could a cranial neural crest origin be determined for **any** of the GnRH3 cells. A more recent model put forward by Whitlock and colleagues (Whitlock et al., 2009) has suggested that hypothalamic precursors may be the source for the hypothalamic GnRH neurons, and this may explain why no external origin for the *'early accumulation'* GnRH3 cells could be determined during our study. Evidence for this model comes from work by Markakis and co-workers who showed that rat hypothalamic progenitor cells cultured externally gave rise to GnRH-expressing cells (Markakis et al., 2004). However, further work will be required to find out whether the *early-accumulation* GnRH cells do actually arise *in situ*, and indeed whether the *'later wave'* have a similar origin, and are therefore quite separate from the terminal nerve GnRH cells which extend into the telencephalon from around 7-12dpf (i.e. the *'later wave'* may not actually be a 'wave' of migration either).

The zebrafish GnRH immuno-labelling and *in situ* hybridisation data in this study was generally in agreement with the previously-published data. That is, GnRH-expressing cells remain localised to the terminal nerve region (and to their associated axonal tracts) during early embryogenesis (up to 6dpf), and there is little or no hypothalamic expression during these stages. Whilst GnRH-immuno-labelled

cells have been reported *en route* to the hypothalamus at 56hpf (Whitlock et al., 2005b), such migrating GnRH cells were not detected in our study. Without such GnRH immuno-labelling data, it has been difficult to ascertain the authenticity of the *'early accumulation'* of GnRH cells i.e. whether or not they really are hypophysiotropic GnRH neurons.

However, it does remain possible that the 'early accumulation' is truly an *'early wave'* of migration, which sets out the migratory pathway for the *later wave*, in a similar manner to that which has been proposed in primates, but where the cells don't express GnRH transcript/ protein, in this case. Alternatively, if the *'early wave'* of GnRH cells are in fact 'born' within the hypothalamus itself, perhaps they still nevertheless have some type of '*attractive'* role for the *later wave* of migration. If this is the case, the '*early'* GnRH cells may not have any hypophysiotropic role as such; but their role in the migration of the *second* wave of GnRH neurons may nevertheless still be fundamental for the correct formation of the forebrain (hypophysiotropic) GnRH system.

However, the fact still remains that the *'early'* GnRH cells do not express GnRH protein or transcript at 36-60hpf. The reason for their being visualised in the G3MC fish may be because the GnRH3 promoter lacks a repressor element that would normally ensure that GnRH is 'switched off' in these cells at this developmental stage. If this is the case, mCherry fluorescent protein has been acting as a 'lineage tracer' for these early cells; which, if proven, may have revealed a hitherto unreported important step during early GnRH neuronal development in the zebrafish. Moreover, while speculative at this stage, it may turn out that the *'early wave'* is in actual fact the only wave of hypothalamic GnRH neuronal migration (or accumulation), and that subsequent 'waves' of migration are simply the same hypothalamic population down- and upregulating GnRH expression over developmental time.

Regardless of whether or not the terminal nerve GnRH cells contribute to the hypothalamic (hypophysiotropic) GnRH cells, or simply form an essential part of their migratory environment *en route* to the hypothalamus, the terminal nerve GnRH cells are likely to have their own, separate, important 'neuromodulatory role' in

adulthood. For this purpose, the terminal nerve GnRH neuronal projections across the forebrain commissures, and in the region of the olfactory projections, could provide plenty of opportunity for the GnRH system to interact with the olfactory system, perhaps by regulation of reproductive capability in response to certain odours, as well as other external cues.

In amniotes, such as the mouse and chick, GnRH neurons dispersed within the hypothalamus extend their axonal processes to the median eminence portal capillary loops, so that secreted GnRH can reach its receptor on gonadotrophin-releasing cells (gonadotrophs) within the anterior pituitary. In teleost fish, the hypothalamic GnRH cells directly innervate the gonadotrophs, delivering GnRH decapeptide directly to their target receptor. In both medaka and zebrafish, this final, but essential, stage in the development of the hypothalamic GnRH system is thought to occur much later in development. So, regardless of whether GnRH cells migrate to the hypothalamus, or are specified from within the hypothalamus, this final step will need to take place in order to ensure the reproductive capability of the animal. Therefore, the establishment of these important synaptic connections should be investigated further, using the G3MC line, as this may be an essential 'check-point' in the regulation of fish puberty and fertility.

Despite the Kisspeptin-Gpr54 signalling pathway having an essential role in GnRH secretion at the time of puberty, upregulating this signalling pathway during early embryogenesis had no noticeable influences on GnRH expression. But, most disappointingly, this experiment was not able to 'reveal' quiescent (mCherry-expressing, non-GnRH-expressing) cells that have migrated to the hypothalamus during the *'early wave'*; meaning that these cells remain undetectable by GnRH immuno-labelling, due to their lack of GnRH expression. However, to avoid the possibility of a false-negative from this experiment (caused by early mRNA degradation), plasmid constructs which allow temporal control of Kisspeptin/Gpr54 expression will allow us to further investigate the effects of upregulating this pathway during early (and late) embryogenesis. Of course, it remains possible that kisspeptin-Gpr54 signalling upregulation affects only the *'later wave'* of GnRH migration to the hypothalamus, from 12dpf onwards; this would need to be further investigated as well.

It is not known what triggers kisspeptin signalling at the time of puberty; and it may be the case that other signalling pathways (e.g. leptin pathway) may be required for the proper action of kisspeptin signalling. So, upregulating kisspeptin signalling alone may be ineffective; hence, perhaps this is the reason for there being no effect on early hypothalamic GnRH secretion. In fact the concept of what triggers amplification of kisspeptin signalling at the time of puberty remains an important question in this field of research (Oakley et al., 2009).

So, in summary, we have generated a zebrafish GnRH3 reporter line which recapitulates some of the immuno-labelling and *in situ* GnRH expression; but also reveals a novel early hypothalamic GnRH population that was not detected using these analyses (Figure 3.20). The requirement of these '*early'* GnRH cells during hypothalamic GnRH neuronal development is yet to be fully characterised. This GnRH3 reporter line, as well as several olfactory reporter lines, can confidently be used to readily identify the terminal nerve GnRH cells, the forebrain commissures, and the olfactory projections, in normal and genetically-manipulated developing zebrafish. However, some caution will need to be used when interpreting putative terminal nerve GnRH defects, as this may represent defects in the neuromodulatory GnRH system and/or the migratory behaviour of the *'later wave'* of GnRH neuronal migration to the hypothalamus. Moreover, any defects in the *'early wave'* of GnRH migration will need to be carefully analysed in the context of the information that we currently have on this novel GnRH population.

It is yet to be proven whether or not the *'two wave model'* for hypothalamic GnRH neuronal migration actually exists in the zebrafish, in the same way that it is thought to occur in primates. Whilst it is interesting to identify unified themes, as well as common molecular and cellular mechanisms, that control forebrain GnRH system development across all vertebrates, it has become evident during the course of this chapter that such mechanisms may have diverged across the different orders (rodentia, primates, teleosts etc). So, while the zebrafish GnRH neuronal system development may be a very useful model for investigating some of the signalling pathways involved in the molecular pathogenesis of Kallmann syndrome, the phenotypes may not be directly comparable to human GnRH ontogeny. Moreover, in some circumstances, where possible, the chick may be a more useful model,

especially for some of the more brain region-restricted comparative analyses where electroporation techniques may be used.

It has become apparent from this chapter that the forebrain commissures, especially the anterior commissure, play a significant role in the connectivity of the olfactory and GnRH systems; and may also play a role as an 'interface' between these two systems, considering terminal nerve GnRH cells and olfactory bulb interneurons both project axons across this same commissure.

Using the zebrafish model that has been characterised in this chapter, the olfactory/ GnRH system phenotypes that results from manipulating the fibroblast growth factor, FGF, (Chapter 4) and anosmin-1 (chapter 5) signalling pathways, will be discussed in the following results chapters.

3.5 Future prospects

A very important future goal will be to further understand the proposed *'two wave'* model of GnRH neuronal migration to the hypothalamus that has been put forward in this thesis. In particular, the *early-accumulation* of GnRH3 neurons at the hypothalamus will need to be independently-proven using several well-characterised hypothalamic GnRH neuronal markers, to ensure that these cells are not just an unfortunate artefact of the G3MC transgenic line. It was hoped that Kiss1, Kiss2, Gpr54a, or Gpr54b could have fulfilled this role, as kisspeptin has been shown to be expressed in the GnRH neurons during human embryogenesis. Perhaps the future availability of antibodies directed against these proteins may help to label the '*early-accumulation'* GnRH neurons at the hypothalamus. Moreover, it would be useful to further characterise '*the later wave'* of GnRH neuronal migration (i.e. the GnRH-expressing cells which appear *after* 12dpf) in this same manner.

Once the *early* and *later wave* GnRH neurons have been more fully characterised, it will be useful to fully determine their embryonic origins (i.e. where they were specified). The presence of GnRH3 cells in the olfactory epithelium, at around 36hpf in G3MC embryos, suggest that at least some of the forebrain GnRH3 neurons may have an olfactory placodal origin. This will need to be investigated further, as the controversy regarding the origins of the hypothalamic GnRH neurons persists.

The midbrain GnRH2 cells are believed to fulfil a *'neuromodulatory role'* which may or may not be related to the role played by the terminal nerve GnRH system. During embryogenesis, these cells consistently occupy a region in the midbrain, which persists on into adulthood. However, it became apparent during this study that there is also GnRH2 expression along the region of the anterior commissure axonal tracts, extending up to the terminal nerve GnRH region. Therefore, we could speculate that the midbrain GnRH2 cells may interact with the terminal nerve, and in turn, perhaps also the hypothalamic GnRH system. Whilst beyond the scope of this thesis, it would be interesting to investigate these putative interactions between the neuromodulatory and hypophysiotropic GnRH systems, and how this influences reproductive competency.

Failure of proper embryonic hypothalamic GnRH neuronal migration is thought to underlie the absence of hypothalamic GnRH secretion at the time of puberty in Kallmann syndrome (KS) patients. So, proper understanding of the molecular and cellular basis of normal embryonic GnRH neuronal migration in humans, and our chosen comparative model (the zebrafish), is essential for understanding the congenital abnormalities that occur in this disease. However, to confirm that these developmental abnormalities persist into adulthood, it will also be necessary to study the adult brains from normal and genetically-altered zebrafish. One way to do this is to carry out GnRH immuno-labelling on adult brain sections, to identify any reduction in hypothalamic GnRH cell number. An alternative way is to study GnRH gene expression levels in adult zebrafish. This could be done by dissecting out adult brains (or, more specifically, their forebrains) and carry out quantitative RT-PCR for GnRH3, or the gonadotrophin genes (FSHβ and LHβ) whose expression/upregulation should result from normal hypothalamic GnRH secretion. Moreover, in normal reproductively-competent adults, FSHβ and LHβ have been shown to be upregulated upon systemic injection of Kisspeptin 2 (Kitahashi et al., 2009), so this 'normal' response could also be investigated. Finally, another way to determine adult reproductive competency would be to actually look at breeding success in 'normal' and genetically-manipulated (KS-model) adult zebrafish.

Chapter 4
Results (II)

Investigating the role of FGFR signalling during GnRH and olfactory system development and identification of a specific role for the *Fgf8a* ligand

4.1 Introduction

Fgf signalling has a critical role in vertebrate forebrain development. In particular, *FGFR1* and *FGF8*, two KS genes involved directly in this signalling pathway, are required for proper olfactory bulb morphogenesis and hypothalamic GnRH neuronal development in both humans and mice. Moreover, these gene products also have a significant role in the formation of the forebrain commissures in these two organisms.

Interestingly, the role of FGF signalling during formation of the forebrain commissures has also been conserved in the zebrafish. Consistently, loss of one of the two zebrafish *FGF8* orthologues was shown to give defects in the targeting of olfactory axons to the olfactory bulbs. However, the role of the two *FGFR1* and *FGF8* orthologues during olfactory, vomeronasal and GnRH neuronal development in the zebrafish has, until now, not been *fully* investigated.

4.1.1 Zebrafish have two *FGFR1 & FGF8* orthologues

FGFR1 (*KAL2*) and *FGF8* (*KAL5*) are two of the autosomal genes which have been implicated in approximately 15% of KS cases (Dode et al., 2003;

Falardeau et al., 2008). Zebrafish have two orthologues of *FGFR1* (*Fgfr1a* and *Fgfr1b*) (Scholpp et al., 2004; Rohner et al., 2009) and two orthologues of *FGF8* (*Fgf8a* and *Fgf8b*) (Reifers et al., 1998; Reifers et al., 2000). *Fgf8b* was previously misnamed '*Fgf17a*' (or *Fgf17*) before it was realised, by looking at conserved sytenic regions, that it was an *FGF8* orthologue instead of an *FGF17* orthologue (Jovelin et al., 2007). *Fgf8a* is also known as '*ace*', in reference to the *Fgf8a* '*acerebellar*' mutant (Reifers et al., 1998). The second *FGFR1* orthologue (*Fgfr1b*) was only recently identified, so *Fgfr1a* was previously known more simply as '*Fgfr1*'(Scholpp et al., 2004).

4.1.2 Expression of Fgfr1a/Fgfr1b and *Fgf8a*/*Fgf8b* during zebrafish brain development

The expression patterns of *Fgf8a* and *Fgf8b* have both previously been well-characterised, and were found to be largely over-lapping (Reifers et al., 2000), although there were some notable differences, which may have resulted in sub-functionalisation of certain ancestral gene functions. The characteristic mid-hindbrain (MHB; 'isthmic') labelling seen by around 24hpf (20-somite stage) is broadly overlapping for both *Fgf8a* and *Fgf8b*; however, only *Fgf8a* is expressed in the dorso-anterior forebrain by this stage. *Fgf8b* is only detected in a medial sub-population of *Fgf8a*-expressing cells in the optic stalk, but, unlike *Fgf8a*, is not seen at all in the olfactory placode, and only very weakly in the dorsal diencephalon, by around 30hpf. So, to summarise, whilst the characteristic MHB staining is largely shared with both *Fgf8a* and *Fgf8b*, only *Fgf8a* is expressed in the forebrain primordium and olfactory placodes (Reifers et al., 2000; Shanmugalingam et al., 2000l; Jovelin et al., 2007).

Like *Fgf8a*, *Fgfr1a* is expressed in the prospective forebrain from around bud stage (~10hpf), and begins to be expressed in the MHB region by around 14hpf (10-somite stage). *Fgfr1a* is also detected at low levels in the hindbrain at this stage. Later, by around 24hpf, *Fgfr1a* transcript is detected in the pharyngeal arches, the MHB, several domains of the telencephalon and the diencephalon, as well as the optic stalk and olfactory placode. Again, this is a very similar expression pattern to

Fgf8a, suggesting that these two orthologues belong to the same synexpression group, like their murine orthologues, *Fgf8* and *Fgfr1* (Scholpp et al., 2004). In contrast, *Fgfr1b* is expressed in much broader domains of the diencephalon, midbrain, cerebellum and ventral hindbrain by 24hpf, whereas the telencephalon completely lacks *Fgfr1b* transcript at this stage (Rohner et al., 2009). However, because knowledge of the existence of *Fgfr1b* has been much more recent than *Fgfr1a*, further expression analyses are required to confirm these results.

4.1.3 The role of Fgf signalling during zebrafish forebrain development

The *Fgf8a* null mutant zebrafish, named 'acerebellar' due to the conspicuous lack of a cerebellum in these mutants, have several prominent forebrain defects as well. This includes fewer olfactory axonal condensations at the anterior telencephalon; neuronal connections which are a necessary pre-requisite for normal glomeruli formation within the future olfactory bulbs. Moreover, whilst the olfactory epithelium was present, differentiation of some ORNs appeared to be disturbed in these *Fgf8a* mutant embryos, and particular subsets of ORNs (expressing a certain odorant receptor, 'Or2.0') were reduced or absent. Other forebrain defects included a variable failure in the establishment of the two forebrain commissures (*see Figure 4.01*): the anterior commissure (AC) and the post-optic commissure (POC) at the rostral tip of the developing forebrain (Shanmugalingam et al., 2000). The AC defect is of particular interest because the AC comprises, in part, some axonal projections from both olfactory and GnRH neurons traversing the midline (Whitlock, 2004), and would be expected to contribute to a failure in coordination of the olfactory and GnRH systems.

During zebrafish development, at around 16hpf, bilateral clusters of neurons appear within the forebrain which will form the two forebrain commissures. These include a pair of ventrorostral clusters in the diencephalon which project axons towards the midline from around 18hpf onwards to form the POC; and a pair of dorsorostral clusters in the telencephalon which extend axons soon after to form the

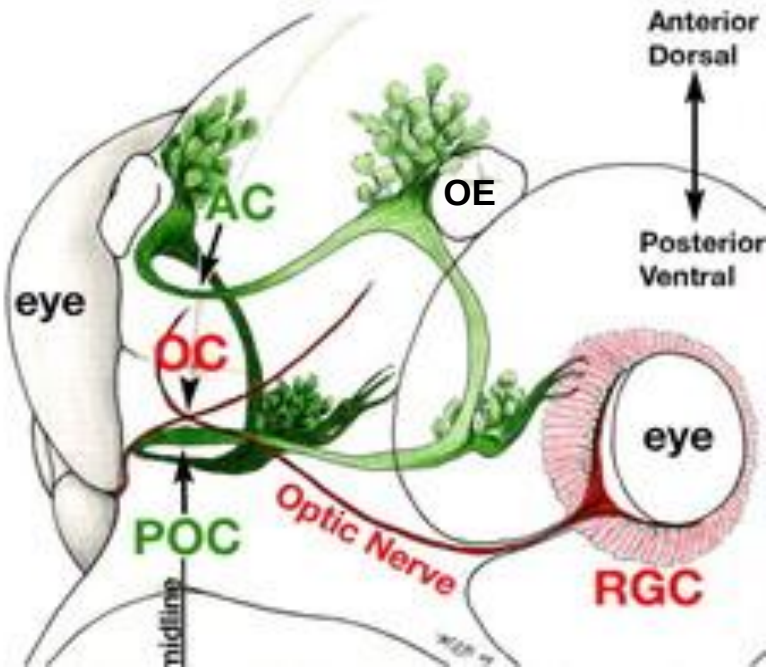

Figure 4.01 The zebrafish forebrain commissures

A three dimensional schematic representation of the forebrain tracts and commissures is depicted for a 48hpf zebrafish embryo, with the anterior dorsal axis projecting towards the top. Commissural axons (in green) traverse the midline to form the anterior commissure (AC) in the telencephalon and the post-optic commissure (POC) in the diencephalon. Retinal ganglion cells (RGCs; *in red*) from the eye form the optic nerve and optic chiasm (OC) close to the where the POC had formed..

OE= olfactory epithelium

Figure 4.01 reproduced with permission from Development (Barresi et al., 2005). doi:10.1242/dev.01929

AC. The outline of both forebrain commissures (POC and AC) have formed by around 27hpf in the zebrafish (Walshe and Mason, 2003; Barresi et al., 2005). A schematic diagram illustrating the formation of these two forebrain commissures is illustrated in Figure 4.02.

4.1.4 Fgfr1 during mammalian forebrain development

The specific loss of *Fgfr1* within the telencephalon of mice results in olfactory bulb aplasia (Hebert et al., 2003). However, despite this lack of normal olfactory bulb morphogenesis, neurons in the anterior part of the *Fgfr1*-deficient telencephalon, although not organised in a typical bulb like structure, still project to their normal targets within the olfactory cortex. Also, the anterior and posterior branches of the anterior commissure fail to project across the midline once they have joined at the anterior olfactory nucleus, even though the initial formation of these neurons is apparently normal. This data would suggest that the olfactory bulb and anterior commissure neurons are indeed generated normally in the *Fgfr1* mutant embryos, but that they are unable to project properly to their intended targets (Hebert et al., 2003; Lindwall et al., 2007). Interestingly, mice which are null for *Ext1* (which encodes an enzyme involved in HS polymerisation), specifically within the telencephalon, have a phenotype which is very similar to the *Fgfr1*-deficient telencephalon mutants i.e. they also have missing olfactory bulbs and loss of the forebrain commissures and midline structures (Inatani et al., 2003). This emphasises the critical role played by HS in the FGF signalling pathway during these developmental processes.

4.1.5 Role of Fgf8 during mammalian forebrain development

Mice with a specific telencephalic deficiency of *Fgf8* survive gestation but die at birth, lacking olfactory epithelium, vomeronasal organ, nasal cavity, and forebrain. During embryogenesis, *Fgf8* is expressed in the rim of the invaginating nasal pit, in a small group of cells that, later in gestation, partially overlaps with putative

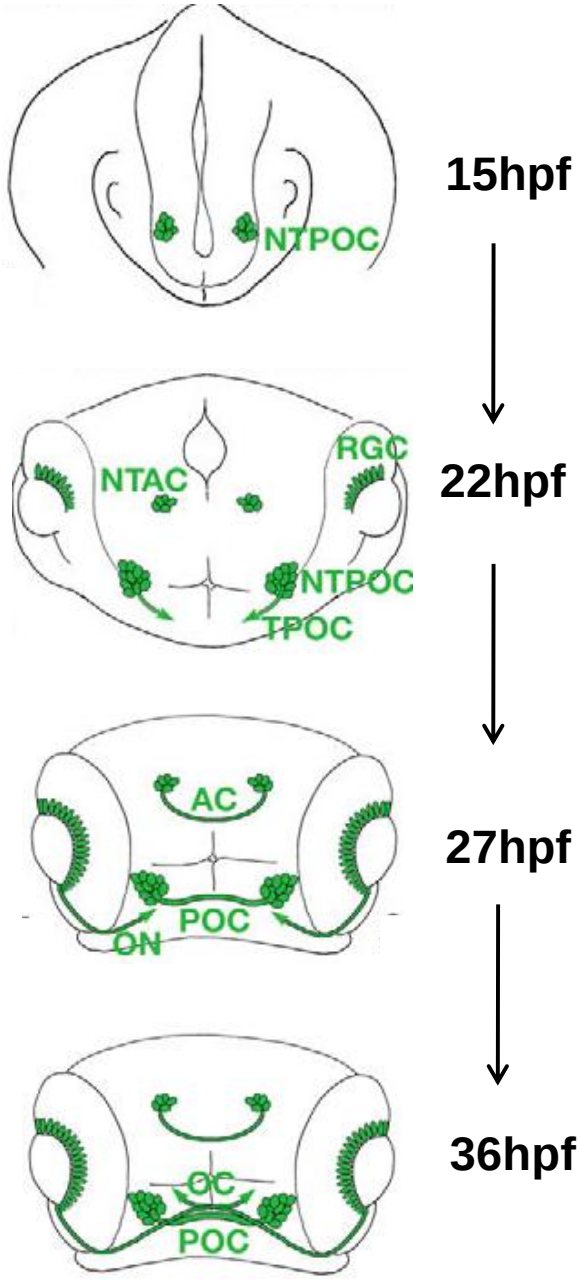

Figure 4.02 Formation of the zebrafish forebrain commissures

A diagram illustrating the progress of anterior commissure (AC) and post-optic commissure (POC) formation between 15hpf and 36hpf. From around 16hpf, clusters of neurons appear in the forebrain that will form the AC and POC: the NTPOC, Nucleus of the tract of the POC; and NTAC, nucleus of the tract of the AC. The NTOC axons begin to project across the midline to form the POC from around 18hpf; and the NTAC axons begin to form the AC soon after. By around 27hpf, the AC and POC have formed; and by 36hpf, the optic nerve (ON) has also formed from retinal ganglion cells (RGCs) in the eyes.

Figure 4.02 adapted with permission from Development (Barresi et al., 2005). doi:10.1242/dev.01929

olfactory epithelium neural stem cells. In fact, E10.5 mouse embryos in which the *Fgf8* gene is inactivated in the anterior neural structures do have at least a rudimentary olfactory pit. However, olfactory neurons within the *Fgf8*-expressing domain of the olfactory pit subsequently undergo high levels of apoptosis in these mutants, resulting in failure of nasal cavity invagination, combined with loss of most of the olfactory epithelium neuronal cell types. This demonstrates that Fgf8 signalling is essential for development of the olfactory epithelium, nasal cavity, and vomeronasal organ in the mouse (Kawauchi et al., 2005).

A model has thus been put forward whereby Fgf8 expression defines an *'anterior morphogenetic center'* which is required for the correct morphogenesis of the nasal cavity, as well as maintenance of olfactory epithelium and vomeronasal neural stem and progenitor cells thereafter. In the mutants, absence of *Fgf8* gene function results in severe deficits in primary olfactory neurogenesis due to the elevated levels of apoptosis in the *Fgf8* expression domain of the olfactory pit (Kawauchi et al., 2005) (*see Figure 4.03*).

4.1.6 Evolutionary conservation of the FGF8/FGFR1 signalling pathway during forebrain development

As already mentioned in Chapter 1, mice homozygous for a hypomorphic *Fgf8* allele lack hypothalamic GnRH neurons (Falardeau et al., 2008; Chung et al., 2008), and similarly, mice which are homozygous for hypomorphic *Fgfr1* allele also have a reduction in hypothalamic GnRH neurons too (Chung et al., 2008). This data, along with the observations above that these mutants also have missing olfactory bulbs, demonstrates that the role played by FGF8 and FGFR1 signalling during olfactory and GnRH system development has been well-conserved from mice to man. In this chapter, it will be investigated whether this role has been well conserved in zebrafish too.

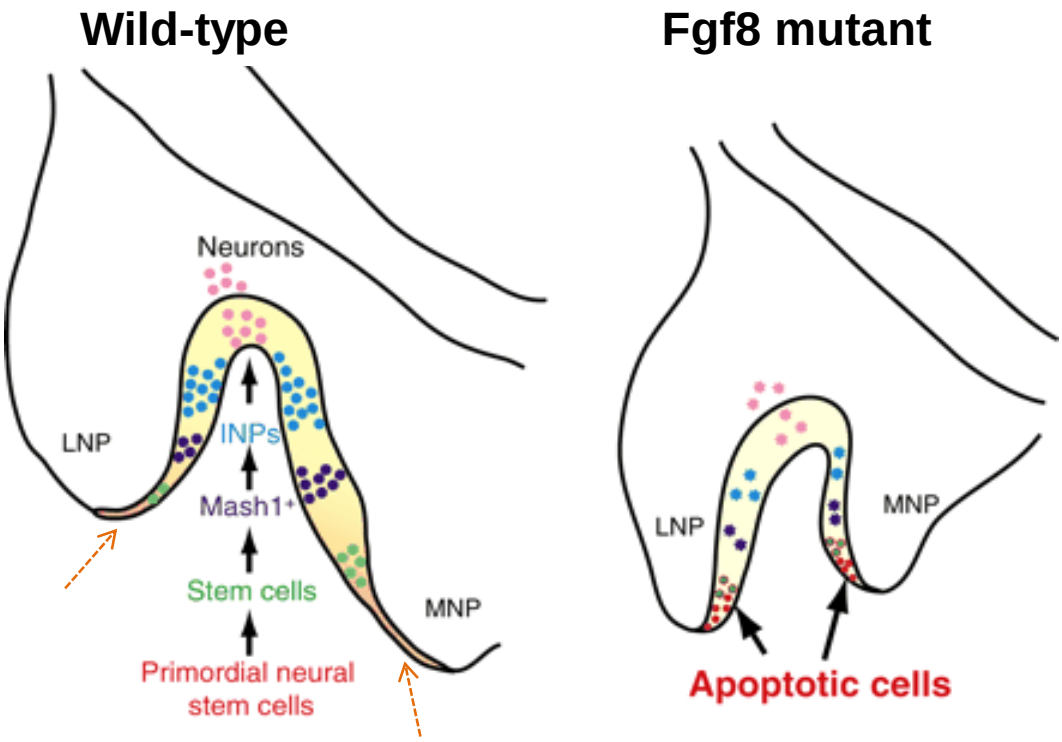

Figure 4.03 The proposed role of Fgf8 in mouse olfactory neurogenesis

This diagram illustrates the Fgf8 expression domain ('anterior morphogenetic center' in orange; emphasised by orange arrows) and the different neuronal cell types during primary olfactory neurogenesis at E10.5 in wild type and conditional Fgf8 mutants that lack Fgf8a expression in the olfactory epithelium. Sox2 expressing cells (definitive neuroepithelium) are yellow; primordial neural stem cells (co-expressing Sox2 and Fgf8), are green; Mash1-expressing committed neuronal progenitors are dark blue; INPs (Ngn1-expressing immediate neuronal precursors) are light blue; and Ncam1-expressing neurons are pink. Cells that undergo apoptosis when Fgf8 is inactivated in the olfactory epithelium are shown in red, and apoptotic primordial neural stem cells are green with a red jagged border.

LNP: lateral nasal placode; MNP: medial nasal placode.

Figure 4.03 adapted with permission from Development (Kawauchi et al., 2005). doi:10.1242/dev.02143

4.1.7 Aims of this chapter

It is well understood that Fgf signalling plays an important role in zebrafish forebrain commissure formation, and that zebrafish *Fgf8a* mutants have fewer olfactory bulb glomeruli. However, a detailed analysis of how the Fgf receptors and Fgf8a/Fgf8b ligands are involved in olfactory and vomeronasal axonogenesis and GnRH system development in the zebrafish has hitherto not been reported.

So, using the olfactory and GnRH transgenic reporter lines that were characterised in the previous chapter, the following aims are set out for this chapter:

-To ascertain the spatio-temporal expression of the Fgf receptors, ligands and downstream effectors during zebrafish forebrain commissure formation and olfactory system development.

-To temporally modulate FGFR signalling by means of pharmacological inhibitors and dominant negative approaches to determine how this affects zebrafish GnRH and olfactory system development.

-To use antisense oligonucleotide (morpholino) and mutant approaches to investigate whether Fgf8a and/or Fgf8b are involved in the development of the zebrafish GnRH and olfactory systems.

-To investigate whether Fgf8b is involved in zebrafish forebrain commissure development, either alone or synergistically with Fgf8a.

4.2 Results

The *in situ* hybridisation spatio-temporal expression pattern for the two zebrafish *FGFR1* and *FGF8* orthologues has been described previously (Scholpp et al., 2004; Rohner et al., 2009; Reifers et al., 1998; Reifers et al., 2000). The aim of this part was therefore to look at their expression specifically during forebrain development, focussing particularly on olfactory and forebrain commissure axonogenesis. Therefore, two significant stages were chosen: 17hpf, when the olfactory placode first forms (*see Chapter 3*) and when the two bilateral clusters which give rise to the AC and POC are first apparent (*see discussion below*); and 23hpf, when ORN and forebrain commissure axonogenesis is becoming active (Walshe and Mason, 2003).

For comparative purposes, the expression pattern for Fgf3 ligand and the other Fgf receptors is also considered. Although Fgf3 does not belong to the same Fgf subfamily as Fgf8a and Fgf8b, its essential role in zebrafish AC and POC formation means that it could also have an important role in forebrain developmental processes where Fgf8 has been implicated, including the olfactory and GnRH systems (*see discussion*).

Finally, expression analysis of two modulators of Fgf signalling, *Dusp6* and *Sprouty4*, are also considered, due to their use as read-outs of active Fgf signalling within the forebrain during embryogenesis (Molina et al., 2007).

4.2.1 *In situ* hybridisation expression analysis of members of the Fgf signalling pathway during olfactory axonogenesis and forebrain commissure formation

Fgfr1a, Fgfr1b, Fgfr2, Fgfr3, and Fgfr4

As expected, at 17hpf, Fgfr1a transcript is present at high levels in the anterior forebrain (Figure 4.04A); whilst the other orthologue, Fgfr1b, shows

indistinct weak labelling throughout the whole head region at this stage (Figure 4.04C). By 23hpf, Fgfr1a is more ubiquitously expressed in several regions throughout the forebrain (Figure 4.04B, B'); however, it remains difficult to decipher spatial expression of Fgfr1b at this stage (data not shown), which only begins to become marginally more distinct by around 26hpf in the diencephalic/midbrain/hindbrain regions (Figure 4.04D, D'). Acetylated tubulin immuno-labelling was carried out on the 23hpf embryos to visualise the newly forming olfactory and commissural axons, in relation to the *in situ* expression. This showed that *Fgfr1a* is expressed in regions of the telencephalon and diencephalon where olfactory and forebrain commissural axonogenesis is occurring (Figure 4.04B; *see inset*); however, analysis of sections from these embryos would need to be carried out in order to distinguish the exact regions of Fgfr1a expression in relation to axon formation (*see discussion*).

Fgfr2, Fgfr3, and Fgfr4 are all expressed throughout most, if not all, regions of the forebrain at 17hpf (Figure 4.04E, G, I). By 23hpf, Fgfr2 is still expressed throughout the forebrain, but shows strongest expression in the ventral telencephalon and anterior diencephalon (Figure 4.04F). Fgfr3 and fgfr4 expression is strongest in the diencephalon by 23hpf, but are both still expressed in some telencephalic regions, including the ventral telencephalon (Figure 4.04H, J). The anti-acetylated tubulin immuno-labelling on these embryos showed that all three receptors are expressed in regions of olfactory and commissural axon formation; especially where the POC forms in the diencephalon (Figure 4.04F', H', J'; *see insets*).

Fgf8a, Fgf8b, and Fgf3

At 17hpf, *Fgf8a*, but *not Fgf8b*, is expressed in the anterior forebrain (Figure 4.05A, C). By 23hpf, *Fgf8a* and *Fgf8b* are both expressed in the optic stalk, but only *Fgf8a* is expressed in the telencephalon, dorsal diencephalon (Figure 4.0B') and olfactory epithelium (*red arrow*, Figure 4.05B'') at this stage. The *Fgf8a* forebrain staining was strongest towards the midline region.

Figure 4.04 Fgf receptor expression during olfactory and commissural axonogenesis

In situ hybridisation analysis for Fgfr1a (A, B, B'), Fgfr1b (C, D, D'), Fgfr2 (E, F, F'), Fgfr3 (G, H, H'), and Fgfr4 (I, J, J') at 17hpf (A, C, E, G, I), 23hpf (B, F, H, J) and 26hpf (D). Magnified pictures are shown for the 23hpf and 26hpf images in B', D', F', H' and J'. The insets in B', F', H', and J' show anti-acetylated tubulin (AT) immuno-labelling (in green) of the commissural tracts for those corresponding embryos: the asterisk in these images indicates the centre of the olfactory placode (-which was identified using the AT labelling). The labelling for Fgfr1b was quite indistinct at 17hpf (C) and there was no labelling at 23hpf *(not shown)*, so a 26hpf embryo was used in D and D' *(with no AT labelling)*.

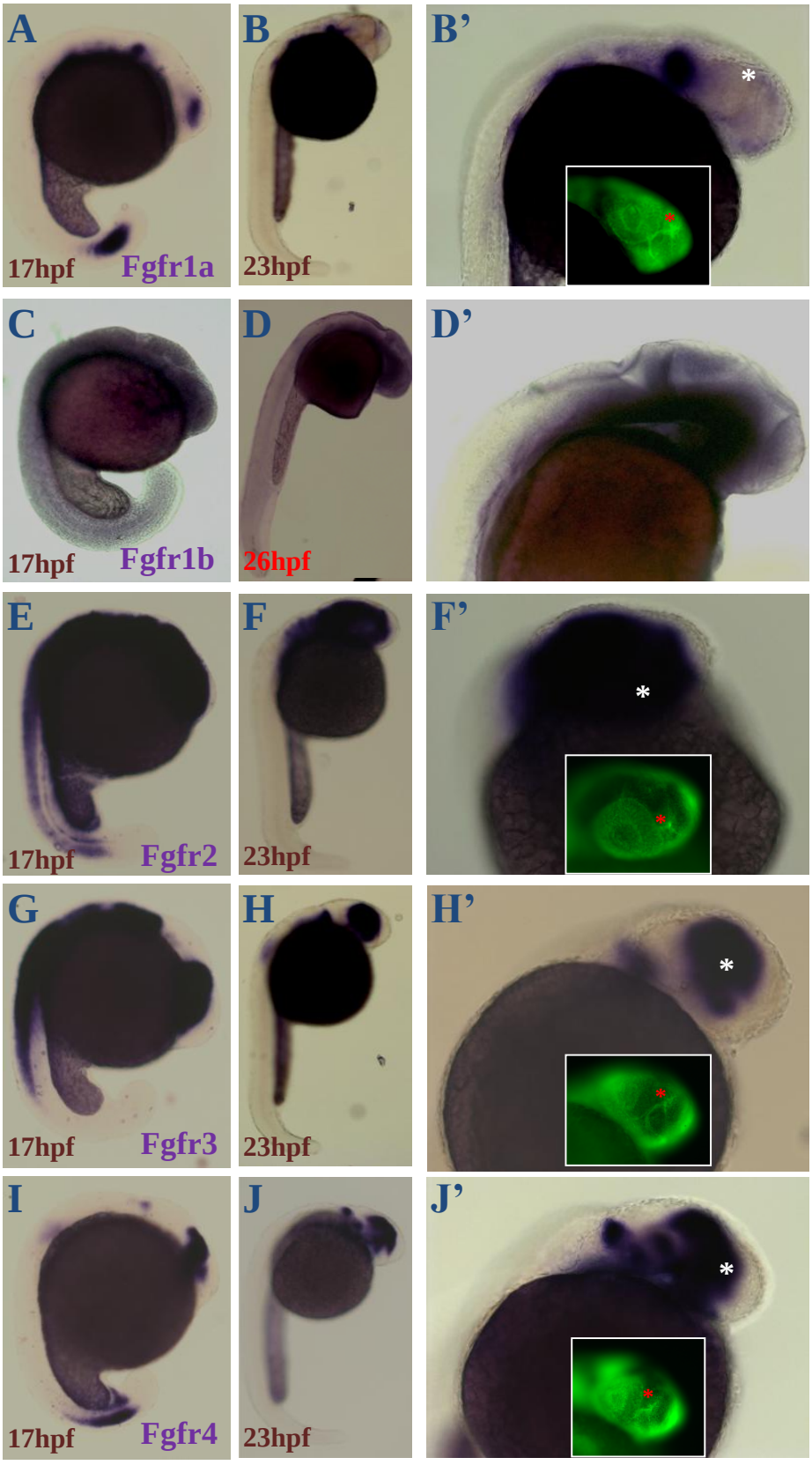

Figure 4.04 Fgf receptor expression during olfactory and commissural axonogenesis

Fgf3 showed weak forebrain labelling at 17hpf (Figure 4.05E), which became stronger by 23hpf, especially in the diencephalon and anterior telencephalon (Figure 4.05F), as well as some weak expression in the region of the olfactory pits (Figure 4.05F'; *see asterisk*).

4.2.2 Expression of Fgf downstream modulators during olfactory & GnRH neuronal development

Sprouty4 (Spry4), an Fgf signalling antagonist, has an expression pattern that is very similar to Fgfr1a and Fgf8a, including the very distinctive isthmic (MHB) expression at 17hpf and 23hpf (Figure 4.06A, B). Moreover, there is anterior forebrain staining at 17hpf (Figure 4.06A), as well as staining of the optic stalk, telencephalon (weakly) and dorsal diencephalon at 23hpf (Figure 4.06B, B'). However, olfactory epithelium expression for Sprouty4 was not detectable at these stages (Figure 4.06B'; *see asterisk*).

Dusp6, another Fgf antagonist, is strongly expressed throughout the forebrain at 17hpf and 23hpf, particularly in the ventral diencephalon and anterior telencephalon (Figure 4.06C, D). Dusp6 is also expressed in the olfactory placodes throughout these stages, as well as within the region of the bilateral clusters which project across the midline to form the AC and POC (Figure 4.06D').

The Dusp6 reporter line (pDusp6:d2GFP) was crossed with G3MC (pGnRH3:mCherry; *see Chapter 3*), and the resulting double transgenic offspring were visualised between 24-30hpf (Figure 4.06E, F). At 24hpf, GFP expression indicated Dusp6 expression at the olfactory pits (Figure 4.06E), which remained until at least 30hpf (Figure 4.06F); however, due to the dynamic nature of d2GFP expression, not all of the same ORNs will still be expressing d2GFP at this time-point. However, the terminal nerve GnRH3 (G3MC) cells do not co-express d2GFP (Dusp6) between 24hfp and 30hpf, and neither do the initial hypothalamic GnRH3 (G3MC) cells at 30hpf (Figure 4.06F). Moreover, there was some dynamic d2GFP (Dusp6) expression in some cells in the anterior telencephalon at 24hpf and 30hpf, in a region where the olfactory bulbs will form (Figure 4.06E, F).

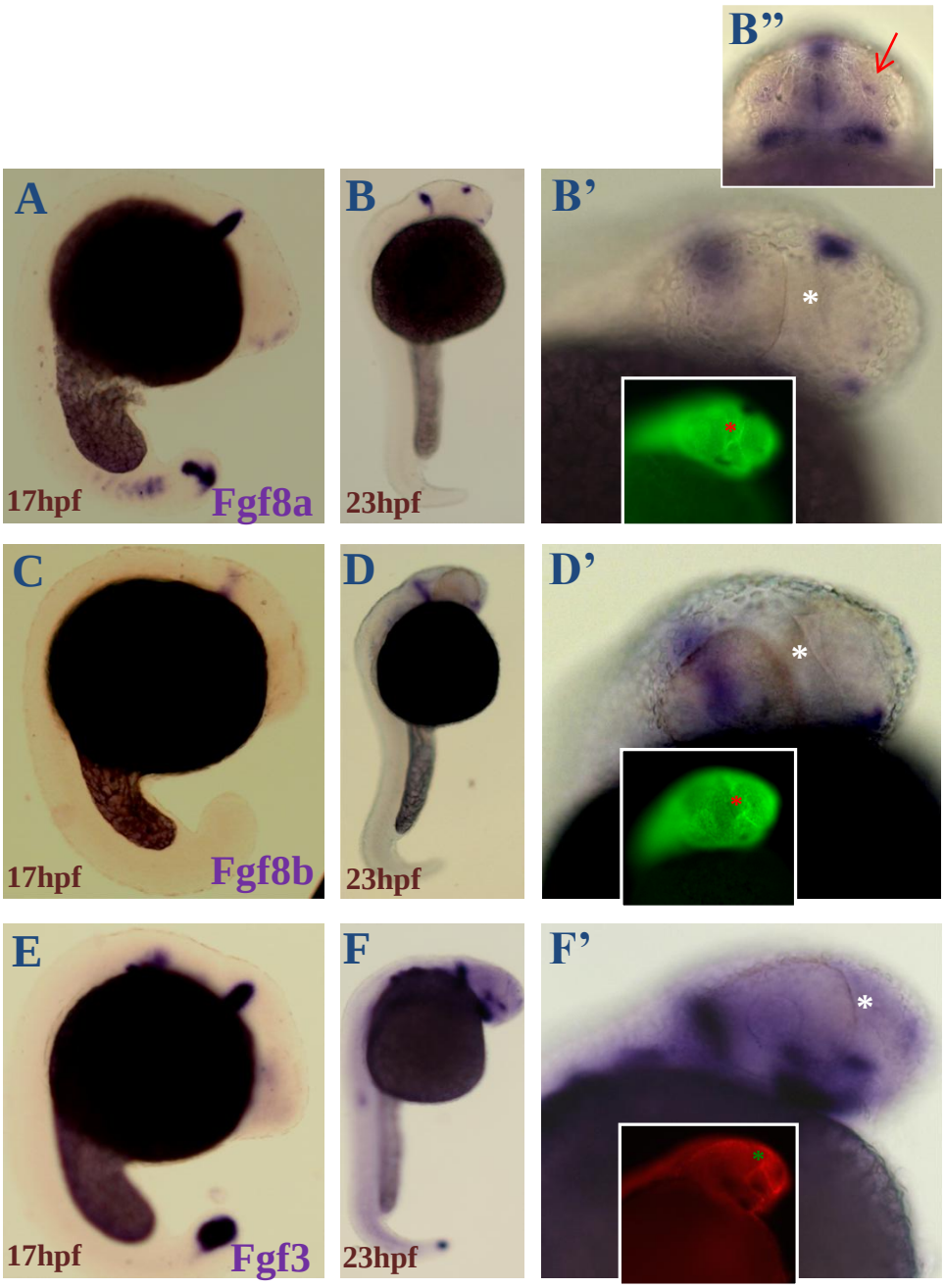

Figure 4.05 Fgf8a, Fgf8b, and Fgf3 ligand expression during olfactory and commissural axonogenesis

In situ hybridisation analysis for Fgf8a (A, B, B', B''), Fgf8b (C, D, D'), and Fgf3 (E, F, F') at 17hpf (A, C, E) and 23hpf (B, D, F). Magnified pictures are shown for the 23hpf images in B', D', and F'. The insets in B', D', and F' show anti-acetylated tubulin (AT) immuno-labelling (in green or red) of the commissural tracts for those corresponding embryos: the asterisk in these images indicates the centre of the olfactory placode (which was identified using the AT labelling). B'' shows B' viewed from the ventral view with a red arrow indicating Fgf8a labelling in the olfactory epithelium.

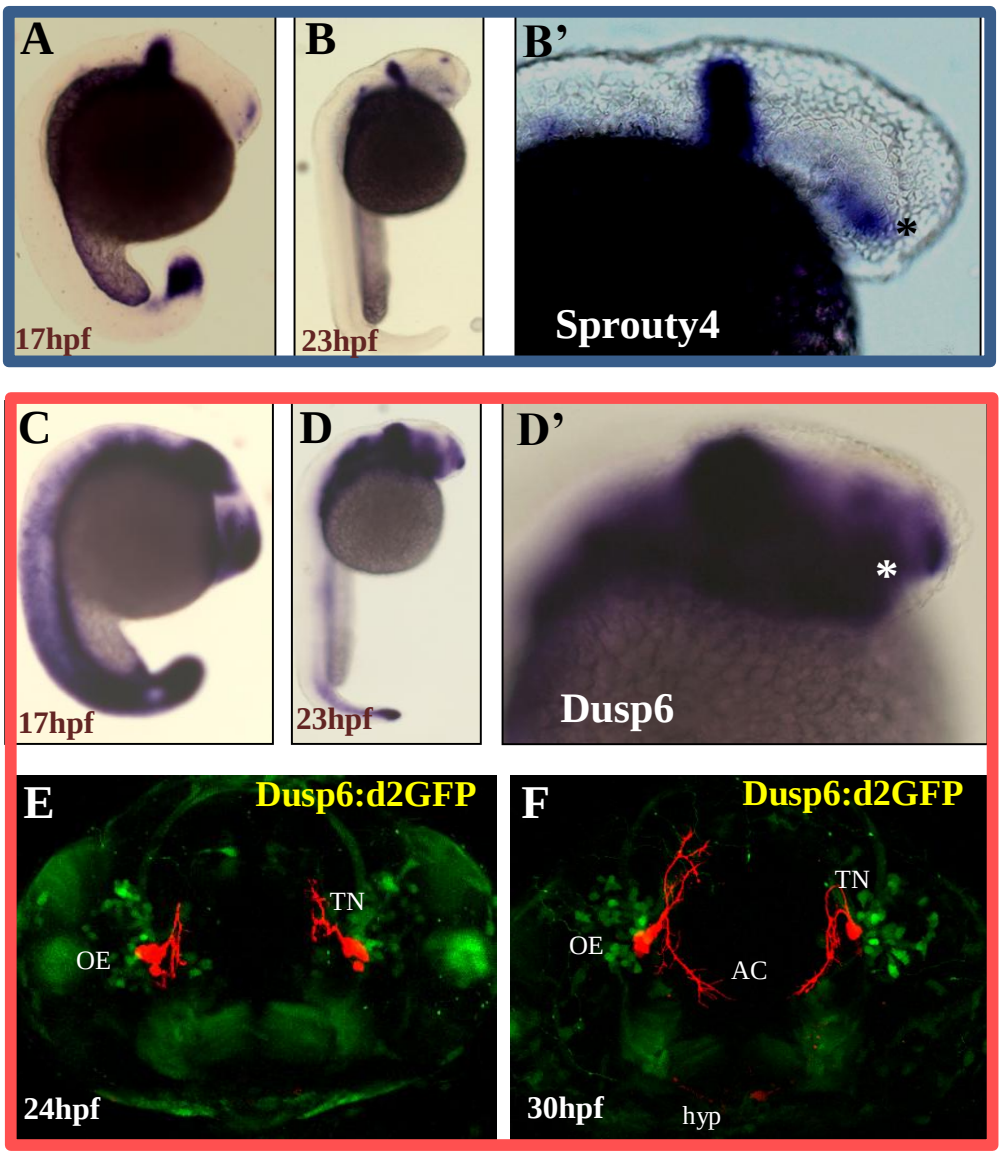

Figure 4.06 Expression of FGFR downstream signalling markers during olfactory and commissural axonogenesis

In situ hybridisation analysis for Sprouty4 (A, B, B') and Dusp6 (C, D, D'), at 17hpf (A, C) and 23hpf (B, D). Magnified pictures are shown for the 23hpf images in B' and D' with asterisks marking the centre of the olfactory placode (-which was identified using the AT labelling). E and F show a ventral view from a cross of Dusp6:d2GFP (in green) with G3MC (in red) at 24hpf (E) and 30hpf (F). E and F are confocal views from the same embryo.
OE= olfactory epithelium; TN= terminal nerve; AC= anterior commissure; hyp= hypothalamus.

Anti-pERK immuno-labelling was carried out on G3MC embryos at 24hpf, 30hpf and 48hpf. However, there was no brain pERK immuno-labelling detected at either 24 or 30hpf (data not shown); whereas by 48hpf, pERK labelling was clearly visible in the presumptive olfactory bulb region of the anterior forebrain, and also in a few cells within the olfactory pits (*represented as white dotted circles* in Figure 4.07). However, there was no anti-pERK and G3MC (GnRH3) co-expression detectable at 48hpf in the terminal nerve (Figure 4.07) and hypothalamic GnRH3 cells (data not shown).

4.2.3 Modulation of FGFR signalling by SU5402 inhibition and dominant negative approaches

Dechorionated embryos were incubated in aquarium water containing 10μM SU5402 (a global FGFR signalling inhibitor) at either 22-36hpf or 14-22hpf, as summarised in Figure 4.08. Some of those embryos incubated in SU5402 from 22hpf to 36hpf were fixed immediately at 36hpf, whilst the remaining embryos were left to develop in aquarium water (without additives) until 60hpf, and then fixed. Similarly, embryos incubated in SU5402 from 14hpf to 22hpf, were subsequently incubated without SU5402 until 36hpf and then fixed, or incubated until 60hpf.

Embryos incubated in SU5402 at 22-36hpf and fixed at 36hpf (n=44/44, 2 experiments) and 60hpf (n=40/40, 2 experiments[3]) had an apparently normal external morphological phenotype. However, those embryos incubated in SU5402 at 14-22hpf had some morphological defects: specifically, those fixed at 36hpf showed some evidence of lower trunk cell necrosis (n=11/43, 2 experiments), whereas those left to develop until 60hpf were all dead by this time-point (n=38/38, 2 experiments), and therefore not fixed or analysed further.

[3] The number of embryos representing a stated phenotype (n=?/?), are recorded as fraction of a pooled total from a specified number of experiments. E.g. '***n=40/40*, 2 experiments**' means that 40 out of a total of 40 embryos showed a particular phenotype across two separate experiments (within a certain experimental group).
NOTE: Numbers for dead embryos is not mentioned, unless the number is significantly higher in one group compared to the others.

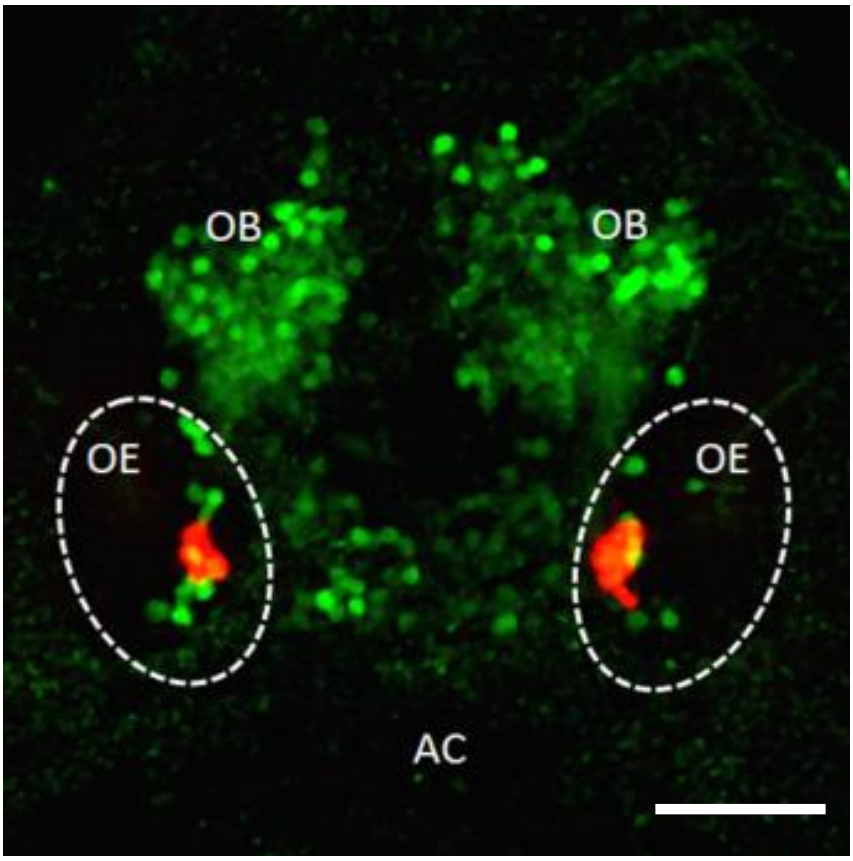

Figure 4.07 phosphoERK immuno-labelling in the zebrafish forebrain

A ventral view of a 48hpf G3MC embryo which has been immuno-labelled with anti-phosphorylated-ERK (anti-pERK, in green). The olfactory epithelia regions are broadly demarcated with white dotted circles. Within these demarcated regions the terminal nerve G3MC cells are visualised alongside approx. 8 pERK-positive cells. The olfactory bulbs, at the anterior end of the forebrain, have distinctly high pERK immuno-labelling. *(No forebrain pERK immuno-labelling was visualised prior to 48hpf; data not shown).*
Scale bar is 50μm.
OE= olfactory epithelium; OB= olfactory bulbs; AC= anterior commissure.

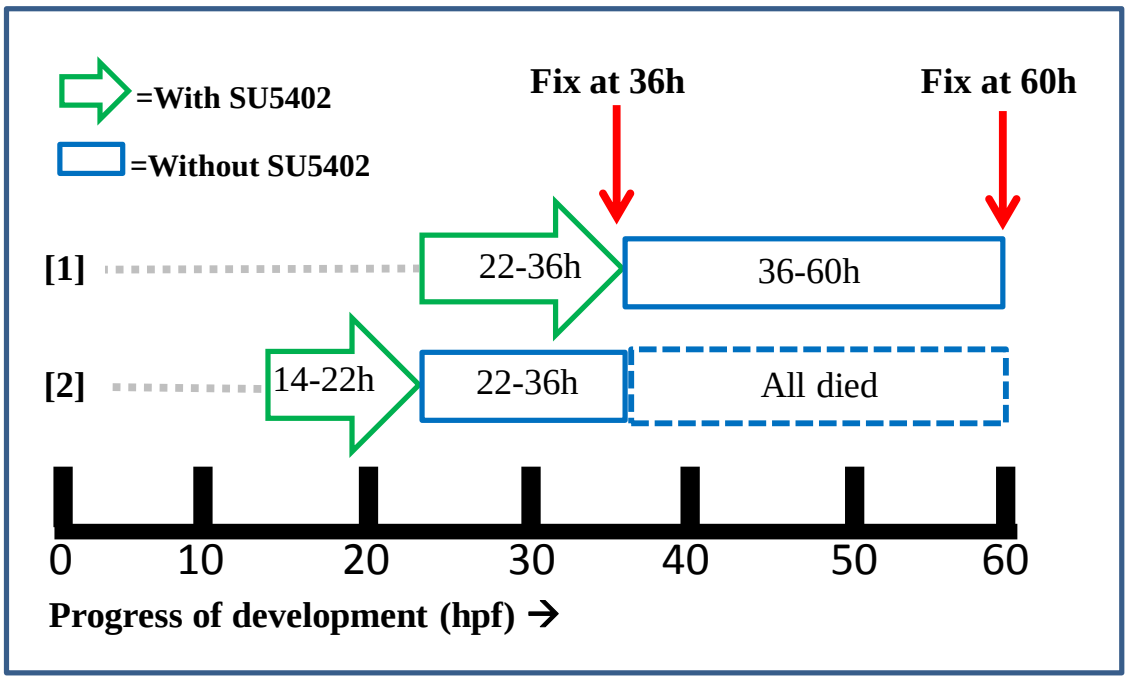

Figure 4.08 Diagram illustrating plan for FGFR inhibition using SU5402

This diagram shows the two routes, [1] and [2], for specific temporal FGFR inhibition using SU5402. The progress of development is illustrated at the bottom of the diagram as a linear time-scale from 0-60hpf. The dotted lines indicate progress of development prior to SU5402 incubation; the green 'boxed' arrows represent times of SU5402 incubation; and blue boxes show times of post-SU5402 development. The embryos from routes [1] and [2] were fixed at either 36hpf or 60hpf (see red arrows): however, embryos treated by route [2] were either dead or dying by 60hpf, and were therefore not analysed further. Control embryos were incubated in 'DMSO only' from 14hpf until 36hpf and showed identical phenotypes to wild-type non-treated embryos (*data not shown)*, thus permitting one 'universal' DMSO control for figures 4.06, 4.08, 4.09, and 4.10.

As an alternative to FGFR down-regulation by use of exogenous inhibitors, a dominant negative approach was also adopted, using the HSP70:dnFGFR-EGFP (Lee et al., 2005) transgenic line. Specifically, the bacterial heat shock promoter (HSP70) was utilised to control the concurrent expression of dominant negative FGFR (dnFGFR) and EGFP, upon activation by means of 'heat-shock' (i.e. 45mins incubation at 37°C). Heat-shock was carried out 2 hours prior to the intended activation of dnFGFR i.e. at 18hpf and 22hpf, to down-regulate FGFR signalling from ~20hpf and ~24hpf onwards, respectively. After heat-shock, embryos were then incubated normally and fixed when they reached 36hpf, by which time dnFGFR was presumably still active (i.e. not yet degraded).

Forebrain commissure phenotype

As SU5402 was dissolved in DMSO before application to the embryos, the same volume of DMSO was also applied to the control embryos, and incubated in this way between 14hpf and 36hpf. These DMSO control embryos had no external morphological abnormalities, and upon acetylated tubulin immuno-labelling had normal (wild-type) forebrain commissure (AC and POC) formation at 36hpf (n=48/48, 2 experiments, Figure 4.09A, A') and 60hpf (n=41/41, 2 experiments, Figure 4.09B). Embryos incubated with SU5402 between 22hpf and 36hpf were either apparently normal (n=37/44, 2 experiments, i.e. similar to Figure 4.09A, A') or with slight AC defects, such as a subtle reduction in the number of axons crossing the midline (n=7/44, 2 experiments, Figure 4.09C, C'). But, by 60hpf, it was no longer possible to detect any of these subtle defects, and the AC looked apparently normal in all embryos (n=40/40, 2 experiments, Figure 4.09D).

In contrast, for embryos incubated with SU5402 between 14hpf and 22hpf, and then fixed at 36hpf, defective forebrain commissure formation phenotypes were much more severe. In some cases, both the AC and POC had formed, but there were several axons mis-projecting between the two commissures (n=14/43, 2 experiments, Figure 4.09E, E', G, G'); whilst in other cases, the AC failed to form correctly (n=13/43, 2 experiments, Figure 4.09F), or didn't form at all (n=9/43, 2 experiments, Figure 4.09H). Also, in just one case, the POC hadn't formed at all (data not shown), or was highly defasciculated (n=3/43, 2 experiments, Figure

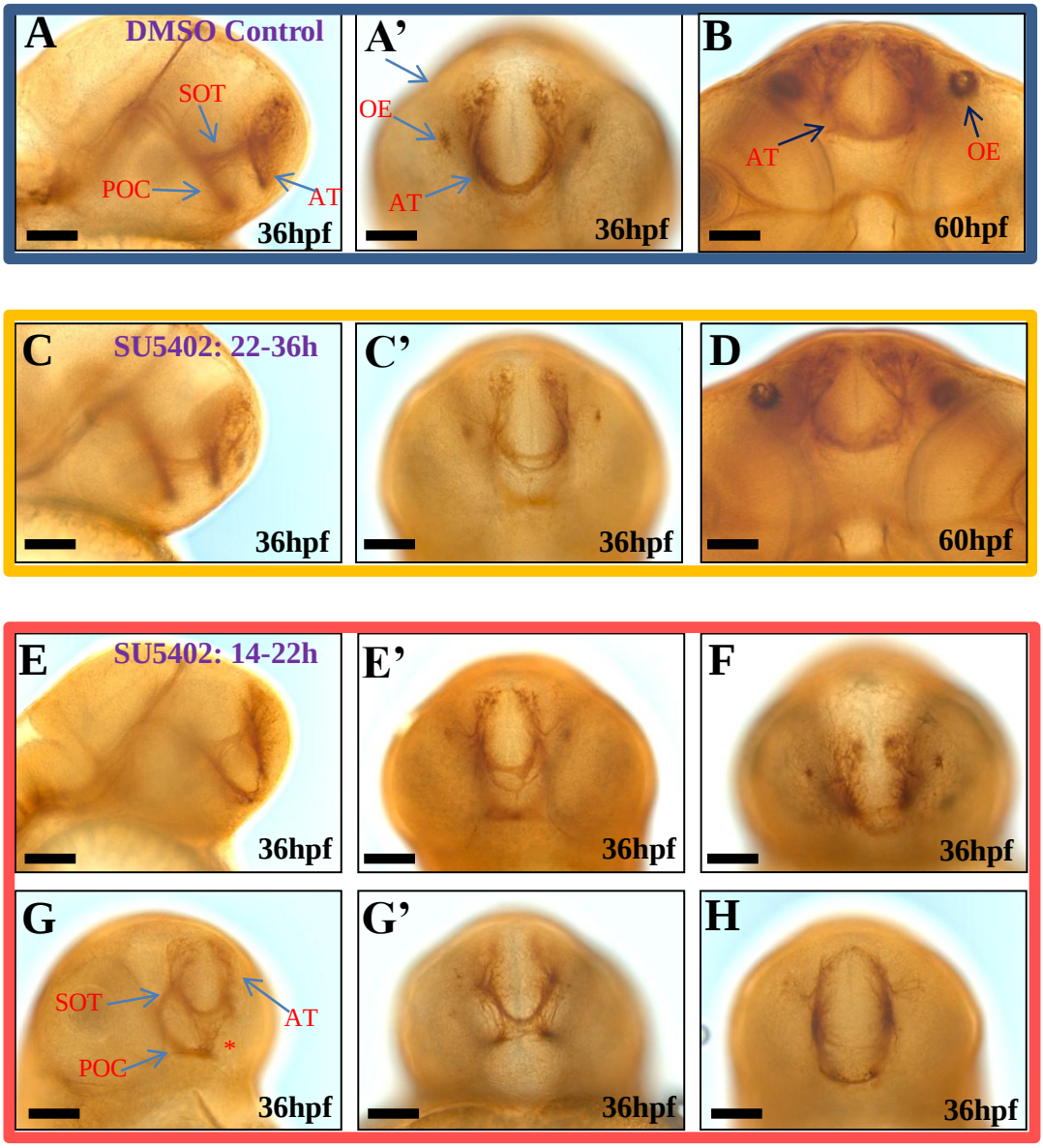

Figure 4.09 FGFR inhibition using SU5402: forebrain commissure phenotype

Anti-acetylated tubulin (AT) immuno-labelled embryos (with DAB) are shown for the 'DMSO control' (A, A', B), 'SU5402 : 22-36h' (C, C', D), and 'SU5402: 14-22h' (E, E', F, G, G', H) embryos, all at 36hpf , except B and D, which are at 60hpf (the 'SU5402: 14-22h' 60hpf embryos all died: *data not shown*). Lateral views for A, C, E and ventral-lateral for G; the rest are all ventral views. E-H demonstrate increasing severity of phenotype for this group. Blue arrows indicate relevant AT immuno-labelling (*see key below*).
Scale bars are 100µm.
POC= post-optic commissure; SOT= supra-optic tract; AC= anterior commissure; OE= olfactory epithelium

4.09G, G'). The remaining six embryos from this group were dead at 36hpf. All embryos from this group which were incubated until 60hpf were dead by this stage and not analysed further (n=39/39, 2 experiments, data not shown).

All HSP70:dnFGFR-EGFP embryos heat-shocked at 18hpf were dead (n=32/42, 2 experiments) or dying (n=10/42, 2 experiments) by 36hpf and not processed further (data not shown). Whilst embryos heat-shocked at 22hpf were mostly apparently normal by 36hpf, and were immuno-labelled for acetylated tubulin in order to visualise their forebrain commissures, as a comparison with the SU5402-treated embryos. Control embryos, which were heat-shocked at 18hpf, but did not express the dnFGFR-EGFP transgene (Figure 4.10A), showed normal forebrain commissure development at 36hpf (n=36/36, 2 experiments, Figure 4.10B, B'). HSP70:dnFGFR-EGFP embryos that were heat-shocked at 22hpf were fluorescing green by 23-24hpf, demonstrating that the dnFGFR/EGFP transgene was successfully switched on. These dnFGFR embryos were fixed at 36hpf, and it was found that all had normal forebrain commissure phenotypes (n=40/40, 2 experiments, Figure 4.10D, D'), although several embryos showed signs of cell necrosis along their trunks (data not shown).

Olfactory and vomeronasal axonal phenotype

Once applied to embryos, the autofluorescence emitted by SU5402 is retained long after the SU5402 has been removed. As a result of this, visualisation of EGFP, Venus, and mCherry fluorescence by confocal microscopy from the olfactory, vomeronasal, and GnRH3 transgenic reporter lines was considerably hindered. Therefore, in order to improve the clarity and sensitivity of this analysis, embryos treated with SU5402 (and their controls) were immuno-labelled with anti-GFP (for pOMP:tauEGFP and pTRPC2:Venus) or anti-mCherry (for pGnRH3:mCherry), followed by HRP-conjugated secondary antibodies and DAB colour reactions (*see Chapter 2*). This meant that standard (non-fluorescent) light microscopy could then be used to visualise these embryos.

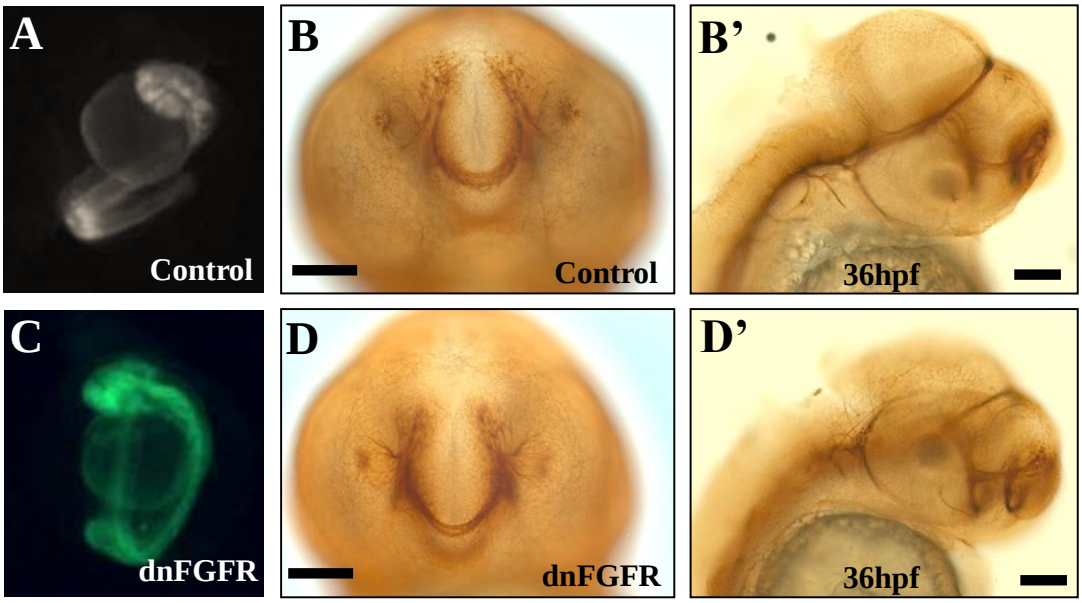

Figure 4.10 FGFR inhibition: using the dominant negative FGFR approach

HSP:dnFGFR-GFP (C, D, D') and wild-type control embryos (A, B, B') were heat-shocked at 22hpf and imaged for fluorescence (A and C) or fixed at 36hpf for anti-acetylated tubulin immuno-labelling, with DAB (B, B', D, D'). GFP (green) fluorescence in C indicates that dnFGFR expression has been switched on, compared with the control (A) which shows no GFP fluorescence (and no dnFGFR). (Embryos heat shocked at 18hpf, or earlier, were dead or dying by 36hpf (*data not shown*).
Scale bars are 100µm.
HSP= heat-shock promoter.

For embryos treated with SU5402 between 22hpf and 36hpf, no defects in olfactory axonogenesis were detected by 36hpf (n=45/45, 2 experiments, Figure 4.11D, E) or 60hpf (n=39/39, 2 experiments, Figure 4.11F). On the contrary, olfactory axonal defects were present in those embryos treated with SU5402 between 14hpf and 22hpf (Figure 4.11G-N). For these embryos, in some cases there were axons extending towards the olfactory bulbs, but they appeared to be less ordered, and not tightly fasciculated as they approached the forebrain (n=32/49, 2 experiments, Figure 4.11G-J), whilst in other cases, this olfactory axonal bundle appeared to be entirely missing or much reduced in axonal number (n=17/49, 2 experiments, Figure 4.11K-N). Moreover, the actual olfactory pits often sometimes appeared to be disorganised or irregular, less shaped like the wild-type 'rosette' olfactory pit, (n=29/49, 2 experiments, Figure 4.11I, N), compared with the DMSO control embryos, which all had the wild-type morphology at 36hpf (n=43/43, 2 experiments, Figure 4.11A, B) and 60hpf (n=40/40, 2 experiments, Figure 4.11C). Whilst there was considerable variability in olfactory pit size amongst the three experimental groups, including the controls, it was not possible to detect a significant decrement in average OMP-positive olfactory pit size in the SU5402-treated embryos, compared with the DMSO-treated controls (data not shown).

The vomeronasal (pTRPC:Venus) neurons within the olfactory pit were not immuno-labelled as strongly by anti-GFP, partly because this cell type is much fewer in number compared to the OMP-positive ('olfactory') neurons. This made it somewhat difficult to determine whether there were any defects in vomeronasal axonogenesis as well. It was, however, evident that the embryos treated with SU5402 between 22hpf and 36hpf (n=37/37, 2 experiments, Figure 4.12B) were similar in appearance to the DMSO controls (n=39/39, 2 experiments, Figure 4.12A) at 36hpf; whilst many of the embryos treated with SU5402 between 14hpf and 22hpf appeared to have 50% or fewer the number of vomeronasal axons and soma (n=31/39, 2 experiments, Figure 4.12C, D) at 36hpf, compared with the controls.

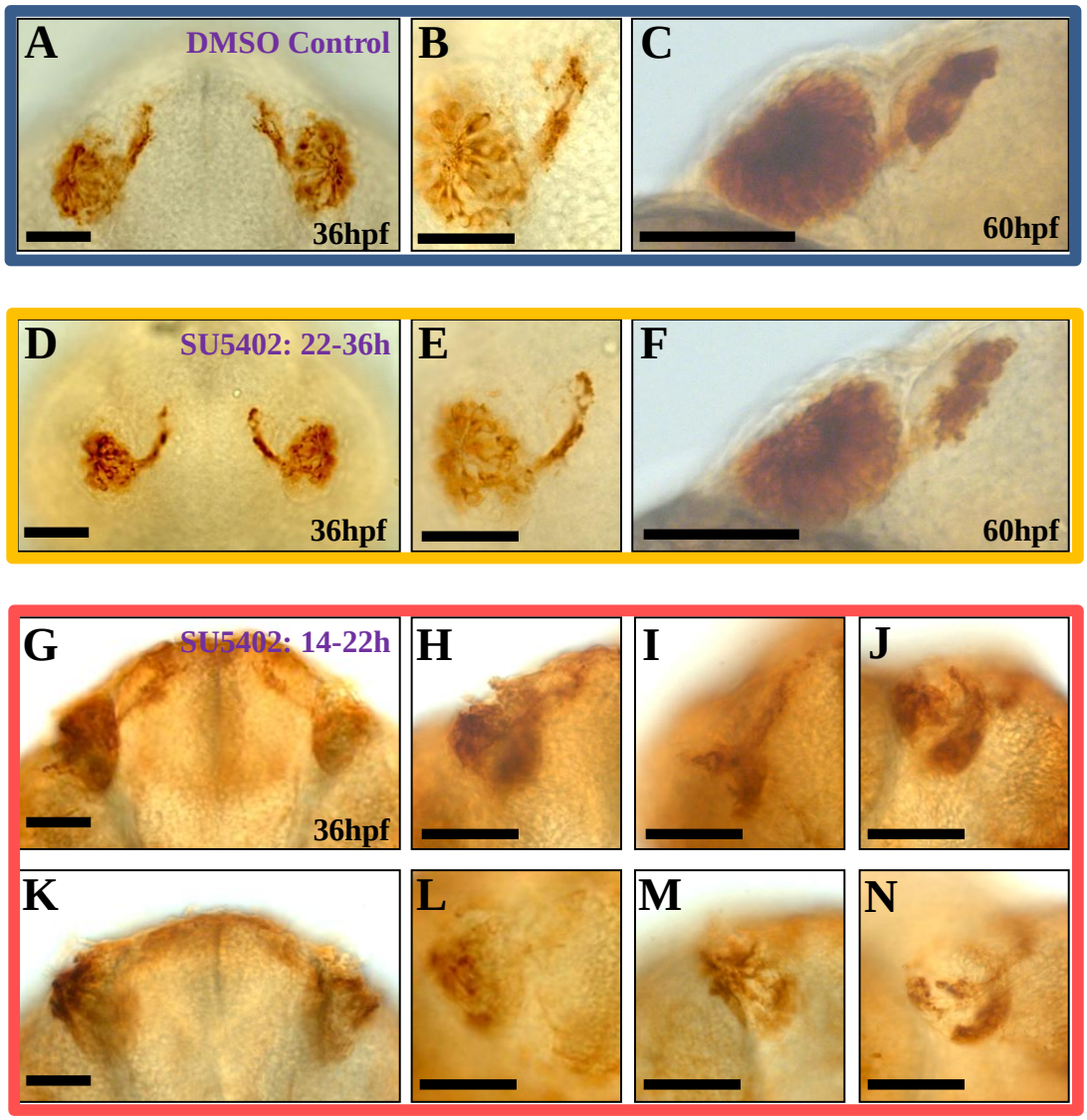

Figure 4.11 FGFR inhibition using SU5402: olfactory phenotype

Anti-GFP immuno-labelled OMPG embryos (with DAB) are shown for the 'DMSO control'(A-C), 'SU5402: 22-36h' (D-F), and 'SU5402: 14-22h' (G-N) embryos, all at 36hpf , except C and F, which are at 60hpf (the 'SU5402: 14-22h' 60hpf embryos all died: *data not shown*). All views are ventral. A, D, G, and K show both olfactory pits; all other images depict a single olfactory pit. G-N demonstrate increasing severity of phenotype for this group.
Scale bars are 50μm.

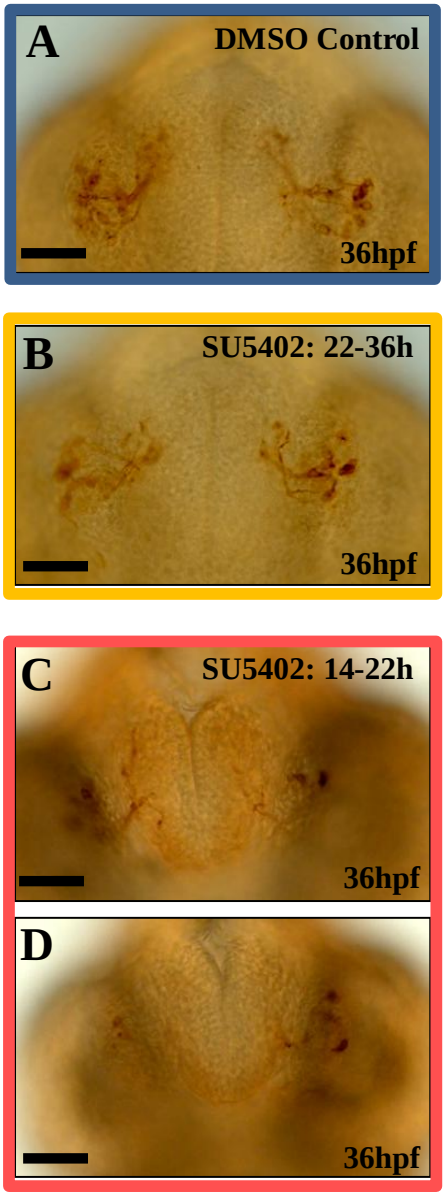

Figure 4.12 FGFR inhibition using SU5402: vomeronasal phenotype

Anti-GFP immuno-labelled pTRPC2:Venus embryos (with DAB) are shown for the 'DMSO control'(A), 'SU5402 : 22-36h' (B), and 'SU5402: 14-22h' (C and D) embryos, all at 36hpf. All views are ventral. C and D illustrate the two types of phenotype that are found in this group. Scale bars are 50μm.

GnRH3 neuronal phenotype

It was difficult to quantify hypothalamic GnRH cells from DAB-stained embryos, so a qualitative approach was used to assess the size of the hypothalamic GnRH cell clusters for the SU5402 treated embryos, compared with the controls.

Embryos treated with SU5402 between 22hpf and 36hpf (n=47/47, 2 experiments, Figure 4.13E-H) had the same G3MC phenotype at 36hpf as the DMSO control embryos (n=45/45, 2 experiments, Figure 4.12B) i.e. normal terminal nerve GnRH3 cell clusters which project axons across the anterior commissure, as well as a 'normal-sized' cluster of *'early wave'* GnRH3 cells at the hypothalamus (*see Chapter 3 for further discussion on the expected size of these GnRH populations*). In contrast, embryos treated with SU5402 between 14hpf and 22hpf have normal-sized terminal nerve GnRH3 cell clusters which don't project axons correctly across the midline via the anterior commissure (n=44/50, 2 experiments, Figure 4.13I-K). Moreover, the hypothalamic cluster of GnRH3 cells is absent (n=19/50, 2 experiments, Figure 4.13L) or reduced in cell number by less than 50% compared with the DMSO controls (n=31/50, 2 experiments, data not shown) at 36hpf.

4.2.4 Modulation of *Fgf8a* & *Fgf8b*: olfactory, GnRH, and forebrain commissure phenotype

Fgf8a ('ace') mutants

It has previously been reported that *Fgf8a* mutant (*'ace'*) zebrafish have defective forebrain commissure formation by 36hpf (Shanmugalingam et al., 2000). This experiment has been repeated here for control purposes (*see Figure 5.12A-E*). Surprisingly, the forebrain commissural defect was found to be very variable in the *ace* embryos, despite them all sharing the same mutant *Fgf8a* allele, and being homozygous for this allele, as confirmed by a missing cerebellum (*red arrow*, Figure 5.12B). Specifically, some *ace* embryos had an apparently normal AC and

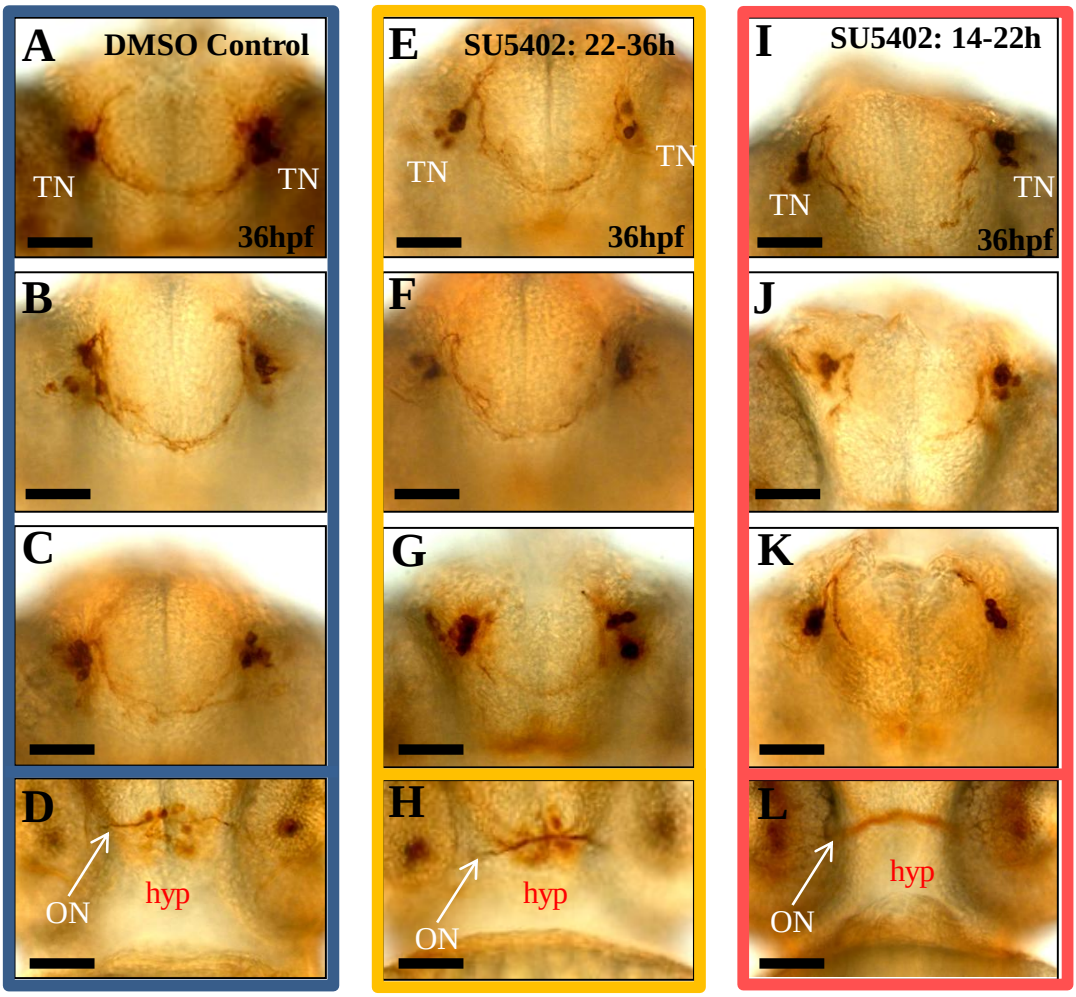

Figure 4.13 FGFR inhibition using SU5402: GnRH (G3MC) phenotype

Anti-mCherry immuno-labelled G3MC embryos (with DAB) are shown for the 'DMSO control'(A-D), 'SU5402 : 22-36h' (E-H), and 'SU5402: 14-22h' (I-L) embryos, all at 36hpf. All views are ventral. A-C, E-G, and I-K illustrate the terminal nerve G3MC phenotype; and D, H, and L illustrate the hypothalamic G3MC phenotype. Scale bars are 50µm.

TN= terminal nerve' hyp= hypothalamus; ON= optic nerve

POC, but with a few axons mis-projecting between the two commissures (n=24/104, 2 experiments, Figure 4.14B-B''), whilst other embryos had the same phenotype, but with many more axons mis-projecting across the two commissures (n=34/104, 2 experiments, Figure 4.14C, D); whilst other *ace* embryos had an aberrant POC with much fewer commissural axons (n=4/104, 2 experiments, Figure 4.14E), or a completely absent AC (n=29/104, 2 experiments, Figure 4.14E). In a few cases, both commissures were intact with no obvious defects (n=10/104, 2 experiments, data not shown). Rarely, both AC and POC were both missing in the same embryo; but these embryos had abnormally small heads with some necrosis, so it is likely that a developmental delay was the cause of the commissure malformation (n=3/104, 2 experiments, data not shown). Due to the rarity of this last phenotype, these severely malformed embryos were not studied further here. Of the controls, all embryos that were scored had normal forebrain commissure formation (n=42/42, 2 experiments, Figure 4.14A-A'').

Anti-GnRH immuno-labelling was also carried out on *ace* embryos, at 60hpf (Figure 4.14F, G). Terminal nerve GnRH cell clusters were labelled for both the *ace* (Figure 5.12G) and control (KWT, Figure 4.14F) embryos, except that whilst AC and POC GnRH-positive axonal projections could be detected in the control embryos (n=28/28, 2 experiments), these commissural projections were often absent or deficient in the *ace* embryos (n=18/32, 2 experiments, Figure 4.14G). Anti-GnRH does not detect hypothalamic GnRH cells at this stage, so it is not possible to comment on whether or not the hypothalamic GnRH cells are also affected in the *ace* embryos at 60hpf (using this method).

Similarly, inhibitors which target specific cascades that occur downstream of FGF signalling were also used. Specifically, these were LY294002, which inhibits PI3K signalling; and U0126, which inhibits MAPK signalling (via MEK1/2). These were used in a similar manner to SU5402 (i.e. external incubation). However, no potency was obtained for these inhibitors i.e. there was no lethality even at high concentrations and no defective phenotypes were obtained suggesting that these inhibitors did not penetrate the zebrafish external epithelium and therefore had no effect on embryogenesis (data not shown).

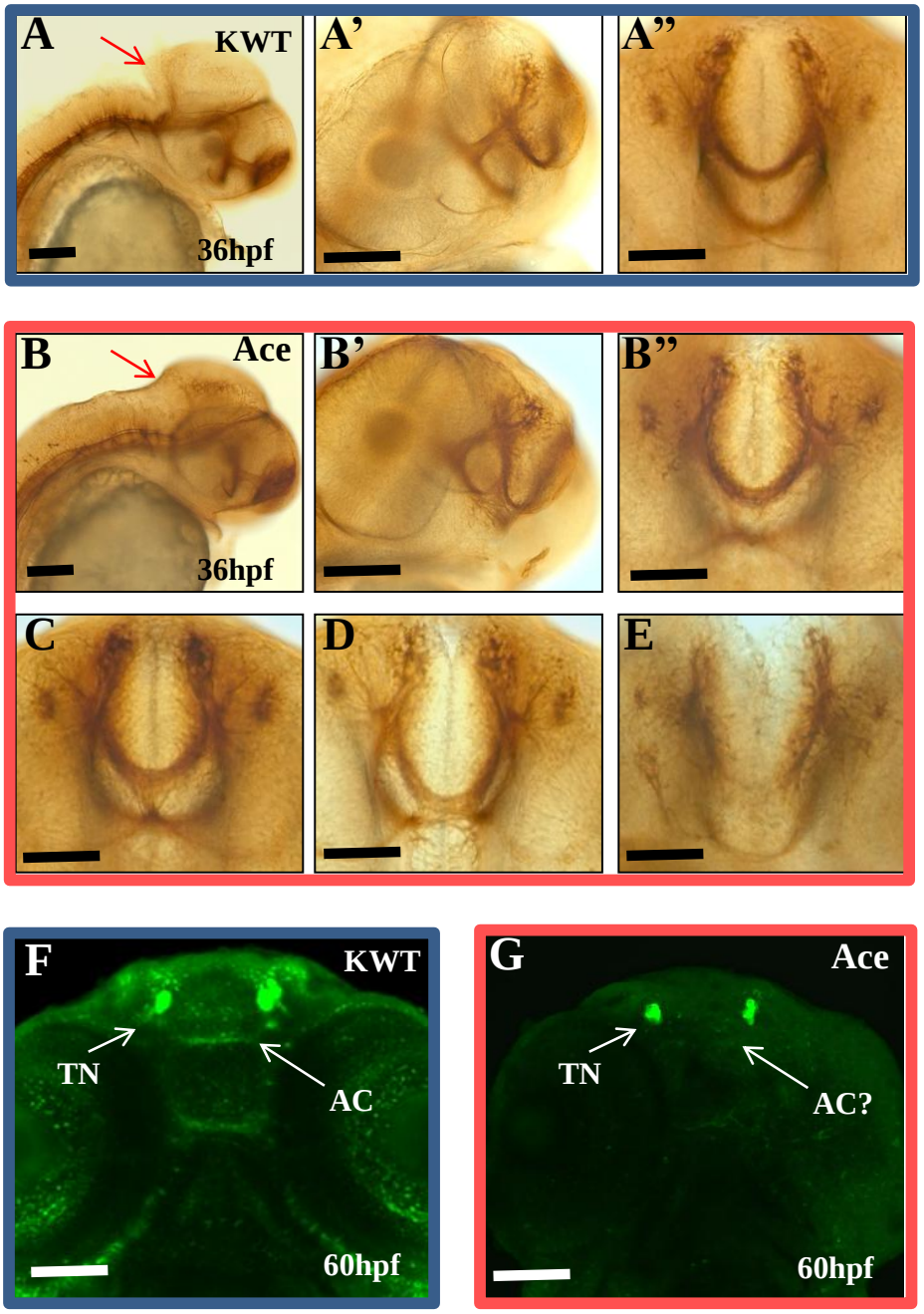

Figure 4.14 Do *Fgf8a* mutants (*ace*) have GnRH defects?

Anti-acetylated tubulin (AT) immuno-labelled embryos (with DAB) are shown for the wild-type (KWT) control (A), and *Fgf8a* mutants (*ace*; C-E) at 36hpf. Confocal images of anti-GnRH immuno-staining are shown for the wild-type (F) and Fgf8a mutant (G) at 60hpf. A , A', and B show lateral views; B' shows a ventral-lateral view; A'', B'', and C-E show ventral views. The red arrow in A points to the cerebellum, which is missing in the Fgf8a mutant (red arrow, B). B-E demonstrate increasing severity of commissural phenotype for the *ace* embryos. Scale bars are 100µm.

TN= terminal nerve; AC= anterior commissure

Fgf8a & Fgf8b knockdown by morpholinos

Whilst *ace* mutants do not have any normal copies of *Fgf8a*, they do have two functioning copies of the other *FGF8* orthologue: *Fgf8b*. So, does losing both *Fgf8a* and *Fgf8b* gene function increase the severity of the mutant phenotypes described for *ace*; and does the *Fgf8b* morphant have any of these abnormalities by itself (i.e. with a normal *Fgf8a* background)?

The Fgf8a morpholino has previously been well characterised, and, like *ace*, gives an acerebellar phenotype which can be used as a positive indication for the high-efficiency of *Fgf8a* knockdown (*black arrow*, Figure 4.15B). However, the Fgf8b morpholino used ('8bMO') was novel, and used for the first time in this study, so its knockdown efficiency needed to be characterised further. The Fgf8b morpholino targets the loss of exon 3 from the *Fgf8b* transcript (Ensembl no.: ENSDART00000057885); a predicted loss of 187 nucleotides of sequence (*see Figure 2.02 & Figure 5*.08 *for an explanation of the splice-blocking morpholino mechanism*). So, when the *Fgf8b* gene is amplified, the wild-type '1486bp' PCR product will be reduced to a 1299bp PCR product in the morphant embryos (if only exon 3 is lost, as predicted). However, upon RT-PCR of the control and *Fgf8b* morphant embryos, only the '1486bp' PCR product was obtained, which, when sequenced, corresponded to full length *Fgf8b* PCR product for both control and morphant cDNA samples. Although, this might suggest that the morpholino is not working, it was noticeable that the intensity of the morphant PCR product was on average around 50% less intense than the control PCR product (Figure 4.15C; repeated 3 times, for 3 different morphant/control cDNA samples, using equal amounts of total cDNA in the PCR reaction; data not shown). Although this would need to be proven quantitatively (i.e. by quantitative PCR, 'qPCR'), it does suggest that less *Fgf8b* transcript is present in the *Fgf8b* morphants. An explanation for this could be that there was partial knockdown of *Fgf8b* (perhaps up to 50% knockdown), but that the morphant mRNA was unstable and readily degraded, so was therefore undetectable by RT-PCR. However, if this is correct, it still means that the Fgf8b morpholino knockdown efficiency is only around 50% at best; nowhere near the approximately 100% knockdown efficiency obtained using other

splice-blocking morpholinos, including the Fgf8a and Kal1a/-1b morpholinos (*see chapter 5*).

The *Fgf8a* morphants had defects in one or both of the forebrain commissure (n=46/54, 3 experiments, Figure 4.15E), similar to what was seen for the ace embryos, *as discussed above*. These *Fgf8a* morphants also had abnormal olfactory pits with stunted axonal growth (n=22/58, 3 experiments, Figure 4.15I) or mis-projections (n=29/58, 3 experiments, data not shown) and a disorganised olfactory pit 'rosette' (n=39/58, 3 experiments, Figure 4.15I). In contrast, in the *Fgf8b* morphants, the forebrain commissures had formed correctly in most embryos (n=47/49, 3 experiments, Figure 4.15F), and the olfactory pits were apparently normal in most cases (n=49/52, 3 experiments, Figure 4.15J), although the poor knockdown efficiency needs to be considered when interpreting this result (*see discussion*). Knocking down both *Fgf8a* and *Fgf8b* together gave commissural (n=53/55, 3 experiments, Figure 4.15G) and olfactory (n=50/56, 3 experiments, Figure 4.15K) defects similar to knocking down *Fgf8a* alone (*see above*). The control (coMO-injected) embryos had normal forebrain commissure formation (n=47/47, 3 experiments, Figure 4.15D) and olfactory axonogenesis (n=51/51, 3 experiments, Figure 4.15H) in all cases.

Consistent with the mouse *Fgf8* mutant, there was a noticeable reduction in olfactory pit size when both *FGF8* orthologues were knocked down, which, whilst also noticeable in the single *Fgf8a* morphants (Figure 4.15I), was more severe in the *Fgf8a+Fgf8b* double morphants (Figure 4.15K). In order to quantify the reduction in olfactory pit size in these morphants, both olfactory pits from 10 embryos (i.e. 20 olfactory pits in total) from each morphant group were measured digitally from a confocal stack, in the anterior-posterior (A-P) direction (*see double-headed arrow in Figure 4*.15*H*). The average A-P length (in brackets, with corresponding standard deviation, as calculated using Microsoft Excel) of the four morphant groups are as follows: coMO (77.2μm $\pm$4.90); Fgf8a MO (61.5μm $\pm$5.96); Fgf8b MO (76.6μm $\pm$6.64); and Fgf8a+Fgf8b MO (56.9μm $\pm$10.73).

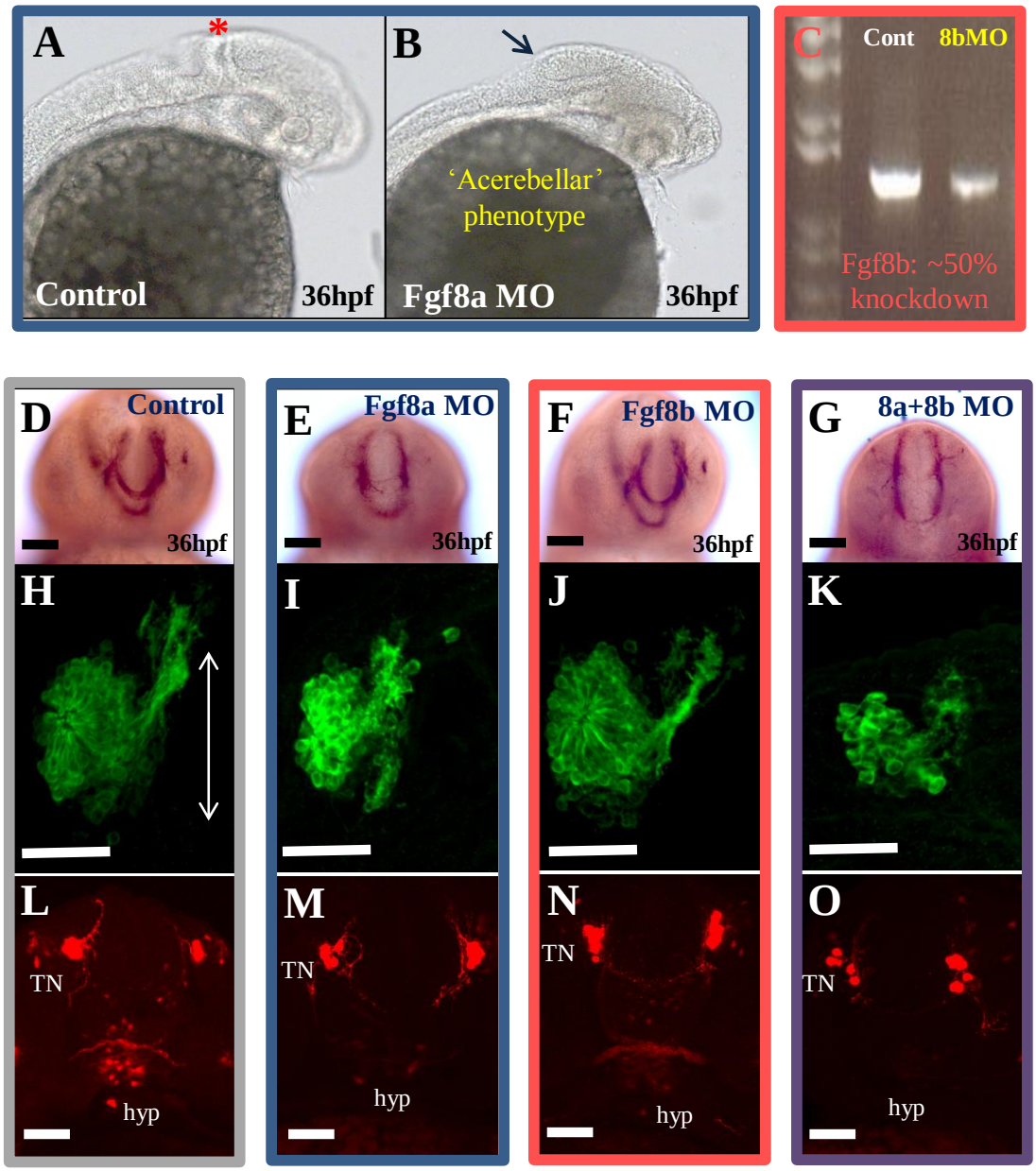

Figure 4.15 Using morpholinos to knock down both *Fgf8a* and *Fgf8b*

A and B: light microscopy images (lateral views) of the 'acerebellar' phenotype of Fgf8a morphants (B; blue arrow), compared to a control morpholino (CoMO) -injected embryo (A) with cerebellum present (asterisk). Fgf8b morpholino (8bMO) knockdown was confirmed by RT-PCR (C). The anti-acetylated tubulin (D-G), OMPG (H-K), and G3MC (L-O) phenotypes are shown for the control (D, H, L), the Fgf8a morphants (E, I, M), Fgf8b morphants (F, J, N), and Fgf8a+Fgf8b double morphants (G, K, O). A single olfactory pit is shown for OMPG phenotypes. For D-O all views are ventral . For A-O all embryos are at 36hpf.

Scale bars are 50µm. *TN= terminal nerve; hyp= hypothalamus.*

The *Fgf8a* morphants had significantly fewer (i.e. ≤50%[4]) hypothalamic GnRH3 ('G3MC') cells by 36hpf (n=38/47, 3 experiments, Figure 4.15M), compared with the controls which had normal hypothalamic GnRH clusters (n=52/52, 3 experiments, Figure 4.15L). Moreover, of the 38 *Fgf8a* morphants which had 50% or fewer hypothalamic GnRH3 cells, 7 embryos had apparently completely absent hypothalamic GnRH3 cells by 36hpf. This was not the case for the *Fgf8b* morphants, which mostly had similar cell numbers to the controls, although these cells often expressed mCherry much more weakly (n=45/49, 3 experiments, Figure 4.15N). Moreover, compared with the *Fgf8a* single morphants, the knockdown of *Fgf8a* and *Fgf8b* together did not make much difference to the number of embryos with less than 50% hypothalamic GnRH neurons, (n=46/51, 3 experiments, Figure 4.15O). However, the hypothalamic GnRH cells in these double *Fgf8a*/-8b morphants, whilst fewer in number, also expressed mCherry (GnRH3) much more weakly, so were more difficult to detect fluorescently (Figure 4.15O). Moreover, the *Fgf8a*/-8b morphants had disrupted terminal nerve GnRH3 cells (n=38/51, 3 experiments, Figure 4.15O).

[4] Hypothalamic cells were not counted individually, but were instead estimated qualitatively. The defective hypothalamic GnRH phenotypes were scored by whether they had less than 50% of the average number seen in the control embryos.

4.3 Discussion

4.3.1 *Fgf8a*, *Fgf3*, and all five Fgf receptors have expression profiles consistent with their putative roles during forebrain commissure formation & olfactory axonogenesis

As the telencephalic-specific *Fgf8* mutant mouse has a more severe forebrain defect than the Fgfr1 mutant, it seems plausible that Fgf8 may be acting via more than one Fgf receptor during mouse forebrain development (Hebert et al., 2003; Meyers et al., 1998; Chung et al., 2008). Assuming that the same may be true in zebrafish, the expression pattern for all five zebrafish Fgf receptors (including both Fgfr1 orthologues) was investigated, in respect to forebrain development. In summary, the expression analyses carried out at 17hpf and 23hpf, would suggest that four of the Fgf receptors (Fgfr1a, Fgfr2, fgfr3, and Fgfr4) could possibly have a role in commissure formation and olfactory system development in the forebrain, but that Fgfr1b may be involved later (from around 23-26hpf).

At 17hpf, when the olfactory placode forms and the cell clusters which give rise to the AC and POC can be first distinguished, Fgfr1a, is expressed quite strongly in the telencephalon (a region where the AC will form). Fgfr1b is expressed very weakly, or not at all, in the forebrain, whilst the other Fgf receptors (Fgfr2, Fgfr3, and Fgfr4) are all expressed strongly throughout the forebrain at this stage. Of the Fgf ligands looked at, *Fgf8a*, and more weakly, Fgf3 were also expressed in the forebrain, but not *Fgf8b*. This data may suggest that Fgf8a, Fgf3, Fgfr1a, Fgfr2, Fgfr3, and Fgfr4 may all have a role in determining the cells which give rise to the olfactory placode and forebrain commissure cell clusters at around 17hpf; but that Fgf8b and Fgfr1b are less likely to have a role in this process. However, because Fgfr1a expression is more restricted to the telencephalon at this stage, the role of Fgfr1a may be more restricted to olfactory and AC (not POC) formation. Further investigation will be required to confirm whether these putative functional roles exist for each of these receptors or ligands at this stage.

At 23hpf, when forebrain commissure and olfactory axonogenesis has become active, Fgfr1a is expressed in regions of the telencephalon and diencephalon where these olfactory and AC/POC tracts are forming. However, Fgfr1b labelling remains diffuse at this stage, and only becomes distinct in these regions by around 26hpf. However, it is uncertain whether this is 'real' expression and not just 'background' signal due to poor *in situ* probe quality. Generation of alternative Fgfr1b probes will be required to further investigate the Fgfr1b expression pattern in relation to olfactory/commissural axonogenesis.

Fgfr2, Fgfr3, and Fgfr4 are all broadly expressed in the forebrain region, so it can be envisaged that any of these receptors may putatively have a role in olfactory/commissural axonogenesis; although this would of course need to be confirmed. Of the Fgf ligands studied here, only Fgf8a and Fgf3 (but not Fgf8b) showed expression in the diencephalon, telencephalon, and olfactory placodes at 23hpf, suggesting that these two ligands may putatively have a role in olfactory/commissural axonogenesis too. The expression of these Fgf receptors and ligands around this stage is also consistent with their putative role in terminal nerve GnRH neurogenesis and axon formation, as well as *'early wave'* GnRH neuronal migration to the hypothalamus. Whilst Fgf8b is less likely to have a role in these forebrain developmental processes (at this stage), it remains possible that this ligand is expressed very weakly, below the detection limit of this analysis, and does indeed have a role in this forebrain development; this possibility is addressed in the functional studies that were carried out (*see below*).

Within the course of this chapter, it will not been possible to determine which of these individual Fgf receptors is involved in these forebrain developmental processes because the methods used herein to block the Fgf receptors are global, that is they target all Fgf receptors equally (*see conclusions/future work*).

Previous investigations in mice suggest that Fgf8 is likely to act mainly through Fgfr1 during telencephalic development (Chung et al., 2008). However, given that telencephalic-specific Fgf8 mutant mice have malformed forebrains that lack olfactory bulbs, whereas the Fgfr1 mutants have a less severe forebrain phenotype with defective olfactory bulb formation, it seems highly plausible that

another Fgf receptor is also used by Fgf8 during these developmental processes. Considering that Fgf8 has significant affinity for Fgfr3 (Ornitz et al., 1996; Chellaiah et al., 1999), this receptor would seem to be a likely candidate. However, mice deficient for Fgfr3 have normal telencephalons (including normal olfactory bulbs), and no reduction in hypothalamic GnRH neuronal number (Deng et al., 1996; Chung et al., 2008); so Fgfr3 is unlikely to be a very significant interactant of Fgf8 during mouse telencephalon development. It remains to be seen whether the same is true for the zebrafish.

4.3.2 Requirement for early Fgfr signalling during zebrafish forebrain commissure formation (the midline glia hypothesis)

Commissural tracts must, during vertebrate development, traverse across long distances within the forebrain to form the necessary connections that will allow coordination of activity between contralateral regions of the brain. The navigation of commissural growth cones therefore requires a well-defined extracellular environment with gradients of specific molecular guidance cues and scaffolds of glia and pioneering axons to ensure that the forebrain commissural neuronal circuit is formed accurately (Lindwall et al., 2007).

In particular, the glial cells which surround the forebrain commissures have been shown to act as a very important source of these guidance cues, helping to make sure that the traversing commissural axons do not stray into surrounding adjacent structures. In mice, as with other mammals, there are well-characterised groups of these glial cells, including the ‘midline zipper glia’, which have an important dual role in regulating fusion of the brain hemispheres, as well as facilitating the passage of commissural axons across the midline. Mammals have three distinct commissural tracts that traverse the telencephalic midline: *the corpus callosum, the hippocampal commissure* and *the anterior commissure*. The ‘glial wedge’ and ‘indusium griseum glia’, ventral and dorsal to the corpus callosum, are two groups of glial cells which have an essential role in the guidance of callosal

fibres across the midline, by secreting specific guidance cues including the chemorepellant, Slit2 (Tole et al., 2006; Lindwall et al., 2007).

Similarly, in zebrafish, cells expressing glial fibrillary acidic protein (GFAP; a glial cell marker) span regions of the forebrain midline where the AC and POC will later cross. Commissural axon extension across the midline is determined partly by the spatio-temporal expression of Sonic hedgehog (Shh) and the slit proteins, Slit1a, Slit2, and Slit3 (*see Figure 4.16*). Disrupting the slit signalling pathway results in disorganised midline glia, concomitant with subsequent severe defects in commissure formation (Barresi et al., 2005). As another example, the *belladonna* mutant zebrafish, which lacks the transcription factor Lhx2, have highly disorganised midline glia associated with failure of the AC and POC axons to cross the midline, but instead associating with misplaced glial cells (Seth et al., 2006). This further illustrates the importance of the midline glia in the formation of the forebrain commissures.

Fgf signalling has an essential role in zebrafish and mouse forebrain commissure formation. Whilst *Fgfr4* is not expressed in the mouse telencephalon, of the three FGFRs which are expressed, only Fgfr1 is present in the midline precursors at E12.5, a stage before the midline glial structures have appeared. *Fgfr1* expression remains in these midline precursor cells through to E15.5, including in the region where the glial wedge forms. Fgf8, a putative ligand for FGFR1 within the telencephalon, is also expressed in the midline at this stage, further supporting an interaction between these two proteins (Tole et al., 2006).

Mice which are brain-specifically null for *Fgfr1*, or those which are glial-specifically null for *Fgfr1*, lack the major commissural tracts, including the corpus callosum. It was subsequently shown by GFAP staining that the *Fgfr1* deficiency resulted in loss of the midline glial structures, including the glial wedge, indusium griseum glia and the midline zipper glia. Whilst there were no telencephalic midline deficiencies in expression of *Slit2*, *Slit3*, or *Robo1*, *Bmp4*, *GAP43*, and only a slight decrease in *Netrin1*, displacement of these midline glial structures, and the short-range guidance cues that they express, was apparently sufficient to cause failure of commissure formation in these *Fgfr1* null mutants (Smith et al., 2006;

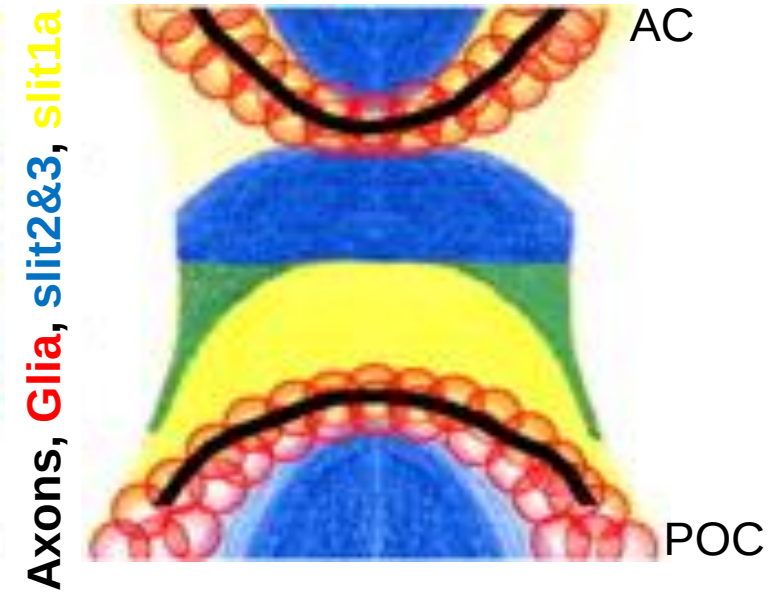

Figure 4.16 The role of glial bridges during zebrafish forebrain commissure formation

This schematic diagram illustrates the glial cells (in red) which support the correct pathfinding of anterior commissure (AC) and post-optic commissure (POC) axons (in black) across the midline. Specific expression of slit2/slit3 (in blue) and slit1a (in yellow) ensures that commissural axons are correctly guided across their glial bridges (in red).

Figure 4.16 reproduced with permission from Development (Barresi et al., 2005). doi:10.1242/dev.01929

Tole et al., 2006). Similarly, agenesis of the corpus callosum was also seen in a KS patient who was homozygous for a certain deleterious missense mutation (Dode et al., 2003), illustrating that the role of FGFR1 in forebrain commissure formation has been well conserved in different vertebrate species.

However, unexpectedly, *heterozygous* Fgfr1 mutants have normal midline glial structures despite the corpus callosum and hippocampal commissures failing to cross the midline. This would suggest that an FGF-dependent mechanism which is separate from the generation of midline glia may also be required for callosal and hippocampal commissure formation. In fact, Fgfr1 is also expressed by midline cingulate cortical neurons, which could imply that Fgfr1 is also required for the differentiation of the callosal pioneering axons which extend across the midline (Tole et al., 2006; Lindwall et al., 2007). In summary, Fgf signalling does have an important role in forming the midline glial structures, but the entire mechanism by which this signalling pathway effects forebrain commissure formation is yet to be fully elucidated.

The role of Fgfr signalling during zebrafish forebrain commissure formation has previously been investigated (Shanmugalingam et al., 2000) using the global FGFR inhibitor, SU5402 (Mohammadi et al., 1997). It was reported in this paper, that those embryos incubated from 90% epiboly (~9-12hpf) showed the most severe defects, consisting of absent forebrain commissures combined with smaller eyes and brains, compared with the controls. Those embryos treated at 6 somite stage (~12-15hpf) gave similar commissural defects to the *Fgf8a* mutant embryos (*see section 4.1.3 above*); and those treated at 18 somite stage (~18-21hpf) gave the weakest phenotype, with only mild defects in AC and POC formation. So, in summary, the severest commissural defects were caused by early FGFR inhibition (~9-12hpf); suggesting that FGFs other than Fgf8a (i.e. expressed earlier than *Fgf8a*) could be involved in AC and POC formation (Shanmugalingam et al., 2000). Indeed, it has since been shown that the AC and POC also fail to form correctly in the absence of another Fgf ligand, Fgf3. But, the most severe AC/POC defects were observed when both *Fgf8a* and *Fgf3* gene function were knocked down together (Walshe and Mason, 2003).

To investigate the effects of Fgf receptor inhibition on olfactory/vomeronasal axonogenesis and GnRH neuronal development, embryos were treated with SU5402 at two different time-points. The first SU5402 incubation ('route [1]' on Figure 4.08) was between 14hpf and 22hpf, with the aim of inhibiting Fgf signalling during olfactory placode formation (at 17hpf), and any GnRH neuronal specification associated with the nasal compartment at this time-point, as well as AC/POC bilateral cell cluster formation and early axonogenesis. The second SU5402 treatment ('route [2]' on Figure 4.08) was between 22hpf and 36hpf, with the aim of inhibiting Fgf signalling during olfactory/vomeronasal/commissural axonogenesis, and GnRH neuronal specification and/or migration.

Embryos treated with SU5402 (as described above), as well as DMSO controls, were analysed for forebrain commissure defects. This analysis acted as a 'control experiment' to ensure that the SU5402 treatments were working, and confirm the forebrain commissure defects which were described previously (Shanmugalingam et al., 2000). Consistent with previous findings, embryos treated with SU5402 at 14hpf showed much more severe AC/POC defects compared with those treated at 22hpf, which showed only minor AC defects in a few embryos; whilst the DMSO control embryos were all normal, as expected. In previous studies, embryos treated with SU5402 between 9hpf and 12hpf, or 12hpf and 15hpf, showed comparable phenotypes to the embryos treated with SU5402 between 14hpf and 22hpf in this study, but without the head/eye defects that were reported for the early-treated SU5402 (9-12hpf) embryos. This is perhaps a bit surprising, as the later-treated (18-21hpf) embryos from that study showed the subtlest defects, whereas as this group closely matches the 14-22hpf incubation time used in this study. However, critically, the later-treated (18-21hpf) embryos from that study had already proceeded past the point of specification of AC/POC (and olfactory placodal, *see below*) cells, whereas the 'early' time-point used in this study (14-22hpf) covered this critical cell-specification period. Fgf signalling is still required past 18hpf for commissure formation, especially AC formation, which is defective in some embryos in the later-treated (22-36hpf) embryos in this study; however, Fgf signalling has a *more essential* role in correct AC/POC cell specification up to around 16-18hpf.

Alternatively, Fgf signalling may have a critical role in determining specification and/or positioning of midline-spanning glial cells (the so-called 'glial-bridge') at around 15-18hpf. This 'glial bridge' contains cells which co-express Gfap and Slit1a providing a 'favourable substrate' for forebrain commissure growth cones projecting across the midline. Previous experiments in mice suggest that Fgf signalling plays a crucial role in determining correct organisation of similar midline glial structures required for correct commissure formation in the mouse. This could explain why the early-treated SU5402 embryos showed a more severe AC/POC defect, as they are the ones with the disorganised midline glial structures. Consistently, Fgf signalling is required for commissure formation at post-glial structure formation stages in both zebrafish and mice, as late-treated SU5402 (22-36hpf) embryos still have some AC defects and heterozygous Fgfr1 mutant mice have normal midline glial structures, but still have commissure defects (Tole et al., 2006). Therefore, as already mentioned, the glial cell hypothesis is not the entire explanation for the role of Fgf signalling during commissure formation, but it may nonetheless play a significant part in the process.

It was not possible to determine from this study which of the five Fgf receptors are involved in forebrain commissure formation, although we can assume from previous studies in the mouse that one or both of the Fgfr1 orthologues (Fgfr1a and Fgfr1b) are likely to have a key role. Morpholino approaches will be required to investigate the role of each individual Fgf receptor in commissure formation. Certainly, the spatio-temporal expression pattern of all five receptors would suggest that they could putatively have a role, but this is yet to be proven experimentally.

4.3.3 Is Fgf8b signalling required for forebrain commissure formation?

As mentioned in the introduction to this chapter, it has been reported previously that both forebrain commissures, the AC and the POC, are disrupted in the *Fgf8a* ('ace') mutant zebrafish. Specifically, commissural axons were visualised 'meandering' as they approached the midline, and were shown at slightly later

stages wandering in between the two forebrain commissures, close to the optic stalks, in a region where axons would normally be excluded. By around 36hpf, one, or sometimes both, of the forebrain commissures had failed to form. The severity of these commissural defects, combined with morphological analyses, suggested that midline tissue was disrupted in these *Fgf8a* mutants. However, many markers of telencephalic domains (*bf1*, *dlx2*, *eph-A4d*, *arx1*, *unc4*, *eome*), with the exception of *nk2.1b* (which was reduced) showed no obvious differences in expression, suggesting that overall induction and patterning of the telencephalon is not severely affected by loss of Fgf8a signalling in zebrafish (Shanmugalingam et al., 2000).

In order to assess the variability of the forebrain commissure defects found in the *Fgf8a* mutants, acetylated tubulin immuno-labelling was carried out on some ace and non-ace embryos at 36hpf. In this analysis, the most predominant phenotype was mis-projected axons between the AC and POC, accounting for about 56% of the embryos. The next most common phenotype was a missing AC, accounting for another 28% of the embryos. A missing POC was much less frequent, accounting for approximately 4% of the embryos. Approximately 3% of the embryos had both commissures missing, giving the appearance of '4 dots', '2 dots' for the AC cell clusters and '2 dots' for the POC cell clusters, both of which failed to extend axons across the midline. However, this last phenotype was accompanied by a significantly smaller head, suggesting that the failed commissure formation may have been secondary to forebrain malformation in these embryos.

The higher penetrance of AC failure, compared with POC failure, suggest that Fgf8a signalling is more important for AC formation, than POC formation. Or, it may indicate that the POC is more resilient to deficient Fgf8a signalling, perhaps because there is more redundancy in the signalling pathways which bring about POC formation. Alternatively, it may have something to do with the POC forming shortly before the AC: if the POC fails to form correctly, perhaps by mis-projecting axons towards the AC, this could in turn cause the AC axons to aberrantly project towards the mis-projected POC axons, somewhere between where the AC and POC should form (as occurs in approximately 56% of cases). If the POC manages to form, by overcoming the Fgf8a signalling deficiency, the AC axons will, instead of projecting towards mis-projected POC axons, fail to project across the midline at all

(and the AC fails to form). This last scenario suggest that the AC axons are either attracted to the mis-projected POC axons, or attracted to something that the mis-projected POC axons were attracted to i.e. disorganised midline cells (e.g. glial cells secreting guidance cues, *see below*).

To ascertain whether or not the other *FGF8* orthologue, *Fgf8b*, also has a role in forebrain commissure formation, morpholino approaches were used to knock down *Fgf8a* and *Fgf8b* gene function. Like the *Fgf8a* ('ace') mutant, *Fgf8a* morphants have a missing cerebellum; a useful confirmation of successful *Fgf8a* gene knockdown. The Fgf8b morpholino did not result in an acerebellar phenotype, so an RT-PCR approach was used to confirm knockdown of *Fgf8b*. However, this showed that *Fgf8b* potentially only gave approximately 50% knockdown, although this would need to be proven more quantitatively by qPCR. Time restraints meant that an alternative Fgf8b morpholino could not be used in order to try and obtain 100% knockdown of *Fgf8b*; but this would be a future goal.

Unsurprisingly, given that gene knockdown levels were only 50% efficient (at best), forebrain commissure formation was normal in the *Fgf8b* (partial) morphants. Moreover, knocking down *Fgf8a* and *Fgf8b* together gave AC/POC defects which were equivalent to knocking down *Fgf8a* alone. It is not possible, however, to summarise from this that Fgf8b is not required for forebrain commissure formation, as these morphants were only hypomorphic for *Fgf8b*, and not true *Fgf8b* morphants. Until 100% (or close to 100%) knockdown of *Fgf8b* is achieved, it isn't possible to confirm its involvement in forebrain commissure formation, although the lack of *Fgf8b* expression in the forebrain during AC/POC development may suggest that its involvement is less likely.

4.3.4 Identification of *active* Fgf signalling during olfactory/vomeronasal axonogenesis and GnRH neuronal specification

Two downstream antagonists of Fgf signalling, Sprouty4 and Dusp6, were investigated in terms of their spatio-temporal expression during early development within the nasal compartment (i.e. during olfactory axonogenesis and GnRH neuronal specification). Whilst both Fgf antagonists were expressed in forebrain regions at 17hpf and 23hpf, Dusp6 was expressed more broadly throughout the forebrain and olfactory placodes, and was investigated further using a recently published Dusp6 reporter line, pDusp6:d2GFP (Molina et al., 2007).

Dusp6 (also known as MKP3 or Pyst1) is an inhibitor of phosphorylated Erk1/2 (pERK); but is itself upregulated by increased MAPK signalling, in an important negative feedback regulatory loop. *Dusp6* expression may therefore act as a dynamic read-out of MAPK signalling, and, indirectly, as an indication of putative Fgf signalling (Molina et al., 2007). For this reason, the Dusp6 transgenic reporter line is a useful tool for investigating not only dynamic Dusp6 expression, but also putative forebrain Fgf signalling during olfactory and/or terminal nerve axonogenesis.

Dusp6 expression correlates well with many sites of Fgf signalling during mouse embryogenesis, including the olfactory system. This means that Dusp6 expression is a useful read-out of Fgf signalling during mouse and zebrafish development. In fact, Dusp6 is expressed in the rim of the invaginating olfactory pit during mouse embryogenesis, the same site as Fgf8 expression. In Fgf8 mutant mice, this Dusp6 expression is strongly down-regulated in this region, demonstrating that loss of Fgf8 severely reduces Fgf signalling in the olfactory region (i.e. Dusp6 down-regulation indicates reduced Fgf signalling) (Dickinson et al., 2002).

When the Dusp6 reporter line was crossed with the GnRH3 reporter, there was no GnRH3/Dusp6 co-expression detectable at 24hpf or 30hpf in the terminal nerve region. However, their d2GFP (Dusp6) was dynamically expressed within

some olfactory epithelial cells and presumptive olfactory bulb cells at these stages. If we assume that this Dusp6 expression represents active MAPK signalling in these forebrain regions, it can be concluded that active signalling may also be active in the olfactory epithelium and presumptive olfactory bulbs at 24hpf and 30hpf; stages at which olfactory axonogenesis is active. However, by extension, there does not seem to be active Fgf signalling in the terminal nerve or early hypothalamic GnRH3 cells at these stages; although it remains possible that the Dusp6 reporter transgene is silenced in the GnRH3-expressing cells, and not reporting Dusp6 activity. Also, because d2GFP is intentionally unstable, in order to show dynamic Dusp6 expression, it remains possible that Fgf signalling occurs briefly in GnRH3-expressing cells and was missed from this analysis. By 48hpf, d2GFP signal had reduced significantly in forebrain/olfactory regions (data not shown), suggesting that Dusp6 expression was down-regulated in these regions by this stage, or that the reporter transgene had been silenced in this region.

To judge the reliability of the pDusp6:d2GFP line as a reporter of MAPK activity, anti-pERK immuno-labelling was also carried out on G3MC embryos. Surprisingly, no pERK immuno-labelling was detected in 24hpf or 30hpf embryos, suggesting that there was actually no active MAPK signalling in these embryos. However, this is unlikely given the importance of this signalling pathway during development. It is more plausible that some technical error (i.e. poor antibody penetration or epitope presentation) prevented pERK immuno-labelling at these early stages. pERK immuno-labelling was detected throughout the presumptive olfactory bulbs, and in some cells in the olfactory epithelium at 48hpf, but was absent from all GnRH3-expressing cells at this stage. This pERK immuno-reactivity is in agreement with the Dusp6 reporter line expression in these regions, although these analyses were of course carried out at different developmental stages. It cannot therefore be conclusively determined how reliably the dynamic d2EGFP/Dusp6 expression represents active MAPK signalling in the forebrain.

Anosmin-1 increases MAPK signalling to levels equivalent to or higher than high levels of FGF2 ligand alone in primary olfactory neuroblast culture (Gonzalez-Martinez et al., 2004b), suggesting that pERK may be an important downstream effector of Fgf signalling during olfactory/GnRH neuronal development. Therefore,

the implied pERK signal at 24hpf and 30hpf (from the Dusp6 reporter line analysis), and actual pERK immuno-labelling at 48hpf, in the olfactory epithelium and presumptive olfactory bulbs, demonstrates that pERK, putatively downstream of Fgf signalling, potentially has an important role in olfactory system development in the zebrafish.

4.3.5 Early inhibition of FGFR signalling causes abnormal olfactory & vomeronasal axonogenesis, as well as defects in GnRH system formation

Taking into consideration the natural variability in the olfactory/vomeronasal axonal phenotype at 36hpf, embryos treated with SU5402 between 22hf and 36hpf had apparently normal olfactory and vomeronasal axonogenesis, which was comparable to the DMSO-treated control embryos. In contrast, embryos treated with SU5402 between 14hpf and 22hpf, showed a very noticeable defect in olfactory/vomeronasal axonogenesis. Specifically, these embryos had fewer or no olfactory axons correctly projecting to the olfactory bulbs. The vomeronasal axons were similarly affected, except that these axonal defects were associated with fewer vomeronasal soma too; whereas the OMP-positive olfactory soma were not apparently reduced in number. Despite no apparent significant reduction in olfactory pit size amongst the SU5402-treated embryos, the olfactory epithelial cells were disorganised in the 14-22hpf embryos; their olfactory pits no longer pertained to a well-ordered ‘rosette’ structure that is seen in wild-type embryos (Yoshida et al., 2002). In summary, Fgf signalling has an essential role in olfactory and vomeronasal axonogenesis, as well as vomeronasal neuronal cell survival or proliferation, between 14hpf and 22hpf.

It has been shown previously that Fgf signalling has a crucial role in the correct morphogenesis of the mouse nasal cavity; hence, *Fgf8* mouse mutants have elevated levels of apoptosis (not *decreased* cell proliferation, as may be expected) in the Fgf8-expressing site of the olfactory pit (Kawauchi et al., 2005). Therefore, it may at first seem surprising that blocking total FGFR activity did not result in any

noticeable decrease in olfactory pit size in the zebrafish (excepting the reduction in vomeronasal neuronal number which didn't significantly affect overall olfactory pit size). However, unlike the *Fgf8* mouse mutant, FGF signalling was blocked for only a finite period of developmental time in the zebrafish (i.e. 14-22hpf or 22-36hpf); as blocking all Fgf signalling from 0hpf would not have been viable, resulting in very early embryonic lethality. It therefore remains possible that early olfactory placodal neurogenesis begins prior to 14hpf in the zebrafish, and so therefore isn't significantly affected by blocking Fgf signalling past 14hpf. In fact, it's probable that olfactory epithelial cells will begin to die by apoptosis after prolonged SU5402 exposure from 14hpf onwards, but that this effect is not apparent by 36hpf (and the olfactory epithelium may have recovered by 60hpf in the 22-36hpf SU5402-treated embryos).

Furthermore, if olfactory epithelial cell survival is significantly reduced in embryos treated with SU5402 between 14hpf and 22hpf, it is possible that the reduced/absent olfactory/vomeronasal axonogenesis is the result of the olfactory/vomeronasal soma becoming less viable, and beginning to become apoptotic (or going through the early stages of apoptosis) and hence not capable of extending axons to the olfactory bulbs. In fact, on closer inspection, it is apparent that the OMP-positive olfactory pits from these early SU5402 treated embryos do have 'gaps' in OMP expression. This could represent apoptotic cells which are no longer viable, and so do not express OMP (GFP), explaining the 'disorganised' olfactory epithelia that were observed. Therefore, whilst the overall olfactory pit may be comparable in size to the control pits, in fact, the olfactory epithelial cell number is likely to be reduced in the 14-22hpf SU5402 treated embryos. So, in summary, it is not only the vomeronasal neurons which are reduced in number, but the OMP-positive olfactory neurons too. Further work is required to assess the olfactory OMP-positive neuronal cell number in the olfactory pits of SU5402-treated embryos, compared with controls, and whether or not these cells are apoptotic (*see Future work, section 4.5*). A significant elevation in apoptosis in the olfactory epithelium, and other putative sites, may explain why the 14-22hpf SU5402 treated embryos fail to survive to 60hpf.

Consistently, G3MC embryos treated with SU5402 between 22hpf and 36hpf had the same GnRH neuronal phenotype as the DMSO controls, taking into consideration the normal variation in the wild-type GnRH3 phenotype (*see chapter 3*). Whilst embryos treated with SU5402 between 14hpf and 22hpf had absent or reduced hypothalamic GnRH3 neuronal clusters at 36hpf, combined with absent terminal nerve GnRH3 neuronal projections across the anterior commissure. Due to the uncertainty of the origins of the hypothalamic GnRH neurons which appear at 36hpf, it is not possible to say whether or not the defect seen in these early SU5402-treated embryos, resulting from loss of Fgf signalling, is due to a GnRH3 neuronal migration failure/delay and/or failure in specification of the GnRH cells. Moreover, the significance of the failure of GnRH3 projections to cross the AC is unclear: although it seems likely that such projections may be important for the neuromodulatory activity of the terminal nerve GnRH system (Palevitch et al., 2007), and its proposed role in regulating reproductive competence.

Previous analyses (*described in section 4.3.4*) indicated that there may not be any Fgf signalling occurring in the GnRH3-expressing cells at 24hpf, 30hpf, or 48hpf, suggesting that Fgf signalling may not be required for GnRH3 neuronal development in the zebrafish. However, the SU5402 experiment indicated that Fgf signalling *is required* between 14hpf and 22hpf; stages much earlier than the dusp6 transgenic/ pERK immuno-labelling analyses could detect Fgf signalling. Alternatively, it remains possible that the effects of Fgf signalling loss on the GnRH neuronal development may occur by a more indirect mechanism, i.e. caused by loss of Fgf signalling in cells within the nasal compartment and/or forebrain where the GnRH cells are specified and/or migrate from. In summary, the loss of Fgf signalling between 14hpf and 22hpf results in a putative loss (by apoptosis) of Fgf8-expressing cells within the nasal compartment. This results in the failure of olfactory and vomeronasal axonogenesis, and blocks normal specification of GnRH cells and/or their putative migration to the hypothalamus following olfactory/vomeronasal tracts (which are now missing).

4.3.6 *Fgf8a* is an important ligand for olfactory & GnRH neuronal development

It was shown previously that *Fgf8a* ('ace') mutants have fewer Or2.0-positive olfactory projections and fewer olfactory bulb glomeruli (Shanmugalingam et al., 2000). To find out if these *ace* embryos also have defects in GnRH neuronal development, GnRH immuno-labelling was carried out on these embryos at 60hpf. GnRH immuno-expression was detected in terminal nerve cells in these *ace* embryos, but the expression levels were weaker than the control (wild-type) embryo at the same stage. Moreover, the GnRH-positive axons, which project across the AC in all wild-type embryos analysed, are missing in approximately half of the *ace* embryos. Whilst this could be because of the weaker GnRH expression levels, this failure of GnRH-projections to cross the AC is more likely to be the result of variable failure of AC formation in *ace* embryos i.e. the terminal nerve GnRH3 neuronal axons require a pre-existing AC scaffold before they too can project axons across the AC. This, of course, will prevent coordination between both sides of the terminal nerve GnRH3 system, and may, in turn, affect reproductive competence, as already mentioned above for the SU5402-treated embryos with the same phenotype.

It was previously reported that the *Fgf8a* ('ace') mutants have a defect in the midline tissue between the two forebrain commissures, the so-called 'preoptic area' (Shanmugalingam et al., 2000); a region believed to encompass part of the migratory route of the *'later wave'* (and *'early wave'*?) GnRH neurons migrating to the presumptive hypothalamus in zebrafish (*see chapter 3*). Moreover, by 3dpf, there was a reported gross distortion in the shape of the brain in the region of the AC and POC; although the hypothalamus appeared superficially normal. The anti-GnRH antibody (LRH13) used in this project does not label the early-arising hypothalamic GnRH neurons at 30-60hpf, so an alternative (morpholino) approach was required to investigate GnRH neuronal development in *Fgf8a* mutants.

The *Fgf8a* and *Fgf8b* genes were knocked down individually and together to investigate their role during olfactory and GnRH neuronal development. The *Fgf8a* morphants had similar olfactory and GnRH phenotypes to 14-22hpf SU5402-treated embryos. Specifically, the OMP-positive olfactory axons were missing or mis-

projected and the olfactory epithelia were disorganised in the *Fgf8a* morphants. Whilst there was an approximately ≤50% reduction in hypothalamic GnRH neurons at 36hpf in 81% of embryos analysed. In contrast, the majority of *Fgf8b* morphants had normal olfactory axons and pits, as well as normal-sized hypothalamic GnRH populations; however, this may reflect the poor *Fgf8b* knockdown levels, and can not therefore be concluded from this data that *Fgf8b* does not have a role in these developmental processes. Embryos that had both *Fgf8a* and *Fgf8b* knocked down had olfactory and GnRH defects that were similar to those described for *Fgf8a* single knockdown. However, there is a bigger reduction in average olfactory pit size (A-P length) for the *Fgf8a+Fgf8b* double morphants (26.4% reduction in size, relative to the control), compared with the *Fgf8a* single morphants (20.3% reduction). The *Fgf8b* single morphants had a less than 1% reduction in olfactory pit size compared to the control olfactory pits. To be more statistically significant, a larger group of olfactory pits will need to be measured for these morphant groups. However, this initial data suggests that *Fgf8b may* also be involved in olfactory epithelium development, especially when *Fgf8a* gene function is lost (i.e. it may compensate for reduced *Fgf8a* signalling), but this will need to be investigated further. Moreover, it would seem that *Fgf8b* signalling may not be required when *Fgf8a* expression is normal. Of course, a more complete knockdown of *Fgf8b* is required to prove for sure that *Fgf8b* does not itself have a role in olfactory neurogenesis when *Fgf8a* signalling levels are normal, and confirm whether it has a significant role when *Fgf8a* signalling is lost (i.e. a redundant role).

Despite the reduction in olfactory pit size obtained by *Fgf8a* knockdown, it is perhaps surprising that the reduction was not larger, given the severe olfactory epithelium defects that are seen in the *Fgf8* mouse mutant. There are several possible reasons for this. Firstly, morpholino knockdown is not permanent and not 100% efficient, so its effects will decrease over developmental time, as the morpholino itself degrades. Secondly, there may be other Fgfs which have an important role in olfactory development in the zebrafish, including *Fgf8b* (as described) and Fgf3, which has previously been implicated along with *Fgf8a* in forebrain commissure development, and may be required together during forebrain development more generally (*this needs to be investigated*).

4.4 Conclusions

4.4.1 Olfactory bulb morphogenesis upon arrival of olfactory axons: the role of Fgf signalling

It has been proposed that olfactory bulb morphogenesis is induced by the arrival of ORN axons from the olfactory epithelium (Gong and Shipley, 1995). This hypothesis is supported by the fact that ORN axons reach the anterior telencephalon before any signs of olfactory bulb formation, but soon after their arrival there is an increase in proliferation of the anterior subventricular zone cells, which supply the olfactory bulb with new neuroblasts via the rostral migratory stream. Furthermore, a model has been suggested, whereby the arrival of ORN axons induces an FGF-dependent decrease in cell proliferation in that particular region of the anterior telencephalon causing initial olfactory bulb evagination (*see Figure 4.17*). Here is the mechanism that has been proposed: soon after first contact between ORN axons and the rostral telencephalon, neuroepithelial cells in close proximity to the axon terminals stop dividing and instead differentiate into neuroblasts, whereas cells located further away from the point of contact continue dividing. The local decrease in cell proliferation at the point of ORN axonal contact results in evagination of the olfactory bulb relative to the rest of the telencephalon. Without an Fgf-induced reduction in proliferation at the anterior telencephalon, no morphologically distinguishable bulbs could be formed (Gong and Shipley, 1995; Hebert et al., 2003).

Fgfr1 and Fgf8 both have an essential role in olfactory bulb morphogenesis in mice and humans (*see chapter 1 and section 4.1 from this chapter*). Olfactory bulb dysgenesis resulting from mutations in these two genes is the proposed cause of anosmia/hyposmia in KS patients (MacColl et al., 2002). However, according to our current understanding of olfactory bulb morphogenesis (as outlined above), ORN axonogenesis from the olfactory epithelium is a necessary pre-requisite for olfactory bulb formation (Gong and Shipley, 1995). Therefore, the focus of this chapter has been to look at olfactory axonogenesis, instead of olfactory bulb formation, in order

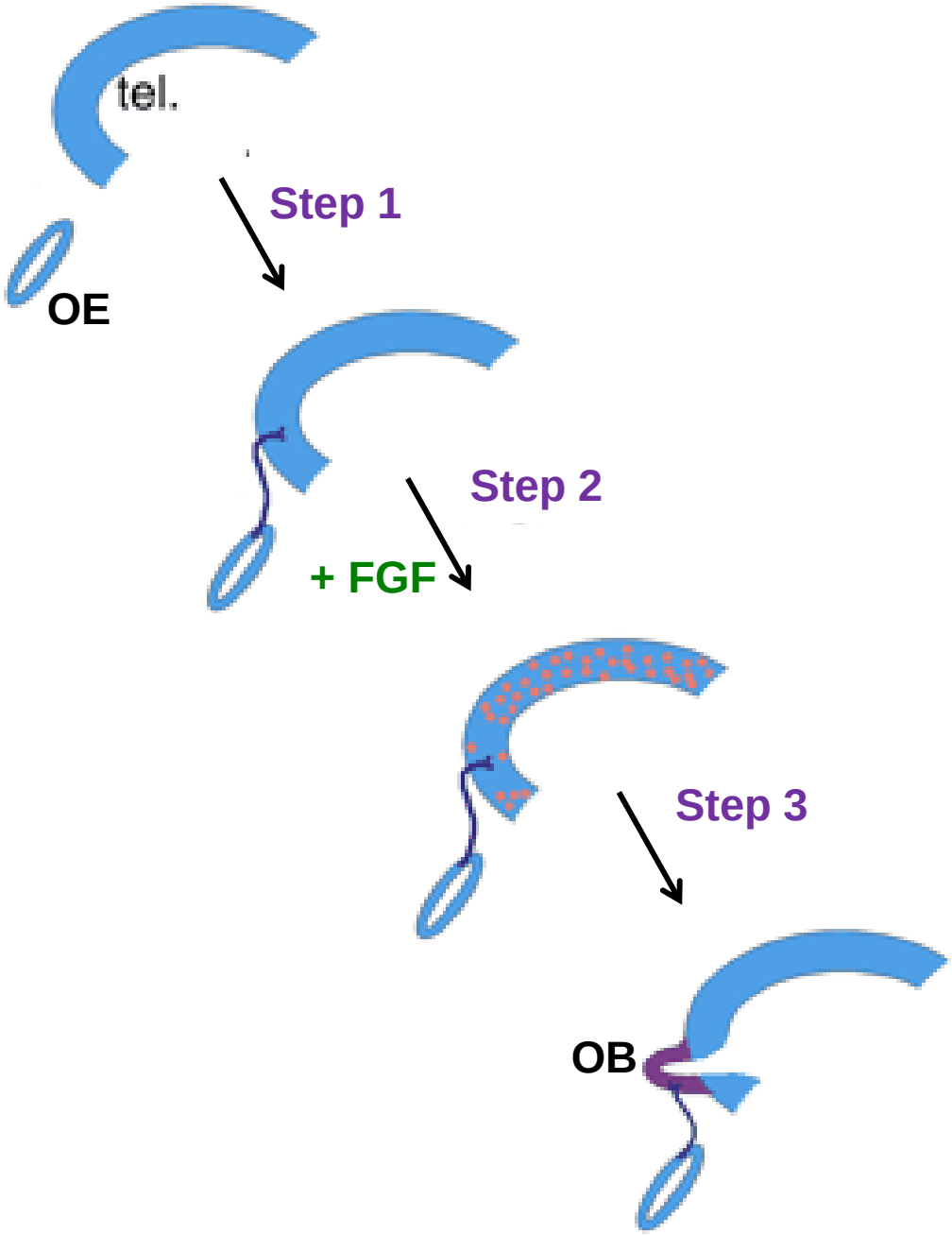

Figure 4.17 A model for the proposed mechanism of olfactory bulb morphogenesis

There are three proposed steps to olfactory bulb (OB) morphogenesis. In 'Step 1', axons from the olfactory epithelium (OE) project to and make contact with the anterior telencephalon (tel.). In 'Step 2', there is an FGF-dependent reduction in the number of proliferating cells (orange spots) at the anterior end of the telencephalon, in the specific site where the olfactory nerve terminals arrived; concurrent with an increase in olfactory bulb-specific neuronal differentiation in these cells (not shown). In 'Step 3', the decrease in cell proliferation results in initial OB evagination (in purple).
Figure modified from Hébert et al., 2003.
Figure 4.17 adapted with permission from Development (Hébert et al., 2003). doi:10.1242/dev.00334

to understand how Fgf signalling is involved in development of the zebrafish olfactory system.

In the mouse, *Fgf8* is expressed in and around primordial neural stem cells in the olfactory epithelium which are responsible for initiating primary olfactory neurogenesis at the olfactory epithelium. When *Fgf8* expression is absent, these primordial stem cells undergo apoptosis, resulting in fewer ORNs being generated (Kawauchi et al., 2005). Consistent with these findings, zebrafish with loss of *Fgf8a* (one of two *FGF8* orthologues) have reduced and/or aberrant olfactory axons, coupled with smaller, more disorganised olfactory epithelia (Shanmugalingam et al., 2000). It would therefore seem that the role of Fgf8 signalling during olfactory system development has been conserved in mice and zebrafish; however, further analysis is required to confirm that increased apoptosis in the olfactory epithelium (*see Figure 4*.06), is the cause of olfactory epithelium defects in zebrafish. Assuming that Fgf8 signalling does have a similar role in zebrafish olfactory neurogenesis, it's likely that the olfactory axonal mis-projections obtained were secondary to the ORN neurons becoming less viable (i.e. becoming apoptotic).

Blocking all Fgf receptors between 14hpf and 22hpf also caused defective olfactory (and vomeronasal) axonogenesis. However, it was not possible from this study to distinguish which of the five Fgf receptors were involved. All five Fgf receptors are expressed in the anterior forebrain during this developmental period, so all could putatively be involved in olfactory axonogenesis, and subsequent olfactory bulb morphogenesis, but it remains to be determined which particular Fgf receptors are involved. However, given that Fgfr1 loss in the mouse causes olfactory bulb agenesis, it can be assumed that one of the two zebrafish Fgfr1 (Fgfr1a and fgfr1b) orthologues is a likely candidate (although there may be more than one Fgf receptor involved). Of the two Fgfr1 receptors, Fgfr1a showed the strongest expression in the anterior forebrain between 17hpf and 23hpf.

Fgfr1a belongs to the *Fgf8a* synexpression group and it has been demonstrated that Fgfr1a knockdown phenocopies many of the defects observed in the *Fgf8a* mutant zebrafish, including loss of the MHB structure (Scholpp et al., 2004). This study demonstrated that *Fgf8a* apparently exerts its function mainly via

Fgfr1a, although a functional role for other Fgf ligands and/or Fgf receptors with overlapping expression patterns cannot be ruled out.

Both Fgfr1a and *Fgf8a* are expressed in the olfactory placode and anterior forebrain between 16-26hpf (Scholpp et al., 2004; Shanmugalingam et al., 2000). Therefore a mechanism can be speculated whereby *Fgf8a* signalling via Fgfr1a has a role in firstly maintaining olfactory neurogenesis in the olfactory epithelium, and secondly, in initiating a reduction in proliferation (or onset of differentiation) at the point of contact between the arriving ORN nerve endings and the anterior forebrain, prior to normal olfactory bulb morphogenesis. According to this model, it can be envisaged that reduced *Fgf8a* signalling may cause less olfactory neurogenesis at the olfactory epithelium (and increased apoptosis), leading to reduced olfactory (and vomeronasal) axonogenesis. This has the knock-on effect of fewer olfactory axons reaching the anterior telencephalon, and a lower reduction in local cell proliferation, causing abnormal (dysgenesis) or failed (agenesis) olfactory bulb formation. Upon MRI inspection, not all KS patients have missing olfactory bulbs, but nonetheless still have anosmia (or hyposmia) (Gonzalez-Martinez et al., 2004a). The likely explanation for this is that these patients have a mutation in *FGF8* or *FGFR1* (or *KAL1*, *see next chapter*), which causes varying degrees of FGF8/FGFR1 signalling, depending on the specific mutation, resulting in varying degrees of olfactory bulb dysgenesis.

Regardless of the exact mechanism of olfactory bulb morphogenesis, accurate pathfinding of the olfactory axons to their targets in the anterior telencephalon is of paramount importance for proper connectivity and correct functioning in the olfactory system (Gong and Shipley, 1995). Whilst it is unclear whether Fgf signalling itself has a direct role in olfactory/vomeronasal axonogenesis, there are many other guidance and signalling molecules which help to ensure that the olfactory axons project to the correct region of the anterior forebrain.

The olfactory axonal mis-projection defects caused by *Fgf8a* knockdown suggest that *Fgf8a*/Fgfr1a signalling may also have a role in olfactory axonogenesis. However, as already mentioned, it seems more likely that these mis-projection defects are caused by reduced neurogenesis in the nasal compartment. It can be

envisaged that fewer olfactory and vomeronasal neurons in the olfactory epithelium results in fewer axons capable of projecting to the anterior forebrain. Moreover, because olfactory axonogenesis is a concerted process whereby many olfactory/vomeronasal axons project to the anterior telencephalon within a relatively short time period between 24hpf and 48hpf, it could be speculated that in a situation of fewer neighbouring olfactory axons, some olfactory/vomeronasal axons may more easily deviate from the normally otherwise well-ordered axonal bundle 'scaffold' and mis-project away from the anterior telencephalon. Furthermore, because the pioneer olfactory axons are affected by *Fgf8a* signalling loss, as the olfactory axonal defects are observed by 36hpf, it is likely that all subsequent (secondary) olfactory axons are denied their 'guided path' towards the presumptive olfactory bulb region, and will mis-project too.

Dusp6 transgenic and pERK immuno-labelling analyses indicated that Fgf signalling was active mainly in the olfactory placodes at 24hpf and 30hf, consistent with its role in olfactory neurogenesis at these stages. However, there is very little Fgf signalling in the presumptive olfactory bulb region at these stages, probably because the majority of olfactory axons have not yet arrived. By 48hpf, Fgf signalling levels have greatly elevated within many cells located at the anterior telencephalon, consistent with olfactory morphogenesis onset in this region.

The exact mechanism whereby Fgf signalling from arriving olfactory axons brings about a reduction in proliferation at the telencephalon (the pre-requisite for olfactory bulb morphogenesis) is yet to be determined. However, it can be speculated that the arriving olfactory neuron growth cones may secrete *Fgf8a* upon their arrival at the target telencephalic neuroepithelial cells. *Fgf8a* freely diffuses through the extracellular space and binds to its receptor (Fgfr1a?) and activates Fgf signalling in those cells. As there is widespread Fgfr1a expression throughout the zebrafish embryonic anterior forebrain, a mechanism is required to ensure that the *Fgf8a* remains local to the olfactory nerve endings which secreted it. A 'source-sink mechanism' has been previously described, whereby Fgf8a morphogen gradients are established by fast, free diffusion of Fgf8a molecules away from the source, combined with a 'sink function' of receiving cells, regulated by receptor-mediated endocytosis (Yu et al., 2009). Extrapolating from this, it can be envisaged that local

telencephalic receiving cells may ensure that the greatest concentration of *Fgf8a* is maintained at the source of the olfactory nerve endings, using the same mechanism. Also, HS in the extracellular matrix maybe specifically modified in the presumptive olfactory bulb region to prevent the free diffusion of *Fgf8a* to neighbouring cells (Ford-Perriss et al., 2002). Either way, the result is that only the target neuroepithelial cells will undergo intracellular changes, via the Fgf signalling pathway, that culminate in those cells switching from a proliferative state, to a differentiative state instead.

An alternative explanation for why olfactory fibres fail to enter and establish contact with the anterior forebrain and initiate olfactory bulb morphogenesis in *Fgf8* deficient embryos is that they have a defect in the olfactory ensheathing cells (OECs). OECs are glial cells which originate from the olfactory epithelium and have been shown to be permissive for elongation/growth of olfactory axons (Tisay and Key, 1999; Chung et al., 2008). OECs express high levels of Fgfr1, and it has been proposed that reduced Fgf8 signalling in these cells impairs their specification and/or functioning in olfactory axonogenesis (Hsu et al., 2001); thus maybe demonstrating why peripherin-immunoreactive olfactory axons are disorganised in *Fgf8* hypomorphs. Despite defects in olfactory neurogenesis and axonogenesis in these mutants, not all olfactory-placodal derived cells are affected equally, and these mutants do have olfactory epithelia, as indicated by the presence of Olf-1 (olfactory neuron-specific transcription factor) positive neurons (Chung et al., 2008).

4.4.2 A problem of GnRH neuronal specification(?): the role of Fgf signalling

Previous studies in mice have shown that deficiencies in Fgf8 or Fgfr1, but not Fgfr3, results in a loss or reduction in hypothalamic GnRH neurons. In homozygous *Fgf8* hypomorphs, the GnRH neurons never emerge from the olfactory epithelium, and are missing from all developmental stages looked at; whereas *Fgfr1* hypomorphy severely reduces the number of GnRH neurons. The discrepancy between these two phenotypes may be explained by the fact that the Fgfr1 gene

knockdown is variable- somewhere between 66 and 80%. Alternatively, it could be because Fgf8 is signalling via more than one Fgf receptor, such as Fgfr3- although there was no GnRH neuronal loss caused by Fgfr3 gene loss, even though Fgfr1 and Fgfr3 are both present in GnRH neurons from E15.5 mouse embryos. Together this data suggests that Fgf8 signals predominantly via Fgfr1 during the generation and/or maintenance of GnRH neurons (or their progenitors) within the nasal compartment, in mice embryos (Chung et al., 2008).

GnRH neuronal migration to the hypothalamus is a very important process in the development of the GnRH system; and it has been well accepted that a failure in this migration is the cause of hypogonadotrophic hypogonadism in patients with KS. Previous studies have shown that peripherin-immunoreactive olfactory/vomeronasal axonal fibres do not enter the forebrain in homozygous *Fgf8* hypomorphic mice (Meyers et al., 1998), suggesting that the loss of GnRH neurons may be a migrational defect, resulting from the loss of the axonal scaffold required for their forebrain migration. However, GnRH neurons were absent from very early embryonic stages (i.e. E11.5) in the *Fgf8* hypomorphs, suggesting that Fgf signalling was instead required for GnRH neuronal specification within the nasal compartment. In support of this hypothesis, mice which were homozygous for the *Fgf8* hypomorphic allele had a 50% reduction in GnRH neurons, despite having normal morphogenesis of the nasal region and olfactory bulbs, demonstrating that some GnRH neurons failed to enter the forebrain even when their migratory scaffold was intact. It was therefore hypothesised that defects in early GnRH neurogenesis, not migration, caused hypothalamic GnRH neuronal loss in Fgf8 and Fgfr1 deficient mouse embryos (Chung et al., 2008).

To investigate the role of Fgf signalling during GnRH neuronal specification, a nasal explant culture which supported emergence of GnRH neurons from E10.5 was utilised. When Fgf signalling was blocked in this system, using SU5402, it was found that the GnRH neurons failed to emerge i.e. they were no longer specified. Furthermore, it was found that addition of FGF2 to dispersed GnRH neurons from E15.5 embryos resulted in neurite outgrowth (Gill et al., 2004). Together this data illustrates that Fgf signalling has a crucial role in GnRH neuronal specification in the nasal compartment, and plays a role in GnRH axon targeting.

Although a direct role for Fgf signalling in GnRH migration cannot be ruled out, the fact that Fgf signalling may be involved in GnRH neuronal axonogenesis suggest that it may have an indirect role in GnRH neuronal migration, as GnRH neurons are believed to migrate along their own (and neighbouring) neuronal processes during their hypothalamic migration in zebrafish (*see chapter 3*).

As mentioned above, Fgf8 deficiency has been shown to result in elevated levels of apoptosis in specific Fgf8-expressing regions of the olfactory placode and surrounding nasal compartment, causing a significant reduction in olfactory neurogenesis (Kawauchi et al., 2005). Similarly, GnRH progenitor cells which are generated within the olfactory placodal region may also be prematurely eliminated in the *Fgf8* mutants, or, if present, may be prevented from becoming GnRH neurons. Unfortunately, the absence of a specific GnRH progenitor cell marker prevents further investigation of the role of Fgf signalling in early GnRH neuronal specification.

Consistent with the mouse *Fgf8* mutant analysis, *Fgf8a* morphant zebrafish embryos had 50% or fewer hypothalamic GnRH neurons by 36hpf. Similarly, blocking Fgf signalling by SU5402 between 14hpf and 22hpf gave similar reduction in hypothalamic GnRH neurons. However, unlike the mouse *Fgf8* mutants, even in the seven *Fgf8a* morphant embryos which lacked all hypothalamic GnRH neurons, GnRH-expressing cells were still present in the terminal nerve region. As already discussed in chapter 3, it is unclear whether terminal nerve GnRH cells (or cells which migrate alongside the terminal nerve) or other cells within the nasal compartment contribute to the hypothalamic GnRH cells, or whether these so-called *'early wave'* hypothalamic GnRH cells actually arise within the hypothalamus itself. This affects how the GnRH defects caused by Fgf signalling loss are analysed.

Firstly, if the *'early wave'* hypothalamic GnRH3 neurons (or their progenitors) arise in the olfactory placode, or an adjacent region (including the anterior pituitary placode), then the proposed increase in apoptosis which occurs in the Fgf8-expressing cells of the nasal compartment in zebrafish, upon loss of Fgf8/Fgfr1 signalling, will also affect specification and subsequent emergence of hypothalamic GnRH3 neurons (or their progenitors) from this region, as is believed

to occur in the mouse *Fgf8* hypomorph. Moreover, as Fgf signalling has been shown to induce GnRH neurite elongation in primary cell culture (Gonzalez-Martinez et al., 2004b), this could result in the loss of the GnRH axonal scaffold that GnRH neurons are believed to utilise for their migration in to the forebrain. In fact, the projections from terminal nerve GnRH cells which normally extend across both forebrain commissures are missing or defective in the *Fgf8a* morphants, thus potentially hindering migration of the GnRH neurons into the hypothalamus. The loss of GnRH-positive projections across the POC, in the preoptic area of the brain, are particularly significant because this is the same region where the *'early wave'* GnRH cells migrate to by 36hpf.

Alternatively, if some or all of the *'early wave'* hypothalamic GnRH cells originate within the hypothalamus itself, the loss of hypothalamic GnRH cells by blocking Fgf signalling must result from an defect in proper GnRH neuronal specification. This may be due to an increase in apoptosis in the hypothalamic GnRH cells or their progenitors; similar to the mechanism of Fgf8 action at the olfactory placode, which may have been conserved from the common rodent/fish ancestor.

Although the Fgf receptors and *Fgf8a* are expressed within the telencephalon/diencephalon between 17-23hpf, it remains to be determined whether they are expressed within the GnRH cells or their progenitors; although the absence of a GnRH progenitor marker prevents such analysis being carried out at earlier stages, when such investigations would be most informative.

Another possibility is that the reduction in hypothalamic GnRH cell number secondary to the midline structural defects that are observed in *Fgf8a* mutant embryos. Specifically, the disorganisation of the area between the two forebrain commissures (the preoptic area) in the *Fgf8a* ('ace') mutant has previously been described (Shanmugalingam et al., 2000), suggesting that neuronal cell types (such as the GnRH neurons) which arise within this region may be disorganised and/or lost.

Using the GnRH3 transgenic reporter line (G3MC), it is has not been possible to observe migration of the hypothalamic GnRH neurons from the nasal

compartment, if such a migration exists in the zebrafish for these *'early wave'* GnRH cells. It is therefore not possible to comment on 'migrational defects' for these cells. However, the *'later wave'* of GnRH neuronal migration that was discussed in chapter 3 may be affected by loss of Fgf signalling in a different manner; this will be a future direction of this project. However, it is unknown whether Fgf8a morpholino will remain active long enough to block Fgf8a signalling when the later wave of GnRH migration into the hypothalamus occurs from around 120hpf onwards. Moreover, as SU5402 approaches can no longer be used at these later stages (due to lack of inhibitor penetration), a dominant negative FGFR approach may be required instead.

The disruption of the terminal nerve GnRH3 cells in the *Fgf8a*/*Fgf8b* double morphants suggest that Fgf8b may also have a role in the development of the zebrafish GnRH system, although this role may be restricted to these neuromodulatory neurons. Again, a more complete knockdown of *Fgf8b* is required to ascertain its full role in zebrafish GnRH development.

The analyses hitherto carried out on mouse and zebrafish to elucidate the role of Fgf8 and Fgfr1 during olfactory and GnRH neuronal development has already enhanced our understanding of the pathogenesis of human KS. In *Fgf8/Fgfr1* mutants, olfactory and vomeronasal neurons are reduced in number in the olfactory epithelium, and their axons are also fewer in number and fail to project correctly to their forebrain neuronal targets. This results in failure of olfactory bulb (and vomeronasal organ) morphogenesis, due to failure of local proliferation reduction (according to the model described above). GnRH cells and/or their progenitors which originate in the nasal compartment (or possibly from within the hypothalamus in zebrafish) do not emerge because they fail to get correctly specified, perhaps because they or their progenitors die through increased apoptosis. Moreover, if there is sufficient Fgf8 signalling, some GnRH cells may be specified, but they fail to project neurites into the forebrain, a necessary pre-requisite for their migration into the hypothalamus, as they migrate along their own axons. Moreover, if the Fgf8 signalling is reduced to levels that cause defects in olfactory axonogenesis, the GnRH neurons may be denied a navigational pathway into the

forebrain; so regardless of whether they have been specified correctly, they will remain outside the forebrain in the olfactory compartment region.

During human embryogenesis, GnRH neurons have been shown to originate at the olfactory placode (Schwanzel-Fukuda et al., 1996; Gonzalez-Martinez et al., 2004a), so they are more likely to follow the mechanism that has been described in mice, if it unfolds that zebrafish have sole hypothalamic origin for their hypothalamic GnRH neurons. KS patients with *FGFR1* and *FGF8* mutations present with HH with or without anosmia/ hyposmia, and, more rarely, isolated anosmia (Pitteloud et al., 2006). This demonstrates that the processes of olfactory and GnRH system development can be affected independently by reduced Fgfr1/Fgf8 signalling. For example, GnRH neuronal specification may be more susceptible to reduced Fgfr1/Fgf8 signalling, so patients who have *FGF8* or *FGFR1* mutations which bring signalling below a certain threshold, GnRH neurons are not specified at the olfactory placode. However, at the same level of Fgf8/Fgfr1 signalling olfactory neurogenesis may proceed, because its threshold hasn't been reached; such patients will have isolated HH, not KS.

Furthermore, some patients with FGFR1 mutations have HH that is reversible. For example, a male KS patient who discontinued his testosterone therapy, recovered from his HH, as evidenced by normal LH secretion, normal serum testosterone levels, and spermatogenesis (Pitteloud et al., 2005). Olfactory stem cells present in the olfactory epithelium continue dividing postnatally, and may potentially be a source of GnRH cells that migrate into the hypothalamus into adulthood (Calof and Chikaraishi, 1989). Moreover, it is possible that, as *may* occur during zebrafish embryogenesis (*see Chapter 3*), a stem cell population within the hypothalamus can give rise to new GnRH neurons, in response to specific maturation signals, such as sex steroids (Pitteloud et al., 2005). Another possibility is that despite the olfactory defects, a sub-optimal number of GnRH neurons were able to migrate into the hypothalamus, but were insufficient in number to initiate pulsatile GnRH secretion at the time of puberty; but this was overcome by the intake of sex steroids which help to initiate pulsatile GnRH release.

4.4.3 Other forebrain defects: the forebrain commissures

Vertebrate commissure formation is a highly organised developmental process whereby axons must traverse long distances in order to navigate towards their neuronal targets and form functional connections between both hemispheres of the brain. Fgf signalling has been shown to play an essential role in the development of the forebrain commissures in mice and zebrafish. Loss of *Fgf8* or *Fgfr1* cause severe defects in forebrain commissure formation in zebrafish and mice (Meyers et al., 1998; Shanmugalingam et al., 2000; Tole et al., 2006). It is therefore likely that Fgf8 is acting via Fgfr1 during this process, and this mechanism probably involves the specification of glial structures at the midline which help to ensure the correct navigation of the commissural axons. However, another, more direct, role for Fgf8/Fgfr1/HS in commissural axon pathfinding has also been postulated, although this is yet to be fully tested and proven (Tole et al., 2006).

Zebrafish deficient in *Fgf8a* have missing or abnormal AC and POC formation (Shanmugalingam et al., 2000); as do embryos that are treated with SU5402 to block Fgf signalling between 14hpf and 22hpf. Although not immediately apparent, these defects in forebrain commissure formation are relevant to our understanding of the pathogenesis of KS. During zebrafish embryogenesis, olfactory and terminal nerve GnRH neuronal axons both project across the forebrain commissures (AC and POC) and their associated tracts, and it is likely that such 'axonal scaffolds' are important for migration of the hypothalamic GnRH neurons (*early wave* and/or *late wave*). Moreover, these forebrain commissure projections permit coordination of GnRH and/or olfactory neuronal communications between both sides of the brain. Finally, defects in forebrain commissure formation may help in our understanding of the biological mechanism of bimanual synkinesis (upper body mirror movements) which is a symptom experienced by around 75% of KS patients with *KAL1* mutations (Kim et al., 2008).

There are two main hypotheses which have been proposed to explain the cause of bimanual synkinesis in KS patients. One proposed mechanism involves dysfunctional decussation (crossing over at the midline) of corticospinal tracts resulting in the majority of these axons instead projecting down the ipsilateral side

of the spinal cord, leading to abnormal development of the primary motor system. The other mechanism involves a lack of contralateral motor cortex inhibitory mechanisms i.e. abnormal formation of the trans-callosal fibres (of the corpus callosum) which coordinate both hemispheres of the brain by inhibiting the generation of a motor impulse in the opposite hemisphere during voluntary upper body movements (Koenigkam-Santos et al., 2008). In an analysis of patients with KS and bimanual synkinesis, cases of hypertrophy of the corpus callosum were found in both X-linked and autosomal KS patients, whereas a case of hypertrophies corticospinal tracts was found in an X-linked patients. This indicates that both hypotheses may be true and that there is may be more than one mechanism involved in bimanual synkinesis in KS patients (Krams et al., 1999).

Abnormalities in zebrafish spinal cord development were not investigated in this chapter; however the defects in AC and POC formation in the zebrafish *Fgf8a* morphants may be mechanistically similar to the corpus callosum defects that are present in the mouse *Fgfr1* and *Fgf8* mutants, as well as humans with X-linked KS and bimanual synkinesis. Moreover, corpus callosum defects have been described in at least one KS patient with an *FGFR1* mutation (Dode et al., 2003), further supporting the second mechanism described above.

However, incidence of bimanual synkinesis is far higher in X-linked KS patients (i.e. those with *KAL1* mutations), compared to autosomal KS patients (e.g. those with *FGFR1* or *FGF8* mutations) (Kim et al., 2008). This may be partly down to the genetics of these genes: *FGFR1* and *FGF8* mutations are normally (but not always) heterozygous mutations, meaning that these patients will be *hypomorphic* for these genes; whereas males with *KAL1* mutations have no other functioning copy of *KAL1*, and are therefore likely to be 'true' *KAL1* knockouts. This effectively means that these X-linked KS patients have no *KAL1* gene function; whereas those with *FGFR1* or *FGF8* mutations will still have at least 50% *FGFR1* or *FGF8* expression. In regions where *KAL1* is expressed, and its function required, loss of anosmin-1 signalling will have a more severe defect, compared with the same regions where *FGF8* or *FGFR1* are also required, giving a less severe (more variable) phenotype. This could be why bimanual synkinesis, and its putative associated defects in corpus callosum formation, is more strongly associated with

KAL1 mutations, compared with *FGFR1* or *FGF8* mutations; and why mouse conditional *Fgfr1* or *Fgf8* knockouts, but not human *FGF8*/*FGFR1* heterozygotes have more penetrant defects in corpus callosum formation.

4.5 Future prospects

Fgf signalling has a critical role in bridging the two hemispheres of the brain by forming midline cell types, including glial structures, which help to promote the midline crossing of commissural axons. Loss of Sonic hedgehog (Shh) signalling also causes loss of midline cell types, leading to a disorder called holoprosencephaly in humans and mice (Hayhurst and McConnell, 2003). It would therefore be interesting to ascertain whether there are any interactions between the Shh and Fgf signalling pathways in the induction of midline cell types and subsequent formation of the forebrain commissures.

Whilst defects in corpus callosum formation has already been described in both autosomal and X-linked KS patients (Krams et al., 1999), it will be informative to investigate whether the other brain commissures are affected in humans, included the anterior commissure, using standard MRI techniques. Moreover, it will be useful to find out how these putative commissure defects relate to any upper body mirror movement they may be present in these patients, and how this relates to their specific *FGF8*/*FGFR1* mutations (i.e. their FGF8/FGFR1 signalling levels).

Fgf3, *Fgf15*, *Fgf17* and *Fgf18* are all expressed at the anterior end of the developing mouse telencephalon, and may also have a role in the developing telencephalon (Hebert et al., 2003). In fact, Fgf3 was shown to have an important role in formation of the AC and POC in the zebrafish; and when *Fgf3* was knocked down with *Fgf8a*, a more severe forebrain commissure phenotype was obtained (Walshe and Mason, 2003). Using similar morpholino approaches, the effects of knocking down *Fgf3* on olfactory/vomeronasal axonogenesis and GnRH system development will be investigated.

Fgf8 mutants have more severe defects in forebrain development, including a much more complete loss of hypothalamic GnRH neurons, compared with the Fgfr1 mutants (Chung et al., 2008). This indicates that Fgf8 may not be acting solely through Fgfr1 during these developmental processes. Fgfr3 is likely candidate because it is expressed in GnRH neurons of E15.5 mouse embryos. Although mouse Fgfr3 mutants do not have a noticeable reduction in hypothalamic GnRH neurons

(Chung et al., 2008), a role for this Fgf receptor cannot completely ruled out. In order to determine which of the five individual zebrafish Fgf receptors are involved olfactory axonogenesis, commissure formation, and/or GnRH neurogenesis, it will be necessary to use specific morpholinos against each one. However, it is unlikely that 100% knockdown can be achieved in these embryos without resulting in early embryonic lethality; therefore each morpholino will need to be carefully titrated down to a knockdown level which is still viable. Moreover, to further investigate the role of Fgf signalling in these developmental processes, various available constructs can be injected into zebrafish embryos which modulate the Fgf signalling pathway, including constitutively active FGFR constructs. Furthermore, in order to fully investigate the role of the second *FGF8* orthologue (*Fgf8b*) during zebrafish forebrain development, it will be necessary to design new morpholinos against this gene, which permit higher (i.e. closer to 100%) knockdown levels.

Moreover, if any novel Fgf ligands, Fgf receptors, or downstream modulators are identified as being involved in olfactory/GnRH neuronal developmental, the KS patient DNA database (at the Centre of Neuroendocrinology, Royal Free hospital) may be utilised to discover whether there are mutations present in the human orthologous genes.

In order to further investigate the mechanism of forebrain commissure failure in the *Fgf8a* morphant zebrafish, it will be necessary to find out if the midline glial structures are disrupted, as they are in the *Fgf8* mouse mutant, using GFAP immuno-labelling between 16-22hpf to label the glial cells. Moreover, by titrating the Fgf8a morpholino, it can be investigated whether there is a threshold of Fgf8a signalling where the midline glial structures are normal, but the commissures are disrupted, thus confirming that Fgf8a signalling may be required for more than just specifying the midline glial structures. Then, by targeting dnFGFR specifically to a subset of commissural axons, e.g. by using the GnRH3 promoter to drive dnFGFR expression, it can be determined whether Fgf signalling is required for AC/POC axonogenesis, when the midline glial structures are normal. For example, if the GnRH-positive commissure axons fail to cross the midline correctly, this would suggest that Fgf signalling is essential for forebrain commissure axonogenesis, assuming that the terminal nerve GnRH cells are specified normally

in these mutants. Indeed, such an experiment will also be useful in determining whether Fgf signalling is required in GnRH3-expressing cells which migrate to the hypothalamus.

Similarly, it is unknown whether the Fgf8a signalling is required for olfactory/vomeronasal axonogenesis, or whether the failure in correct axonal formation is due to an increase in apoptosis in the olfactory epithelium. It may be expected that using the OMP promoter to control dnFGFR may caused too much apoptosis in the olfactory epithelium, and this will not allow us to answer this question. Therefore, instead, a promoter, such as that of an odorant receptor gene, may be used to control dnFGFR specifically in a small subset of olfactory neurons; the TRPC2 promoter may be used in a similar manner to inhibit Fgf signalling specifically in the vomeronasal axons. If Fgf signalling is required in those specific olfactory neurons that have their Fgf signalling blocked, their axons will be expected to mis-project away from the well-organised, tightly fasciculated olfactory nerve bundle which normally projects to the presumptive olfactory bulb region by around 36hpf. It is assumed that by the time that the odorant receptor has been expressed (at around 24hpf), the olfactory neuron's fate has already been established; so it won't be fated to go through apoptosis when Fgf signalling has been lost (as happens to early olfactory stem cells with Fgf signalling loss). Similarly, if Fgf signalling can be blocked specifically in a subset of zebrafish OECs, by using an OEC-specific promoter, it may be determined whether Fgf signalling is required for the correct functioning of the OECs, which are required for normal olfactory axonogenesis. Finally, to confirm that Fgf8a signalling is required for cell survival within the olfactory placode/ nasal compartment region in zebrafish, as happens in mouse embryos, cell apoptosis analyses (such as the Lysotracker assay, Invitrogen) will be need to be carried out on *Fgf8a* morphants, to identify increased olfactory neuronal cell death. Moreover, identification of a marker for early GnRH progenitor cells, which putatively originate in the nasal compartment, will permit an analysis of GnRH progenitor cell survival within the *Fgf8a*-expressing domain of the nasal compartment (and how this may hinder their subsequent migration to the hypothalamus).

Chapter 5
Results (III)

Indentifying combinatorial roles for *Kal1a* & *Kal1b* during GnRH/olfactory system development and forebrain commissure formation.

5.1 Introduction

In the past few years, several reports regarding the role of *KAL1* orthologues in zebrafish olfactory and GnRH neuronal ontogeny have, for the first time in a vertebrate model organism, helped to advance our understanding of the molecular pathogenesis of X-linked Kallmann syndrome *in vivo*. However, during this time, there has also been further progress in our fundamental understanding of the development of the zebrafish GnRH and olfactory systems. Specifically, using transgenic approaches, it is now well understood that there are two major groups of olfactory receptor neurons in the zebrafish (an 'olfactory-type' and a 'vomeronasal-type'), and perhaps two 'waves' of GnRH neuronal migration to the hypothalamus. Moreover, the use of splice-blocking morpholinos has helped achieve improved knockdown efficiencies, which can be more accurately assessed using standard molecular biological techniques. Also, the search for defects in forebrain commissure formation in these morphants, similar to those caused by another of the other KS genes, *Fgf8a*, may provide a new avenue for identifying the interaction of anosmin-1 in the FGF8 signalling pathway, *in vivo*.

5.1.1 Zebrafish have two *KAL1* orthologues: *Kal1a* & *Kal1b*

Zebrafish have two orthologues of the human *KAL1* gene: *Kal1a* and *Kal1b*, which share an overall homology with *KAL1* of 75.5% and 66.5%, respectively (Figure 5.01B). The proteins encoded by *Kal1a* (anosmin-1a[5]) and *Kal1b (*anosmin-1b) share the same domain structure as human anosmin-1: that is, an N-terminal cysteine-rich region, followed by a whey acidic protein-like (WAP) four disulphide core motif, and four fibronectin type III domains, finishing with a C-terminal histidine-rich region; except for anosmin-1b, where this last domain is missing (Figure 5.01A) (Ardouin et al., 2000). Moreover, the WAP motif in Kal1b has three amino acid substitutions which are conserved in the anosmin-1 proteins found in all other vertebrates; and, two highly conserved cysteine residues are substituted in the N-terminal cysteine-rich domain of Kal1b too (Yanicostas et al., 2009).

Ardouin and colleagues carried out initial *in situ* hybridisation analysis and found that *Kal1a* transcript was detected from around 37hpf onwards in the presumptive olfactory bulbs, whereas *Kal1b* was detected later, from around 48hpf onwards, in the epithelium of the nasal cavity, suggesting that Kal1a and Kal1b may have a role in the development of the zebrafish olfactory system (Ardouin et al., 2000).

5.1.2 A role for Kal1a in teleost fish GnRH system development

The effects of *Kal1a* and *Kal1b* gene knockdown on the GnRH system of two teleost fish models, the zebrafish (Whitlock et al., 2005b) and the medaka (Okubo et al., 2006), have been reported.

Medaka, like zebrafish, have two *KAL1* orthologues. However, unlike zebrafish, they have GnRH1- and GnRH3-expressing cells present in the preoptic area of the hypothalamus; but, only the GnRH1 cells project axons to the anterior

[5] To avoid confusion, anosmin-1a and anosmin-1b are referred to throughout as Kal1a and Kal1b, respectively; and the genes are referred to as *Kal1a* and *Kal1b* (i.e. italicised, as per convention).

A (i) anosmin-1a:

(ii) anosmin-1b

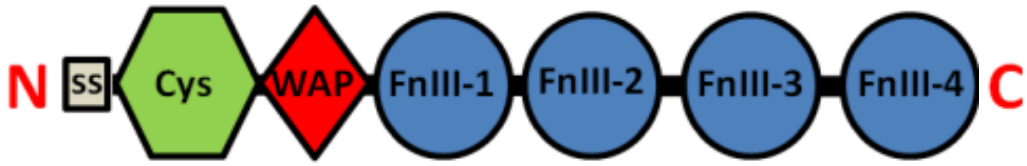

B

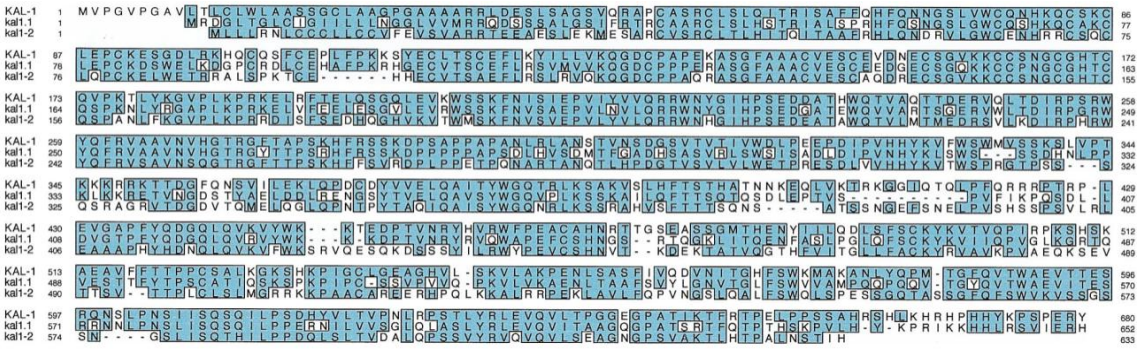

Figure 5.01 Zebrafish anosmin-1a & anosmin-1b

A: Schematic domain-structure diagrams (drawn to relative scale) of (i) anosmin-1a and (ii) anosmin-1b. They both have the same domain structure as human anosmin-1, except anosmin-1b lack the histidine-rich C-terminus. B: Amino acid sequence alignment of human anosmin-1 ('KAL-1') with zebrafish anosmin-1a ('kal1.1') and anosmin-1b ('kal1.2') . Regions of conservation are highlighted in blue

SS =Secretory signal sequence; Cys box = cysteine-rich region; WAP = whey acidic protein-like four disulphide core motif; FnIII-1, FnIII-2, FnIII-3, FnIII-4 = fibronectin type III domains; H = histidine-rich region.

Figure 5.01 (B) reprinted from Mech. Dev. 90, Ardouin et al., 'Characterization of the two zebrafish orthologues of the KAL-1 gene underlying X chromosome-linked Kallmann syndrome.', pp.89-94, Copyright 2000, with permission from Elsevier.

pituitary, thus making GnRH1 the hypophysiotropic form of GnRH in the medaka. However, Okubo and colleagues showed that knocking down *Kal1a*, but not *Kal1b*, resulted in both GnRH1 and GnRH3 neurons failing to migrate into the hypothalamus, and instead accumulating in the olfactory compartment (Okubo et al., 2006).

Similarly, Whitlock and co-workers reported that knocking down *Kal1a* in the zebrafish resulted in specific and complete loss of the 'endocrine' GnRH cells of the hypothalamus, but did not affect the 'neuromodulatory' cells of the midbrain and terminal nerve. Moreover, knocking down *Kal1b* resulted in only a slight decrease in the number of migratory hypothalamic GnRH cells by 56hpf (Whitlock et al., 2005b).

5.1.3 A role for Kal1a in zebrafish olfactory system development

Using anti-anosmin-1a polyclonal antibodies, it was also recently reported that anosmin-1a is expressed from as early as 22hpf in the pioneer olfactory receptor neurons (ORNs) and that knockdown of *Kal1a*, but not *Kal1b*, impaired the proper fasciculation of olfactory axons and their terminal targeting at the olfactory bulbs. Moreover, there was a severe decrease in the number of GABAergic and dopaminergic olfactory bulb neurons caused by the knockdown of anosmin-1a, thus demonstrating once again the need for correct innervations by the ORNs for proper olfactory bulb neuronal differentiation (Yanicostas et al., 2009).

5.1.4 Aims of this chapter

Kal1a has been implicated in olfactory and GnRH system development in the zebrafish. Using novel technological approaches, the role of both Kal1a and Kal1b will be further examined, and then studied in the context of its involvement in the Fgf8a signalling pathway, *in vivo*. These are therefore the aims for this chapter:

- To characterise the spatio-temporal expression of *Kal1a* and *Kal1b* in relation to olfactory and GnRH system development in the forebrain.

-To knockdown *Kal1a* and *Kal1b* using translation- and splice-blocking morpholinos, confirm their knockdown efficiencies, and identify any GnRH, olfactory, and/or vomeronasal mutant phenotypes caused by their knockdown.

-Establish whether the *Kal1a* and/or *Kal1b* morphants, like *Fgf8a* morphants, have defects in forebrain commissure formation.

-To over-express *Kal1a* and *Kal1b* by micro-injection of *in vitro* transcribed mRNA, and identify any developmental defects this may cause.

-If no measurable olfactory, GnRH, or commissural defects are caused by over-expression, the *Kal1a* and/or *Kal1b* mRNA can then be used to 'rescue' any morphant defects caused by knockdown of *Kal1a* and/or *Kal1b*.

-To identify whether or not Kal1a and/or Kal1b are acting via the Fgf8a signalling pathway i*n vivo*.

5.2 Results

5.2.1 *Kal1a* and *Kal1b* expression during head development

In situ hybridisation expression analysis of Kal1a and Kal1b

Kal1a transcript was first detected at around 24hpf in the otic vesicle and the posterior lateral line primordium (PLLP); where it has been shown to have an essential role in positioning lateral line neuromasts along the trunk (Yanicostas et al., 2008) (Figure 5.02A). However, head expression could not be detected until around 32hpf, broadly within the diencephalic and hindbrain regions (Figure 5.02B). This expression pattern broadened to encompass some of the midbrain by 45hpf (Figure 5.02C), but became weaker and more diffuse by 60hpf in these regions (Figure 5.02D). Notably, *Kal1a* transcript *could not* be reliably detected in the telencephalon or olfactory placodes throughout these stages (Figure 5.02A-D).

Kal1b was detected in the tailbud regions from as early as 17hpf *(*data not shown*)*, as previously reported (Ardouin et al., 2000). However, more anteriorly, *Kal1b* transcript is first detected in the PLLP and otic vesicle, and, more weakly, in diencephalic and midbrain regions from around 24hpf (Figure 5.02E). Significantly, *Kal1b* was also detected in the olfactory placodes at this stage (Figure 5.02E); particularly in a group of cells at the medial edges, which share a similar appearance and localisation to the terminal nerve GnRH3 cells (Figure 5.02E', E''). From around 32hpf, olfactory epithelium staining could no longer be reliably detected, and *Kal1b* brain expression was similar to that reported above for *Kal1a* at these stages, but weaker and more diffuse (Figure 5.02F-G).

Interestingly, at 60hpf, in the forebrain, both *Kal1a* and *Kal1b* transcripts appear to be restricted to regions where the forebrain commissure and terminal nerve projections have formed (Figure 5.02D', H').

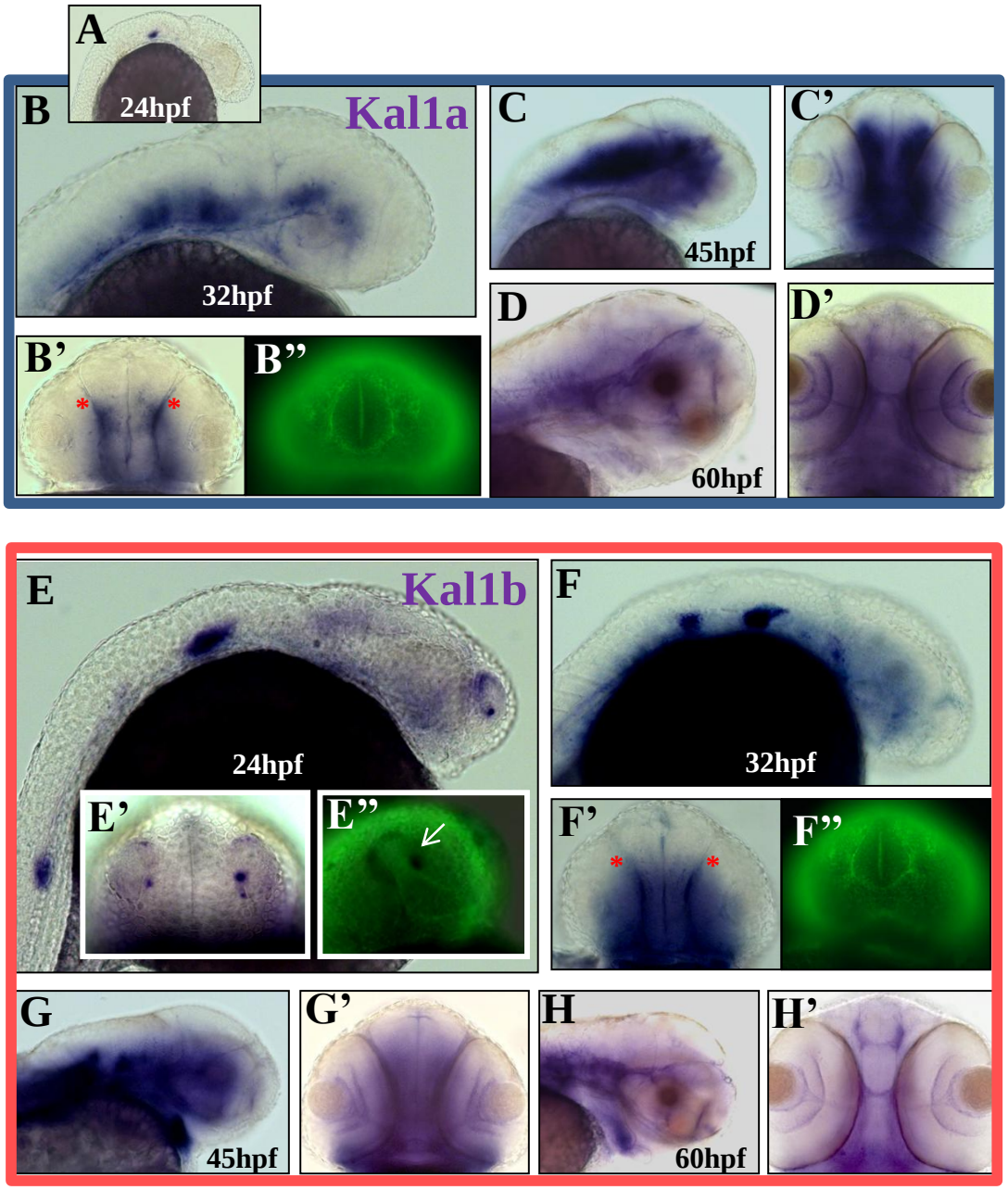

Figure 5.02 Kal1a & Kal1b *in situ* hybridisation expression analysis

Expression of Kal1a (A-D') and Kal1b (E-H') at 24hpf (A, E), 32hpf (B, F) 45hpf (C, G) and 60hpf (D, H). B', B'', C', D' are ventral views; A, B, C, D, E, F, G, H are lateral views. B'' and F'' show anti-acetylated tubulin (AT) immuno-labelling for B' and F', respectively. The asterisks in B' and F' indicate the location of the olfactory placodes. E'' shows the overlay of AT labelling on a ventral-lateral view of a Kal1b *in situ* at24hpf. The arrow in E'' indicates the terminal nerve position.

Immuno-expression of anosmin-1a and anosmin-1b in the olfactory epithelium and pituitary

Between 24hpf and 60hpf, anosmin-1a and anosmin-1b are both expressed throughout the whole olfactory epithelium and its associated axonal projections to the olfactory bulbs, as well as some projections which extend across the anterior commissure (Figure 5.03A-H). Anosmin-1b expression also extended to the pituitary region from around 36hpf onwards (Figure 5.03D, F, H; and Figure 5.04A). Anosmin-1a and anosmin-1b were not detected in any other brain region during these stages; however, there was some expression of both orthologues in the otic vesicle, PLLP, and pronephric duct from around 30hpf onwards (appendix, Figure A1).

Anti-anosmin-1b immuno-labelling was also carried out on 48hpf pGnRH3:mCherry (G3MC) embryos, in order to characterise the position of the hypothalamic G3MC cells in relation to the anosmin-1b-labelled pituitary (Figure 5.04B-C). The presumptive pituitary cells were found to closely abut the hypothalamic G3MC cells; however, there was no co-expression of mCherry and anosmin-1b in any of these cells, except, perhaps at the interface between the pituitary and hypothalamic G3MC cells. Using 3D rendering software, it was possible to view the pituitary and hypothalamic cells from the dorsal and side view too (Figure 5.04C, C'). This showed that the pituitary is in the same anterior-posterior plane as the hypothalamic G3MC cells, and that some of the G3MC cells (2-3) are actually positioned on the dorsal side of the pituitary. Whilst it is impossible to say from this data whether or not the hypothalamic G3MC cells are interacting with the pituitary gonadotrophs (or other pituitary cell-types) at this stage, such interactions seem plausible, but would need to be investigated further.

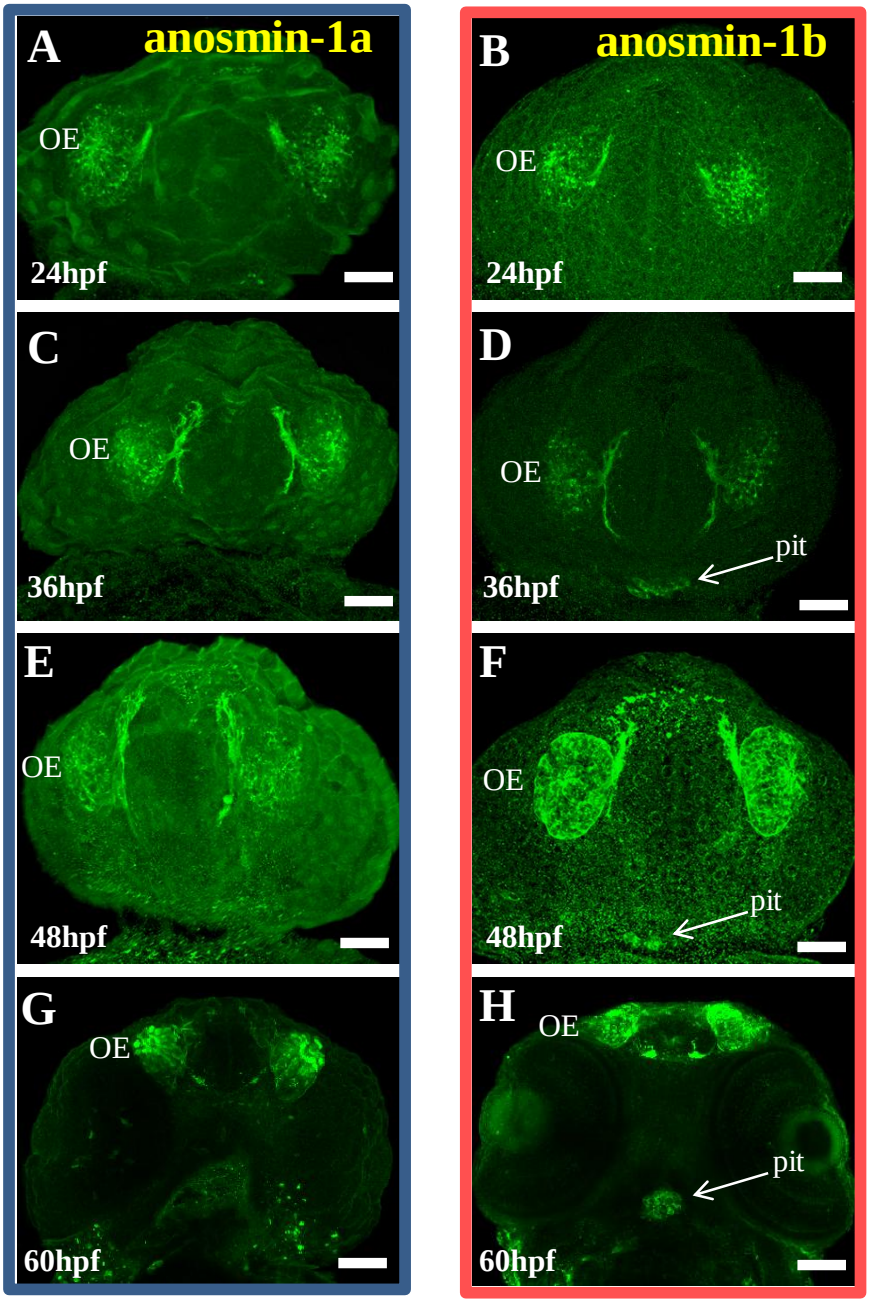

Figure 5.03 Anosmin-1a & anosmin-1b immuno-expression during head development

Anti-anosmin-1a (A, C, E, G) and anti-anosmin-1b (B, D, F, H) immuno-labelling in zebrafish embryos at 24hpf (A, B), 36hpf (C, D), 48hpf (E, F), and 60hpf (G, H). A-H are all confocal images from ventral view.
Scale bars are 50µm.
OE= olfactory epithelium; pit= pituitary

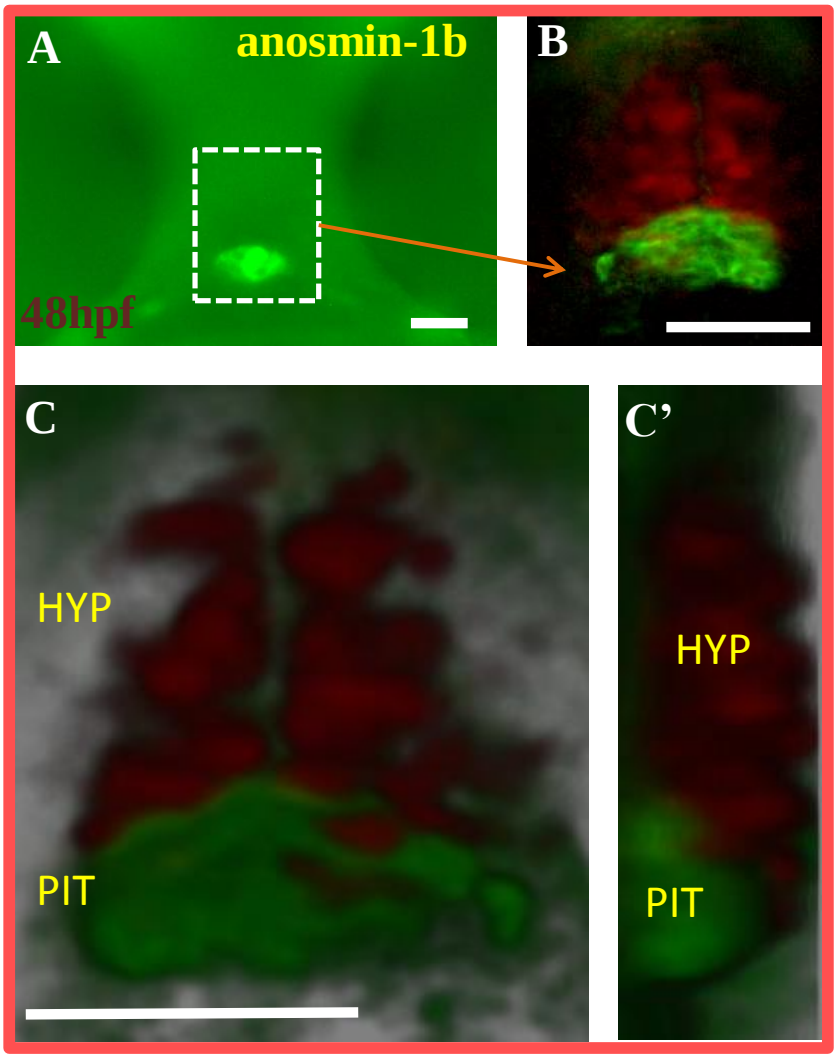

Figure 5.04 Anosmin-1b immuno-expression in the pituitary

Anti-anosmin-1b immuno-labelling in the pituitary (in green, A-C). A: a dotted box indicates the presumptive pituitary labelling at 48hpf; in B this region is shown in more detail relative to hypothalamic G3MC cells (in red). A and B are both ventral views. 3D rendering analysis was carried out on B (shown in C and C'). The hypothalamic cells closely abut the presumptive pituitary anosmin-1b positive cells- as seen from a dorsal view (C) and a lateral view (C'). Scale bars are 50μm.
HYP= hypothalamic G3MC cells; PIT= presumptive pituitary

5.2.2 Knocking down *Kal1a* and *Kal1b* using translation-blocking morpholinos

To begin with, translation-blocking morpholinos (tbMOs) were used to specifically knock down *Kal1a* (A-MO) and *Kal1b* (B-MO) gene function. But, due to their unfavourable knockdown efficiency and lack of significant morphological defects (*see below*), these were later replaced with splice-blocking morpholinos (sbMOs, *see section 5.2.4*) for the remainder of the *Kal1a*/*Kal1b* knockdown studies in this chapter.

Knockdown is incomplete

To verify the knockdown efficiency of the tbMOs (A-MO and B-MO), Western immuno-blotting was carried out using embryonic lysates harvested from 24hpf embryos previously injected with control MO (coMO, at 1.5mM) or A-MO or B-MO at 0.5mM, 1.0mM, or 1.5mM (Figure 5.05A).

Immunoblots probed with anti-anosmin-1a antibody (Figure 5.05A, *top left*) produced two bands for each lane: one at ~95kDa and another at ~85kDa. Two bands of similar molecular weight were also detected when anti-anosmin-1b antibody (Figure 5.05A, *top right*) was used, except that the equivalent ~85kDa band was much weaker in intensity. Whilst only a ~95kDa band had previously been reported for these antibodies, the ~85kDa band may be a differentially glycosylated form of anosmin-1a and anosmin-1b. However, for the purposes of this analysis, only the higher ~95kDa band will be assessed.

Previous titration experiments had shown (*see appendix*) that the highest non-lethal concentrations for A-MO and B-MO were 1.5mM. However, at 1.5mM some embryos showed severe overall morphological deformities such as heart oedema and 'curved trunk' (especially the B-MO injected embryos); but, these defects were much less apparent at either 1.0mM or 0.5mM (*see appendix*).

'Visual comparisons' of relative reduction in band intensities of coMO-injected embryos were compared with the A-MO and B-MO morphants to obtain

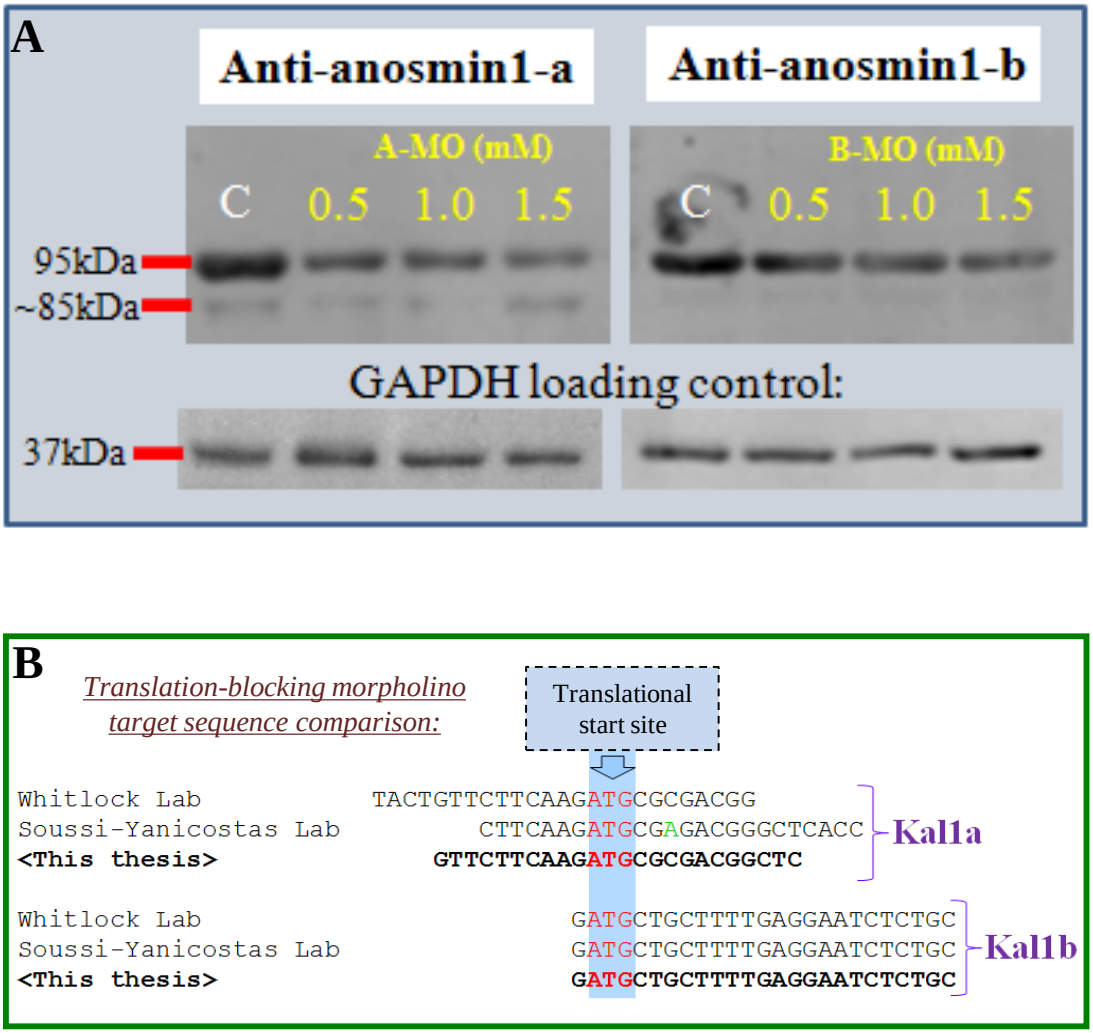

Figure 5.05 Confirmation of Kal1a & Kal1b knockdown by translation-blocking morpholinos

A: Immunoblotting of 24hpf control ('C') and morphant* (*see below*) embryo lysates, probed with anti-anosmin-1a (top left), anti-anosmin-1b (top right), or anti-GAPDH (bottom).

B: Diagram comparing target sequences for Kal1a (top) or Kal1b (bottom) translation-blocking morpholinos used in this thesis (see Figure 5.05 for phenotype) or papers published by the Whitlock (Whitlock et al., 2005b) or Soussi-Yanicostas (Yanicostas et al., 2009) laboratories.

**Translation-blocking morpholinos against Kal1a (A-MO) and Kal1b (B-MO) were used at concentrations of 0.5, 1.0 or 1.5mM*

approximate *Kal1a*/*Kal1b* gene knockdown levels. Lysates from embryos injected with 1.5mM of A-MO showed no more than 75% decrease in band intensity (*Kal1a* knockdown) compared with the coMO lysate (Figure 5.05A, *top left*); whilst the knockdown efficiencies for 0.5mM and 1.0mM A-MO were ~50-75%. For B-MO, these knockdown efficiencies were ~50% at 1.0mM and 1.5mM, and only ~25% at 0.5mM (Figure 5.05A, *top right*). The GAPDH loading controls (~37kDa bands) showed that the amount of total embryonic protein lysate loaded in each lane was approximately equal across all lanes, thus making these calculated knockdown efficiencies more reliable (Figure 5.05A, *bottom*).

Whilst densitometry analysis of these band intensities would have been far more accurate, this analysis was sufficient to prove that the knockdown was incomplete, and that the 'average' morphant had no more than around 75% knock down of *Kal1a*/*Kal1b* gene expression (*see discussion*).

Subtle olfactory and commissural defects

There were no noticeable defects caused by knocking down *Kal1a* and *Kal1b* individually using the translation-blocking morpholinos A-MO and B-MO *(*data not shown*)*; however, there were some subtle phenotypes caused by co-injecting A-MO and B-MO together (Figure 5.06).

The G3MC phenotype was virtually unaffected at 36hpf (data not shown) or later at 60hpf in the A-MO+B-MO morphants (n=28/31, 2 experiments, Figure 5.06B). In Figure 5.06B, the G3MC hypothalamic cluster and G3MC-positive optic nerve and tract appear fainter (less mCherry fluorescence), but, on closer inspection these tracts and cells nevertheless still appear to be grossly present and intact, compared with the wild-type G3MC phenotype seen in the coMO-injected controls (n=28/28, 2 experiments, Figure 5.06A).

The olfactory pits had formed correctly by 48hpf in the A-MO+B-MO double morphants, and the ORN axons had extended towards the telencephalon in a approximately normal tightly-fasciculated bundle (n=47/50, 2 experiments, Figure 5.06D), similar to the control embryos (n=44/44, 2 experiments, Figure 5.06C).

Figure 5.06 Morphant phenotypes for translation-blocking morpholinos targeted against Kal1a and Kal1b

No observable defects were observed for knocking down Kal1a or Kal1b alone ,using translational-blocking morpholinos . Therefore, only the double knockdown of both Kal1a and Kal1b is shown here.

G3MC (in red; A, B), OMPG (in green; C, D), anti-calretinin immuno-labelling (in purple; E, F), and anti-acetylated tubulin immuno-labelling (in blue; G, H) is shown for control* (A, C, E, G) or Kal1a+Kal1b (B, D, F, H) morphants at 60hpf (A,B), 48hpf (C-F), or 36hpf (G, H). All views are ventral. The asterisk indicates the loss/reduction of some calretinin-positive axons in the 'central zone' region of the olfactory bulb in F.
Scale bars are 50μm (C-H) 100μm (A, B).

**Henceforth , 'control' means control morpholino (CoMO)-injected.*

TN= terminal nerve; hyp= hypothalamus; OE= olfactory epithelium; OB= olfactory bulb; AC= anterior commissure; POC= post-optic commissure.

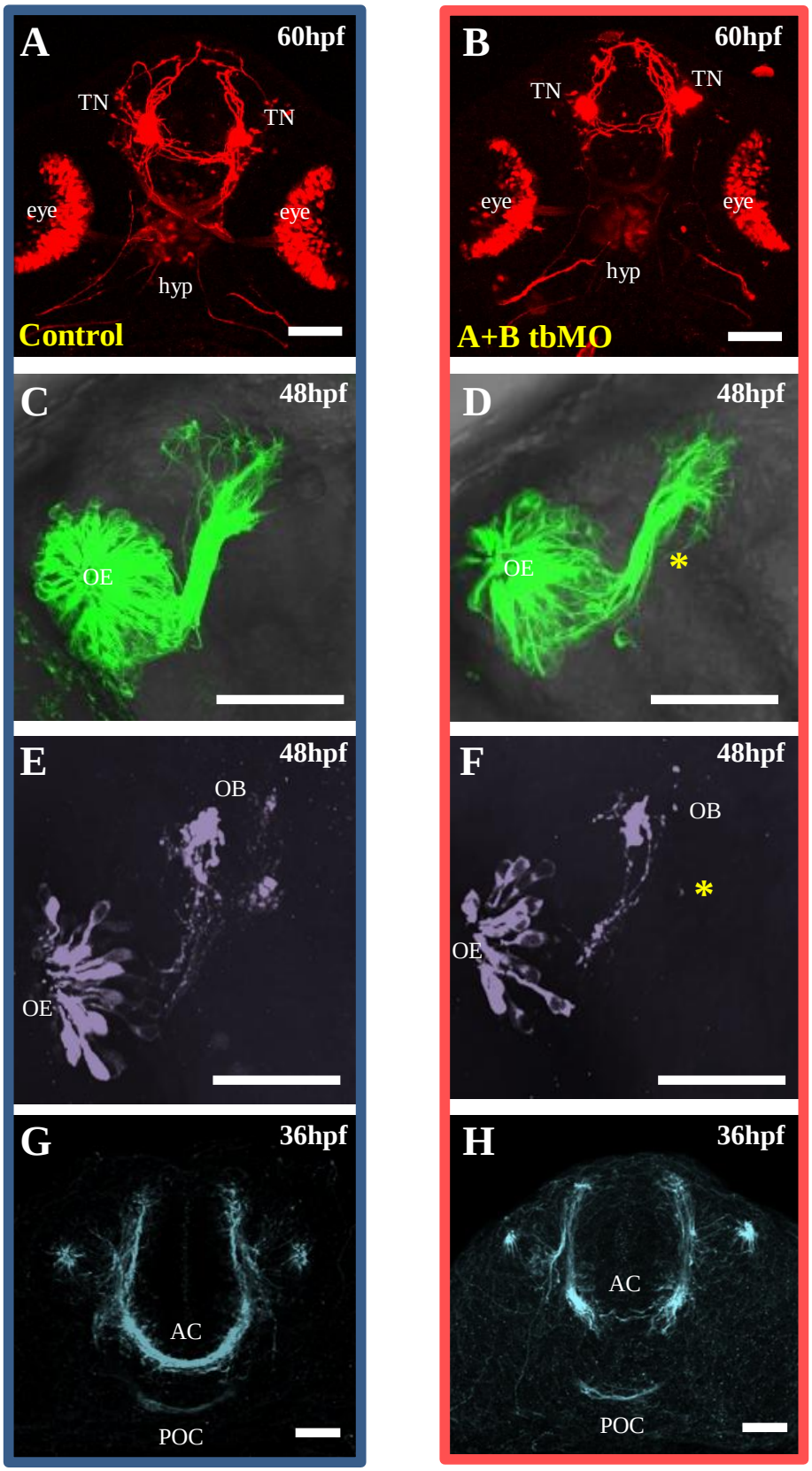

Figure 5.06 Morphant phenotypes for translation-blocking morpholinos targeted against Kal1a and Kal1b

However, whilst the pOMP:EGFP labelled ORNs in the control embryos had begun to defasciculate at the presumptive olfactory bulb region and had formed specific axonal condensations (glomeruli) by 48hpf (n=44/44, 2 experiments, Figure 5.06C), many of the A-MO+B-MO morphants were less-defasciculated in this region and had formed a different, less ordered, pattern of glomeruli at the presumptive olfactory bulbs by this stage (n=34/50, 2 experiments, Figure 5.06D). Moreover, the A-MO+B-MO morphants often also had mis-projected ORNs (n=19/50, 2 experiments, Figure 5.06D), which, in the case of Figure 5.06D, sometimes appeared to be repelled from the presumptive olfactory bulb region and reversed their direction of elongation back towards the olfactory pits (*see asterisk in Figure 5.06D*).

To further investigate this olfactory phenotype, anti-calretinin immuno-labelling was used to label a subset of the ORNs at 48hpf. Consistently, the A-MO/B-MO morphants were found to have fewer medial calretinin-positive ORN projections in the 'central zone area' of the olfactory bulbs (n=38/48, 2 experiments, Figure 5.06F), compared with the controls which labelled all expected calretinin-positive projections (n=42/42, 2 experiments, Figure 5.06E); whereas those projections which form the 'lateral glomeruli' were much less affected (data not shown). See Figure 5.07 for a schematic map of a zebrafish olfactory bulb at approximately 48hpf, illustrating the locations of the different glomeruli regions referred to above.

Finally, anti-acetylated tubulin immuno-labelling was also carried out to see if the forebrain commissures (AC and POC) were also affected (Figure 5.06G, H), as they in *Fgf8a* morphants. At 36hpf, whilst the AC had formed in most of the A-MO/B-MO double morphants; in some cases, fewer axons had projected across the midline (n=28/56, 3 experiments, Figure 5.06E), compared with the control embryos which all had normal commissure formation (n=51/51, 3 experiments, Figure 5.06E), whereas the POC appeared normal morphants and control embryos.

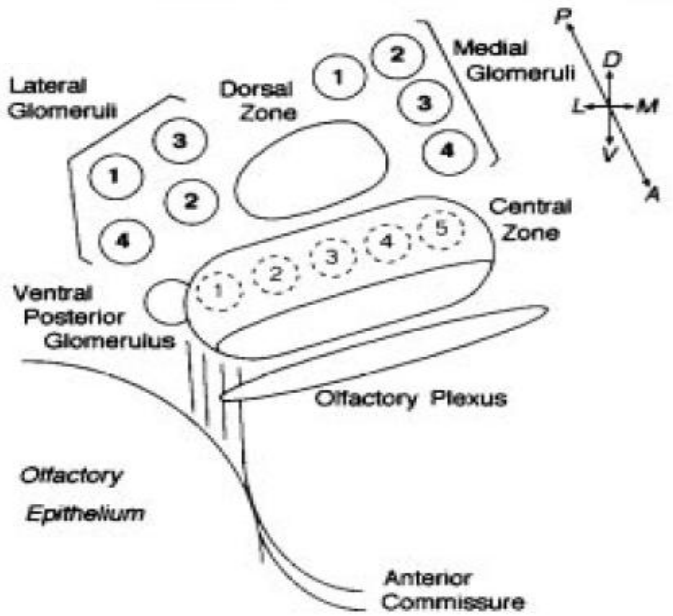

Figure 5.07 Glomerular map of a zebrafish olfactory bulb

A schematic map showing the glomerular pattern in the olfactory bulb of a 3.5dpf zebrafish embryo, based on a study by Dynes and Ngai, using lipophilic tracer dyes in live embryos. Bilaterally symmetric and distinct structures in the developing olfactory bulb that were characterised include: the olfactory plexus, four lateral glomeruli, four medial glomeruli, five glomeruli in the central zone, a ventral posterior glomerulus, and a dorsal zone. Glomeruli within the central zone region are indicated by dotted lines, as their boundaries are less distinct.

Figure 5.07 reprinted from Neuron 20, Dynes and Ngai., 'Pathfinding of olfactory neuron axons to stereotyped glomerular targets revealed by dynamic imaging in living zebrafish embryos.', pp.1081-1091, Copyright 1998, with permission from Elsevier.

5.2.3 Kal1a and Kal1b over-expression causes no observable forebrain defects

In vitro transcribed *Kal1a* and *Kal1b* capped mRNA (Figure 5.08A) were injected individually at a concentration of 0.5μM, 1.0μM, or 2.0μM (data not shown) or co-injected together at 0.5μM each, at the one-cell stage (Figure 5.08B-E). At 1.0μM *Kal1a* or *Kal1b*, there were occasionally some trunk-shortening defects, but the heads appeared normal. At 2.0μM of *Kal1a* or *Kal1b*, the majority of embryos died by 24hpf: an effect which was, to a lesser extent, mirrored by using1.0μM *Kal1a* + 1.0μM *Kal1b*. However, embryos injected with 0.5μM *Kal1a* or *Kal1b* had normal morphologies; and those injected with 0.5μM *Kal1a* + 0.5μM *Kal1b* were mostly normal, and only occasionally had subtle trunk defects (*see appendix for summary of lethalities and gross morphological abnormalities in these Kal1a/Kal1b mRNA titration experiments*). *In vitro* transcribed GFP mRNA, at a concentration of 1.0μM, was injected into the control embryos that were subsequently immuno-labelled with acetylated tubulin (Figure 5.08B), and there did not appear to be any morphological abnormalities (controls for the pOMP:EGFP embryos were uninjected, as injecting GFP would have interfered with transgenic EGFP fluorescence).

Both forebrain commissures had formed correctly by 36hpf for those embryos injected with 0.5μM *Kal1a* + 0.5μM *Kal1b* mRNA (n=32/32, 2 experiments, Figure 5.08C) or GFP mRNA (*controls*; n=29/29, 2 experiments, Figure 5.08C); and by 48hpf, the olfactory pits also appeared normal, with typical tightly fasciculated bundles of ORNs projecting to the telencephalon. Moreover, the pattern of defasciculation at the presumptive olfactory bulbs fell within the range of accepted natural variability for the *Kal1a*/*Kal1b* mRNA-injected embryos (n=36/36, 2 experiments, Figure 5.08D) and GFP controls (n=30/30, 2 experiments, Figure 5.08E); and consistently, there were no observable defects in the G3MC phenotype at 36hpf or 60hpf (data not shown). Fortuitously, this meant that *Kal1a* and *Kal1b* mRNA (at 0.5μM + 0.5μM) could be used in subsequent experiments to *'rescue'* the Kal1a/Kal1b morpholino-induced phenotypes, and thereby proving the specificity of those morphant phenotypes *(see below)*.

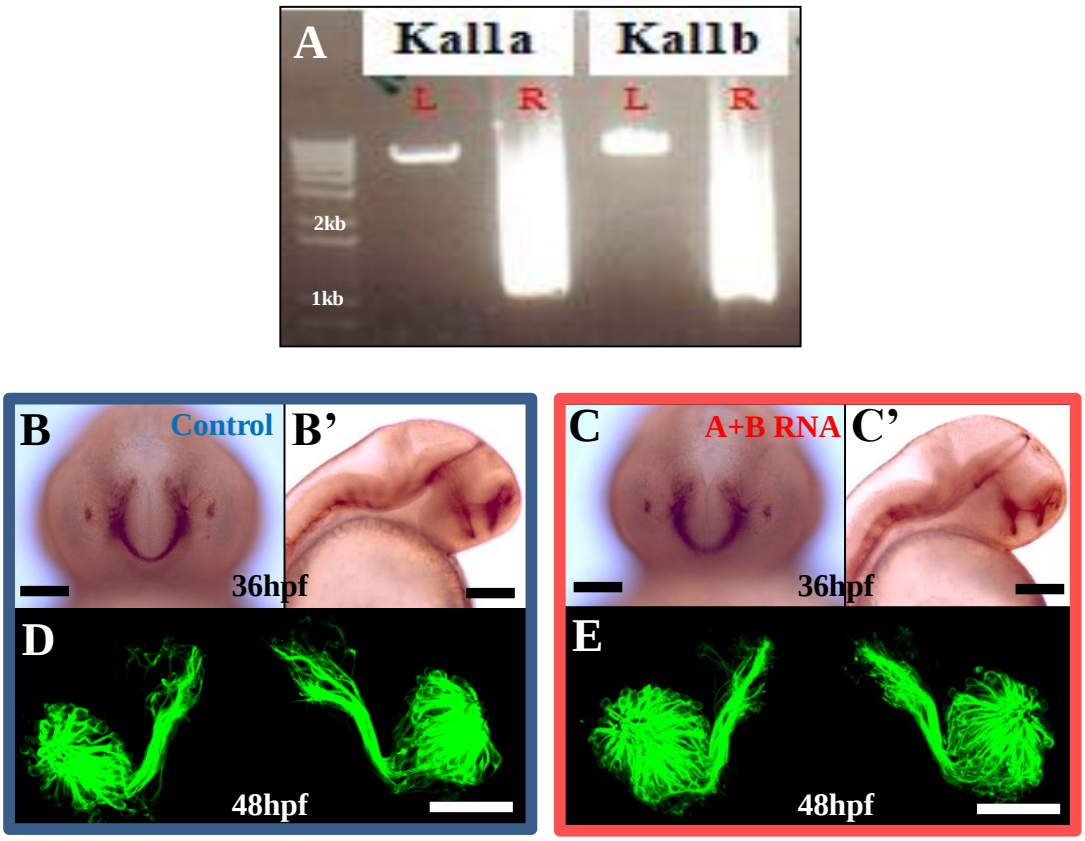

Figure 5.08 Kal1a and Kal1b over-expression causes no observable defects

A: An agarose gel showing that RNA for Kal1a and Kal1b was successfully transcribed *in vitro*. Anti-acetylated-tubulin immuno-labelling with DAB at 36hpf (B, C) and OMPG confocal analysis at 48hpf (D, E) are shown for the Control (B, B', D) and Kal1a+Kal1b RNA-injected (C, C', E) embryos . Ventral views are shown for B, C, D, and E; lateral views for B' and C'. No observable defects were observed for embryos injected with Kal1a or Kal1b RNA alone (*data not shown*) or together (*shown here*). Scale bars are 50µm (D, E) 100µm (B, C).
L= linearised plasmid; R= RNA

5.2.4 Knocking down *Kal1a* and *Kal1b* using splice-blocking morpholinos which target the loss of exon 4

Splice-blocking morpholinos (sbMOs), which target the loss of either exon 4 (*see below*) or exon 6 (*see section 5.2.5*) from *Kal1a* or *Kal1b*, were used in order to try and achieve higher levels of knockdown (i.e. 75-100%) compared with the tbMOs (A-MO and B-MO). Figure 5.09 schematically illustrates the mechanism for the morpholinos which target the loss of exon 4 from *Kal1a* or *Kal1b* ('KA4' and 'KB4'). The exact same mechanism is also true for the morpholinos which target the loss of exon 6 from *Kal1a* and *Kal1b* ('KA6' and 'KB6'), and all other sbMOs, including the Fgf8b morpholino used in chapter 4. The resulting mis-spliced *Kal1a* and *Kal1b* transcripts are predicted to be shorter than their wild-type versions due to the expected loss of a whole exon; and this was confirmed when this region of the transcripts was amplified by RT-PCR *(see below)*.

High knock-down efficiency confirmed by RT-PCR

Initially, to confirm that the KA4 and KB4 sbMOs were successfully targeting the loss of the whole of exon 4 from *Kal1a* and *Kal1b*, RT-PCR was carried out on cDNA pooled from 10 embryos (Figure 5.10A). GAPDH control PCR reactions were used to confirm that cDNA synthesis was successful in all of the pooled cDNA samples, in case the morphant Kal1a/Kal1b PCR products were degraded.

The expected PCR product sizes for wild-type *Kal1a* and *Kal1b* of (750bp) and (754bp), respectively, were obtained for the control cDNA sample (Figure 5.10A[1]). These PCR products were excised from the gel and sequenced to confirm that they were indeed amplified from *Kal1a* and *Kal1b*, respectively *(*data not shown*)*.

For the KA4 morphant cDNA sample (Figure 5.10A[2]), the *Kal1a* PCR reaction gave a band of reduced size, which was equivalent to the size predicted for the loss of the whole of exon 4 (527bp); whereas the *Kal1b* PCR reaction from the

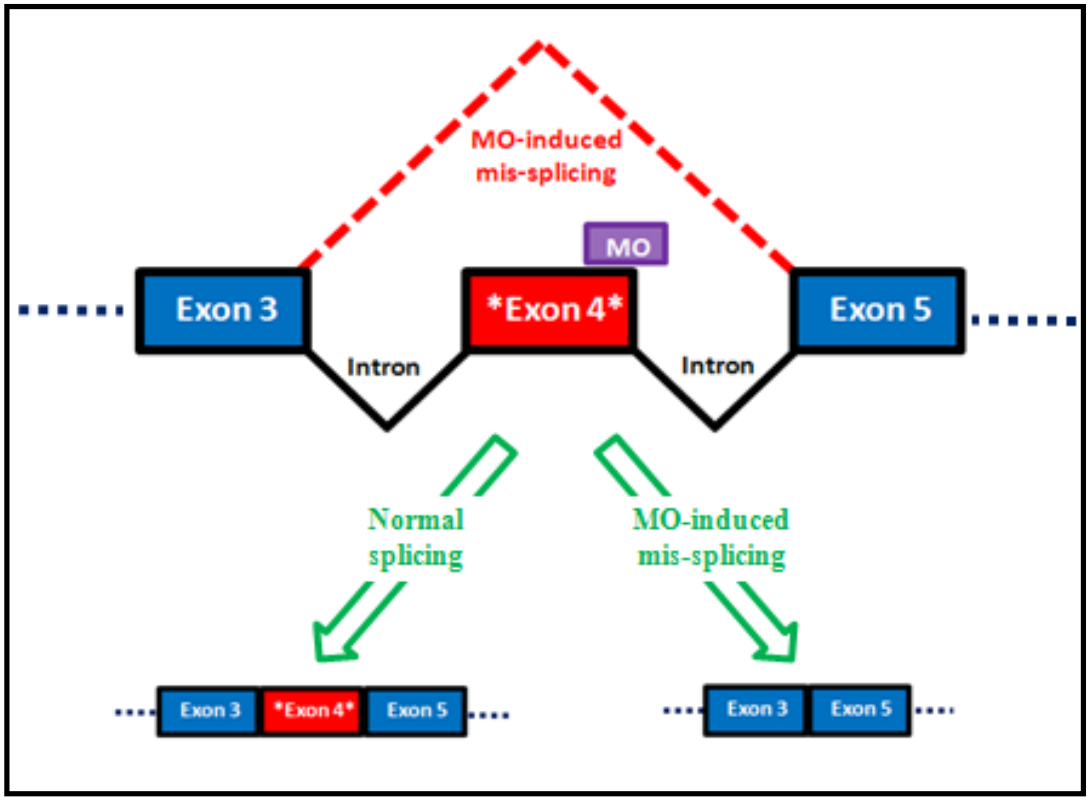

Figure 5.09 Schematic diagram illustrating the mechanism for splice-blocking morpholino gene-targeted knockdown

Exons 3, 4, and 5 from a Kal1a or Kal1b mRNA transcript are represented as boxes separated by 'V' shapes (two introns). The dotted line before exon 3 represents exons 1 and 2; and the dotted line after exon 5 represents exons 6-14. During normal splicing, both introns will be spliced out and the spliced transcript will contain all three of the pictured exons (*bottom left*). However, if the morpholino (purple box) is present, it will bind to a specific exon-intron junction - in this case exon 4 (red box). The splicing machinery 'skips' the whole intron-exon4-intron sequence, and the resultant (morphant) spliced transcript will lack exon 4 (*bottom right*).

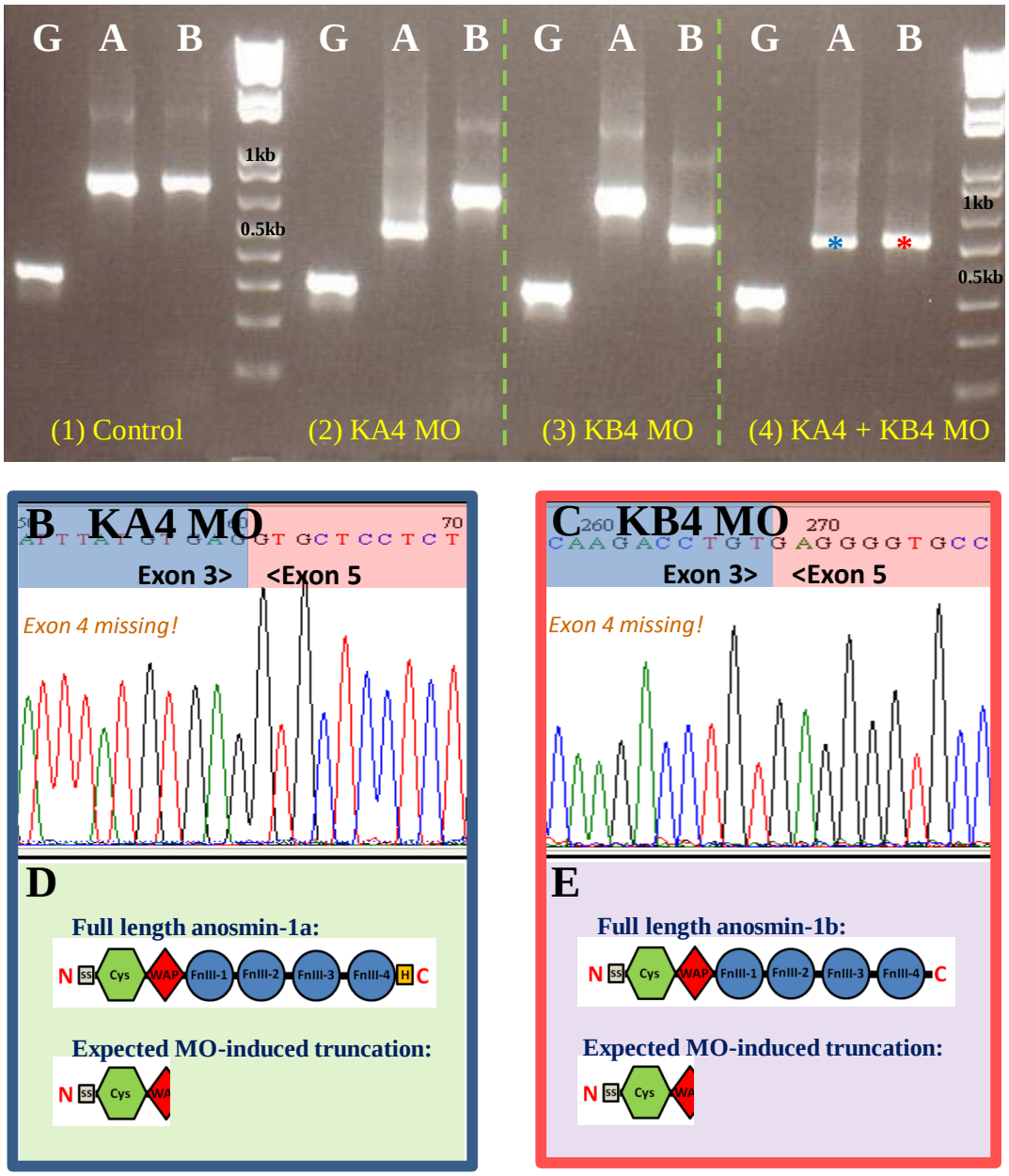

Figure 5.10 Confirming knockdown of Kal1a and Kal1b by exon-4-targeted splice-blocking morpholinos

A: An agarose gel depicting RT-PCR analysis of Kal1a and Kal1b transcript from morphant cDNA samples synthesised from the pooled RNA of twenty36hpf embryos. A GAPDH control PCR reaction ('G' lanes) and a PCR reaction encompassing exon4-6 for Kal1a ('A' lanes) or Kal1b ('B' lanes) is shown for control (1), KA4* morphant (2), KB4*morphant (3), or KA4+KB4 morphant cDNA samples. B and C show the raw sequencing data from the bands in A marked by blue and red asterisks, respectively: demonstrating that exon 4 is missing from Kal1a (B) and Kal1b (C) morphants. D and E illustrate the expected WAP-truncated Kal1a (D) and Kal1b (E) proteins that would result from loss of exon 4.
** Splice-blocking morpholinos targeted against exon 4 of Kal1a (KA4) and Kal1b (KB4) were used at concentrations of 1.0mM*

same cDNA sample gave the wild-type product size, thus demonstrating that *Kal1b* transcripts were unaffected by the KA4 sbMO. The converse was true for the KB4 cDNA sample, i.e. the predicted 549bp band was obtained for the *Kal1b* PCR lane (Figure 5.10A[3]). Finally, unsurprisingly, when KA4 and KB4 sbMOs were co-injected, both *Kal1a* and *Kal1b* PCR reactions gave the shorter 'morphant' PCR products (Figure 5.10A[4]).

The KA4 *(blue asterisk)* and KB4 *(red asterisk)* morphant PCR products in (Figure 5.10A[4]) were gel-extracted, cloned into TOPO, and sent off for DNA sequencing; and they were both found to lack the whole of exon 4, as predicted (Figure 5.10B,C). The loss of exon 4 from *Kal1a* and *Kal1b* transcripts means that exon 3 is spliced to exon 5, causing a frame-shift that introduces a stop codon in to the early part of exon 5. Post-translation, this means that the resulting anosmin-1a and anosmin-1b proteins will be WAP-domain truncated, thus lacking all succeeding C-terminal domains, including the remainder of the WAP domain and all four FnIII domains, as shown schematically in Figure 5.10D, E.

To get a better understanding of the knockdown efficiency of KA4 and KB4 in individual embryos, RT-PCR was carried out on eight single KA4 and KB4 morphants (Figure 5.11A, B). For KA4, there was virtually complete (~100%) knockdown of *Kal1a* for six embryos (lanes 1, 3-6, and 8), and ~75% knockdown (lanes 2 and 7) for the remaining two embryos (Figure 5.11A). For KB4, there was ~100% knockdown for 7 embryos (lanes 1-5, 7 and 8), and ~75% knockdown (lane 6) for the remaining one embryo (Figure 5.11B). Whilst this was a very small group of embryos, it can be estimated that in approximately three quarters of the KA4 or KB4 morphants there is ~100% knockdown, whilst the remainder will have ~75% knockdown, and that on average there is more than 90% knockdown of *Kal1a*/*Kal1b* gene function by these morpholinos (KA4 and KB4).

GnRH system phenotype

Two developmental stages were chosen for G3MC phenotype analysis in KA4/KB4 morphants: 36hpf and 60hpf. 36hpf was chosen because it represents the time when the number of (*'early wave'*) hypothalamic and terminal nerve GnRH3

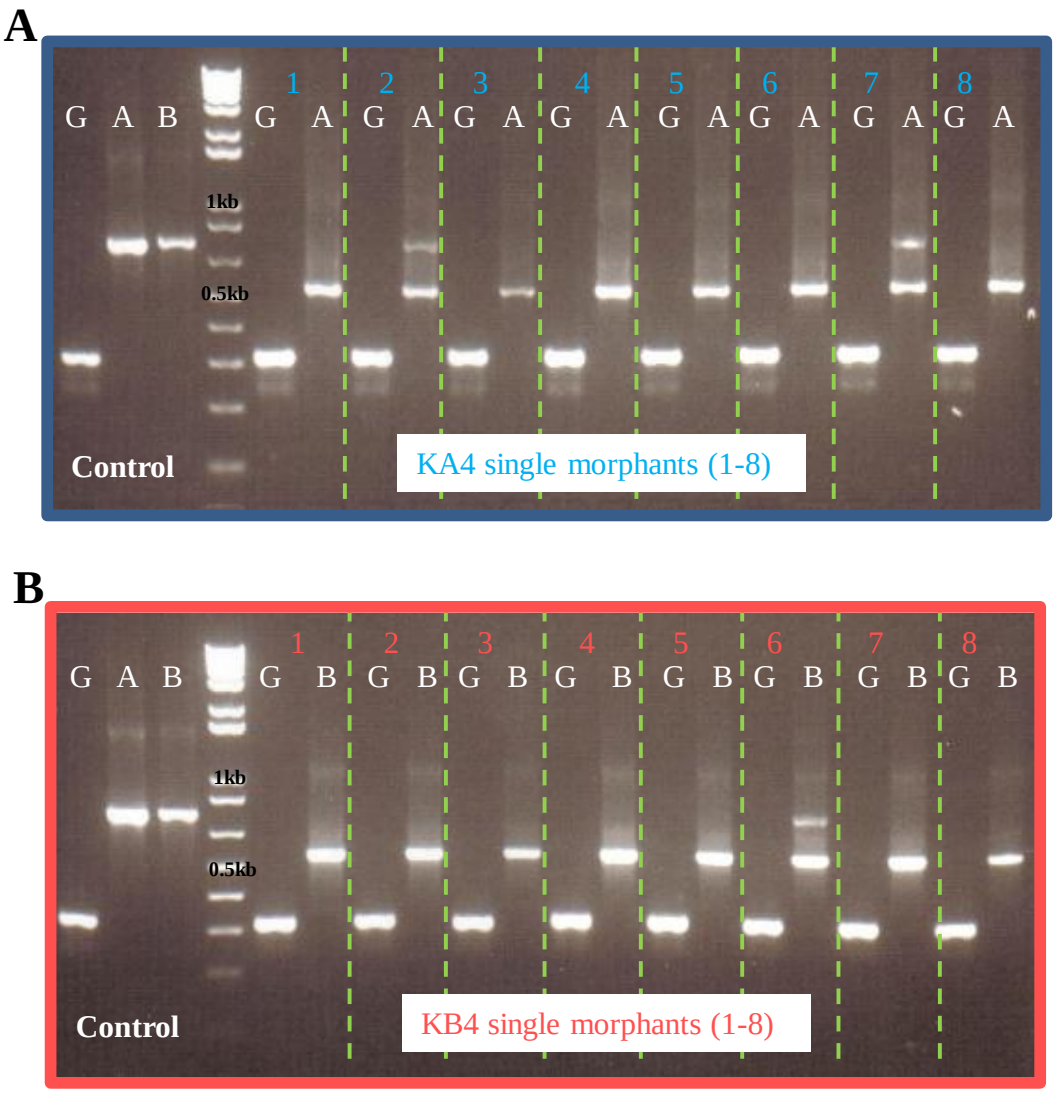

Figure 5.11 Demonstrating the efficiency of KA4 or KB4 morpholinos in individual morphant embryos

Agarose gels depicting the RT-CR analysis of knockdown levels for eight individual KA4 (A) or KB4 (B) morphants at 36hpf. The 'control' cDNA is to the left of the DNA ladder (with 0.5 and 1.0kb bands labelled) and individual morphant cDNA (labelled '1' through to '8') is to the right of the ladder. 'G' indicates GAPDH (control) PCR reactions; 'A' and 'B' indicate the Kal1a and Kal1b PCR reactions, respectively.

(G3MC) cells has stabilised and is maximal in number, for most embryos of the same stage. However, there are two caveats for using 36hpf G3MC embryos. Firstly, there are some cells which transiently appear in the region of the anterior commissure at 36hpf, often obstructing/interfering with the detection of the mCherry-positive projections here; and secondly, there are extra mCherry-positive cells that begin to appear in the olfactory epithelia, which can sometimes make it confusing to distinguish the terminal nerve G3MC cells in this region. 60hpf was the other stage which was chosen because it may allow late-emerging (*'early wave'*) hypothalamic GnRH cells to finally show their presence at the hypothalamus; which may be a possible morpholino-induced defect.

G3MC defects were present in embryos injected with both KA4 and KB4 together (both at 1mM; Figure 5.12 & Figure 5.13); whereas embryos injected with either KA4 (1mM) or KB4 (1mM) alone were apparently normal *(*data not shown*)*. The number of hypothalamic G3MC cells (referred to as the *'early wave'* in chapter 3), and their position in the forebrain, was really quite variable amongst the KA4+KB4 double morphants at 36hpf (Figure 5.12B-E), compared to the control (Figure 5.12A). Sometimes the actual number of hypothalamic G3MC cells fell within the normal range (*as discussed in chapter 3*), but their spatial arrangement was quite disorganised (n=25/29, 3 experiments, Figure 5.12B). Whilst in other morphants, the hypothalamic G3MC cells were much fewer in number i.e. $\leq$50% of the number found in the control embryos of the same stage (n=29/70, 3 experiments, Figure 5.12C), or even completely absent/undetectable at 36hpf (n=16/70, 3 experiments, Figure 5.12D, E). The majority of the coMO-injected (control) embryos had a cluster of hypothalamic G3MC cells that fell within the previously stated normal range (n=40/42, 3 experiments, Figure 5.12A).

There was also an apparent disruption in the organisation of the terminal nerve G3MC cells for some of these KA4+KB4 morphants (Figure 5.12B-E), but this was difficult to quantify due to the appearance of other G3MC cells in the olfactory compartment around this stage. Indeed, the disruption of these terminal nerve cells is likely to be due to the disruption of the adjacent olfactory epithelium in these morphants (*see below*).

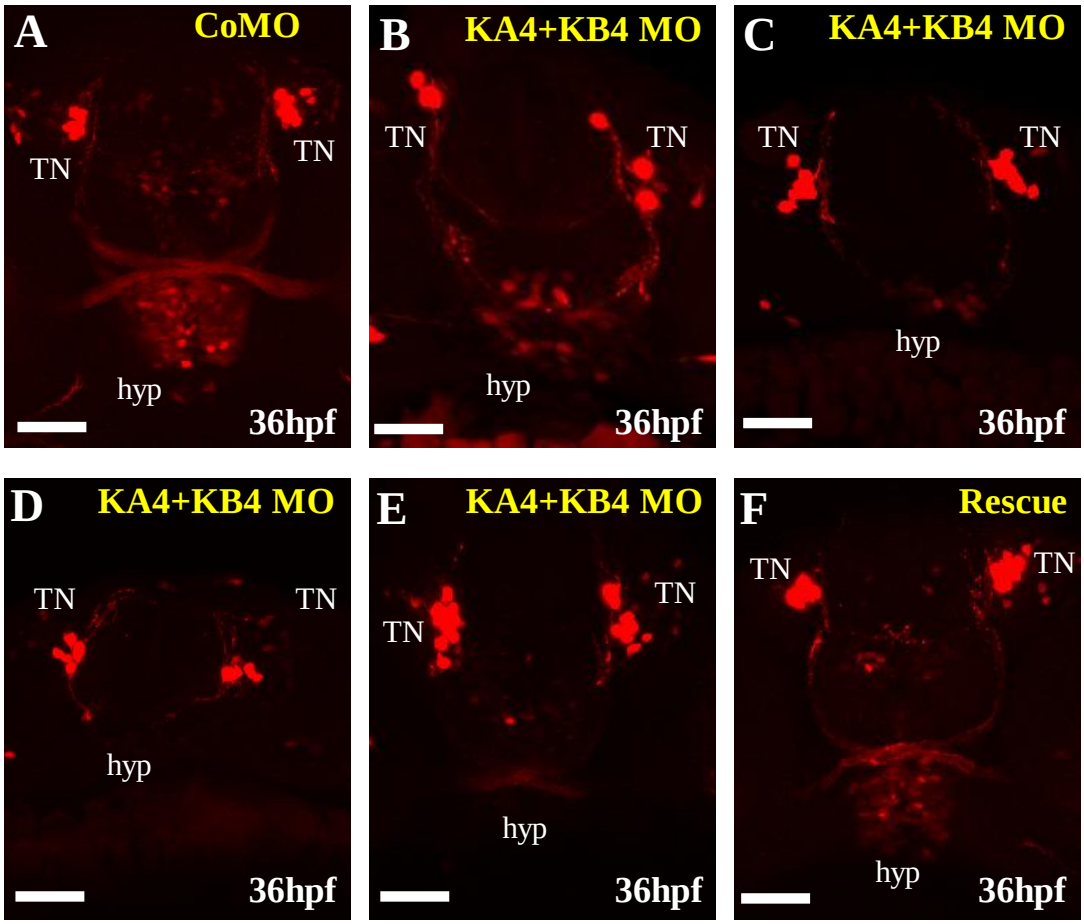

Figure 5.12 GnRH (G3MC) phenotype for KA4+KB4 morphants at 36hpf

A-F show confocal images (ventral views) of the G3MC phenotype at 36hpf for the control (A); 'KA4+KB4' morphants (B-E); and 'rescue*' embryos. B-E illustrates variability in the morphant phenotype. There was no apparent G3MC mutant phenotype when KA4 or KB4 morpholinos were injected alone (*data not shown*). Scale bars are 50μm

**Henceforth 'rescue' means KA4+KB4 MOs co-injected with Kal1a+Kal1b RNA*

TN= terminal nerve; hyp= hypothalamus

Most of the G3MC phenotypic abnormalities at 36hpf could be 'rescued' by co-injecting the *Kal1a* and *Kal1b* mRNA together with the KA4 and KB4 sbMOs (n=17/24, 1 experiment, Figure 5.12F). That is, the majority of the rescued embryos had 'normal'-appearing hypothalamic and terminal nerve G3MC clusters (which fell within the aforementioned normal range in turns of cell number); and it may therefore be concluded that the GnRH3 neuronal defects reported above were specific for the knockdown of *Kal1a* and *Kal1b* by the KA4 and KB4 sbMOs *(see discussion).* However, some embryos had 50% or fewer hypothalamic GnRH neurons (n=7/24,, 1 experiment, data not shown), demonstrating that the rescue was not complete.

KA4+KB4 morphants continued to exhibit a variable G3MC phenotype at 60hpf, as demonstrated using anti-mCherry immuno-labelled embryos in Figure 5.13B-D. Control (coMO) embryos had the expected tightly-clustered terminal nerve G3MC cells with associated forebrain commissural projections, as well as hypothalamic and retinal G3MC cells (n=44/45, 2 experiments, Figure 5.12A). Of the KA4+KB4 morphants, most had fewer mCherry-positive projections across the anterior commissure compared to the control (n=39/48, 2 experiments, Figure 5.13B-D) and some had disrupted terminal nerve G3MC cells (n=23/48, 2 experiments, Figure 5.13D). However, the hypothalamic G3MC cell clusters seemed to be largely present and intact by 60hpf, with most embryos having similar (n=29/48, 2 experiments, Figure 5.13D) or moderately reduced i.e. 50-75% (n=19/48, 2 experiments, Figure 5.13B, C) the number hypothalamic GnRH cells compared to the controls.

Olfactory and vomeronasal axonal phenotype

Olfactory (pOMP:tauEGFP) phenotype

At 36hpf, the pOMP:tauEGFP wild-type phenotype comprises a tightly-fasciculated olfactory bundle which projects towards the anterior telencephalon and defasciculates in the presumptive olfactory bulb region. This is the phenotype that was seen in the coMO-injected embryos (n=56/56, 3 experiments, Figure 5.14A).

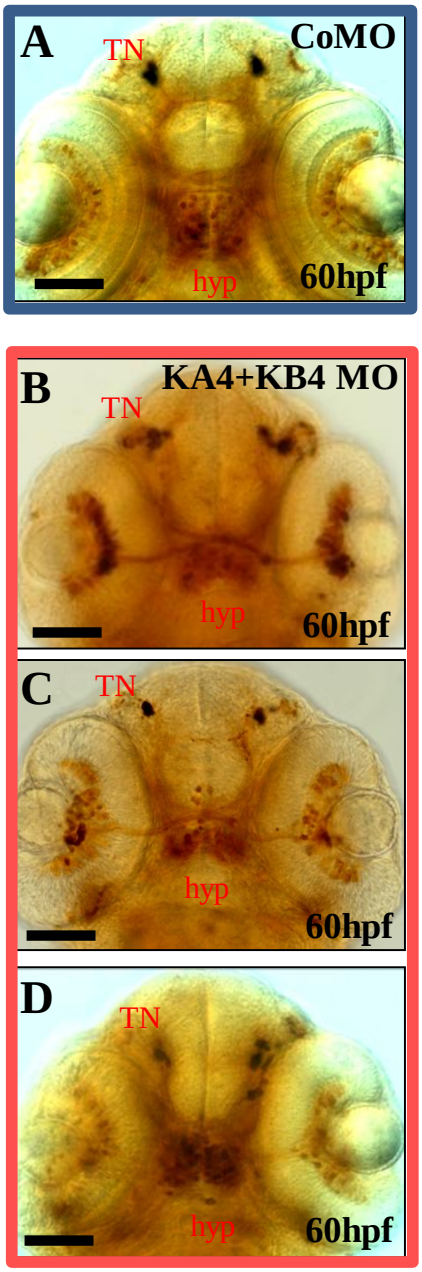

Figure 5.13 G3MC phenotype for KA4+KB4 morphants at 60hpf

G3MC embryos immuno-labelled with anti-mCherry (with DAB) at 60hpf are shown for control (A) and KA4+KB4 morphants (B-D). B-D illustrates variability in the G3MC morphant phenotype at 60hpf.
Scale bars are 100µm.
TN= terminal nerve; hyp= hypothalamus

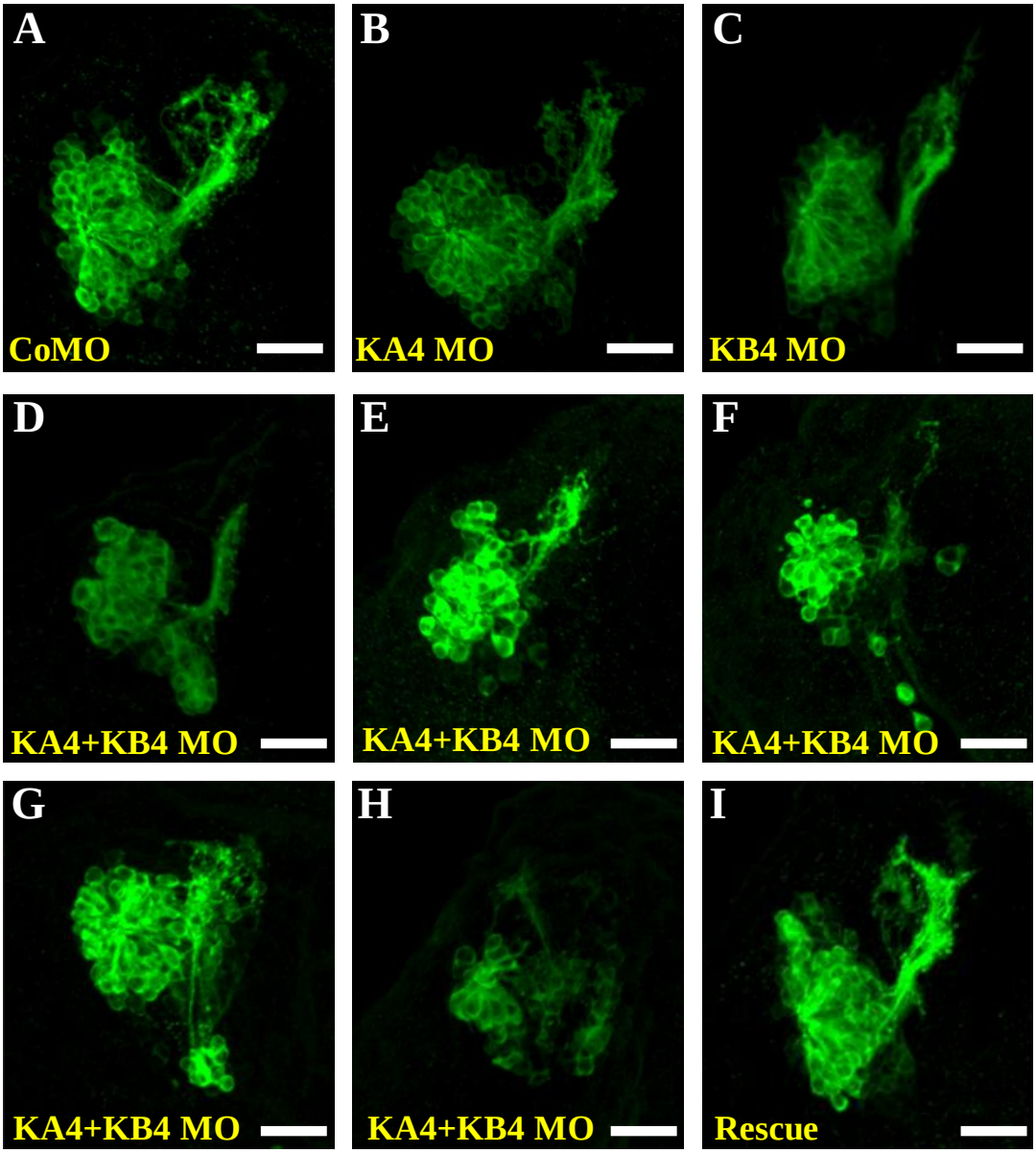

Figure 5.14 Olfactory (OMPG) phenotype for KA4 and KB4 morphants at 36hpf

A-I show OMPG confocal images of single olfactory pits at 36hpf for the control (A); KA4 morphant (B); KB4 morphant (C); 'KA4+KB4' morphant (D-H); and 'rescue' (I) embryos. D-H illustrates variability in the KA4+KB4 morphant phenotype. Scale bars are 25μm.

Most of the KA4 and KB4 single morphants had a similar wild-type-like phenotype, except several KA4 morphants which had a slightly defasciculated olfactory nerve bundle (n=8/52, 3 experiments, Figure 5.14B), and several KB4 morphants which showed a failure in defasciculation at the presumptive olfactory bulb region (n=17/58, 3 experiments, Figure 5.14C), but this may represent a delay in terminal axonogenesis, because, by 60hpf, the defasciculation pattern at the telencephalon appeared quite normal i.e. similar to the control embryo (data not shown). Similarly, the KA4 morphants had an apparently normal phenotype by 60hpf, when taking into account the natural variance in olfactory axonal phenotype (data not shown), suggesting that the defect in the pioneer olfactory axonogenesis at 36hpf was rectified by the later, secondary, round of olfactory axonogenesis by 60hpf.

Whilst there was some variability in the KA4+KB4 double morphant phenotype (Figure 5.14D-H), it was, in general, a more severe olfactory phenotype than any of the KA4 or KB4 single morphants. The actual morphology of the olfactory pit was more disorganised compared with the coMO embryos, where the olfactory pit had a much rounder 'rosette' appearance. Sometimes, in fact, it would appear that some of the olfactory epithelial cells were 'displaced' away from the normal perimeter of the olfactory pit (n=19/92, 3 experiments, Figure 5.14F, G); a phenotype that was never seen in any of the control embryos. Whilst most of the time the olfactory axons did project in, at least a 'rudimentary', fasciculated olfactory bundle towards the presumptive olfactory bulb region, despite an often premature defasciculation and/or failure to fasciculate properly at all (n=47/92, 3 experiments, Figure 5.14D-F); in some embryos, this bundle of axons appeared to be completely missing at 36hpf (n=33/92, 3 experimentsFigure 5.14G, H). Also, in the majority of embryos which did have axons projecting to the olfactory bulb, there was an apparent failure of proper defasciculation of the olfactory axons at the presumptive olfactory bulb region i.e. abnormal terminal targeting of the olfactory axons (n=76/92, 3 experiments, Figure 5.14D-H); which is always seen in the control embryos (n=56/56, 3 experiments, Figure 5.14A).

For the majority of the 'rescue' (, KA4+KB4 & *Kal1a/Kal1b* RNA co-injected) embryos (n=37/44, 2 experiments, Figure 5.14I), the olfactory pits were largely intact, though not completely 'roundish' ('rosette-shaped') in morphology.

Moreover, there were no displaced epithelial cells apparent; and, an apparently 'normal' fasciculated bundle of axons projecting towards the olfactory bulbs was present (n=42/44, 2 experiments, Figure 5.14I). However, the defasciculation of olfactory axons in the presumptive olfactory bulb region was perhaps not completely 'wild-type' in character in some embryos (n=23/44, 2 experiments, Figure 5.14I); and therefore not completely rescued. Overall though, it can be concluded that the rescue was largely successful, and that the olfactory defects present in the KA4+KB4 morphants were mostly specific consequences of knocking down *Kal1a* and *Kal1b* by KA4 and KB4 *(see discussion)*.

Amongst the KA4+KB4 double morphants, there was an apparent reduction in olfactory pit size at 36hpf. To quantify this reduction in olfactory pit size in these morphants, both olfactory pits from 18 embryos (i.e. 36 olfactory pits in total) from each morphant group were measured digitally from a confocal stack, in the anterior-posterior (A-P) direction; the same method that was used to assess olfactory pit size in the *Fgf8a* morphants in chapter 4. The average A-P length (in brackets) of the four morphant groups are as follows: coMO (76.9μm $\pm$4.53); KA4 (76.7μm $\pm$4.86); *KB4* (72.9μm $\pm$7.72); KA4+KB4 (58.2μm $\pm$13.11); and rescue embryos (73.4μm $\pm$6.12).

For the KA4+KB4 morphants, some of these olfactory defects had persisted until 60hpf (Figure 5.16C, E); but, for the KA4 or KB4 single morphants, the phenotype was apparently normal *(*data not shown*)*, compared to the control embryos, which had 'rosette'-shaped olfactory pits and normal-appearing olfactory axonal projections (n=35/35, 2 experiments, Figure 5.16A). For some of the KA4+KB4 double morphants, the olfactory pits were largely intact, but with some 'displaced' cells, and, for most of these embryos, it was apparent that many olfactory axons had projected towards, and defasciculated at, the olfactory bulbs (n=17/41, 2 experiments, Figure 5.16C; *see asterisks*). For other KA4+KB4 morphants, the olfactory pits were even more disrupted, and were barely recognisable as olfactory pits (n=7/41, 2 experiments, Figure 5.16E), whilst the remaining KA4+KB4 morphants embryos had apparently normal olfactory pits (n=17/41, 2 experiments, data not shown). The majority of the rescued embryos (n=13/18, 1 experiment, Figure 5.16G) did have more 'spherical' olfactory pits, with

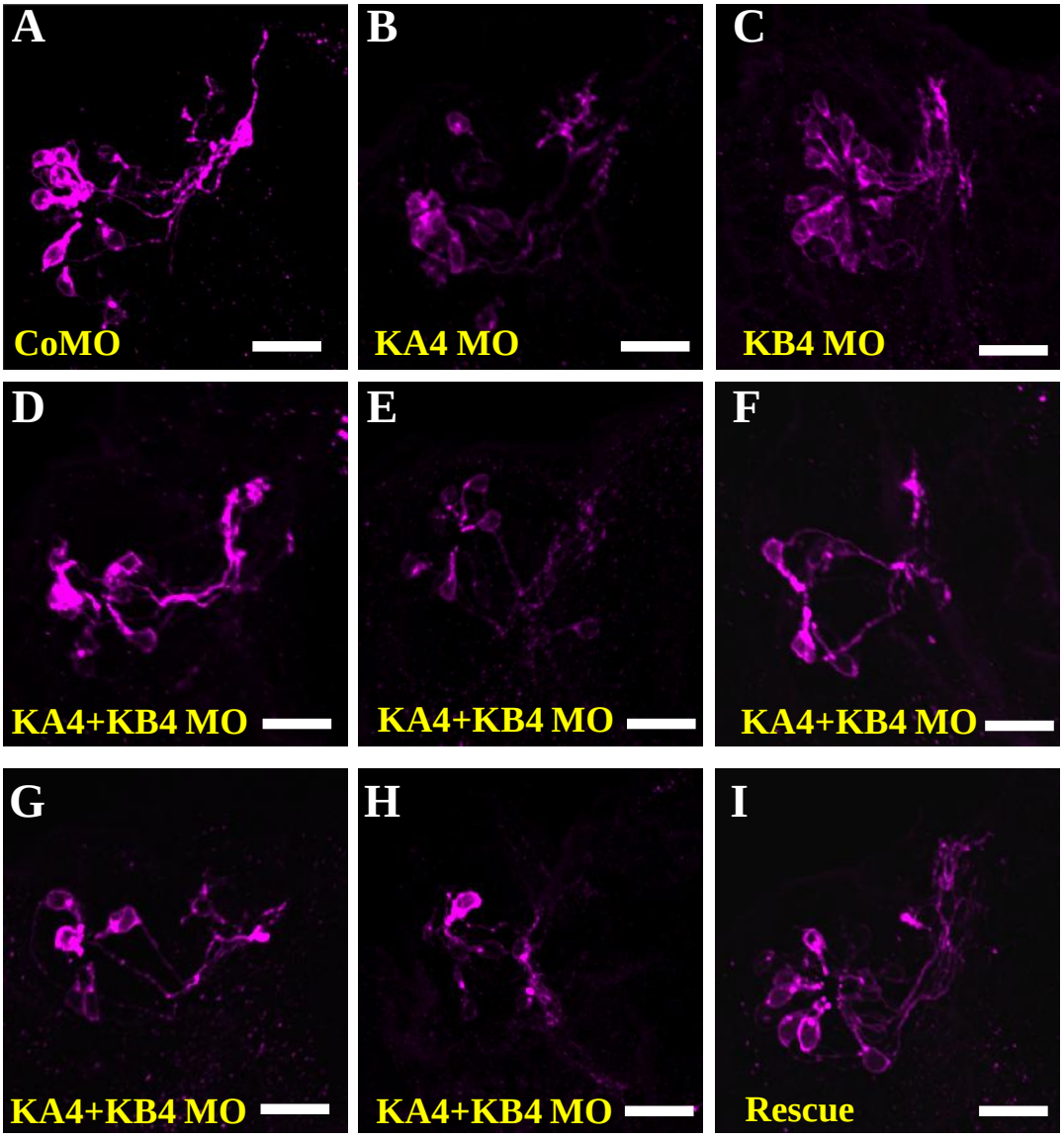

Figure 5.15 Vomeronasal phenotype for KA4 and KB4 morphants at 36hpf

A-I show TRPC2:Venus confocal images of single olfactory pits at 36hpf for the control (A); KA4 morphant (B); KB4 morphant (C); 'KA4+KB4' morphant (D-H); and 'rescue' (I) embryos. D-H illustrates variability in the KA4+KB4 morphant phenotype. Scale bars are 25μm.

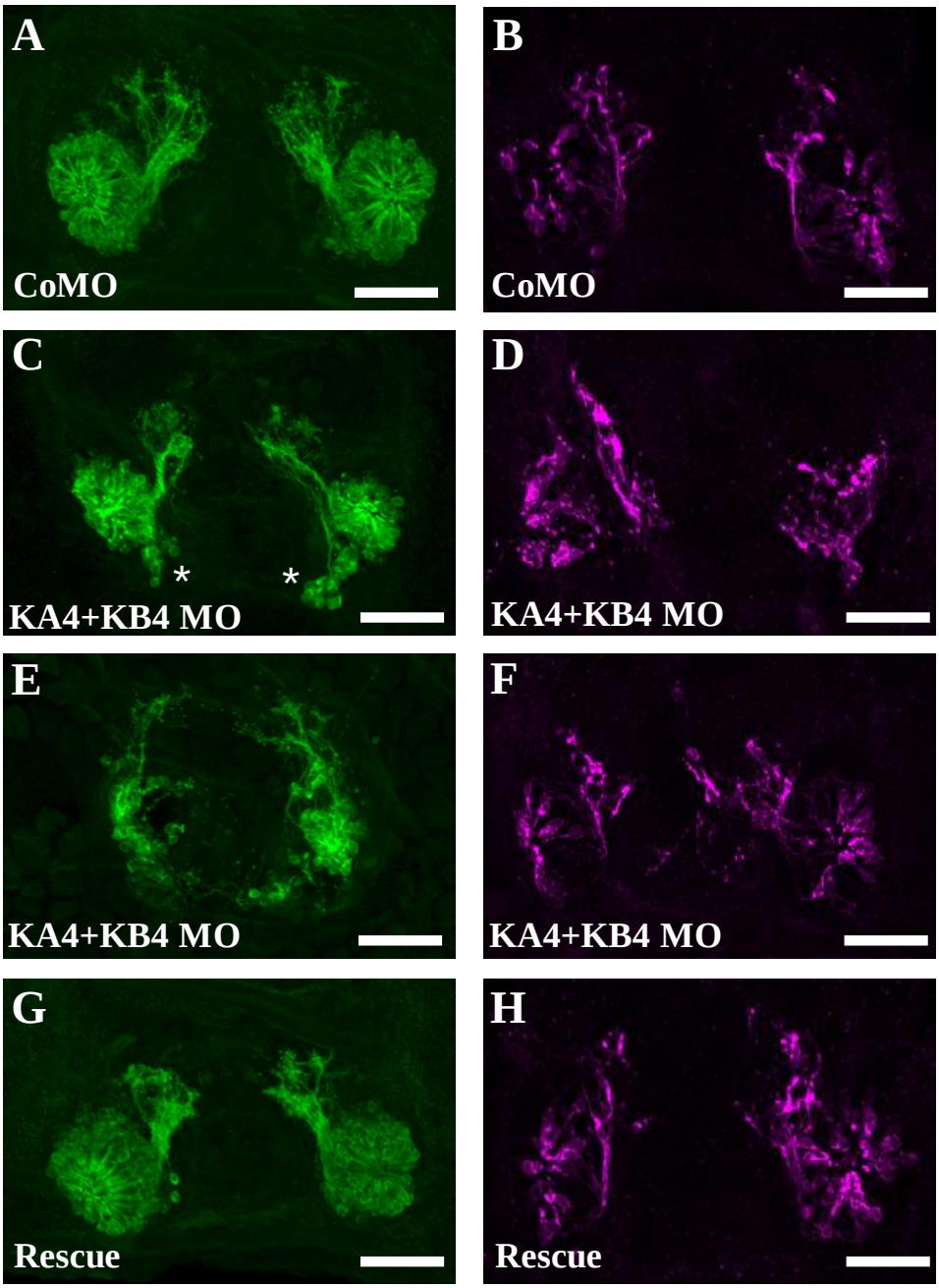

Figure 5.16 Olfactory and vomeronasal phenotype for KA4 and KB4 morphants at 60hpf

OMPG (A, C, E, G) and TRPC2:Venus (B, D, F, H) is shown for control (A, B); KA4+KB4 morphant (C-F) ; and Rescue (G, H) embryos at 60hpf . C-F illustrates variability in the KA4+KB4 morphant phenotype.
Scale bars are 50mm.

an apparently 'normal' olfactory axonal bundle extending to the olfactory bulbs; whilst a few embryos did show some evidence of 'displaced' olfactory epithelial cells (n=5/18, 1 experiment, data not shown).

Vomeronasal (pTRPC2:Venus) axonal phenotype

Whilst taking into account the high levels of natural variance in the wild-type pTRPC2:Venus phenotype, a representative control (coMO) phenotype is shown in Figure 5.15A. Both the KA4 (n=40/40, 2 experiments, Figure 5.15B) and KB4 (n=37/37, 2 experiments, Figure 5.15C) single morphants fell within the same range of wild-type variance, so therefore did not appear to have defective vomeronasal axonal phenotypes. It was also difficult to ascertain whether or not the KA4+KB4 double morphants had any defective vomeronasal axonal morphologies (Figure 5.15D-H). In most cases, there was evidence of vomeronasal axonal projections to the presumptive olfactory bulb region (n=37/45, 2 experiments, Figure 5.15D-G); although it was difficult to assess whether these axonal projections were normal, due to the inherent variability in early vomeronasal axonogenesis in the zebrafish, even in wild-types at 36hpf. However, a proportion of the KA4+KB4 embryos did have vomeronasal axons that were deficient (n=14/45, 2 experiments, Figure 5.15E, F, H), or appeared more disordered i.e. putatively mis-projecting (n=18/45, 2 experiments, Figure 5.15D, G) compared with the controls. The majority of the rescue embryos had vomeronasal axons which projected normally, taking into consideration the variance in wild-type variation in vomeronasal phenotype (n=15/17, 1 experiment, Figure 5.15I).

To find out if there were any defects at the level of actual vomeronasal (Venus-positive) *cell number*, a cell count was carried out. Control (coMO) embryos had an average of 13.3 vomeronasal cells, for KA4 morphants this was 12.8, for KB4 morphants this was 14.2, for KA4+KB4 morphants this was 6.8, and for the rescue embryos this was 11.6 (averages were based on cell counts from 10 embryos i.e. 20 olfactory pits from each morphant group). So, in summary, the KA4+KB4 morphants had 49% fewer vomeronasal cells than the control embryos, whilst the

KA4 single morphants had only 3.8% fewer cells, and the KB4 single morphants had 6.8% *more* cells.

By 60hpf, the KA4 and KB4 single morphants still had apparently normal vomeronasal morphologies *(*data not shown*)*, whereas vomeronasal axonal defects in some KA4+KB4 morphants had become more clearly apparent. Specifically, in some KA4+KB4 morphants, the vomeronasal axons were missing entirely on one (n=4/19, 1 experiment, Figure 5.16D; *right side*) or both (n=1/19, 1 experiment) sides. In other KA4+KB4 morphants, there were mis-projected vomeronasal axons across the midline (n=5/19, 1 experiment, Figure 5.16F). Whilst in the remaining embryos, the vomeronasal axons were apparently normal on both sides (n=9/19, 1 experiment) i.e. comparable to the control phenotype (n=16/19, 1 experiment, Figure 5.16B). For the rescue embryos, the vomeronasal axons were apparently projecting to the olfactory bulbs normally on both sides for most embryos (n=9/15, 1 experiment, Figure 5.16); whilst, in the remainder, some embryos had mis-projected vomeronasal axons (n=6/15, 1 experiment), suggesting that the 'rescue' was not complete.

Forebrain commissure phenotype

Anti-acetylated tubulin immuno-labelling was used to visualise both forebrain commissures (AC and POC) in the KA4 and KB4 morphants (Figure 5.17). At 36hpf, in the KA4 morphants, there was a subtle deficiency in the number of axons crossing over at the AC (n=33/54, 3 experiments, Figure 5.17B). Whilst, in the KB4 morphants, there was a more significant reduction in the number of axons crossing the midline (at the AC) at this stage (n= 37/59, 3 experiments, Figure 5.17C). For the KA4+KB4 morphants, this anterior commissure formation defect became even more apparent, as the commissure either failed to form altogether (n= 31/72, 3 experiments, Figure 5.17D), or the AC commissural axons were mis-projected across other midline regions, including towards the POC (n= 37/72, 3 experiments, Figure 5.17D). The POC was present and normal for the KA4 single morphants (n=54/54, 3 experiments, Figure 5.17B), but was slightly defasciculated in some KB4 morphants (n=6/59, 3 experiments, Figure 5.17C) and more severely

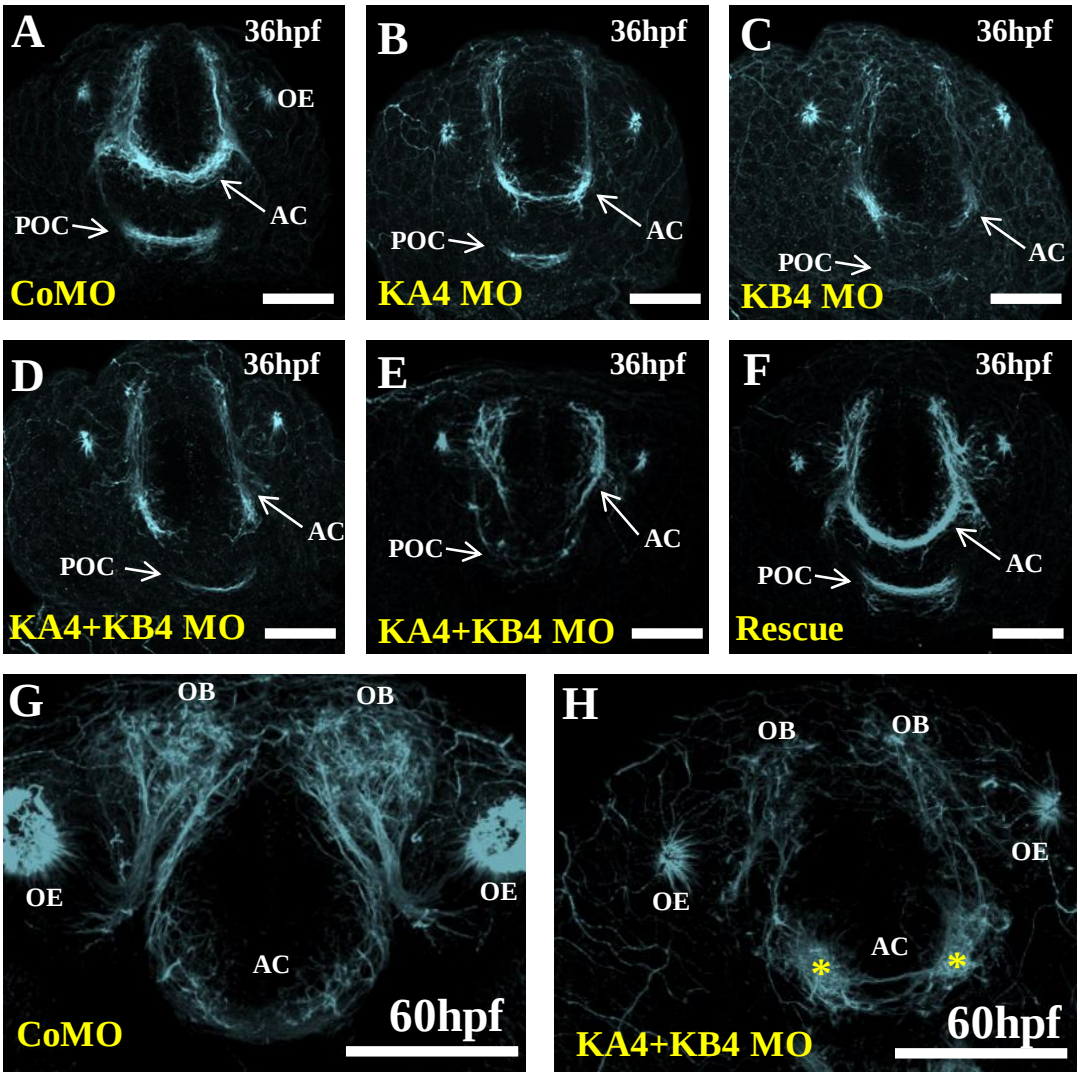

Figure 5.17 Forebrain commissural phenotype for KA4 and KB4 morphants at 36hpf and 60hpf

Confocal images of anti-acetylated tubulin immuno-labelling is shown for control (A, G); KA4 morphant (B); KB4 morphant (C); KA4+KB4 morphant (C-E, H) ; and Rescue (F) embryos at 36hpf (A-F) and 60hpf (G and H). D and E illustrates variability in the KA4+KB4 morphant phenotype. Scale bars are 100µm.

OE= olfactory epithelium; OB= olfactory bulb; AC= anterior commissure; POC= post-optic commissure.

defasciculated in some KA4+KB4 morphants (n=11/72, 3 experiments, Figure 5.17E). Both commissures (AC and POC) were present and normal (tightly fasciculated) in most of the 'rescue' embryos (n=29/35, 2 experiments, Figure 5.17E), apart from a few which had slightly fewer axons crossing at the AC (n=6/35, 2 experiments; data not shown).

By 60hpf, a very significant number of axons have crossed the midline across the AC in the coMO-injected embryos (n=42/42, 2 experiments, Figure 5.17G), but not all of these axons will be labelled by acetylated tubulin antibody, as this antibody will only label *newly-formed* axons. Most of the KA4+KB4 double morphants had a few axons crossing over at the midline at the AC by 60hpf, but these axons were much fewer in number compared to the controls (n=33/45, 2 experiments, Figure 5.17H). In fact, a 'tangle' of probable '*arrested'* axons can be seen gathered at either side of the midline, where the AC should have formed (*see asterisks in Figure 5.17H*).

From Figure 5.17H, it is also apparent that there are much fewer glomeruli (olfactory axonal condensations) within the presumptive olfactory bulbs of the KA4+KB4 morphants (n=29/45, 2 experiments, compared with the control embryos (n=42/42, 2 experiments, Figure 5.17G); further supporting the olfactory/ vomeronasal axon defects reported above in the KA4+KB4 morphants.

5.2.5 Exon-6-targetted splicing-blockers: confirming the specificity of the phenotypes caused by loss of exon 4

In order to confirm the morphant phenotypes described above for KA4 and KB4 sbMOs, a second pair of sbMOs were also used. These sbMOs were designed to target the loss of exon 6 from *Kal1a* and *Kal1b* mRNA, and are therefore named 'KA6' and 'KB6', respectively.

High knock-down efficiency confirmed by RT-PCR

Initially, to confirm that these new morpholinos could knockdown *Kal1a* and *Kal1b* just as efficiently as the KA4 and KB4 sbMOs, RT-PCR analysis was carried out (Figure 5.18), as described above in the previous section.

From KA6 morphant cDNA samples, a lower (620bp) 'morphant' band was obtained (blue asterisk, Figure 5.18A); which, after DNA sequencing, was shown to completely lack exon 6 (Figure 5.18B), as predicted. This causes a frame-shift in the mRNA and introduces an early stop codon, resulting in a truncation of anosmin-1a within the first fibronection type III domain (shown schematically in Figure 5.18D).

A new set of primers were used for *Kal1b* PCR, as the primers used to confirm KB4 knockdown did not encompass exon 7 and would therefore not amplify the exon 6 region (or lack thereof). The new primer pair successfully amplified pat of *Kal1b* (an 858bp PCR product) as confirmed by DNA sequencing *(*data not shown*)*. However, there were also two other PCR products amplified by this new primer set (marked by green crosses in Figure 5.18A) which could not be identified by sequencing, so are most probably non-specific (i.e. not *Kal1b*), and, as such, have been disregarded from this analysis.

From KB6 morphant cDNA samples, a lower (728bp) 'morphant' band was obtained (*red asterisk*, Figure 5.18A); which, after DNA sequencing, was shown to completely lack exon 6 (Figure 5.18B), which, similar to KA6 above, resulted in a fibronectin-domain truncated anosmin-1b (shown schematically in Figure 5.18E). However, there were also two other lower bands for the *Kal1b* PCR of the KB6 morphant cDNA. The lower of the two was sequenced and shown to lack both exon 5 and 6 (resulting in the loss of the whole of the first fibronectin domain, data not shown); however, the other band could not be sequenced. Because the 'top' morphant band (marked by red asterisk) is the most prominent, it can be assumed that most of the anosmin-1b is fibronectin-domain-truncated, as shown in Figure 5.18E.

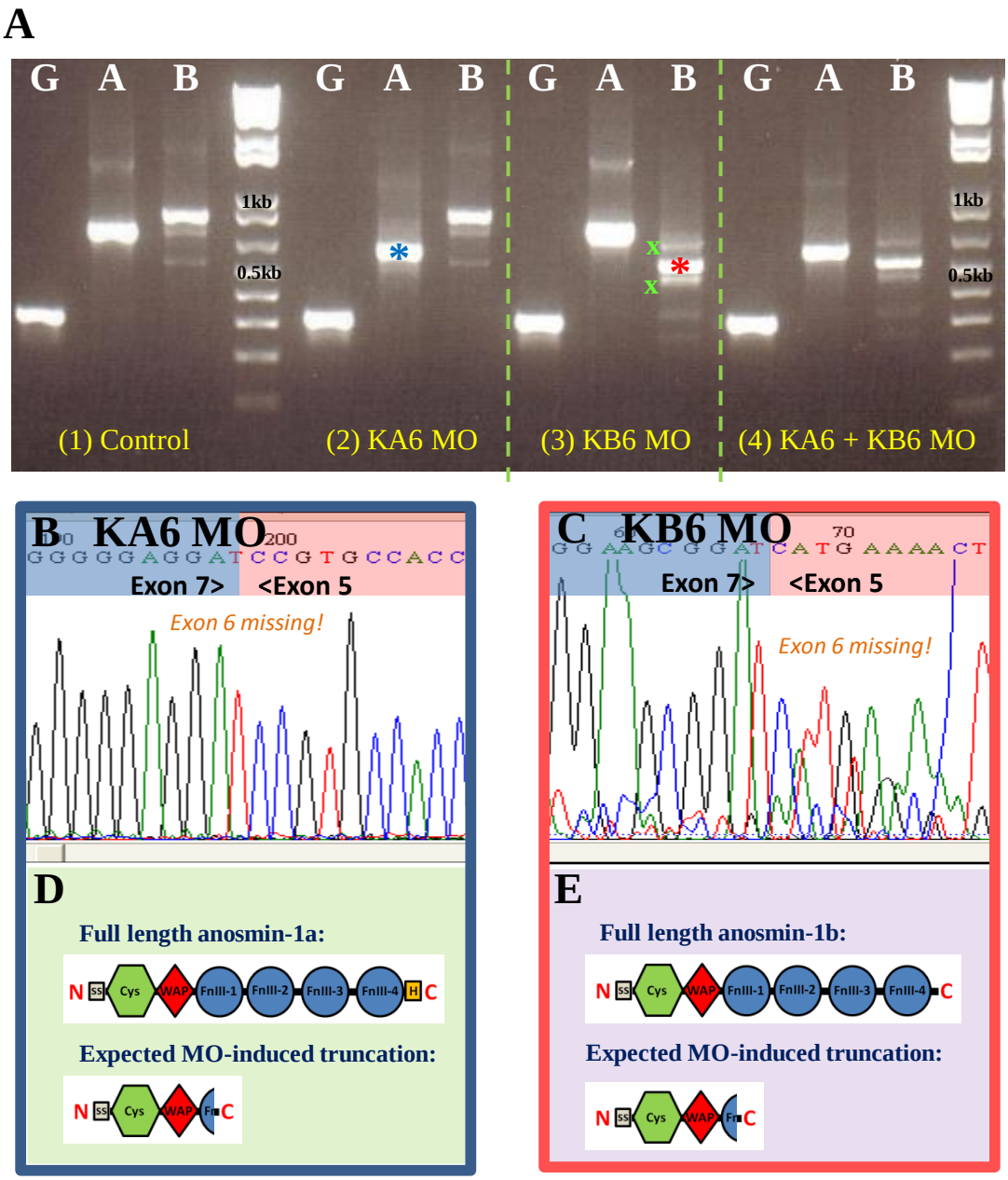

Figure 5.18 Confirming knockdown of Kal1a and Kal1b by a second set of splice-blocking morpholinos: targeted loss of exon 6

A: An agarose gel depicting RT-PCR analysis of Kal1a and Kal1b transcript from KA6 and KB6 morphant cDNA (as figure 5.08). A GAPDH control PCR reaction ('G' lanes) and a PCR reaction encompassing exon5-7 for Kal1a ('A' lanes) or Kal1b ('B' lanes) is shown for control (1), KA6* morphant (2), KB6*morphant (3), or KA6+KB6 morphant cDNA samples.
B and C show the raw sequencing data from the bands in A marked by blue and red asterisks, respectively: demonstrating that exon 6 is missing from Kal1a (B) and Kal1b (C) morphants. D and E illustrate the expected FnIII-1-truncated Kal1a (D) and Kal1b (E) proteins that result from loss of exon 6.
** Splice-blocking morpholinos targeted against exon 6 of Kal1a (KA6) and Kal1b (KB6) were used at concentrations of 2.0mM and 1.0mM, respectively.*

Confirmation of the olfactory, GnRH, and commissure phenotypes

Using KA6 and KB6 to knock down *Kal1a* and *Kal1b* resulted in defects in the formation of the anterior commissure (Figure 5.19A, B), in olfactory axonogenesis (Figure 5.19C, E), and in GnRH3 neuronal system development (Figure 5.19D, F), which were analogous to those defects caused by KA4 and KB4 described above. Further proof, therefore, that these defects are specific to the knocking down of *Kal1a* and *Kal1b* gene function *in vivo*.

Specifically, KA6+KB6 morphants had fewer axons crossing over at the AC, in association with mis-projected axons across other regions of the midline, including some axons projecting towards the POC (n=43/51, 2 experiments, Figure 5.19B-B''). KB6 single morphants also had a noticeable reduction in the number of axons crossing the AC (n=29/37, 2 experiments, data not shown), but KA6 single morphants had apparently normal forebrain commissural phenotypes (n=38/39, 2 experiments, data not shown). The KA6+KB6 double morphants also had a reduced number of olfactory axons projecting to the olfactory bulbs, and disrupted olfactory pits at 36hpf (n=17/22, 1 experiment, Figure 5.19E). Finally, the KA6+KB6 morphants also had reduced or absent GnRH3 neuronal projections across the anterior commissure, as well as fewer G3MC neuronal cell bodies localised to the hypothalamus by 42hpf (n=15/20, 1 experiment, Figure 5.19E), compared with the control embryos.

5.2.6 Testing the hypothesis that Kal1a and Kal1b act through the Fgf8a signalling pathway *in vivo*

Loss of either *Fgf8a* or *Kal1a+Kal1b* gene function during zebrafish embryogenesis is sufficient to cause defective anterior commissure formation. Therefore, it can be assumed that all three genes are required for proper anterior commissural development, but it is unclear whether or not these gene products interact in this process, or whether they have separate independent roles (and signalling pathways). So, the question arises, does Kal1a and Kal1b act through the Fgf8a signalling pathway during anterior commissure formation?

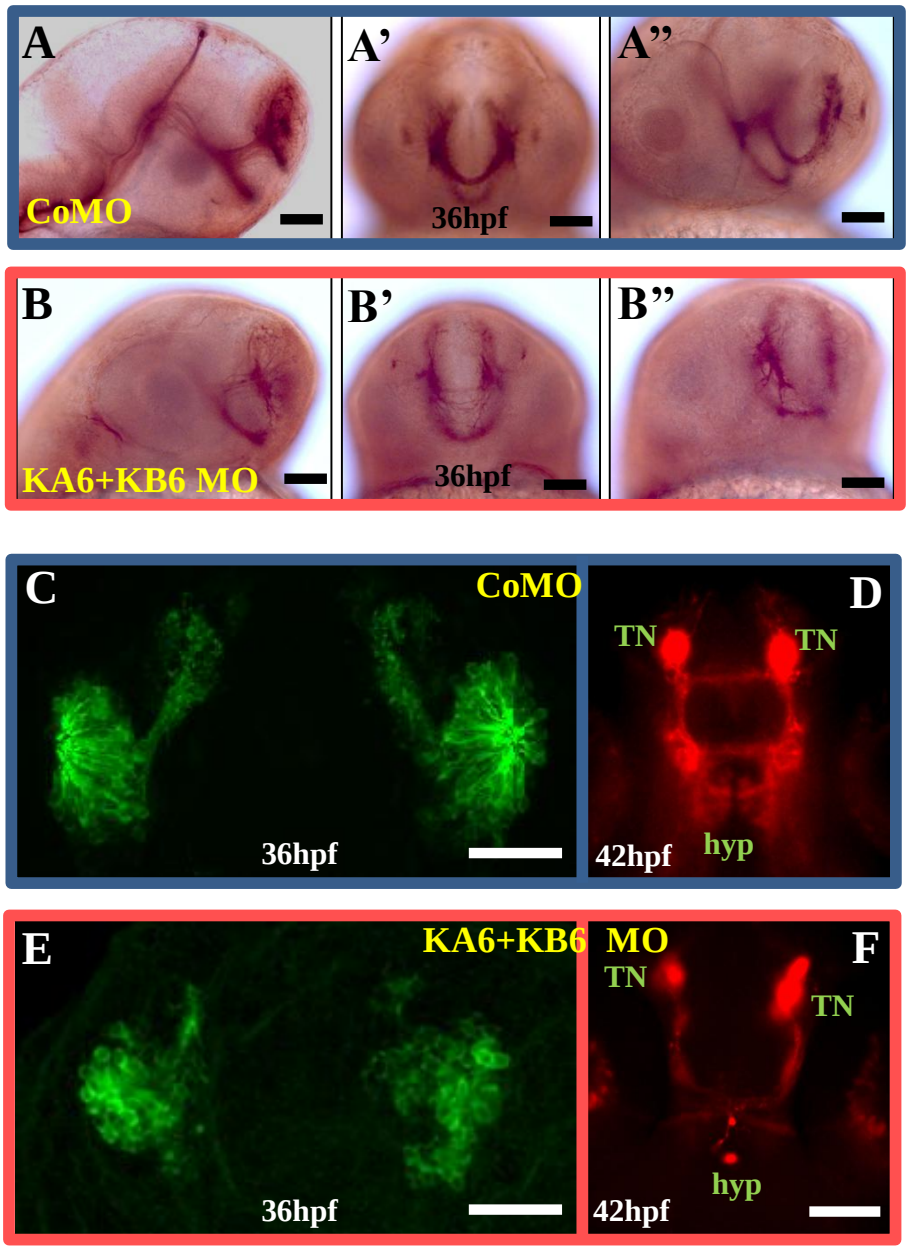

Figure 5.19 KA6 and KB6 replicate the phenotypic aspects of KA4 and KB4 knockdown

Anti acetylated tubulin immuno-staining with DAB at 36hpf (A, B), OMPG at 36hpf(C, E), and G3MC at 42hpf (D, F) is shown for control (A, C, E) and 'KA6+KB6' morphant (B, D, F) embryos. A and B are lateral views; A', B' C-F are ventral views; A'' and B'' are ventral-lateral views. C and E are confocal images. D and F were visualised on a standard light microscope, with fluorescence.

Scale bars are 50µm (C, E) 100µm (A, B, D, F).

TN= terminal nerve; hyp= hypothalamus.

To investigate this, KA4+KB4 and Fgf8a MOs were titrated down to concentrations that brought about no discernible forebrain commissural abnormalities. The functional concentration (i.e. the concentration that causes AC formation defects in ≥80% of embryos) for KA4+KB4 was earlier determined to be 1mM +1mM (n=39/43, 2 experiments, Figure 5.20B) and for Fgf8a MO was also found to be 1mM (n=38/46, 2 experiments, Figure 5.20C).

So, to titrate these morpholinos down to non-functional concentrations (i.e. the concentration that results in mild AC formation defects in less than 20% of embryos), KA4+KB4 or Fgf8a MO concentrations of 0.25mM, 0.5mM, and 0.75mM were tested, and AC formation was assessed in these putative partial morphants at 36hpf. For KA4+KB4 at 0.75mM, embryos still had reduced AC projections (n=12/21, 1 experiment, data not shown); but, at 0.5mM, most embryos had apparently normal AC projections (n=20/24, 1 experiment, Figure 5.20D); and at 0.25mM *all* embryos were apparently normal (n=18/18, 1 experiment, data not shown). Similarly, using Fgf8a MO at 0.75mM, many embryos still had AC defects (n=19/27, 1 experiment, data not shown), but this number was significantly reduced when using Fgf8a MO at 0.5mM, and most embryos showed normal AC formation (i.e. n=21/25, 1 experiment, Figure 5.20E). And, again at 0.25mM Fgf8a MO, all embryos had normal forebrain commissures (n=22/22, 1 experiment, data not shown).

When, KA4+KB4 and Fgf8a MOs were co-injected at 0.25mM concentrations, there were no obvious defects in forebrain commissure formation (n=31/33, 2 experiments, data not shown)*)*. However, when KA4+KB4 and Fgf8a MOs were co-injected at 0.5mM concentrations, many of the embryos had defects in AC formation (n=41/48, 2 experiments, and sometimes both AC and POC formation were defective (n=13/48, Figure 5.20F). This data would suggest that Kal1a and/or Kal1b are acting through the same signalling pathway as Fgf8a during forebrain commissure formation *(see discussion)*.

Finally, for completion, *Kal1a* and *Kal1b* were knocked down separately with *Fgf8a* (i.e. KA4+Fgf8a MO or KB4+Fgf8a MO; all at 0.5mM morpholino concentrations). Preliminary results showed that knocking down *Kal1a* and *Fgf8a*

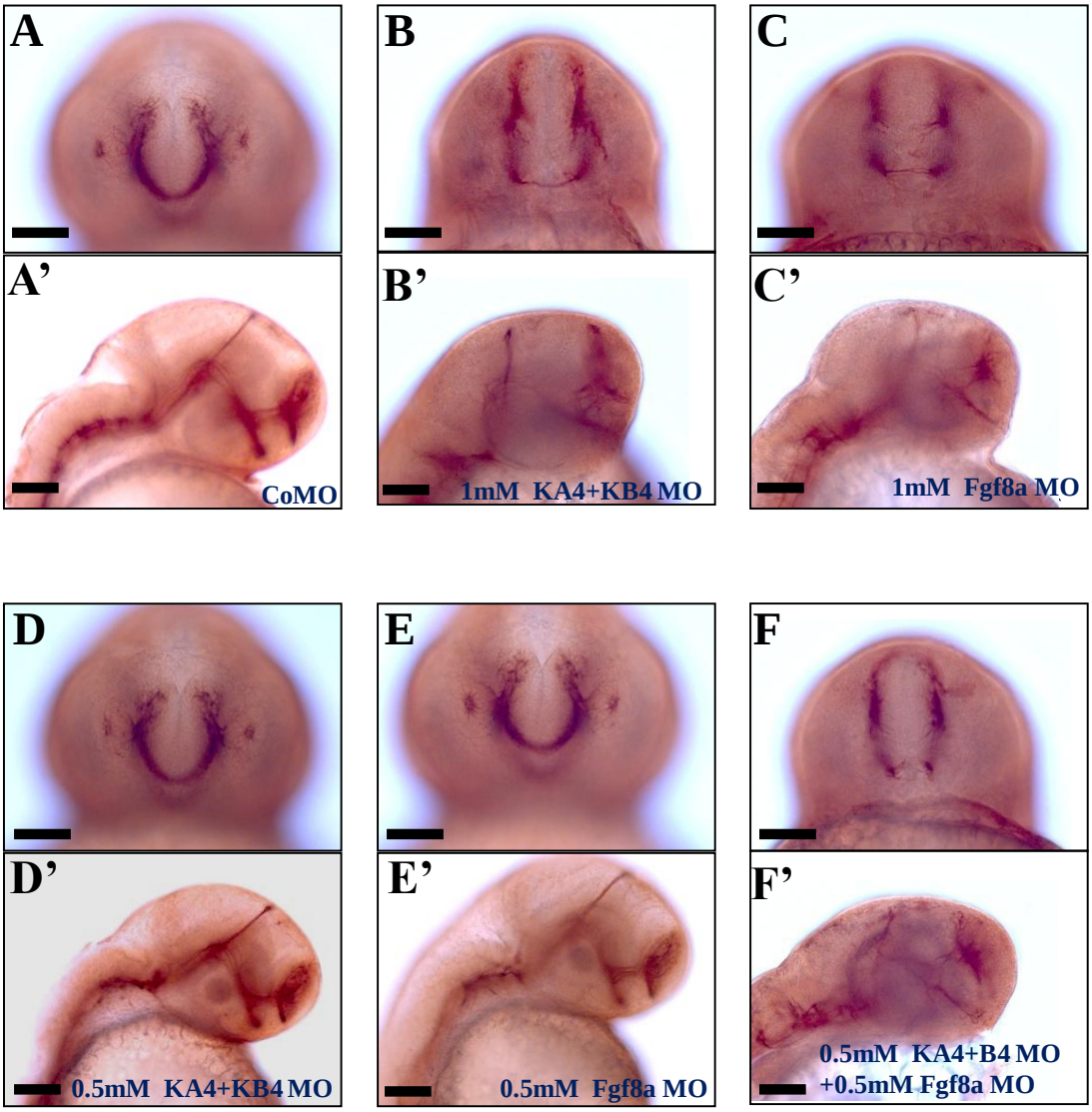

Figure 5.20 Testing the hypothesis that Kal1a/Kal1b act through the Fgf8a signalling pathway *in vivo*

Anti acetylated tubulin immuno-staining with DAB at 36hpf for control (A, A'), '1mM KA4+KB4' (B, B'), '1mM Fgf8a MO' (C, C'), '0.5mM KA4+KB4' (D, D'), '0.5mM Fgf8a MO' (E, E'), and '0.5mM KA4+KB4' + '0.5mM Fgf8a MO' (F, F'). Ventral views for A-F and lateral views for A'-F'. Scale bars are 100µm. *(See Fig5.21 for a summary of these results.)*

together had no noticeable effect on forebrain commissure formation (data not shown), whereas knocking down *Kal1b* with *Fgf8a* had a subtle effect on anterior commissure formation in a few embryos i.e. 3/18 embryos had slightly fewer crossings over at the midline. So, in conclusion, knocking down *Kal1a* and *Kal1b* together with *Fgf8a* (all at 0.5mM morpholino concentrations) was required for the more severe, fully penetrant, failure of AC (and POC) formation.

5.3 Discussion

5.3.1 Anosmin-1a and anosmin-1b are both expressed in the olfactory epithelium region during early embryogenesis

There is a noticeable disparity between the spatio-temporal expression patterns seen for the *Kal1a*/*Kal1b in situ* hybridisation analyses, compared with the anosmin-1a/ anosmin-1b immuno-labelling studies. At 24hpf through to 60hpf, *Kal1a* and *Kal1b* transcripts were detected widely across the midbrain/hindbrain regions, whilst only *Kal1b* was detected in the olfactory placodal region. In contrast, the expression of their protein products, anosmin-1a and anosmin-1b, were both restricted to the olfactory epithelium during these stages, with no other brain-specific expression detectable, except in the presumptive pituitary (*see section 5.3.2*). However, consistently, *Kal1a* and *Kal1b* transcript were both detected in the PLLP and otic vesicle, two regions where their protein products were also detected by immuno-labelling.

Previous *in situ* hybridisation analyses carried out by Ardouin *et al* showed that *Kal1a* transcript is detected in the olfactory pits by 37hpf (Ardouin et al., 2000), but in the current analysis, *Kal1a* transcript could not be detected in this region. In fact, it was *Kal1b* that was detected in the olfactory pit region, in this study, at around 24hpf; whereas, previously it had been shown to localise to the olfactory bulb region from around 48hpf. However, this previous study, and our current study, both showed significant staining throughout several midbrain and hindbrain regions during these stages, suggesting that *Kal1a*/*Kal1b in situ* expression is largely reproducible.

The anti-anosmin-1a and anti-anosmin-1b that were used in this study were two rabbit polyclonal antibodies raised against the N-terminal residues 151 to 197 of anosmin-1a (Genbank AF163310) and the N-terminal residues 51 to 102 of anosmin-1b (Genbank AF163311), respectively. Moreover, their specificity for either anosmin-1a or anosmin-1b only was previously confirmed by Western blot analysis (Yanicostas et al., 2008; Yanicostas et al., 2009). It can therefore be assumed that these antibodies are highly specific for their respective proteins, and

that the immuno-labelling analysis faithfully portrays the expression of anosmin-1a and anosmin-1b during development.

Whilst there are notable differences in our *in situ* analysis, in terms of which of the two *KAL1* orthologues are expressed in the olfactory epithelium (compared to a previous report), it is clear that the midbrain/hindbrain staining reported by both studies cannot be recapitulated by immuno-labelling analysis. This could simply be because the *Kal1a*/*Kal1b* transcript is not translated into protein in the midbrain/hindbrain; and that they are expressed in the olfactory epithelium region, at low levels or for short periods of time, such that they are not always detectable by *in situ* hybridisation analysis.

Significantly, both anosmin-1a and anosmin-1b are expressed in the pioneer olfactory axons as they first begin to establish the olfactory axonal pathway to the presumptive olfactory bulb region from around 24hpf. By 48hpf, they both continue to be expressed in the secondary ORN axons, which, by this stage, have replaced the earlier pioneer axons, suggesting that anosmin-1a and anosmin-1b may have a continued role in olfactory axonogenesis throughout early zebrafish development.

Interestingly, at 60hpf, *Kal1a* and *Kal1b* transcripts are clearly detected in the region of the anterior commissure and terminal nerve projections, and may be expressed in this region much earlier than this, but their expression in this region is obscured by broad midbrain/diencephalon labelling. In fact, in the immuno-labelling analysis, anosmin-1a and anosmin-1b can both clearly be seen expressed along the anterior commissure between 36hpf and 60hpf (Figure 5.03C-H), and even as early as 30hpf (data not shown). Whilst not proof that Kal1a and Kal1b were involved in the formation of the anterior commissure, this data suggested that they could have such a role, similar to two of the other KS gene orthologues, *Fgf8* and *Fgfr1*, which were discussed in the previous chapter.

The *in situ* analysis also showed expression of *Kal1b* in the region of the terminal nerve GnRH cells, medial to the olfactory pits, at 24hpf. It would need to be confirmed by double *in situ* hybridisation analysis with *GnRH3* probes that this expression was actually in the same GnRH cells in this region. However, analysis of a single confocal ‘z-layer’ through the olfactory pit region of anosmin-1a/-1b

immuno-labelled embryos reveals that both anosmin-1a and anosmin-1b are both expressed in a 'broad' olfactory pit region which also encompasses the terminal nerve GnRH3 cells (appendix, Figure A2). This suggests that anosmin-1a and anosmin-1b could also be involved in the development of the terminal nerve GnRH system; and subsequent hypothalamic GnRH neuronal migration that putatively depends on the correct development of the terminal nerve GnRH system and its associated axonal projections.

5.3.2 Anosmin-1b is highly expressed in the presumptive pituitary during early embryogenesis

Anosmin-1b was highly expressed in the presumptive pituitary between 36hpf and 60hf, whereas anosmin-1a was apparently absent from this region during these times points. However, because the 'background' (non-specific) labelling of the anti-anosmin-1a antibody was higher than anti-anosmin-1b, it may simply be the case that anosmin-1a was expressed in the pituitary too, but perhaps at a lower level, which was 'masked' by the high 'background' labelling. Further analysis would need to be carried to confirm that this structure labelled by anti-anosmin-1b was definitely the pituitary, perhaps by using a pituitary-specific marker, such as POMC (proopiomelanocortin) transgenic reporter line (Liu et al., 2003). However, its spatial localisation within that area of the brain, as well as its overall morphology, would certainly suggest that this is the pituitary.

Anti-anosmin-1b immuno-labelling was carried out on G3MC embryos, in order to visualise the *'early wave'* hypothalamic GnRH3 neurons in relation to the pituitary, at 48hpf. After confocal imaging was carried out on a representative embryo, 3D rendering image analysis was then performed. This demonstrated that the presumptive pituitary was located caudal to the hypothalamic GnRH3 (mCherry-positive) cells at 48hpf, and that the pituitary cells closely abutted these GnRH3 cells. No evidence of neurite interactions between the hypothalamic GnRH3 cells and the putative gonadotrophs was detectable; however, this is not surprising, given the close proximately of the two cell types, and the technical difficulties in visualising such an interaction. In fact, specific synapse markers would be required

to identify specific synapse formation in this region, in early embryos. Moreover, if such synapses were identified at this stage, or some later stage, it would then need to be confirmed that they were actually 'functional' (hypophysiotropic) interactions between GnRH-secreting cells and pituitary gonadotrophs, perhaps by upregulation of specific GnRH receptor genes in those target gonadotrophs, or GnRH secretion at the synaptic junction from the GnRH axon terminals.

However, it remains to be established what the role of anosmin-1b is in the pituitary at these stages, and how this may reflect upon the role of its related orthologues in the pituitary of other vertebrates, such as humans. Whilst a functional role for anosmin-1b cannot be assumed simply from its pituitary expression, it is tempting to speculate on some of the possibilities. For example, anosmin-1b may be required as a chemoattractant cue for GnRH3 cell migration to the hypothalamus in zebrafish, or perhaps as a cell survival or GnRH cell differentiation factor once they arrive at the hypothalamus. Or, anosmin-1b activity at the pituitary may be required for proper synapse formation between hypothalamic GnRH cells and the pituitary gonadotrophs; or perhaps may be required to keep such synapses functional. Moreover, because pituitary expression appears to be restricted to anosmin-1b only (not anosmin-1a), these putative roles would seem to be a sub-function of this particular orthologue only.

5.3.3 Translation-blocking morpholinos against *Kal1a* & *Kal1b* show incomplete knockdown, resulting in only subtle olfactory/ commissural defects

Incomplete knockdown

So far, according to the scientific literature, only translation-blocking morpholinos have been used to knockdown *Kal1a* and *Kal1b* in zebrafish. However, whilst the same *Kal1b* tbMOs ('B-MOs') have been used in this project, our *Kal1a*

tbMO ('A-MO') target sequences have differed (*see Figure 5.05B*). So, whilst all three A-MOs target the same 'ATG' translational start site of *Kal1a*, the A-MO used by one group has 14 upstream target nucleotides (Whitlock et al., 2005b), whereas that used by another group has only 6 (Yanicostas et al., 2008; Yanicostas et al., 2009), and the A-MO used in this project had 10.

The tbMOs used in this thesis, were acquired prior to any of these other research papers being published, so it was not possible to use the same A-MO from the start. However, since the publication of the first *Kal1a*/*Kal1b* knockdown several years ago by Whitlock and colleagues, we have ordered, and tested, the same A-MO that was reported in their publication (Whitlock et al., 2005b). However, in our hands, we were unable to obtain levels of knockdown that were any higher than our existing A-MO, as assessed by Western immuno-blot analysis (data not shown). The A-MO used by Soussi-Yanicostas and colleagues was published more recently (Yanicostas et al., 2008; Yanicostas et al., 2009), and has therefore not been independently tested by us.

The knockdown efficiencies for our A-MO and B-MO were assessed qualitatively by immunoblot analysis, and both of these morpholinos were found to have an approximately 50-75% knockdown at 1.5mM, with A-MO having the slightly higher knockdown efficiency. These approximate knockdown efficiencies were based upon analysis of pooled lysates from ten embryos, and were assessed visually, based on the relative intensity of the 'knockdown band' compared with the 'control band'. Of course, using pooled lysates meant that the knockdown level visualised is indicative of an 'average knockdown', so, in fact, some embryos may have had higher/lower levels of knockdown than this average. However, as this analysis was carried out on several pooled lysates (data not shown), this 'average knockdown' was found to be representative of the tbMO morphants' knockdown efficiencies.

Immunoblotting on *single* embryos was not permissible because the anti-anosmin-1a/-1b signal from this analysis was too weak. Also, densitometry analysis of the band intensities would have given far greater accuracy in the relative comparisons; however, the more important outcome of this analysis was to show

that the tbMOs did not give close to 100% knockdown i.e. ~25% of the anosmin-1a/-1b protein expression was unaffected in the 'average' tbMO morphant embryo. Therefore, an alternative knockdown approach would need to be considered, to achieve higher levels of knockdown (*see section 5.3.5*).

In contrast, Soussi-Yanicostas and colleagues did manage to demonstrate approximately 100% knockdown of *Kal1a* and *Kal1b*, using tbMOs at concentrations of 0.5mM (Ayari and Soussi-Yanicostas, 2007; Yanicostas et al., 2008; Yanicostas et al., 2009). However, as mentioned, using the same B-MO, and their same anti-anosmin-1b antibody, we were unable to reproduce such high levels of knockdown. Perhaps this was due to the different strain of zebrafish they were using ("AB strain"), which may have a different genetic background to the strain that we used, which may have influenced the knockdown efficiency.

GnRH3 neuronal phenotype apparently normal

The GnRH neuronal defects reported by K. Whitlock and colleagues, in *Kal1a* morphants, could not be verified in this study because when GnRH immuno-labelling was carried out earlier in this thesis (*see chapter 3*) in the same way that had been described (Whitlock et al., 2005b), hypothalamic GnRH cells were not detectable at 56hpf (*see Fig.3.04*). Therefore, as the pGnRH3:mCherry (G3MC) transgenic line labels the same terminal nerve GnRH cells as the GnRH antibody (LRH13), as well as am *'early wave'* hypothalamic GnRH cluster by around 36hpf, the G3MC line was used instead to assess the GnRH3 neuronal phenotype in this project.

The A-MO+B-MO double morphant embryos had an apparently normal G3MC phenotype at 36hpf, and only at 60hpf were there some subtle differences noticeable in these double morphants (whereas the A-MO and B-MO single morphants remained normal throughout). Specifically, there was no difference in the hypothalamic cluster of cells, with just a slight reduction in GnRH3 (mCherry)

expression) in these cells by 60hpf. Therefore, knockdown of 50-75% *Kal1/Kal1b* was not sufficient to give any observable GnRH3 neuronal defects.

Subtle defects in olfactory axonogenesis and forebrain commissure formation

Despite the lack of a GnRH3 neuronal phenotype in the partial knockdown Kal1a/Kal1b (tbMO) double morphants, subtle olfactory defects and forebrain commissure defects were noticeable. Specifically, the A-MO+B-MO embryos, despite apparently projecting normally to the anterior forebrain, were less defasciculated at the olfactory bulbs, which inevitably resulted in a more disordered pattern of potential glomeruli in this region. Moreover, there was less decussation (crossing over) at the midline in the AC (but not POC) by 36hpf. Together, this indicates that a combined 50-75% reduction in *Kal1a* and *Kal1b* gene function was sufficient to bring about mild-moderate defects in olfactory and AC formation, but did not noticeably affect GnRH system formation. Therefore, another approach was required in an endeavour to obtain closer to 100% *Kal1a*/*Kal1b* knockdown in order to assess the affects of a 'true null' morphant (although, it's probably more reasonable to expect a $\geq$95% knockdown, rather than a true 'knock-out').

5.3.4 *Kal1a*/ *Kal1b* over-expression causes no observable defects in olfactory, GnRH, or forebrain commissure phenotype

The known role of anosmin-1 in modulating Fgf signalling (at least in *ex vivo* culture), and because the Fgf signalling pathway is required extensively during embryogenesis, severe morphological abnormalities are expected to result from anosmin-1 over-expression. In fact, previous experiments in the nematode worm *C. elegans* have indeed demonstrated that anosmin-1 over-expression does cause an axonal branching phenotype in AIY interneurons, which receive synaptic input from olfactory neurons in this organism (Bulow et al., 2002; Bulow and Hobert, 2004).

Therefore, over-expression of anosmin-1 in other organisms such as the zebrafish may also be expected to induce axonal branching defects (or similar phenotypes); however, this was not the case.

At higher concentrations (i.e. 2.0μM) of *Kal1a* and *Kal1b* mRNA, there was a very significant elevation in embryonic death by 24hpf. However, it is not possible to say for sure whether or not this was a non-specific effect of injecting too much exogenous mRNA, or whether it was a specific result of Kal1a/Kal1b interfering with Fgf signalling at critical events during embryogenesis (e.g. gastrulation). When GFP mRNA was injected at a concentration of 2.0μM the embryo lethality was low, but many embryos had shortened trunks, indicative of the non-specific effects caused by excessive mRNA. Therefore, it is highly likely that the lethality caused by 2.0μM of *Kal1a* and *Kal1b* mRNA was also non-specific.

0.5-1.0μM was the most appropriate concentration for *Kal1a* or *Kal1b* mRNA, due to the much lower embryo lethality. However, no neuronal defects were detectable in those systems which were assessed (olfactory, GnRH, and forebrain commissures). Similarly, over-expression of *Kal1a* and *Kal1b* together, at concentrations of 0.5μM, did not affect the formation of these forebrain systems either. This may suggest that zebrafish are more resistant to the effects of *Kal1a/Kal1b* over-expression than *C. elegans*, perhaps because zebrafish have mechanisms to counter-act the putative imbalance in Fgf signalling, brought about by the increased presence of Kal1a/Kal1b; perhaps by upregulating other Fgf modulators which restore Fgf signalling to normal, functioning levels. Similarly, in humans, *KAL1* partially escapes X-inactivation in females, effectively meaning that they may have double the *KAL1* expression levels compared to males (Dode et al., 2003; Cadman et al., 2007). Therefore, it is likely that some mechanism may happen during human embryogenesis to ensure that inappropriately high Fgf signalling levels do not occur in regions where ansomin-1 is expressed (i.e. during olfactory/GnRH neuronal development). It will be useful to investigate which modulators, if any, are up- or down-regulated in response to *Kal1a/Kal1b* over-expression in order to maintain fully-functional levels of Fgf signalling during olfactory and GnRH neuronal development.

Moreover, whilst GnRH/olfactory neuronal development was apparently normal in those embryos where *Kal1a/Kal1b* was over-expressed, it can not be ruled out that development of these systems may have been initiated prematurely i.e. olfactory axonogenesis, for example, may have begun earlier than usual. Whilst this may have resulted in 'apparently normal' olfactory projections, these axons may have reached the anterior forebrain too prematurely for normal olfactory bulb morphogenesis to proceed correctly. Therefore, functional defects in the olfactory and GnRH systems may exist in the *Kal1a/Kal1b* mRNA-injected embryos, and the only way to prove this may be to carry out functional/behavioural studies in adults, to assess reproductive and olfactory capabilities.

5.3.5 Using exon-4 targeted splice-blocking morpholinos against *Kal1a* & *Kal1b* resulted in very efficient knockdown

KA4 and KB4, the splice-blocking morpholinos which targeted the loss of exon 4 from *Kal1a* and *Kal1b*, respectively, gave significantly higher levels of *Kal1a*/*Kal1b* knockdown, compared with the translation-blocking morpholinos described above (A-MO and B-MO). Moreover, upon sequencing of the *Kal1a* and *Kal1b* morphant bands, it was determined that the whole of exon 4 was lost, as predicted, resulting in severely truncated translated protein-product, which part of the WAP domain and all fibronectin domains. This WAP-truncated anosmin-1a/anosmin-1b are very unlikely to retain any of the native functions of the full-length proteins. It is possible that the remaining Cys-box may have some residual signalling capability in some contexts. But, even if this is true, it is unlikely that the truncated anosmin-1a/anosmin-1b would have a very long half-life (i.e. in all likelihood, these truncated proteins will be targeted for degradation soon after translation).

When the knockdown levels were assessed by RT-PCR across eight individual KA4 or KB4 morphant embryos, it was determined that in approximately three quarters of the embryos, an almost complete knockdown of *Kal1a* or *Kal1b* was achieved, whilst in the remaining morphants, a knockdown of around 75% was

achieved. This of course means that in approximately 75% of the KA4 or KB4 morphants there is an almost complete functional loss of *Kal1a* or *Kal1b* activity. However, it is unlikely that there is an actual 100% loss in *Kal1a/Kal1b* in the morphant embryos, due to the mechanism of gene knockdown by morpholinos i.e. it is unlikely that the morpholino can bind to and block correct exon 4 splicing in every single *Kal1a/Kal1b* transcript. Moreover, the RT-PCR analysis will not reveal residual transcripts if the full to levels below around 95% because this will be beyond the detection limits of the agarose gel electrophoresis analysis. However, it can be concluded that Kal1a/Kal1b knockdown was as high as could be measured in the majority of KA4/KB4 morphants, and Kal1a/kal1b activity has effectively been abrogated in these embryos. Currently, the best way to achieve a targeted absolute knock-out of gene function in zebrafish embryos, which has longer-lasting effects, is to use customised zinc finger nucleases (ZFNs) which permit efficient genome modification in zebrafish (Foley et al., 2009).

Disrupted terminal nerve GnRH cells, concomitant with a decrease in hypothalamic GnRH cell number by 36hpf

Knocking down *Kal1a* or *Kal1b* individually did not result in noticeable defects in GnRH3 neuronal development, compared with the controls; whereas, knocking down *Kal1a* and *Kal1b* together did. However, the KA4+KB4 morphant phenotype was very variable: approximately 32% of embryos hypothalamic GnRH neurons which were within the normal range of *'early wave'* hypothalamic cell number at 36hpf, but were often disorganised in their spatial arrangement; whilst another 38% of embryos had approximately 50% or fewer of the 'average' number of hypothalamic cells at this stage; 17% of the embryos had apparently completely absent hypothalamic GnRH cells; whilst the remaining embryos had normal-appearing GnRH3 neuronal phenotypes. Co-injection of *Kal1a/Kal1b* mRNA with the morpholinos 'rescued' much of the abnormalities that were caused by KA4 and KB4; that is, the majority of these embryos did not have disorganised hypothalamic GnRH clusters at 36hpf. This confirms that these defects were specifically caused by *Kal1a/Kal1b* knockdown, because the co-injected *Kal1a/Kal1b* mRNA was able to provide a substitute source of Kal1a/Kal1b protein, when the native *Kal1a/Kal1b*

transcripts were made non-functional by KA4 and KB4. Because the Kal1a/Kal1b mRNA was able to do this, the defects caused by KA4 and KB4 must have been caused predominantly by loss of *Kal1a/Kal1b*. However, whilst none of the rescue embryos had absent hypothalamic GnRH neurons, a minority of them did have 50% or fewer hypothalamic GnRH neurons, suggesting that the injected *Kal1a/Kal1b* mRNA levels were not sufficiently high enough to completely rescue loss of native Kal1a/Kal1b transcript in all embryos.

By 60hpf, the KA4+KB4 morphant phenotype was less variable: around 60% of the embryos had an organised cluster of hypothalamic GnRH neurons of a cell number comparable to the average cell number observed in the control embryos; whilst the remaining 40% of embryos had approximately 50-75% of the average hypothalamic cell number, which were organised closely together in the hypothalamic region, as normal. Combined, this data suggests that Kal1a and Kal1b are both required for the correct positioning of the *'early wave'* hypothalamic GnRH cells neurons by 36hpf; however, these cells may still be able to reach the hypothalamus by 60hpf, if they fail to get there earlier. It is however, unclear whether the early failure in accumulation of GnRH3 cells in the hypothalamus by 36hpf represents a failure in GnRH neuronal migration (from the nasal compartment) or a failure in the specification of these neurons in the hypothalamus (or nasal compartment); or indeed, whether it is a combination of a failure in both processes. Furthermore, there may be a much more significant disruption in the organisation of the brain regions, or their boundaries, as both *Kal1a* and *Kal1b* are expressed throughout the diencephalon during early zebrafish embryogenesis and may have an important role in diencephalon morphogenesis. Moreover, if the loss of hypothalamic GnRH cells is caused by a migrational defect in these cells, this may be caused by a failure in forebrain commissure formation and its associated tracts, which are believed to form part of the axonal scaffold that GnRH neurons use to migrate into the forebrain. Alternatively, if Kal1a/Kal1b are required for GnRH neuronal specification in the nasal compartment, Kal1a/Kal1b may be acting via the Fgf8a signalling pathway in this region; suggesting that the loss of hypothalamic GnRH cells may be associated with an increase in apoptosis in this region, resulting from a reduction in Fgf8a signalling levels (*see conclusion for further discussion*).

The terminal nerve neurons were also noticeably disrupted in approximately half of the KA4+KB4 morphant embryos by 60hpf; and there was a noticeable failure in terminal nerve GnRH neuronal projections across the AC in around 81% of these morphants too. As mentioned above, the axonal scaffold formed by the terminal nerve GnRH cells is believed to have a putative role in the migration of the hypothalamic GnRH neurons, so the disruption of the AC projections may affect this process. Furthermore, it has been proposed that the hypothalamic GnRH neurons may arise from the terminal nerve GnRH neuronal population, as embryos which had their terminal nerve GnRH cells ablated had a missing hypothalamic GnRH neuronal population in adulthood (Abraham et al., 2010); indicating that the disruption of the terminal nerve GnRH cells may affect the *'later wave'* hypothalamic GnRH neuronal migration, even if it does not significantly affect the *'early wave'* hypothalamic GnRH cells. Moreover, the terminal nerve GnRH neuronal system has been shown to have an important role in the neuromodulation of reproductive behaviour, so a loss of the terminal nerve GnRH system, and its likely interactions with the olfactory/vomeronasal systems, may significantly alter the reproductive activity of the KA4+KB4 morphants. Finally, a disruption of the terminal GnRH cells may also be secondary to a disruption in the organisation and/or specification of cells in the nasal compartment (*see below*).

As already discussed in Chapter 3, at 56hpf, Whitlock and colleagues were able to immuno-label a migrating population of 'endocrine' GnRH-expressing cells that were migrating from the nasal compartment region towards the presumptive preoptic area/hypothalamic region. Moreover, when they knocked down *Kal1a* gene function (using tbMOs; *see Figure 5.05B*), these 'migrating' hypothalamic GnRH cells were completely lost; whereas the terminal nerve GnRH immuno-positive cells in these embryos were still present, although mildly disrupted (Whitlock et al., 2005b). In contrast, the 'migrating' hypothalamic GnRH immuno-positive cells were only mildly affected (data not shown) in the *Kal1b* morphants. Even though the same antibody (LRH13) and same protocol was used, it was not possible for us to detect the same 'migrating' population of hypothalamic GnRH immuno-positive cells at 56hpf (*see Figure 3.04B'*); instead, only the terminal nerve GnRH cells were detectable. Whilst the *'early wave'* hypothalamic GnRH cells (from the G3MC transgenic line) were detected during a similar stage (i.e. between 30-60hpf), they

do not seem to occupy the same brain location as the migrating GnRH cells detected by Whitlock and colleagues i.e. the *'early wave'* G3MC cells already reside in the hypothalamus by 36hpf. However, it is possible that the hypothalamic GnRH neurons switch off GnRH gene expression once they reach the hypothalamus, whereas the mCherry (G3MC) expression is switched on only when these cells reach the hypothalamus. This may explain these conflicting observations; although it does not explain why we weren't able to detect the 'migrating' hypothalamic GnRH immuno-positive cells- although this may be an experimental/technical issue (as discussed in chapter 3).

In our analysis it was necessary to knock down both *Kal1a* and *Kal1b* gene function to obtain the GnRH3 neuronal defects described above; conversely, it was necessary to only knockdown one of these genes, *Kal1a*, for Whitlock and colleagues to observe a comparative loss in hypothalamic 'endocrine' GnRH neurons (Whitlock et al., 2005b). Firstly, it should be noted that the G3MC hypothalamic GnRH cells are yet to be fully confirmed as *bona fide* 'endocrine'/hypophysiotropic GnRH cells, so some caution is needed when referring to these cells. Similarly, the migrating hypothalamic GnRH cells reported by Whitlock and colleagues, whilst GnRH immuno-positive, are yet to be identified independently by us, and, in our opinion, are yet to be fully characterised and confirmed as hypophysiotropic GnRH cells. Significantly, these 'migrating' hypothalamic GnRH immuno-positive cells are not detected by GnRH3 or GnRH2 *in situ* analysis (Palevitch et al., 2007), and are not observed in the same brain region in the G3MC transgenic line, or the characterisation of the similar pGnRH3:EGFP transgenic line reported by Abraham and colleagues (Abraham et al., 2008). In summary, assuming that we and K.Whitlock and colleagues are observing the *bona fide* 'endocrine'/hypophysiotropic hypothalamic GnRH cells at between 30-60hpf, it can be concluded that Kal1a and Kal1b both have a role in the accumulation of hypothalamic GnRH neurons by 60hpf.

The development of the proposed second wave of GnRH neuronal migration to the hypothalamus (termed the *'later wave'* in chapter 3), was not assessed in the KA4+KB4 morphants, but remains an important future goal of this project.

Olfactory and vomeronasal projections are missing or mis-projected

In their report describing the loss of 'endocrine' GnRH cells in *Kal1a* morphants, Whitlock and colleagues also observed that the disruption terminal nerve GnRH cells seen in these embryos were probably due to a disrupted adjacent olfactory epithelium. Using similar tbMOs against *Kal1a* and *Kal1b* (*see Figure 5.05B*), Yanicostas and colleagues (Yanicostas et al., 2009) recently reported that Kal1a, but not Kal1b, is required for the proper fasciculation of olfactory axons and their terminal targeting at the olfactory bulbs; using the same pOMP:tauEGFP transgenic line (Yoshida et al., 2002) that was used in this thesis. However, before the publication of this report, our analyses demonstrated that both Kal1a *and* Kal1b were required for normal olfactory axonogenesis in zebrafish embryos.

The KA4 and KB4 single morphants both had olfactory axonal defects; however, the most severe olfactory defects were observed in the KA4+KB4 double morphants. Specifically, some KA4 morphants had some abnormal defasciculation of the olfactory nerve bundle projecting to the presumptive olfactory bulb region, by 36hpf. This is a similar defect to what was reported recently by Yanicostas and colleagues (Yanicostas et al., 2009); however, in our experience, this phenotype was present in only a few of the *Kal1a* morphants. Moreover, they also reported a failure of terminal targeting of the olfactory axons to the olfactory bulbs; however, whilst we also observed this defect, we found that this happened in the *Kal1b morphants* instead, but only in a proportion of the embryos. The most severe, fully penetrant, phenotypes were observed in the KA4+KB4 *double* morphants. Around one third of these embryos had disrupted olfactory pits, often with eptopic olfactory cells outside of the normal 'rosette' arrangement of the olfactory epithelium, suggesting an abnormal specification of the olfactory epithelial cells within the nasal compartment, similar to the *Fgf8a* morphants. Moreover, in approximately 51% of these KA4+KB4 morphants, there was a failure of the olfactory axons to properly fasciculate into an olfactory axonal bundle, whilst in around 21% of these embryos there was a failure to form a recognisable olfactory nerve bundle at all. Moreover, in around 83% of these morphants, there was a failure of terminal axonal targeting i.e. the olfactory axons failed to defasciculate properly at the presumptive olfactory bulb

region; a defect that is likely to cause a failure in subsequent olfactory bulb morphogenesis.

The 36hpf rescue embryos (KA4+KB4 morphants co-injected with *Kal1a/Kal1b* mRNA) mostly had a normal-appearing, apparently tightly-fasciculated, olfactory bundle. However, whilst there was much improvement in terminal olfactory targeting in the rescue embryos, approximately half of the embryos still had some defects in defasciculation at the presumptive olfactory bulbs, but this was more subtle compared with the morphants. Although the rescue was not complete, there was nonetheless a rescue to some significant extent, suggesting that the olfactory defects observed are likely to be specific consequences of loss of Kal1a/Kal1b.

Furthermore, there was an approximately 24% reduction in the average olfactory epithelium size (A-P length) at 36hpf for the KA4+KB4 morphants, compared with the controls. Whereas the reduction in average A-P length for the *Kal1a* and *Kal1b* individual morphants was only 0.3% and 5.2%, respectively. There was still a reduction in the average A-P length for the rescue embryos (4.8%), but it was a much smaller reduction compared with the KA4+KB4 morphants without the rescue *Kal1a/Kal1b* mRNA co-injection, suggesting that the reduction in olfactory pit size was specifically caused by loss of *Kal1a/Kal1b* activity. This is very similar to the 20.3% average olfactory epithelium size that was reported for the Fgf8a morphant embryos (or 26.4% for the *Fgf8a+Fgf8b* morphants). This, together with observations that KA4+KB4 morphants also had disorganised olfactory pits and failure in terminal targeting of olfactory axons, as well as defects in GnRH neuronal development (*see above*) and forebrain commissure formation (*see below*), suggested that Kal1a/Kal1b could be involved in the Fgf8a signalling pathway during these processes (*see sections 5.37 and 5.4*).

The presence of defects in olfactory axonogenesis by 36hpf, suggest that Kal1a and Kal1b are required for the establishment of the pioneer olfactory pathway; however, the secondary olfactory axons which replace these pioneer axons by 60hpf are also affected. Both *Kal1a* and *Kal1b* are expressed in the olfactory epithelium between 24hpf and 60hpf during pioneer and secondary olfactory

axonogenesis so may have a role in establishing both pathways. By 60hpf, despite a persistence of the olfactory pit disorganisation phenotype, the olfactory axons had projected to the presumptive olfactory bulbs in the majority of the KA4+KB4 morphants; although in approximately 17% of these embryos, there was a severe disruption in the olfactory pit formation and axonal pathfinding, with many olfactory axons meandering away from the presumptive olfactory bulbs. In contrast, the majority of the rescue embryos had normal-appearing olfactory pit 'rosettes' with apparently normal olfactory projections; although some embryos still had displaced olfactory cells. Together, this data suggests that *Kal1a* and *Kal1b* have a more important role in establishing the pioneer olfactory pathway, and if enough pioneer axons (above a certain threshold) can establish the pioneer olfactory pathway by 36hpf, the proceeding secondary ORNs may establish a normal-appearing secondary olfactory axonal pathway (although this may be too late for normal olfactory bulb morphogenesis; *see conclusions*) by 60hpf. Conversely, if insufficient pioneer olfactory axons have established the pioneer pathway, the proceeding secondary (ORN) olfactory axons are denied their precisely-guided navigational pathway to the presumptive olfactory bulb region, so instead meander in abnormal directions, as occurs in around 17% of the KA4+KB4 morphants by 60hpf. Similarly, it was demonstrated in the *Cxcr4b* ('odysseus') mutant, which, that if pathfinding by pioneer axons is significantly impaired by 36hpf, the following ORNs fail to exit the olfactory placode, and were found to accumulate instead around the olfactory epithelium by 72hpf (Miyasaka et al., 2007).

Despite the high levels in natural variance with the vomeronasal neuronal phenotype at 36hpf and 60hpf, it was possible to detect some defects in a minority of the KA4+KB4 morphants. Specifically there were absent or mis-projected vomeronasal axonal projections, which were not seen in the controls or the majority of rescue embryos, as well as a 49% reduction in the vomeronasal cell number for the KA4+KB4 morphants at 36hpf, compared to only a 13% reduction in the rescue embryos. In fact, it is likely that the absence in vomeronasal projections in some KA4+KB4 morphant embryos is due to the reduction in vomeronasal cell number in the olfactory pits of these embryos. Whilst the vomeronasal phenotypes were not investigated in the fgf8a morphants, this phenotype was assessed in the SU5402-treated embryos, and similar axonal projection defects and vomeronasal neuronal

loss was observed in those embryos that had their Fgf signalling blocked between 14hhpf and 22hpf. This suggests that *Kal1a* and *Kal1b* may be exerting their action on the Fgf signalling pathway during zebrafish vomeronasal development.

By 60hpf, vomeronasal axons were missing or mis-projected in around half of the KA4+KB4 morphants; a phenotype that was present, but to a lesser extent in fewer rescue embryos. The incomplete rescue suggests that these vomeronasal defects may not be entirely specific to *Kal1a/Kal1b* knockdown, but may instead reflect the difficulty in accurately assessing 'normal' vomeronasal axonogenesis at 60hpf. Nonetheless, the vomeronasal axonal defects were noticeably much more severe in the KA4+KB4 morphants, compared with controls and rescue embryos.

In mice, GnRH neurons are observed closely migrating with vomeronasal axons towards the forebrain. However, unlike mice which have a separate vomeronasal organ and accessory bulb for their vomeronasal projections, zebrafish vomeronasal neurons arise from the olfactory epithelium, along with the olfactory neurons, and navigate to a similar olfactory bulb target region in the forebrain. It remains to be demonstrated whether vomeronasal axons are important for putative GnRH neuronal migration from the nasal compartment in zebrafish, but such a mechanism is possible; so, disruption of these vomeronasal (and olfactory) axons may affect GnRH neuronal migration in the zebrafish too.

So, in summary, although knockdown of *Kal1a* or *Kal1b* alone resulted in mild to moderate olfactory axonal defects in some embryos; knocking down both *Kal1a* and *Kal1b* together resulted in much more severe defects in olfactory epithelium organisation and axon pathfinding, in a greater proportion of morphant embryos. Similarly, vomeronasal axonogenesis was apparently only affected in the KA4+KB4 morphants. This would suggest that there is some redundancy in the action of *Kal1a* and *Kal1b* during olfactory/vomeronasal (and GnRH) neuronal development.

However, the conflicting findings from two other research groups suggesting that *Kal1a* alone has a crucial role during olfactory axonogenesis and hypothalamic GnRH neuronal migration may be unified with our findings by better understanding the different morpholinos strategies used. Firstly, morpholino knockdown is very

unlikely to give a 100% knockdown of gene function, despite immunoblotting or RT-PCR analyses indicating that all protein or full-length transcript has been lost. This is because when protein or transcript levels are reduced to below 5-10% of their normal (wild-type) levels, such levels may no longer be distinguishable by the antibody (for immunoblotting) or the UV spectrophotometer (for RT-PCR/ agarose gel electrophoresis); thus falsely indicating a complete loss of protein or normal transcript, when this may not be the case. Therefore, it is possible that up to ~5-10% of *Kal1a* full length transcript may be retained in the KA4 morphants embryos that appear to show 100% knockdown; which, despite being very low, may, along with normal Kal1b, have some residual activity (i.e. above the combined signalling threshold of Kal1a+Kal1b). Conversely, using translation-blocking morpholinos, it may have actually been possible for other groups to obtain a more complete *Kal1a* knockdown, which made the combined levels of Kal1a+Kal1b for below what is required for active Kal1a/Kal1b signalling. Furthermore, in the complete absence of Kal1a, Kal1b signalling may be insufficient for normal olfactory/GnRH neuronal development; despite having a role at low levels of Kal1a (i.e. when the combined Kal1a+Kal1b threshold is high enough).

However, it was found that Kal1b does have an important role in forebrain commissure formation; a role that could not be fulfilled by normal background *Kal1a* gene expression levels in these embryos, although knocking down *Kal1a* and *Kal1b* together gave more severe defects in AC/POC formation (*see below*).

Anterior commissure does not form correctly- phenocopying the Fgf8a morphants

As discussed already in chapter 4, the forebrain commissure defects that are observed in *Fgf8a* morphants may help to explain the role of Fgf signalling in the molecular pathogenesis of bimanual synkinesis (upper body mirror movements) found in some KS patients with mutations in genes involved in the FGF signalling pathway (*FGF8* and *FGFR1*). As Bimanual synkinesis is found in more than 75% of patients with *KAL1* mutations (Kim et al., 2008), and because anosmin-1 (the *KAL1* gene product) has been implicated as an extracellular modulator of FGFR1 signalling (*in vitro*) (Gonzalez-Martinez et al., 2004b), KA4/KB4 morphants were assessed for defects in forebrain commissure formation too. Moreover, such

analyses also bear direct relevance to the function of the olfactory and terminal nerve GnRH neurons which project across the AC (and POC) (Whitlock, 2004).

Kal1a knockdown resulted in a subtle reduction in the number of axons crossing the AC at 36hpf; whereas the Kal1b morphants had a similar phenotype, but more of their decussating AC axons were affected. However, knocking down both Kal1a and Kal1b together gave the strongest, most penetrant, phenotype at 36hpf. In most of the KA4+KB4 morphants the AC axons failed to project across the midline or mis-projected towards regions of the midline that they would normally be excluded from, including towards the POC. Consistent with the forebrain defects described for the *Fgf8a* morphant in chapter 4, the POC was only affected in around 15% of the KA4+KB4 morphants. Whilst most of the rescue embryos had normal AC and POC formation, a small percentage of embryos had fewer AC axons crossing the midline, demonstrating that the forebrain commissures defects caused by KA4+KB4 were mainly due to the specific loss of *Kal1a* and *Kal1b*. By 60hpf, most embryos had at least a few AC axons crossing the midline, but many more AC axons were observed in an axonal 'tangle' at either side of the defective commissure, presumably caused by their failure to respond to a guidance cue (or absence of said guidance cue) instructing them cross the midline.

As anosmin-1 has previously been implicated in the FGFR1 signalling pathway *in vitro*, and both *KAL1* and *FGFR1* mutations result in corpus callosum defects in humans (and mice: Fgfr1 only), it may be speculated that the mechanisms proposed for the similar AC/POC defects caused by Fgf8a loss (in chapter 4) may be the same mechanism occurring in the zebrafish *Kal1a*/*Kal1b* morphants. That is Fgfr1/Fgf8 signalling at the midline is required for the specification and localisation of midline glial structure (a 'glial bridge') which, by secreting guidance cues, permits the correct pathfinding of the AC and POC axons across the midline. The exact role of Kal1a and Kal1b in these processes may be as modulators of Fgf8/Fgfr1 signalling, a role that has been demonstrated previously *in vitro* (Gonzalez-Martinez et al., 2004b). The putative interaction of Kal1a/Kal1b with the Fgf8a signalling pathway is discussed below.

However, whilst *in situ* hybridisation analyses demonstrated that *Kal1a* and *Kal1b* transcripts are present in cells of the anterior midline during early zebrafish embryogenesis, immuno-labelling analyses showed that Kal1a and Kal1b proteins are detected only in the elongating AC axons between 24hpf and 60hpf, suggesting that Kal1a and Kal1b are more likely to be acting directly on these commissural axons, rather than specifying the midline 'glial bridge' cells. Interestingly, it has been demonstrated in the mouse Fgf signalling is involved in more than use determining the midline glial structures during commissure formation, as *Fgfr1* hypomorphs have normal midline glial structures, but still have missing/aberrant commissures. Therefore, it was proposed that Fgf signalling was also required for the elongation/pathfinding of the commissural growth cones. Assuming this is true, it can be speculated that Kal1a/Kal1b may be modulating Fgf8a signalling in the AC (and to a lesser extent, the POC) and thus altering the pathfinding capabilities of these axons.

The AC defects reported for the KA4+KB4 morphants are consistent with the absence of GnRH3-positive AC projections that were reported above. Given the importance of the AC in both the olfactory and GnRH systems in zebrafish, which both project axons across this commissure, it is likely that loss of the AC may have repercussion for the correct functioning and coordination of both system, and possibly with their interactions which each other.

5.3.6 Olfactory, GnRH, and commissure phenotypes were confirmed by a second pair of morpholinos against *Kal1a* and *Kal1b*

A second pair of splice-blocking morpholinos which targeted the loss of exon 6 from *Kal1a* and *Kal1b*, KA6 and KB6, respectively, was used to further confirm the specificity of the forebrain defects caused by Kal1a and Kal1b knockdown. Firstly, RT-PCR analysis was carried to confirm the knockdown efficiencies of these new morpholinos. KA6 and KB6 were both shown to give

Kal1a/Kal1b knockdown levels of close 100%, like KA4 and KB4. The predominant PCR product for both morphants was the morphant band comprising loss of exon 6; resulting in first-fibronectin domain-truncated mis-spliced proteins which are predicted to be inactive due to the functional loss of the essential first fibronectin domain.

Consistent with the KA4+KB4 morphants, the KA6+KB6 morphants had defects in AC formation (including fewer GnRH3-positive decussating axons), failure in olfactory axons to project correctly to the presumptive olfactory bulb region, and hypothalamic GnRH neuronal deficiency. Therefore, all of the major forebrain defects caused by KA4+KB4 knockdown were shown to be specific (using Kal1a/Kal1b mRNA rescue) and reproducible using a second independent pair of morpholinos against *Kal1a/Kal1b*. Moreover, the use of KA6 and KB6 also confirmed that knocking down Kal1a and Kal1b individually does not, in our experience, result in the severe, fully penetrant defects in forebrain development that were demonstrated by knocking down both genes together.

5.3.7 Kal1a/Kal1b may be acting via the Fgf8a signalling pathway *in vivo* during embryogenesis

Given the extensive similarities of the forebrain defects caused by Fgf8a or *Kal1a/Kal1b* knockdown, including during formation of the AC; the final experiment of this thesis aimed to investigate whether Kal1a/Kal1b may be acting via the Fgf8a signalling pathway in these developmental processes.

Fgf8a or *Kal1a/Kal1b* were sufficiently knocked down at a morpholino concentration of 1mM to cause failure of AC formation; and, if this morpholino concentration was reduced to 0.5mM, this effect was then reduced significantly or abolished (i.e. AC formation was again normal, excepting subtle defects). However, when Fgf8a and Kal1a/Kal1b morpholinos were all co-injected at the same concentration of 0.5mM, the phenotype of defective AC formation re-occurred; suggesting that Fgf8a and Kal1a/Kal1b were acting via the same signalling pathway during AC formation (*see Figure 5.21 for a summary of these findings*).

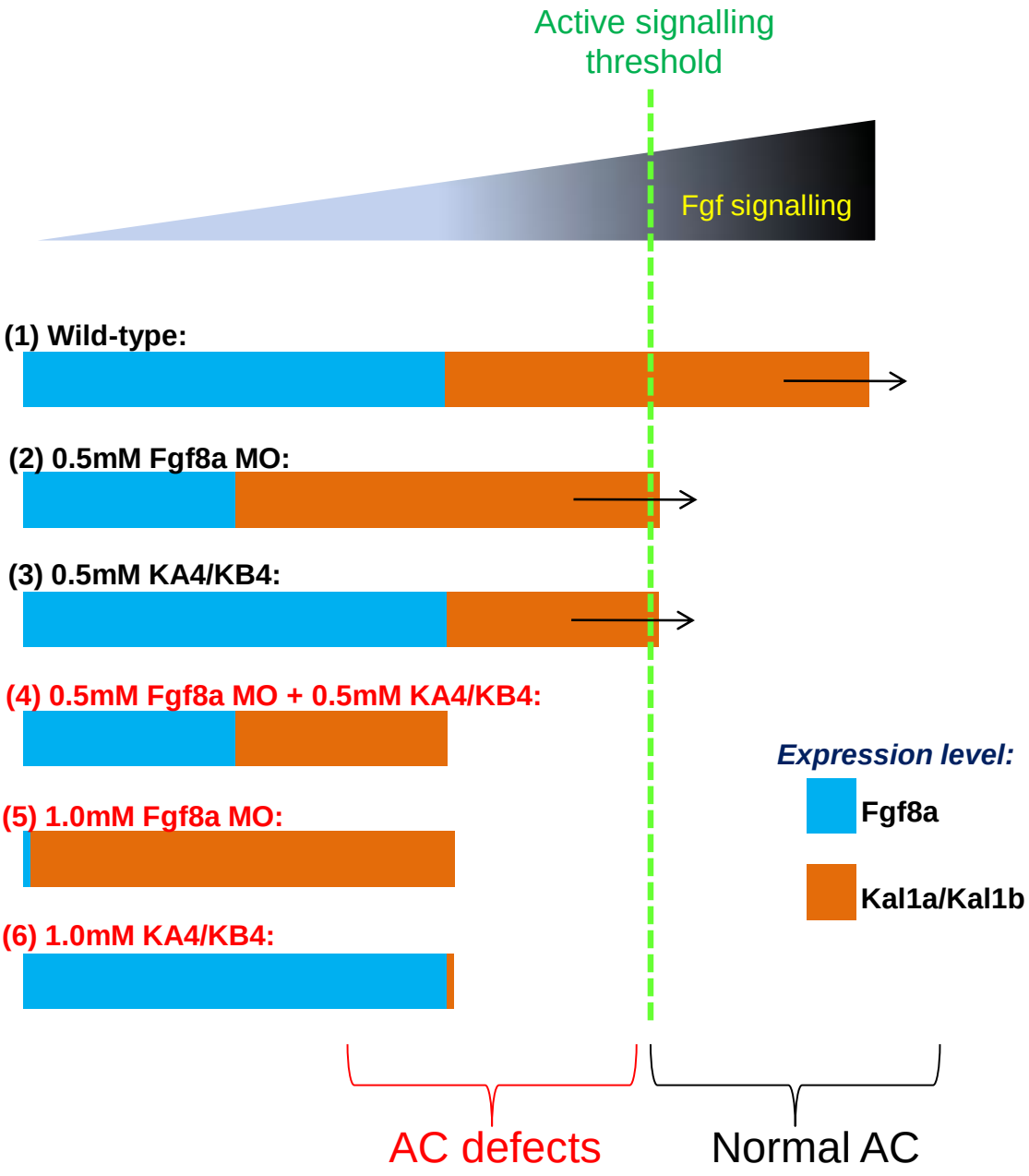

Figure 5.21 The additive effect of Fgf8a & Kal1a/Kal1b during anterior commissure (AC) formation

This schematic diagram summarises the findings from Fig5.20. The level of Fgf8a and Kal1a/Kal1b expression are indicated by blue and orange bars, respectively (*not drawn to scale*). For the purposes of this illustration it is assumed that Fgf8a signalling levels are insufficient for normal AC formation without a certain level of Kal1a/Kal1b, which modulates the Fgf8a signalling levels. The wild-type and morphant groups (1) & (2) have sufficient functional Fgf8a signalling for normal AC formation (as indicated by arrows); whereas morphant groups (4), (5), & (6) have Fgf8a signalling levels which are below the required' threshold (green dotted line), and so fail to initiate normal AC formation.

This data is consistent with the observation *in vitro* analyses that showed that anosmin-1 induces neurite outgrowth and cytoskeletal rearrangements through an FGF2/FGFR1-dependent mechanism (Gonzalez-Martinez et al., 2004b). It may be speculated that the mechanism is used by Kal1a/Kal1b to initiate/maintain commissural axon elongation across the midline during AC formation. Similarly, Kal1a/Kal1b may modulate Fgf8a signalling during its proposed role in olfactory neurogenesis and GnRH neuronal specification at the nasal compartment (*see chapter 4*); although such a mechanism will need to be investigated further.

It may also be possible that Kal1a/Kal1b act though another signalling pathway which converges downstream with the Fgf8a signalling pathway. Or, Kal1a and Kal1b may be acting entirely independently of Fgf8a, perhaps as a directional cue for the commissural axons as they cross the midline, at a similar point along their navigational route when Fgf8a signalling is also required. Therefore, the combined reduction of both the directional cue and signalling activity is sufficient to cause aberrant commissure formation. However, given the extensive *in vitro* and *ex vivo* data supporting the direct action of anosmin-1 on the FGF signalling pathway, a more direct role during AC formation seems highly plausible.

Future work will involve identifying the downstream signalling cascades which propagate the Fgf8a and Kal1a/Kal1b signal intracellularly during AC/POC forebrain commissure formation, and olfactory/GnRH system development; thus allowing novel avenues of investigation into other novel KS disease loci.

5.4 Conclusions

Previous studies have suggested that Kal1a, *but not Kal1b*, are required for hypothalamic GnRH neuronal migration and olfactory axonogenesis in the zebrafish; however, experiments carried out in this chapter have cast doubt on this assertion. It has been demonstrated in the course of this chapter that Kal1a and Kal1b are both required during at least three forebrain developmental processes in zebrafish: 1) the GnRH system, 2) the olfactory system, and 3) the forebrain commissures (AC and POC); although Kal1b notably had an important individual role in AC/POC formation as well.

During zebrafish GnRH system development, Kal1a and Kal1b are required together to ensure that the correct number of GnRH3 cells are accumulated and properly distributed at the hypothalamus by 36hpf i.e. a tight cluster positioned at the midline, rostral to the POC, and caudal to the pituitary in the G3MC transgenic line (termed the *'early wave'* in chapter 3). Moreover, Kal1a and Kal1b are also required to ensure that the terminal nerve GnRH cells remains localised between the olfactory epithelium and anterior forebrain, and project axons across the AC and POC.

During zebrafish olfactory system development, Kal1a and Kal1b are required together for the proper organisation of the olfactory epithelium, by maintaining the right number of cells and ensuring they form a typical 'rosette'-shaped formation. Moreover, Kal1a and Kal1b are also required to ensure that the olfactory and vomeronasal axons project to the anterior forebrain in a tightly-fasciculated bundle, and then defasciculate appropriately in the presumptive olfactory bulb region, a necessary pre-requisite for olfactory bulb morphogenesis.

During zebrafish olfactory system development, Kal1a and Kal1b are required together for correct formation of the AC, and to a lesser extent, the POC. Loss of Kal1b alone was sufficient to cause these AC defects; however, the loss of both Kal1a and Kal1b together resulted in a more severe phenotype, demonstrating that both Kal1a and Kal1b are required during forebrain commissure formation. When *Fgf8a* and *Kal1a/Kal1b* were knocked down together at sub-functional

morpholino concentrations, the AC defects were again observed, demonstrating that Kal1a, Kal1b and Fgf8a are acting together during the formation of the AC.

Given that anosmin-1 induces neurite outgrowth *in vitro*, in an FGFR1-dependent manner, and that *Kal1a* and *Kal1b* are expressed in the forming AC projections; it is likely that Kal1a/Kal1b have a direct role in the pathfinding of the AC/POC axons across the midline, via their modulation of the Fg8a signalling pathway. It is likely that a similar mechanism is used by the terminal nerve GnRH axons which also project across the AC and POC. If confirmed, such a mechanism may explain the malformation of the commissures (including the corpus callosum) in human KS patients with *KAL1* mutations, which is a proposed cause of the upper body mirror movements seen in more than 75% of X-linked KS patients (Kim et al., 2008).

The proposed role of Kal1a/Kal1b in the Fgf8a signalling during forebrain commissure axonogenesis may also be similar to the role played by Kal1a/kal1b during olfactory and GnRH system development, given that the defects in these systems caused by *Kal1a/Kal1b* or *Fgf8a* gene knockdown are so comparable. However, in the nasal compartment, Fgf8a was primarily implicated in olfactory/GnRH neuronal specification (i.e. olfactory/GnRH progenitor maintenance), and not olfactory axonogenesis. Therefore, it can be speculated that *Kal1a/Kal1b*, which are expressed in the olfactory placode soon after it first appears during zebrafish embryogenesis, modulate Fgf8a signalling during olfactory neurogenesis. Assuming the *'early wave'* GnRH3 neurons are also specified in the nasal compartment, their failure to reach the hypothalamus by 36hpf may indicate that their progenitor cells have been lost due to increased levels of apoptosis, due to the reduced Fgf8a signalling that may result from the loss of positive-regulation by Kal1a/Kal1b. It remains to be demonstrated whether the *'later wave'* of GnRH neuronal migration are similarly affected.

Loss of Kal1a/Kal1b apparently primarily affected the pioneer neurons which establish the olfactory pathway by 36hpf, subsequently denying the secondary (ORN) a navigational pathway towards the presumptive olfactory bulb region. Yanicostas and colleagues recently reported that there is a severe decrease in

the number of GABAergic and dopaminergic olfactory bulb neurons in the Kal1a morphant embryos by 5dpf, together with their data showing Kal1a protein accumulation in the presumptive olfactory bulbs from around 72hpf (Yanicostas et al., 2009), suggest that the absence of differentiated olfactory bulb glomeruli in the *Kal1a/Kal1b* morphants may be the cause of incorrect olfactory bulb morphogenesis. In our studies, olfactory projection defects were greater in the embryos at 36hpf, compared with later stage (60hpf) *Kal1a/Kal1b* morphants; suggesting that Kal1a/Kal1b had an important role during establishing the pioneer olfactory pathway (perhaps by maintaining olfactory neurogenesis at the olfactory pit); whereas the secondary olfactory axons may be able to navigate to the presumptive olfactory bulbs following an incomplete pioneer pathway. However, if this proposal is true, it is unknown whether the glomeruli that are formed by 60hpf are precisely formed (and therefore functional); and whether the failure/misrouting of the pioneer olfactory pathway affects olfactory bulb morphogenesis, regardless of whether the secondary ORNs reach the presumptive olfactory bulb region.

In summary, it is hypothesised that Kal1a/Kal1b modulate the Fgf8a signalling pathway in decussating axons of the anterior commissure in the zebrafish, during forebrain commissure formation; and a similar mechanism may be responsible for the corpus callosum malformation that is believed to be a cause of upper body mirror movements in X-linked KS patients. Kal1a/Kal1b are also hypothesised to modulate Fgf8a signalling during olfactory and GnRH neurogenesis and/or olfactory/vomeronasal axonal pathfinding and GnRH *'early wave'* neuronal migration/specification at the hypothalamus.

.

5.5 Future prospects

To further investigate the underlying cause of the various defects in olfactory/GnRH neuronal development and AC/POC formation, several further experiments are required.

Firstly, it will be necessary to use forebrain (and midbrain/hindbrain) regional and boundary markers to assess the morphogenesis of the brain region in the KA4/KB4 morphants, and ensure that the aforementioned defects are not due to a more major failure in brain region formation/specification. However, when the morphant embryos were examined there was not any noticeable reduction in head size, and brain formation appeared morphologically normal, so defects in brain regionalisation/morphogenesis are not expected. For example a loss of specific hypothalamic neuronal lineages or regions may cause the loss of GnRH3 neurons which may putatively arise from within the developing hypothalamus at 36hpf.

Secondly, a glial cell marker, such as GFAP, will be required to immuno-label the 'glial bridge' in the KA4+KB4 morphants at around 16-20hpf (prior to AC/POC formation) to determine whether a loss or disorganisation of the midline glial structure is the cause of forebrain commissure formation in the KA4/KB4 morphants.

Thirdly, apoptosis (and proliferation) analysis will be required to investigate whether there is an increase in cell death at the olfactory epithelium, which may suggest that Kal1a/Kal1b may be involved in the Fgf8a signalling pathway that has been proposed to maintain the cell survival of olfactory progenitor cells (and specification of GnRH neurons) within the olfactory epithelium.

Finally, the availability of a *Kal1a* and *Kal1b* knockout mutant, which has permanent loss of functioning Kal1a or Kal1b genes, will greatly assist in deciphering whether Kal1a/Kal1b are required for olfactory/vomeronasal axonogenesis (and not just olfactory/vomeronasal specification). For example, cells from the olfactory placode of a *Kal1a/Kal1b* knockout mutant (pOMP:tauEGFP transgenic) embryo may be transplanted to the olfactory placode of a wild-type embryo to see if GFP-positive Kal1a/Kal1b–negative olfactory neurons are able to

project axons to the presumptive olfactory bulbs in a wild-type background. If they were able to project axons, it would suggest that Kal1a/Kal1b are not required for olfactory axonogenesis (at least not within the neuron that they are expressed, anyway). Conversely, if the axons fail to project, it would suggest that Kal1a/Kal1b are required for olfactory axonal extension/pathfinding. If mutant *Kal1a/Kal1b* knockouts do not become available, these experiments can be done transplanting olfactory placodal cells from KA4/KB4 morphant embryos. The same experiment can also be carried out using cells transplanted from the olfactory placode of an ace embryo, to investigate whether Fgf8a is required for olfactory axonogenesis, as well as maintenance of olfactory neurogenesis.

In the present study, wild-type *Kal1a* and *Kal1b* mRNA was used to rescue the morpholino-induced phenotypes. However, the plasmid constructs containing the wild-type *Kal1a* or *Kal1b* coding sequence was specifically mutated, by site-directed mutagenesis, to generate mutant *Kal1a* and *Kal1b* constructs with a KS-specific single nucleotide change (i.e. one of the following human *KAL1* mutations: C172R, N267K, or E514K (Kim et al., 2008)). The specific site of these intended nucleotide changes was identified by sequence alignment of *Kal1a* and *Kal1b* with human *KAL1* coding sequence. Time-restraints have meant that these constructs have not yet been used; however, in future experiments the mutant *Kal1a*/*Kal1b* mRNA that they encode will be used in *Kal1a*/*Kal1b* morphant rescue experiments. It is predicted that the mutant *Kal1a*/*Kal1b* mRNAs will not rescue *Kal1a*/*Kal1b* morphant phenotypes, or that the rescue will be incomplete, because they are predicted to be loss-of-function mutations. These experiments would thereby confirm that the KS mutations are disease-causing because the *KAL1* gene product is non-functional, and that the mutated amino acid is therefore essential for the correct activity of anosmin-1.

Now that it has been determined that Kal1a/Kal1b are likely to be acting via the Fgf8a signalling pathway *in vivo*, it may now be investigated whether *Fgf8a* mRNA can rescue the AC defects that were observed in the KA4+KB4 morphants; thus demonstrating that Kal1a/Kal1b are positive regulators of fgf8a signalling during AC formation. However, this experiment will only work if levels of Fgf8a ligand is a limiting factor during AC formation because if functional levels of Fgf8a

are maximal, excess Fgf8a ligand will make no difference to the level of fgf8a signalling (although Kal1a/Kal1a may potentiate the Fgf8a signalling, even at maximum Fgf8a usage). Given the expected role of Kal1a/Kal1b as a modulators of Fgf8a signalling, not an Fgf ligand by themselves (Gonzalez-Martinez et al., 2004b), it is unlikely that *Kal1a/Kal1b* mRNA could rescue *Fgf8a* morphant phenotypes; assuming that most of the Fgf8a ligand is lost in these morphants.

It has been shown previously that Fgf3, like Fgf8a, is another Fgf ligand that is required for the formation of the AC and POC. Therefore, it will be interesting to ascertain whether or not Kal1a/Kal1b can also act through the Fgf3 signalling pathway in the formation of the AC. If so, it would then be logical to find out the putative involvement of Fgf3 in olfactory and GnRH system development too; and, if so, whether *FGF3* mutations are found in KS patients. If Fgf3 morpholinos, when titrated down with KA4/KB4 to non-functioning levels, do not give the same result as the Fgf8a MO (i.e. AC defects), it will indicate that Kal1a/Kal1b do not signal via the Fgf3 pathway, thus permitting Fgf3 to be used as a negative control for similar future experiments testing the role of other putative Fgf ligands.

Up to 30% of KS patients with mutations in the *KAL1* gene also present with a missing kidney (unilateral renal agenesis) (Kim et al., 2008), indicating that anosmin-1 may have a role in human kidney development. In zebrafish, *Kal1a* and *Kal1b* are expressed in the region of the developing pronephric duct, the zebrafish equivalent of a kidney, from around 24hpf onwards (*see appendix, Figure A1*); suggesting that the putative role of anosmin-1 in kidney development is also conserved in the zebrafish. A future aim of this project is to investigate the putative role of Kal1a and Kal1b during zebrafish pronephros morphogenesis, using various early-expressing pronephric markers.

Chapter 6

Final Conclusions

Kallmann syndrome is a congenital disorder of olfactory and pubertal failure, resulting from olfactory bulb dysgenesis and hypothalamic GnRH neuronal loss, respectively. These defects are proposed to result from a failure of olfactory axons to target the anterior telencephalon, combined with a failure of GnRH neurons to migrate into the hypothalamus, during early embryogenesis.

Broadly speaking, the rostral-caudal distribution of GnRH neurons along the ventral telencephalon and diencephalon is evolutionarily conserved across vertebrates, including humans, mice, chickens, and zebrafish. However, there are some distinct differences in the early ontogeny of the GnRH system in these species. Human, chick and mouse embryos exhibit the classical 'migratory stream' of GnRH-immunoreactive neurons detected at their origin in the nasal compartment, migrating across the nasal-forebrain junction, and then on into the hypothalamus. Whereas, in zebrafish embryos, GnRH-immunoreactive cells are first detected in the terminal nerve region (adjacent to the olfactory epithelium), and then much later (in comparative developmental staging) in the hypothalamus from around 1-2 weeks later.

However, using a transgenic reporter line which labelled all GnRH3-expressing cells with a red fluorescent protein, it was possible to detect a much earlier hypothalamic GnRH neuronal population, soon after the appearance of the terminal nerve GnRH cells at the nasal compartment region. Although the GnRH neuronal identity is yet to be verified (i.e. confirmed that they are *bona fide* 'endocrine' GnRH cells), we have speculated that there may be two 'waves' of hypothalamic GnRH neuronal migration and/or accumulation: one occurring around the time of (or before) the olfactory axons reach the anterior forebrain ('the early wave'); and a much later 'wave' occurring after olfactory bulb morphogenesis ('the

later wave'). This hypothesis is consistent with observations of two waves of GnRH neuronal migration during human embryogenesis. The early wave of GnRH cells was detected just rostral to the optic chiasm, and just caudal to (and closely abutting with) the presumptive pituitary.

Whilst the origin of the *'later wave'* of hypothalamic GnRH neuronal migration is likely to be within the nasal compartment (from where they then migrate into the forebrain); the origin of the proposed *'early wave'* of GnRH neurons is less certain. For example, these *'early wave'* GnRH cells may also arise within the nasal compartment region and pioneer a pathway into the hypothalamus, thus, perhaps establishing the migratory route for the much later wave of GnRH neuronal migration. The absence of early GnRH neuronal detection along this pathway may simply indicate the absence of GnRH expression of these cells until they reach the hypothalamus. Unfortunately, the absence of early GnRH neuronal progenitor markers has so far hampered further investigation of this proposal. Alternatively, some or all of the hypothalamic GnRH neurons may arise from a stem cell population within the diencephalon itself, thus negating the requirement for migration of this *'early wave'*. However, using pGnRH3:mCherry, the presence of mCherry-positive cells within the olfactory epithelium around 30-36hpf may suggest that cells within the olfactory epithelium do contribute to the GnRH neuronal system in zebrafish.

The kisspeptin-GPR54 signalling pathway has an important role in the onset of puberty in vertebrates. However, when the two GPR54 and KiSS1 orthologues were upregulated during zebrafish embryogenesis, there were no observable abnormalities in terminal nerve GnRH expression; or premature GnRH immuno-expression within the hypothalamus. Although, gene knockdown strategies will need to be carried out to confirm whether or not kisspeptin-Gpr54 signalling has a role in the formation of the GnRH system during zebrafish embryogenesis.

Two of the autosomal genes which have been implicated in around 10-15% of KS cases are *FGFR1* and *FGF8*. Both genes have previously been shown to have an important role in olfactory bulb morphogenesis and hypothalamic GnRH neuronal development; the two main systems affected in KS patients with mutations

in these genes. Moreover, these genes also have a very important role at the midline where Fgf8/Fgfr1 signalling has been shown to have a very important role in brain commissure formation.

Zebrafish have two orthologues of FGFR1 (Fgfr1a and Fgfr1b), as well as two orthologues of FGF8 (Fgf8a and Fgf8b). Using the zebrafish model system which was established in chapter 3, the role of Fgf8a/Fgf8b, as well as Fgfr signalling in general, during GnRH/olfactory neurogenesis and forebrain commissure formation were further investigated in chapter 4.

It has been proposed that olfactory bulb morphogenesis is induced by the arrival of olfactory axon terminals, which bring about a local Fgf-dependent reduction in proliferation (and increase in differentiation), which allows the olfactory bulb to evaginate from the anterior telencephalon. Therefore, the accurate pathfinding of olfactory axons to the anterior telencephalon is an essential pre-requisite for olfactory bulb morphogenesis; and it has been proposed that a failure in the terminal axonogenesis of the olfactory axons is the cause of olfactory bulb dysgenesis in human KS patients.

Knocking down *Fgf8a* gene function in the zebrafish resulted in smaller olfactory epithelia, combined with fewer and/or mis-projected olfactory axons. Similarly, blocking Fgfr signalling between 14-22hpf gave similar defects in olfactory axonogenesis; demonstrating that this may be the critical period for Fgf8a signalling. It was previously demonstrated in Fgf8 conditional mouse mutants, that Fgf8 is required for olfactory neurogenesis in the olfactory epithelium, and that loss of Fgf8 in this region results in increased olfactory neuronal cell death. We speculate that Fgf8a, which is expressed in the olfactory placodes in zebrafish, may also have a role in olfactory neurogenesis, by maintaining the survival of an olfactory stem cell population in the olfactory epithelium; however, this mechanism is yet to be proven in zebrafish. We propose that the failure and/or abnormalities in olfactory axonogenesis in zebrafish may be secondary to the reduction in normal olfactory neurogenesis in the olfactory epithelium i.e. the increased cell death, and improperly-specified olfactory neurons which may lack their normal olfactory path-finding apparatus. However, further experiments will be required to assess the

specific role of Fgf signalling in the correct navigation of the olfactory axons to the anterior telencephalon e.g. by using constructs which cause the loss of Fgf signalling in a small subset of olfactory neurons (or single neurons) at the expected time of olfactory axonogenesis (around 24hpf). Similarly, transplantation of Fgf-deficient olfactory epithelial cells to the olfactory pits of wild-type embryos will also help us to understand the pathfinding capabilities of Fgf-deficient olfactory axons.

As well as their important role in olfactory bulb morphogenesis, previous studies in mice have also shown that Fgf8 and Fgfr1 are required for development of the GnRH system; hence, mice which are homozygous for hypomorphic *Fgf8* or *Fgfr1* (but not *Fgfr3*) have absent or fewer hypothalamic GnRH neurons. Similarly, zebrafish *Fgf8a* morphants also had reduced/absent *'early wave'* hypothalamic GnRH cells (the effects on 'the later wave' are yet to be assessed). The failure of normal olfactory axonogenesis in these mouse and zebrafish mutants suggests that the loss/reduction of hypothalamic GnRH cells may be caused by the abnormalities/loss of the olfactory/vomeronasal axonal 'scaffold' which they require for their migration. However, in the mouse *Fgf8* mutant, the GnRH cells never emerge from the olfactory pit (i.e. they are not specified); such an absence makes it impossible to comment on whether or not they are capable of migrating into the hypothalamus. Similarly, absence of the *'early wave'* in the zebrafish *Fgf8a* morphants may signify a failure in the specification at the nasal compartment or in the diencephalon. Identification of markers for early GnRH progenitors in zebrafish will assist in the investigation of whether or not the hypothalamic GnRH cells are improperly specified in the *Fgf8a* morphants.

Mice deficient in Fgf8 or Fgfr1 have severe midline defects, which include failure of commissure formation. Similarly, zebrafish *Fgf8a* mutants lack proper forebrain commissure formation; as do embryos which have their Fgfr signalling blocked between 14hpf and 22hpf. It has been demonstrated in mice that loss of Fgf signalling blocks formation of the midline glial structures which have a crucial role in guiding commissural axons across the midline; however, Fgf signalling is also likely to have a second role in commissural axonogenesis as well, as heterozygote *Fgfr1* mutants have normal midline glial structures, but still have failed commissure

formation. Similarly, it is proposed that the anterior commissure (AC) and post-optic commissure (POC) in the zebrafish forebrain also require 'glial bridges' to guide their commissural axons across the midline and by 'channelling' through the correct decussation point.

Although an important role for the second FGF8 orthologue, Fgf8b, during GnRH/olfactory neurogenesis and forebrain commissure formation could not be established, the failure to completely knockdown *Fgf8b* gene function means that such a putative role cannot be ruled out yet. As such, further Fgf8b morpholinos will need to be tested, in order to try and attain an approximately 100% knockdown of *Fgf8b*.

Kal1a and *Kal1b* are the two zebrafish orthologues of *KAL1*, the gene implicated in patients with X-linked KS. At the outset of this project, no reports had been published using zebrafish (or any other vertebrate) as an *in vivo* model to study the role of Kal1/Kal1b during development. However, during this time period, there have been two reports regarding the essential role of Kal1a, but not Kal1b, during development of the 'endocrine' (hypothalamic) GnRH cells and the targeting of the olfactory axons to the presumptive olfactory bulb region. However, using different morpholino approaches, combined with alternative GnRH and olfactory analyses, as well as assessment of the forebrain commissure phenotype, we were able to further advance the understanding of the role played by Kal1a and Kal1b during zebrafish forebrain development.

Specifically, we found that, similar to the *Fgf8a* morphants, *Kal1a+Kal1b* morphants had smaller olfactory epithelia, with absent, fewer and/or aberrant projections to the presumptive olfactory bulb region, combined with loss/reduction of *'early wave'* hypothalamic GnRH neurons. Moreover, a specific role for Kal1b in AC formation was also determined; although, much more severe, fully penetrant, defects in AC/POC formation were obtained in the *Kal1a+Kal1b* morphants. So, in summary, we observed that Kal1a and Kal1b are required together for proper olfactory/GnRH neuronal development and forebrain commissure formation, using splice-blocking morpholino approaches.

The defects in forebrain commissure formation seen in the *Fgf8a* and *Kal1a/Kal1b* morphants are similar to the corpus callosum commissure defects that have been reported in some X-linked and autosomal KS patients, suggesting that defects in commissure formation may be the source of the upper body mirror movements which may be seen in these patients.

It was previously demonstrated, using *in vitro* cell cultures, that anosmin-1 interacts with, and modulates the signalling of FGFR1, which is understood to be the main Fgf receptor for Fgf8 during mouse telencephalic development. Together with the findings here that *Fgf8a* and *Kal1a/Kal1b* expression in the nasal compartment overlap during early development, and that the forebrain defects caused by their knockdown are similar, suggest that Kal1a/Kal1b may be acting via the Fgf8a signalling pathway during olfactory/GnRH neuronal development and forebrain commissure formation. If so, this may suggest that Kal1a/Kal1b may be modulating Fgf8 signalling in the nasal compartment, and thus, by extension, means that Kal1a/Kal1b also have a role in maintenance of olfactory (and GnRH) neurogenesis in this region. Similarly, Kal1a and Kal1b may also have a role in modulating Fgf signalling during olfactory bulb morphogenesis; as well as during midline glial bridge formation and/or commissural axonogenesis. These proposed roles, will, of course, need to be investigated further and confirmed.

In order to try and establish whether Kal1a/Kal1b may be acting via the Fgf8a signalling pathway *in vivo*, Kal1a/Kal1b and Fgf8b morpholinos were titrated down to levels where there were no (or subtle) AC defects; and then injected together at these concentrations. The data is preliminary, and will need to be repeated and confirmed with negative controls, but it does suggest that Kal1a/Kal1b are acting together with Fgf8a during AC formation. However, the mechanism of action will need to be investigated further.

Some of the other future aims include utilising behavioural assays to assess the actual olfactory and reproductive capabilities of the *Kal1a/Kal1b* and *Fgf8a* morphants. Also, the molecular/developmental basis of the other occasional defects, such as kidney dysgenesis, should also be investigated.

Currently, the genes underlying only around 30-40% of KS cases have thus far been identified. Future work will involve using the zebrafish model established in this project, along with the human KS patient DNA database, to identify the remaining 60-70% of causative genes. It is likely that other upstream and downstream modulators and effectors of Fgf signalling will be involved; and possibly other FGF ligands and/or receptors. Understanding the other genes involved in KS, and other hypogonadotrophic hypogonadic disorders may help in the identification of novel targets for modulating puberty and/or reproductive competency in adults. Furthermore, a better understanding of the Fgf signalling pathway, as well as the other molecular pathways required for the development of the reproductive and olfactory systems, may prove beneficial for identifying novel routes to treatments and diagnosis of other conditions, such as spinal repair and some cancers, which also involve the FGF signalling pathway in their pathologies.

References

Abraham,E., Palevitch,O., Gothilf,Y., and Zohar,Y. (2009). The zebrafish as a model system for forebrain GnRH neuronal development. Gen. Comp Endocrinol.

Abraham,E., Palevitch,O., Gothilf,Y., and Zohar,Y. (2010). Targeted gonadotropin-releasing hormone-3 neuron ablation in zebrafish: effects on neurogenesis, neuronal migration, and reproduction. Endocrinology 151, 332-340.

Abraham,E., Palevitch,O., Ijiri,S., Du,S.J., Gothilf,Y., and Zohar,Y. (2008). Early development of forebrain gonadotrophin-releasing hormone (GnRH) neurones and the role of GnRH as an autocrine migration factor. J. Neuroendocrinol. 20, 394-405.

Achermann,J.C., Weiss,J., Lee,E.J., and Jameson,J.L. (2001). Inherited disorders of the gonadotropin hormones. Mol. Cell Endocrinol. 179, 89-96.

Andrenacci,D., Le,B.S., Rosaria,G.M., Rugarli,E., and Graziani,F. (2004). Embryonic expression pattern of the Drosophila Kallmann syndrome gene kal-1. Gene Expr. Patterns. 5, 67-73.

Ardouin,O., Legouis,R., Fasano,L., David-Watine,B., Korn,H., Hardelin,J., and Petit,C. (2000). Characterization of the two zebrafish orthologues of the KAL-1 gene underlying X chromosome-linked Kallmann syndrome. Mech. Dev. 90, 89-94.

Ayari,B. and Soussi-Yanicostas,N. (2007). FGFR1 and anosmin-1 underlying genetically distinct forms of Kallmann syndrome are co-expressed and interact in olfactory bulbs. Dev. Genes Evol. 217, 169-175.

Barresi,M.J., Hutson,L.D., Chien,C.B., and Karlstrom,R.O. (2005). Hedgehog regulated Slit expression determines commissure and glial cell position in the zebrafish forebrain. Development 132, 3643-3656.

Bribian,A., Esteban,P.F., Clemente,D., Soussi-Yanicostas,N., Thomas,J.L., Zalc,B., and de,C.F. (2008). A novel role for anosmin-1 in the adhesion and migration of oligodendrocyte precursors. Dev. Neurobiol. 68, 1503-1516.

Britto,J.A., Evans,R.D., Hayward,R.D., and Jones,B.M. (2002). Toward pathogenesis of Apert cleft palate: FGF, FGFR, and TGF beta genes are differentially expressed in sequential stages of human palatal shelf fusion. Cleft Palate Craniofac. J. 39, 332-340.

Bulow,H.E., Berry,K.L., Topper,L.H., Peles,E., and Hobert,O. (2002). Heparan sulfate proteoglycan-dependent induction of axon branching and axon misrouting by the Kallmann syndrome gene kal-1. Proc. Natl. Acad. Sci. U. S. A 99, 6346-6351.

Bulow,H.E. and Hobert,O. (2004). Differential sulfations and epimerization define heparan sulfate specificity in nervous system development. Neuron 41, 723-736.

Cadman,S.M., Kim,S.H., Hu,Y., Gonzalez-Martinez,D., and Bouloux,P.M. (2007). Molecular pathogenesis of Kallmann's syndrome. Horm. Res. 67, 231-242.

Calof,A.L. and Chikaraishi,D.M. (1989). Analysis of neurogenesis in a mammalian neuroepithelium: proliferation and differentiation of an olfactory neuron precursor *in vitro*. Neuron 3, 115-127.

Cariboni,A., Maggi,R., and Parnavelas,J.G. (2007). From nose to fertility: the long migratory journey of gonadotropin-releasing hormone neurons. Trends Neurosci. 30, 638-644.

Cariboni,A., Pimpinelli,F., Colamarino,S., Zaninetti,R., Piccolella,M., Rumio,C., Piva,F., Rugarli,E.I., and Maggi,R. (2004). The product of X-linked Kallmann's syndrome gene (KAL1) affects the migratory activity of gonadotropin-releasing hormone (GnRH)-producing neurons. Hum. Mol. Genet. 13, 2781-2791.

Chalouhi,C., Faulcon,P., Le,B.C., Hertz-Pannier,L., Bonfils,P., and Abadie,V. (2005). Olfactory evaluation in children: application to the CHARGE syndrome. Pediatrics 116, e81-e88.

Chan,Y.M., de,G.A., Lang-Muritano,M., Plummer,L., Cerrato,F., Tsiaras,S., Gaspert,A., Lavoie,H.B., Wu,C.H., Crowley,W.F., Jr., Amory,J.K., Pitteloud,N., and Seminara,S.B. (2009). GNRH1 mutations in patients with idiopathic hypogonadotropic hypogonadism. Proc. Natl. Acad. Sci. U. S. A 106, 11703-11708.

Chellaiah,A., Yuan,W., Chellaiah,M., and Ornitz,D.M. (1999). Mapping ligand binding domains in chimeric fibroblast growth factor receptor molecules. Multiple regions determine ligand binding specificity. J. Biol. Chem. 274, 34785-34794.

Chung,W.C., Moyle,S.S., and Tsai,P.S. (2008). Fibroblast growth factor 8 signaling through fibroblast growth factor receptor 1 is required for the emergence of gonadotropin-releasing hormone neurons. Endocrinology 149, 4997-5003.

Coatesworth,A.P. and Woodhead,C.J. (2002). Conductive hearing loss associated with Kallmann's syndrome. J. Laryngol. Otol. 116, 125-126.

Danesin,C., Peres,J.N., Johansson,M., Snowden,V., Cording,A., Papalopulu,N., and Houart,C. (2009). Integration of telencephalic Wnt and hedgehog signaling center activities by Foxg1. Dev. Cell 16, 576-587.

Deng,C., Wynshaw-Boris,A., Zhou,F., Kuo,A., and Leder,P. (1996). Fibroblast growth factor receptor 3 is a negative regulator of bone growth. Cell 84, 911-921.

Dhillo,W.S., Chaudhri,O.B., Patterson,M., Thompson,E.L., Murphy,K.G., Badman,M.K., McGowan,B.M., Amber,V., Patel,S., Ghatei,M.A., and Bloom,S.R. (2005). Kisspeptin-54 stimulates the hypothalamic-pituitary gonadal axis in human males. J. Clin. Endocrinol. Metab 90, 6609-6615.

Dickinson,R.J., Eblaghie,M.C., Keyse,S.M., and Morriss-Kay,G.M. (2002). Expression of the ERK-specific MAP kinase phosphatase PYST1/MKP3 in mouse embryos during morphogenesis and early organogenesis. Mech. Dev. 113, 193-196.

Dode,C. and Hardelin,J.P. (2010). Clinical genetics of Kallmann syndrome. Ann. Endocrinol. (Paris) 71, 149-157.

Dode,C., Levilliers,J., Dupont,J.M., De,P.A., Le,D.N., Soussi-Yanicostas,N., Coimbra,R.S., Delmaghani,S., Compain-Nouaille,S., Baverel,F., Pecheux,C., Le,T.D., Cruaud,C., Delpech,M., Speleman,F., Vermeulen,S., Amalfitano,A., Bachelot,Y., Bouchard,P., Cabrol,S., Carel,J.C., Delemarre-van de Waal,H., Goulet-Salmon,B., Kottler,M.L., Richard,O., Sanchez-Franco,F., Saura,R., Young,J., Petit,C., and Hardelin,J.P. (2003). Loss-of-function mutations in FGFR1 cause autosomal dominant Kallmann syndrome. Nat. Genet. 33, 463-465.

Dode,C., Teixeira,L., Levilliers,J., Fouveaut,C., Bouchard,P., Kottler,M.L., Lespinasse,J., Lienhardt-Roussie,A., Mathieu,M., Moerman,A., Morgan,G., Murat,A., Toublanc,J.E., Wolczynski,S., Delpech,M., Petit,C., Young,J., and Hardelin,J.P. (2006). Kallmann syndrome: mutations in the genes encoding prokineticin-2 and prokineticin receptor-2. PLoS. Genet. 2, e175.

Duke,V.M., Winyard,P.J., Thorogood,P., Soothill,P., Bouloux,P.M., and Woolf,A.S. (1995). KAL, a gene mutated in Kallmann's syndrome, is expressed in the first trimester of human development. Mol. Cell Endocrinol. 110, 73-79.

Dynes,J.L. and Ngai,J. (1998). Pathfinding of olfactory neuron axons to stereotyped glomerular targets revealed by dynamic imaging in living zebrafish embryos. Neuron 20, 1081-1091.

Elsalini,O.A. and Rohr,K.B. (2003). Phenylthiourea disrupts thyroid function in developing zebrafish. Dev. Genes Evol. 212, 593-598.

Eswarakumar,V.P., Lax,I., and Schlessinger,J. (2005). Cellular signaling by fibroblast growth factor receptors. Cytokine Growth Factor Rev. 16, 139-149.

Falardeau,J., Chung,W.C., Beenken,A., Raivio,T., Plummer,L., Sidis,Y., Jacobson-Dickman,E.E., Eliseenkova,A.V., Ma,J., Dwyer,A., Quinton,R., Na,S., Hall,J.E., Huot,C., Alois,N., Pearce,S.H., Cole,L.W., Hughes,V., Mohammadi,M., Tsai,P., and Pitteloud,N. (2008). Decreased FGF8 signaling causes deficiency of gonadotropin-releasing hormone in humans and mice. J. Clin. Invest 118, 2822-2831.

Feng,B., Chung,W.C., Au,M.G., Plummer,L., Dwyer,A., Quinton,R., Seminara,S.B., Chenoine,J.P., Sykiotis,J.P., Sidis,Y., Tsai,P., and Pitteloud,N. (2010). SEF Is a Novel Locus for GnRH Deficiency (P2-278). Endocrine Reviews, Supplement 1, 31, S1153.

Filby,A.L., van,A.R., Duitman,J., and Tyler,C.R. (2008). The kisspeptin/gonadotropin-releasing hormone pathway and molecular signaling of puberty in fish. Biol. Reprod. 78, 278-289.

Foley,J.E., Yeh,J.R., Maeder,M.L., Reyon,D., Sander,J.D., Peterson,R.T., and Joung,J.K. (2009). Rapid mutation of endogenous zebrafish genes using zinc finger nucleases made by Oligomerized Pool ENgineering (OPEN). PLoS. One. 4, e4348.

Ford-Perriss,M., Guimond,S.E., Greferath,U., Kita,M., Grobe,K., Habuchi,H., Kimata,K., Esko,J.D., Murphy,M., and Turnbull,J.E. (2002). Variant heparan sulfates synthesized in developing mouse brain differentially regulate FGF signaling. Glycobiology 12, 721-727.

Furthauer,M., Reifers,F., Brand,M., Thisse,B., and Thisse,C. (2001). sprouty4 acts in vivo as a feedback-induced antagonist of FGF signaling in zebrafish. Development 128, 2175-2186.

Gill,J.C., Moenter,S.M., and Tsai,P.S. (2004). Developmental regulation of gonadotropin-releasing hormone neurons by fibroblast growth factor signaling. Endocrinology 145, 3830-3839.

Gong,Q. and Shipley,M.T. (1995). Evidence that pioneer olfactory axons regulate telencephalon cell cycle kinetics to induce the formation of the olfactory bulb. Neuron 14, 91-101.

Gonzalez-Martinez,D., Hu,Y., and Bouloux,P.M. (2004a). Ontogeny of GnRH and olfactory neuronal systems in man: novel insights from the investigation of inherited forms of Kallmann's syndrome. Front Neuroendocrinol. 25, 108-130.

Gonzalez-Martinez,D., Kim,S.H., Hu,Y., Guimond,S., Schofield,J., Winyard,P., Vannelli,G.B., Turnbull,J., and Bouloux,P.M. (2004b). Anosmin-1 modulates fibroblast growth factor receptor 1 signaling in human gonadotropin-releasing hormone olfactory neuroblasts through a heparan sulfate-dependent mechanism. J. Neurosci. 24, 10384-10392.

Graziadei,G.A. and Graziadei,P.P. (1979a). Neurogenesis and neuron regeneration in the olfactory system of mammals. II. Degeneration and reconstitution of the olfactory sensory neurons after axotomy. J. Neurocytol. 8, 197-213.

Graziadei,P.P. and Graziadei,G.A. (1979b). Neurogenesis and neuron regeneration in the olfactory system of mammals. I. Morphological aspects of differentiation and structural organization of the olfactory sensory neurons. J. Neurocytol. 8, 1-18.

Graziadei,P.P. and Monti Graziadei,G.A. (1986). Principles of organization of the vertebrate olfactory glomerulus: an hypothesis. Neuroscience 19, 1025-1035.

Grus,W.E., Shi,P., Zhang,Y.P., and Zhang,J. (2005). Dramatic variation of the vomeronasal pheromone receptor gene repertoire among five orders of placental and marsupial mammals. Proc. Natl. Acad. Sci. U. S. A 102, 5767-5772.

Guimond,S.E. and Turnbull,J.E. (1999). Fibroblast growth factor receptor signalling is dictated by specific heparan sulphate saccharides. Curr. Biol. 9, 1343-1346.

Hall,B.D. (1979). Choanal atresia and associated multiple anomalies. J. Pediatr. 95, 395-398.

Hall,B.D. (1979). Choanal atresia and associated multiple anomalies. J. Pediatr. 95, 395-398.

Hamburger,V. and Hamilton,H.L. (1992). A series of normal stages in the development of the chick embryo. 1951. Dev. Dyn. 195, 231-272.
Hatta,K., Tsujii,H., and Omura,T. (2006). Cell tracking using a photoconvertible fluorescent protein. Nat. Protoc. 1, 960-967.

Hayhurst,M. and McConnell,S.K. (2003). Mouse models of holoprosencephaly. Curr. Opin. Neurol. 16, 135-141.

Hebert,J.M., Lin,M., Partanen,J., Rossant,J., and McConnell,S.K. (2003). FGF signaling through FGFR1 is required for olfactory bulb morphogenesis. Development 130, 1101-1111.

Herzog,W., Sonntag,C., von der,H.S., Roehl,H.H., Varga,Z.M., and Hammerschmidt,M. (2004). Fgf3 signaling from the ventral diencephalon is required for early specification and subsequent survival of the zebrafish adenohypophysis. Development 131, 3681-3692.

Hsu,P., Yu,F., Feron,F., Pickles,J.O., Sneesby,K., and kay-Sim,A. (2001). Basic fibroblast growth factor and fibroblast growth factor receptors in adult olfactory epithelium. Brain Res. 896, 188-197.

Hu,Y. (2005). Functional and structural studies of anosmin-1, the protein implicated in X-linked Kallmann’s syndrome. Ph.D. Thesis. University College London: U.K.

Hu,Y., Gonzalez-Martinez,D., Kim,S.H., and Bouloux,P.M. (2004). Cross-talk of anosmin-1, the protein implicated in X-linked Kallmann's syndrome, with heparan sulphate and urokinase-type plasminogen activator. Biochem. J. 384, 495-505.

Hu,Y., Guimond,S.E., Travers,P., Cadman,S., Hohenester,E., Turnbull,J.E., Kim,S.H., and Bouloux,P.M. (2009). Novel mechanisms of fibroblast growth factor receptor 1 regulation by extracellular matrix protein anosmin-1. J. Biol. Chem.

Hu,Y., Sun,Z., Eaton,J.T., Bouloux,P.M., and Perkins,S.J. (2005). Extended and flexible domain solution structure of the extracellular matrix protein anosmin-1 by X-ray scattering, analytical ultracentrifugation and constrained modelling. J. Mol. Biol. 350, 553-570.

Hu,Y., Tanriverdi,F., MacColl,G.S., and Bouloux,P.M. (2003). Kallmann's syndrome: molecular pathogenesis. Int. J. Biochem. Cell Biol. 35, 1157-1162.

Inatani,M., Irie,F., Plump,A.S., Tessier-Lavigne,M., and Yamaguchi,Y. (2003). Mammalian brain morphogenesis and midline axon guidance require heparan sulfate. Science 302, 1044-1046.

Jovelin,R., He,X., Amores,A., Yan,Y.L., Shi,R., Qin,B., Roe,B., Cresko,W.A., and Postlethwait,J.H. (2007). Duplication and divergence of fgf8 functions in teleost development and evolution. J. Exp. Zool. B Mol. Dev. Evol. 308, 730-743.

Kallmann,F.J., Schönfeld,W.A., and Barrera,S.E. (1944). The genetic aspects of primary eunuchoidism. Am J Ment Defic 48, 203-236.

Kawai,T., Oka,Y., and Eisthen,H. (2009). The role of the terminal nerve and GnRH in olfactory system neuromodulation. Zoolog. Sci. 26, 669-680.

Kawauchi,S., Shou,J., Santos,R., Hebert,J.M., McConnell,S.K., Mason,I., and Calof,A.L. (2005). Fgf8 expression defines a morphogenetic center required for olfactory neurogenesis and nasal cavity development in the mouse. Development 132, 5211-5223.

Kim,H.H., Wolfe,A., Smith,G.R., Tobet,S.A., and Radovick,S. (2002). Promoter sequences targeting tissue-specific gene expression of hypothalamic and ovarian gonadotropin-releasing hormone in vivo. J. Biol. Chem. 277, 5194-5202.

Kim,S.H., Hu,Y., Cadman,S., and Bouloux,P. (2008). Diversity in fibroblast growth factor receptor 1 regulation: learning from the investigation of Kallmann syndrome. J. Neuroendocrinol. 20, 141-163.

Kitahashi,T., Ogawa,S., and Parhar,I.S. (2009). Cloning and expression of kiss2 in the zebrafish and medaka. Endocrinology 150, 821-831.

Klein,V.R., Friedman,J.M., Brookshire,G.S., Brown,O.E., and Edman,C.D. (1987). Kallmann syndrome associated with choanal atresia. Clin. Genet. 31, 224-227.

Kleinjan,D.A., Bancewicz,R.M., Gautier,P., Dahm,R., Schonthaler,H.B., Damante,G., Seawright,A., Hever,A.M., Yeyati,P.L., van,H., V, and Coutinho,P. (2008). Subfunctionalization of duplicated zebrafish pax6 genes by cis-regulatory divergence. PLoS. Genet. 4, e29.

Koenigkam-Santos,M., Santos,A.C., Borduqui,T., Versiani,B.R., Hallak,J.E., Crippa,J.A., and Castro,M. (2008). Whole-brain voxel-based morphometry in Kallmann syndrome associated with mirror movements. AJNR Am. J. Neuroradiol. 29, 1799-1804.

Kotani,M., Detheux,M., Vandenbogaerde,A., Communi,D., Vanderwinden,J.M., Le,P.E., Brezillon,S., Tyldesley,R., Suarez-Huerta,N., Vandeput,F., Blanpain,C., Schiffmann,S.N., Vassart,G., and Parmentier,M. (2001). The metastasis suppressor gene KiSS-1 encodes kisspeptins, the natural ligands of the orphan G protein-coupled receptor GPR54. J. Biol. Chem. 276, 34631-34636.

Kramer,P.R. and Wray,S. (2000). Novel gene expressed in nasal region influences outgrowth of olfactory axons and migration of luteinizing hormone-releasing hormone (LHRH) neurons. Genes Dev. 14, 1824-1834.

Krams,M., Quinton,R., Ashburner,J., Friston,K.J., Frackowiak,R.S., Bouloux,P.M., and Passingham,R.E. (1999). Kallmann's syndrome: mirror movements associated with bilateral corticospinal tract hypertrophy. Neurology 52, 816-822.

Laemmli, U. K. (1970). Cleavage of structural proteins during the assembly of the head of bacteriophage T4. Nature 227, 680-5.

Kuo,M.W., Lou,S.W., Postlethwait,J., and Chung,B.C. (2005). Chromosomal organization, evolutionary relationship, and expression of zebrafish GnRH family members. J. Biomed. Sci. 12, 629-639.

Lee,Y., Grill,S., Sanchez,A., Murphy-Ryan,M., and Poss,K.D. (2005). Fgf signaling instructs position-dependent growth rate during zebrafish fin regeneration. Development 132, 5173-5183.

Legouis,R., Cohen-Salmon,M., del,C., I, Levilliers,J., Capy,L., Mornow,J.P., and Petit,C. (1993a). Characterization of the chicken and quail homologues of the human gene responsible for the X-linked Kallmann syndrome. Genomics 17, 516-518.

Legouis,R., Hardelin,J.P., Petit,C., and Ayer-Le,L.C. (1994). Early expression of the KAL gene during embryonic development of the chick. Anat. Embryol. (Berl) 190, 549-562.

Legouis,R., Lievre,C.A., Leibovici,M., Lapointe,F., and Petit,C. (1993b). Expression of the KAL gene in multiple neuronal sites during chicken development. Proc. Natl. Acad. Sci. U. S. A 90, 2461-2465.

Lindwall,C., Fothergill,T., and Richards,L.J. (2007). Commissure formation in the mammalian forebrain. Curr. Opin. Neurobiol. 17, 3-14.

Liu,N.A., Huang,H., Yang,Z., Herzog,W., Hammerschmidt,M., Lin,S., and Melmed,S. (2003). Pituitary corticotroph ontogeny and regulation in transgenic zebrafish. Mol. Endocrinol. 17, 959-966.

Lo,T.W., Bennett,D.C., Goodman,S.J., and Stern,M.J. (2010). Caenorhabditis elegans fibroblast growth factor receptor signaling can occur independently of the multi-substrate adaptor FRS2. Genetics 185, 537-547.

Lutz,B., Kuratani,S., Rugarli,E.I., Wawersik,S., Wong,C., Bieber,F.R., Ballabio,A., and Eichele,G. (1994). Expression of the Kallmann syndrome gene in human fetal brain and in the manipulated chick embryo. Hum. Mol. Genet. 3, 1717-1723.

MacColl,G., Bouloux,P., and Quinton,R. (2002). Kallmann syndrome: adhesion, afferents, and anosmia. Neuron 34, 675-678.

Maestre de San Juan,A. (1856). Teratolagia: falta total de los nervios olfactorios con anosmia en un individuo en quien existia una atrofia congenita de los testiculos y miembro viril. El siglo medico, Madrid, p 211.

Markakis,E.A., Palmer,T.D., Randolph-Moore,L., Rakic,P., and Gage,F.H. (2004). Novel neuronal phenotypes from neural progenitor cells. J. Neurosci. 24, 2886-2897.

Maroon,H., Walshe,J., Mahmood,R., Kiefer,P., Dickson,C., and Mason,I. (2002). Fgf3 and Fgf8 are required together for formation of the otic placode and vesicle. Development 129, 2099-2108.

Mason,I. (2007). Initiation to end point: the multiple roles of fibroblast growth factors in neural development. Nat. Rev. Neurosci. 8, 583-596.

Matsumoto,S., Yamazaki,C., Masumoto,K.H., Nagano,M., Naito,M., Soga,T., Hiyama,H., Matsumoto,M., Takasaki,J., Kamohara,M., Matsuo,A., Ishii,H., Kobori,M., Katoh,M., Matsushime,H., Furuichi,K., and Shigeyoshi,Y. (2006). Abnormal development of the olfactory bulb and reproductive system in mice lacking prokineticin receptor PKR2. Proc. Natl. Acad. Sci. U. S. A 103, 4140-4145.

Matsuo,T., Okamoto,S., Izumi,Y., Hosokawa,A., Takegawa,T., Fukui,H., Tun,Z., Honda,K., Matoba,R., Tatsumi,K., and Amino,N. (2000). A novel mutation of the KAL1 gene in monozygotic twins with Kallmann syndrome. Eur. J. Endocrinol. 143, 783-787.

Messager,S., Chatzidaki,E.E., Ma,D., Hendrick,A.G., Zahn,D., Dixon,J., Thresher,R.R., Malinge,I., Lomet,D., Carlton,M.B., Colledge,W.H., Caraty,A., and Aparicio,S.A. (2005). Kisspeptin directly stimulates gonadotropin-releasing hormone release via G protein-coupled receptor 54. Proc. Natl. Acad. Sci. U. S. A 102, 1761-1766.

Meyers,E.N., Lewandoski,M., and Martin,G.R. (1998). An Fgf8 mutant allelic series generated by Cre- and Flp-mediated recombination. Nat. Genet. 18, 136-141.

Miura,K., Acierno,J.S., Jr., and Seminara,S.B. (2004). Characterization of the human nasal embryonic LHRH factor gene, NELF, and a mutation screening among 65 patients with idiopathic hypogonadotropic hypogonadism (IHH). J. Hum. Genet. 49, 265-268.

Miyasaka,N., Knaut,H., and Yoshihara,Y. (2007). Cxcl12/Cxcr4 chemokine signaling is required for placode assembly and sensory axon pathfinding in the zebrafish olfactory system. Development 134, 2459-2468.

Mochizuki,Y., Tsuda,S., Kanetake,H., and Kanda,S. (2002). Negative regulation of urokinase-type plasminogen activator production through FGF-2-mediated activation of phosphoinositide 3-kinase. Oncogene 21, 7027-7033.

Mohammadi,M., McMahon,G., Sun,L., Tang,C., Hirth,P., Yeh,B.K., Hubbard,S.R., and Schlessinger,J. (1997). Structures of the tyrosine kinase domain of fibroblast growth factor receptor in complex with inhibitors. Science 276, 955-960.

Mohammadi,M., Olsen,S.K., and Ibrahimi,O.A. (2005). Structural basis for fibroblast growth factor receptor activation. Cytokine Growth Factor Rev. 16, 107-137.

Molina,G.A., Watkins,S.C., and Tsang,M. (2007). Generation of FGF reporter transgenic zebrafish and their utility in chemical screens. BMC. Dev. Biol. 7, 62.

Monnier,C., Dode,C., Fabre,L., Teixeira,L., Labesse,G., Pin,J.P., Hardelin,J.P., and Rondard,P. (2009). PROKR2 missense mutations associated with Kallmann syndrome impair receptor signalling activity. Hum. Mol. Genet. 18, 75-81.

Ng,K.L., Li,J.D., Cheng,M.Y., Leslie,F.M., Lee,A.G., and Zhou,Q.Y. (2005). Dependence of olfactory bulb neurogenesis on prokineticin 2 signaling. Science 308, 1923-1927.

Oakley,A.E., Clifton,D.K., and Steiner,R.A. (2009). Kisspeptin signaling in the brain. Endocr. Rev. 30, 713-743.

Okubo,K. and Nagahama,Y. (2008). Structural and functional evolution of gonadotropin-releasing hormone in vertebrates. Acta Physiol (Oxf) 193, 3-15.

Okubo,K., Sakai,F., Lau,E.L., Yoshizaki,G., Takeuchi,Y., Naruse,K., Aida,K., and Nagahama,Y. (2006). Forebrain gonadotropin-releasing hormone neuronal development: insights from transgenic medaka and the relevance to X-linked Kallmann syndrome. Endocrinology 147, 1076-1084.

Ornitz,D.M., Xu,J., Colvin,J.S., McEwen,D.G., MacArthur,C.A., Coulier,F., Gao,G., and Goldfarb,M. (1996). Receptor specificity of the fibroblast growth factor family. J. Biol. Chem. 271, 15292-15297.

Pagon,R.A., Graham,J.M., Jr., Zonana,J., and Yong,S.L. (1981). Coloboma, congenital heart disease, and choanal atresia with multiple anomalies: CHARGE association. J. Pediatr. 99, 223-227.

Palevitch,O., Abraham,E., Borodovsky,N., Levkowitz,G., Zohar,Y., and Gothilf,Y. (2009). Nasal embryonic LHRH factor plays a role in the developmental migration and projection of gonadotropin-releasing hormone 3 neurons in zebrafish. Dev. Dyn. 238, 66-75.

Palevitch,O., Kight,K., Abraham,E., Wray,S., Zohar,Y., and Gothilf,Y. (2007). Ontogeny of the GnRH systems in zebrafish brain: *in situ* hybridization and promoter-reporter expression analyses in intact animals. Cell Tissue Res. 327, 313-322.

Parhar,I.S. (2002). Cell migration and evolutionary significance of GnRH subtypes. Prog. Brain Res. 141, 3-17.

Park,M.K. and Wakabayashi,K. (1986). Preparation of a monoclonal antibody to common amino acid sequence of LHRH and its application. Endocrinol. Jpn. 33, 257-272.

Pitteloud,N., Acierno,J.S., Jr., Meysing,A., Eliseenkova,A.V., Ma,J., Ibrahimi,O.A., Metzger,D.L., Hayes,F.J., Dwyer,A.A., Hughes,V.A., Yialamas,M., Hall,J.E., Grant,E., Mohammadi,M., and Crowley,W.F., Jr. (2006). Mutations in fibroblast growth factor receptor 1 cause both Kallmann syndrome and normosmic idiopathic hypogonadotropic hypogonadism. Proc. Natl. Acad. Sci. U. S. A 103, 6281-6286.

Pitteloud,N., Acierno,J.S., Jr., Meysing,A.U., Dwyer,A.A., Hayes,F.J., and Crowley,W.F., Jr. (2005). Reversible kallmann syndrome, delayed puberty, and isolated anosmia occurring in a single family with a mutation in the fibroblast growth factor receptor 1 gene. J. Clin. Endocrinol. Metab 90, 1317-1322.

Pitteloud,N., Quinton,R., Pearce,S., Raivio,T., Acierno,J., Dwyer,A., Plummer,L., Hughes,V., Seminara,S., Cheng,Y.Z., Li,W.P., MacColl,G., Eliseenkova,A.V., Olsen,S.K., Ibrahimi,O.A., Hayes,F.J., Boepple,P., Hall,J.E., Bouloux,P., Mohammadi,M., and Crowley,W. (2007). Digenic mutations account for variable phenotypes in idiopathic hypogonadotropic hypogonadism. J. Clin. Invest 117, 457-463.

Plant,T.M., Ramaswamy,S., and DiPietro,M.J. (2006). Repetitive activation of hypothalamic G protein-coupled receptor 54 with intravenous pulses of kisspeptin in the juvenile monkey (Macaca mulatta) elicits a sustained train of gonadotropin-releasing hormone discharges. Endocrinology 147, 1007-1013.

Raisman,G., Carlstedt,T., Choi,D., and Li,Y. (2010). Clinical prospects for transplantation of OECs in the repair of brachial and lumbosacral plexus injuries: Opening a door. Exp. Neurol.

Reifers,F., Adams,J., Mason,I.J., Schulte-Merker,S., and Brand,M. (2000). Overlapping and distinct functions provided by fgf17, a new zebrafish member of the Fgf8/17/18 subgroup of Fgfs. Mech. Dev. 99, 39-49.

Reifers,F., Bohli,H., Walsh,E.C., Crossley,P.H., Stainier,D.Y., and Brand,M. (1998). Fgf8 is mutated in zebrafish acerebellar (ace) mutants and is required for maintenance of midbrain-hindbrain boundary development and somitogenesis. Development 125, 2381-2395.

Rembold,M., Lahiri,K., Foulkes,N.S., and Wittbrodt,J. (2006). Transgenesis in fish: efficient selection of transgenic fish by co-injection with a fluorescent reporter construct. Nat. Protoc. 1, 1133-1139.

Rinaldi,A. (2007). The scent of life. The exquisite complexity of the sense of smell in animals and humans. EMBO Rep. 8, 629-633.

Robertson,A. (2000). Structural and functional studies of anosmin-1, the protein disrupted in X-linked Kallmann's syndrome. Ph.D. Thesis. University College London: U.K.

Rohner,N., Bercsenyi,M., Orban,L., Kolanczyk,M.E., Linke,D., Brand,M., Nusslein-Volhard,C., and Harris,M.P. (2009). Duplication of fgfr1 permits Fgf

signaling to serve as a target for selection during domestication. Curr. Biol. 19, 1642-1647.

Ruitenberg,M.J., Vukovic,J., Sarich,J., Busfield,S.J., and Plant,G.W. (2006). Olfactory ensheathing cells: characteristics, genetic engineering, and therapeutic potential. J. Neurotrauma 23, 468-478.

Sato,Y., Miyasaka,N., and Yoshihara,Y. (2005). Mutually exclusive glomerular innervation by two distinct types of olfactory sensory neurons revealed in transgenic zebrafish. J. Neurosci. 25, 4889-4897.

Scholpp,S., Groth,C., Lohs,C., Lardelli,M., and Brand,M. (2004). Zebrafish fgfr1 is a member of the fgf8 synexpression group and is required for fgf8 signalling at the midbrain-hindbrain boundary. Dev. Genes Evol. 214, 285-295.

Schlessinger,J. (2003). Signal transduction. Autoinhibition control. Science 300, 750-752.

Schwanzel-Fukuda,M., Bick,D., and Pfaff,D.W. (1989). Luteinizing hormone-releasing hormone (LHRH)-expressing cells do not migrate normally in an inherited hypogonadal (Kallmann) syndrome. Brain Res. Mol. Brain Res. 6, 311-326.

Schwanzel-Fukuda,M., Crossin,K.L., Pfaff,D.W., Bouloux,P.M., Hardelin,J.P., and Petit,C. (1996). Migration of luteinizing hormone-releasing hormone (LHRH) neurons in early human embryos. J. Comp Neurol. 366, 547-557.

Schwanzel-Fukuda,M., Zheng,L.M., Bergen,H., Weesner,G., and Pfaff,D.W. (1992). LHRH neurons: functions and development. Prog. Brain Res. 93, 189-201.

Seminara,S.B., DiPietro,M.J., Ramaswamy,S., Crowley,W.F., Jr., and Plant,T.M. (2006). Continuous human metastin 45-54 infusion desensitizes G protein-coupled receptor 54-induced gonadotropin-releasing hormone release monitored indirectly in the juvenile male Rhesus monkey (Macaca mulatta): a finding with therapeutic implications. Endocrinology 147, 2122-2126.

Seminara,S.B., Messager,S., Chatzidaki,E.E., Thresher,R.R., Acierno,J.S., Jr., Shagoury,J.K., Bo-Abbas,Y., Kuohung,W., Schwinof,K.M., Hendrick,A.G., Zahn,D., Dixon,J., Kaiser,U.B., Slaugenhaupt,S.A., Gusella,J.F., O'Rahilly,S., Carlton,M.B., Crowley,W.F., Jr., Aparicio,S.A., and Colledge,W.H. (2003). The GPR54 gene as a regulator of puberty. N. Engl. J. Med. 349, 1614-1627.

Seth,A., Culverwell,J., Walkowicz,M., Toro,S., Rick,J.M., Neuhauss,S.C., Varga,Z.M., and Karlstrom,R.O. (2006). belladonna/(Ihx2) is required for neural patterning and midline axon guidance in the zebrafish forebrain. Development 133, 725-735.

Shaner,N.C., Steinbach,P.A., and Tsien,R.Y. (2005). A guide to choosing fluorescent proteins. Nat. Methods 2, 905-909.

Shanmugalingam,S., Houart,C., Picker,A., Reifers,F., Macdonald,R., Barth,A., Griffin,K., Brand,M., and Wilson,S.W. (2000). Ace/Fgf8 is required for forebrain commissure formation and patterning of the telencephalon. Development 127, 2549-2561.

Silveira,L.F., MacColl,G.S., and Bouloux,P.M. (2002). Hypogonadotropic hypogonadism. Semin. Reprod. Med. 20, 327-338.

Sleptsova-Friedrich,I., Li,Y., Emelyanov,A., Ekker,M., Korzh,V., and Ge,R. (2001). fgfr3 and regionalization of anterior neural tube in zebrafish. Mech. Dev. 102, 213-217.

Smith,K.M., Ohkubo,Y., Maragnoli,M.E., Rasin,M.R., Schwartz,M.L., Sestan,N., and Vaccarino,F.M. (2006). Midline radial glia translocation and corpus callosum formation require FGF signaling. Nat. Neurosci. 9, 787-797.

Smith,T.D., Siegel,M.I., and Bhatnagar,K.P. (2001). Reappraisal of the vomeronasal system of catarrhine primates: ontogeny, morphology, functionality, and persisting questions. Anat. Rec. 265, 176-192.

Soussi-Yanicostas,N., de,C.F., Julliard,A.K., Perfettini,I., Chedotal,A., and Petit,C. (2002). Anosmin-1, defective in the X-linked form of Kallmann syndrome, promotes axonal branch formation from olfactory bulb output neurons. Cell 109, 217-228.

Soussi-Yanicostas,N., Faivre-Sarrailh,C., Hardelin,J.P., Levilliers,J., Rougon,G., and Petit,C. (1998). Anosmin-1 underlying the X chromosome-linked Kallmann syndrome is an adhesion molecule that can modulate neurite growth in a cell-type specific manner. J. Cell Sci. 111 (Pt 19), 2953-2965.

Thisse,B., Thisse,C., and Weston,J.A. (1995). Novel FGF receptor (Z-FGFR4) is dynamically expressed in mesoderm and neurectoderm during early zebrafish embryogenesis. Dev. Dyn. 203, 377-391.

Tirindelli,R., Dibattista,M., Pifferi,S., and Menini,A. (2009). From pheromones to behavior. Physiol Rev. 89, 921-956.

Tisay,K.T. and Key,B. (1999). The extracellular matrix modulates olfactory neurite outgrowth on ensheathing cells. J. Neurosci. 19, 9890-9899.

Tobet,S.A. and Schwarting,G.A. (2006). Minireview: recent progress in gonadotropin-releasing hormone neuronal migration. Endocrinology 147, 1159-1165.

Tole,S., Gutin,G., Bhatnagar,L., Remedios,R., and Hebert,J.M. (2006). Development of midline cell types and commissural axon tracts requires Fgfr1 in the cerebrum. Dev. Biol. 289, 141-151.

Tonou-Fujimori,N., Takahashi,M., Onodera,H., Kikuta,H., Koshida,S., Takeda,H., and Yamasu,K. (2002). Expression of the FGF receptor 2 gene (fgfr2) during embryogenesis in the zebrafish Danio rerio. Gene Expr. Patterns. 2, 183-188.

Topaloglu,A.K., Reimann,F., Guclu,M., Yalin,A.S., Kotan,L.D., Porter,K.M., Serin,A., Mungan,N.O., Cook,J.R., Ozbek,M.N., Imamoglu,S., Akalin,N.S., Yuksel,B., O'Rahilly,S., and Semple,R.K. (2009). TAC3 and TACR3 mutations in familial hypogonadotropic hypogonadism reveal a key role for Neurokinin B in the central control of reproduction. Nat. Genet. 41, 354-358.

Torgersen,J., Nourizadeh-Lillabadi,R., Husebye,H., and Alestrom,P. (2002). In silico and *in situ* characterization of the zebrafish (Danio rerio) gnrh3 (sGnRH) gene. BMC. Genomics 3, 25.

Trarbach,E.B., Abreu,A.P., Silveira,L.F., Garmes,H.M., Baptista,M.T., Teles,M.G., Costa,E.M., Mohammadi,M., Pitteloud,N., Mendonca,B.B., and Latronico,A.C. (2010). Nonsense mutations in FGF8 gene causing different degrees of human gonadotropin-releasing deficiency. J. Clin. Endocrinol. Metab 95, 3491-3496.

Tsai,P.S., Moenter,S.M., Postigo,H.R., El,M.M., Pak,T.R., Gill,J.C., Paruthiyil,S., Werner,S., and Weiner,R.I. (2005). Targeted expression of a dominant-negative fibroblast growth factor (FGF) receptor in gonadotropin-releasing hormone (GnRH) neurons reduces FGF responsiveness and the size of GnRH neuronal population. Mol. Endocrinol. 19, 225-236.

Tsang,M., Maegawa,S., Kiang,A., Habas,R., Weinberg,E., and Dawid,I.B. (2004). A role for MKP3 in axial patterning of the zebrafish embryo. Development 131, 2769-2779.

Van,V.D., Wall,D.P., and Johnson,K.G. (2006). Heparan sulfate proteoglycans and the emergence of neuronal connectivity. Curr. Opin. Neurobiol. 16, 40-51.

Vissers,L.E., van Ravenswaaij,C.M., Admiraal,R., Hurst,J.A., De Vries,B.B., Janssen,I.M., van der Vliet,W.A., Huys,E.H., de Jong,P.J., Hamel,B.C., Schoenmakers,E.F., Brunner,H.G., Veltman,J.A., and van Kessel,A.G. (2004). Mutations in a new member of the chromodomain gene family cause CHARGE syndrome. Nat. Genet. 36, 955-957.

Wada,N., Javidan,Y., Nelson,S., Carney,T.J., Kelsh,R.N., and Schilling,T.F. (2005). Hedgehog signaling is required for cranial neural crest morphogenesis and chondrogenesis at the midline in the zebrafish skull. Development 132, 3977-3988.

Walshe,J., Maroon,H., McGonnell,I.M., Dickson,C., and Mason,I. (2002). Establishment of hindbrain segmental identity requires signaling by FGF3 and FGF8. Curr. Biol. 12, 1117-1123.

Walshe,J. and Mason,I. (2003). Unique and combinatorial functions of Fgf3 and Fgf8 during zebrafish forebrain development. Development 130, 4337-4349.

Whitlock,K.E. (2004). Development of the nervus terminalis: origin and migration. Microsc. Res. Tech. 65, 2-12.

Whitlock,K.E. (2005a). Origin and development of GnRH neurons. Trends Endocrinol. Metab 16, 145-151.

Whitlock,K.E., Smith,K.M., Kim,H., and Harden,M.V. (2005b). A role for foxd3 and sox10 in the differentiation of gonadotropin-releasing hormone (GnRH) cells in the zebrafish Danio rerio. Development 132, 5491-5502.

Whitlock,K.E. and Westerfield,M. (1998). A transient population of neurons pioneers the olfactory pathway in the zebrafish. J. Neurosci. 18, 8919-8927.

Whitlock,K.E. and Westerfield,M. (2000). The olfactory placodes of the zebrafish form by convergence of cellular fields at the edge of the neural plate. Development 127, 3645-3653.

Whitlock,K., Kim,H., Maturana,C., and Letelier,J. (2009). 06-P013 Disrupted patterning of the hypothalamus results in Kallmann Syndrome like defects in the zebrafish. Mechanisms of Development 126, S124.

Wilkie,A.O. (2005). Bad bones, absent smell, selfish testes: the pleiotropic consequences of human FGF receptor mutations. Cytokine Growth Factor Rev. 16, 187-203.

Wirsig,C.R. and Leonard,C.M. (1987). Terminal nerve damage impairs the mating behavior of the male hamster. Brain Res. 417, 293-303.

Wittbrodt,J., Shima,A., and Schartl,M. (2002). Medaka--a model organism from the far East. Nat. Rev. Genet. 3, 53-64.

Woodage,T., Basrai,M.A., Baxevanis,A.D., Hieter,P., and Collins,F.S. (1997). Characterization of the CHD family of proteins. Proc. Natl. Acad. Sci. U. S. A 94, 11472-11477.

Wray,S., Nieburgs,A., and Elkabes,S. (1989). Spatiotemporal cell expression of luteinizing hormone-releasing hormone in the prenatal mouse: evidence for an embryonic origin in the olfactory placode. Brain Res. Dev. Brain Res. 46, 309-318.

Yanicostas,C., Ernest,S., Dayraud,C., Petit,C., and Soussi-Yanicostas,N. (2008). Essential requirement for zebrafish anosmin-1a in the migration of the posterior lateral line primordium. Dev. Biol. 320, 469-479.

Yanicostas,C., Herbomel,E., Dipietromaria,A., and Soussi-Yanicostas,N. (2009). Anosmin-1a is required for fasciculation and terminal targeting of olfactory sensory neuron axons in the zebrafish olfactory system. Mol. Cell Endocrinol. 312, 53-60.

Yoshida,T., Ito,A., Matsuda,N., and Mishina,M. (2002). Regulation by protein kinase A switching of axonal pathfinding of zebrafish olfactory sensory neurons through the olfactory placode-olfactory bulb boundary. J. Neurosci. 22, 4964-4972.

Yu,S.R., Burkhardt,M., Nowak,M., Ries,J., Petrasek,Z., Scholpp,S., Schwille,P., and Brand,M. (2009). Fgf8 morphogen gradient forms by a source-sink mechanism with freely diffusing molecules. Nature 461, 533-536.

Appendix

Table A1 Optimising the morpholino concentrations

	Proportion of embryos dead or with non-specific MO-induced toxicity*							
MO conc. / MO Name	0.5mM		1.0mM		1.5mM		2.0mM	
stage:	36hpf	60hpf	36hpf	60hpf	36hpf	60hpf	36hpf	60hpf
Fgf8A MO	3/64	4/64	9/72#	12/72#	11/76	15/76	35/53	38/53
Fgf8B MO	3/51	5/51	7/63	9/63	7/66#	10/66#	16/58	21/58
A-MO**	2/71	5/71	9/76#	13/76#	17/79	19/79	N/A	N/A
B-MO**	9/85	13/85	19/93#	22/93#	28/74	29/74	N/A	N/A
KA4	8/118	9/118	11/109#	15/109#	16/91	23/91	45/61	46/61
KB4	11/126	14/126	18/133#	25/133#	36/58	39/58	All died	All died
KA6	4/51	5/51	2/48	2/48	5/47	7/47	4/58#	6/58#
KB6	5/67	8/67	14/71#	17/71#	41/49	All died	All died	All died
coMO	4/74	6/74	3/69	4/69	2/64#	4/64#	6/56	6/56

* Including significant levels of head/brain/eye/trunk necrosis and heart oedema (remaining embryos were morphologically normal or with very minor defects).

** Translational-blocking morpholinos against Kal1a and Kal1b (refer to text).

# indicates the morpholino (MO) concentration used for experiments in this thesis.

Table A2 Optimising the mRNA concentrations

	Proportion of embryos dead or with non-specific mRNA-induced toxicity* by 36hpf		
RNA conc. / RNA Name	**0.5μM**	**1.0μM**	**1.5μM**
Kal1a	13/78	19/89	68/82
Kal1b	11/75	17/87	31/81
Kal1a +Kal1b	16/96**	59/86***	ALL DIED

* *Including significant levels of head/brain/eye/trunk necrosis and heart oedema* (remaining embryos were morphologically normal or with very minor defects).

** 0.5μM+0.5μM (1.0μM total).

*** 1.0μM+1.0μM (2.0μM total).

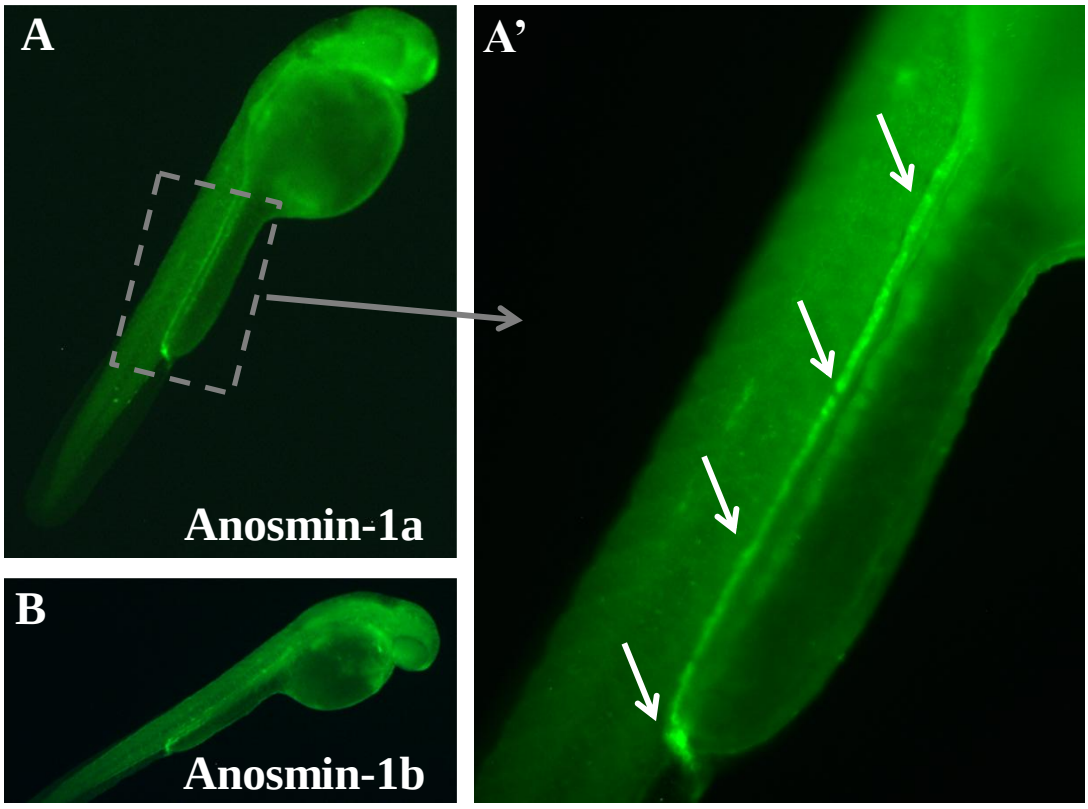

Figure A1 Anosmin-1a & anosmin-1b immuno-reactivity in the pronephric duct

Anosmin-1a (A) and anosmin-1b (B) are both expressed in the pronephric duct region by around 30hpf. The dotted box in A demarcates the region along the trunk which is shown in more detail in A', with arrows pointing out the pronephric duct region.

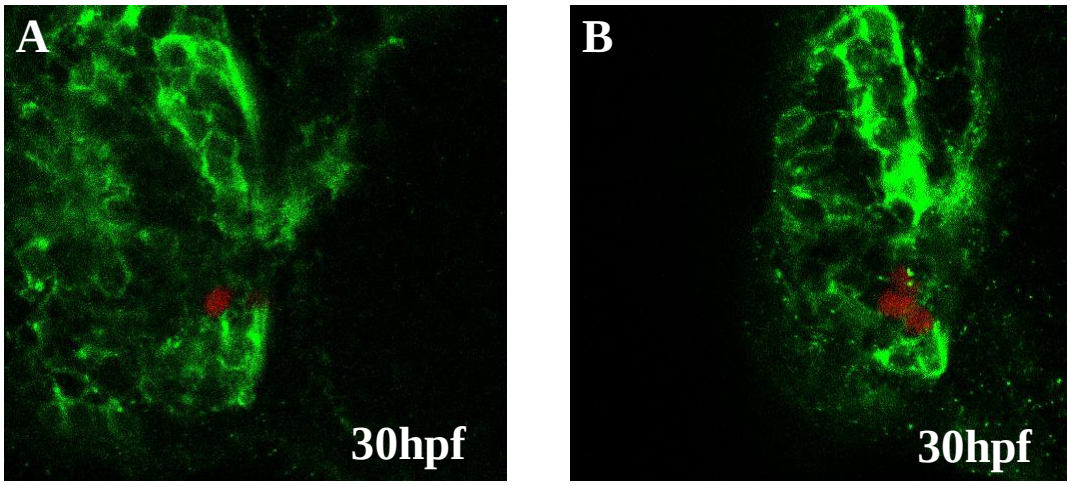

Figure A2 Anosmin-1a/anosmin-1b immuno-expression in the nasal compartment

A and B illustrate a single Z-layer of the olfactory epithelium region from a confocal stack of anosmin-1a and anosmin-1b immuno-labelled G3MC embryos at 30hpf. This demonstrates that anosmin-1a and anosmin-1b are both expressed in a broad olfactory epithelial/ nasal compartment region that includes the terminal nerve GnRH3 -expressing cells.

Publications, presentations & awards

Journal Publications

Cadman, S. M., Kim, S. H., Hu, Y., Gonzalez-Martinez, D., and Bouloux, P. M. (2007). Molecular pathogenesis of Kallmann's syndrome. Horm Res 67, 231-242.

Kim, S. H., Hu, Y., **Cadman, S.,** and Bouloux, P. (2008). Diversity in fibroblast growth factor receptor 1 regulation: learning from the investigation of Kallmann syndrome. J Neuroendocrinol 20, 141-163.

Hu, Y., Guimond, S. E., Travers, P., **Cadman, S.,** Hohenester, E., Turnbull, J. E., Kim, S. H., and Bouloux, P. M. (2009). Novel mechanisms of fibroblast growth factor receptor 1 regulation by extracellular matrix protein anosmin-1. J Biol Chem.

Cadman, S. M., Iyengar, L., Philp, G., Kim, S. H., Bouloux, P. M., and Mason, I.J. Anosmin-1a and anosmin-1b are required together for olfactory axonogenesis, GnRH cell migration and anterior commissure formation in the zebrafish. *(Manuscript in preparation)*

Conference oral presentations

20th Head group meeting (18 January 2008), Institute of Child Health, UCL

Society for Endocrinology BES 2008 (07 April 2008), Harrogate, UK

Joint Meeting of the British Societies for Cell and Developmental Biology (03 April 2008), Warwick, UK

Awards

Best PhD student poster presentation (July 2007)

"Science at The Free" Symposium, Royal Free hospital